



저작자표시-비영리-변경금지 2.0 대한민국

이용자는 아래의 조건을 따르는 경우에 한하여 자유롭게

- 이 저작물을 복제, 배포, 전송, 전시, 공연 및 방송할 수 있습니다.

다음과 같은 조건을 따라야 합니다:



저작자표시. 귀하는 원저작자를 표시하여야 합니다.



비영리. 귀하는 이 저작물을 영리 목적으로 이용할 수 없습니다.



변경금지. 귀하는 이 저작물을 개작, 변형 또는 가공할 수 없습니다.

- 귀하는, 이 저작물의 재이용이나 배포의 경우, 이 저작물에 적용된 이용허락조건을 명확하게 나타내어야 합니다.
- 저작권자로부터 별도의 허가를 받으면 이러한 조건들은 적용되지 않습니다.

저작권법에 따른 이용자의 권리는 위의 내용에 의하여 영향을 받지 않습니다.

이것은 [이용허락규약\(Legal Code\)](#)을 이해하기 쉽게 요약한 것입니다.

[Disclaimer](#)



博士學位論文

Chemical Constituents and  
Cosmetics-Related Activities from  
Plants in Jeju Island

濟州大學校 大學院

化 學 科

高 麗 暎

2012年 2月



# 제주 식물로부터 화장품 관련 유효성분 규명 및 활성 연구

指導教授 李 南 昊

高 麗 暎

이 論文을 理學 博士學位 論文으로 提出함

2012年 2月

高麗暎의 理學 博士學位 論文을 認准함

審査委員長	_____	Ⓜ
委 員	_____	Ⓜ
委 員	_____	Ⓜ
委 員	_____	Ⓜ
委 員	_____	Ⓜ

濟州大學校 大學院

2012年 2月

Chemical Constituents and Cosmetics-Related  
Activities from Plants in Jeju Island

Ryeo Kyeong Ko

(Supervised by Professor Nam Ho Lee)

A thesis submitted in partial fulfillment of the requirement  
for the degree of Doctor of Philosophy

2012. 2.

This thesis has been examined and approved.

.....  
.....  
.....  
.....  
.....

.....  
Date

DEPARTMENT OF CHEMISTRY  
GRADUATE SCHOOL  
JEJU NATIONAL UNIVERSITY

# LIST OF CONTENTS

<b>LIST OF CONTENTS</b> .....	i
<b>LIST OF PHOTOGRAPHS</b> .....	x
<b>LIST OF SCHEMES</b> .....	x i
<b>LIST OF TABLES</b> .....	x ii
<b>LIST OF FIGURES</b> .....	x iii
<b>LIST OF ABBREVIATIONS</b> .....	x x
<b>ABSTRACT (In English)</b> .....	x x iv
<b>초록 (국문)</b> .....	x x vii
<b>I. INTRODUCTION</b> .....	<b>1</b>
1. Natural product and cosmetics.....	1
1-1. Need for cosmeceuticals from nature.....	1
1-2. Botanical extract and cosmetic uses.....	2
1-3. Characteristics of the phytochemical component used for the cosmetics.....	5
2. Trend of development of functional cosmetics ingredients.....	8
2-1. The natural product and functional cosmetic.....	8
2-2. The overseas technology trend.....	9
2-3. The domestic technology trend.....	9
3. Antioxidants.....	14
3-1. Water-soluble antioxidants.....	16
3-2. Lipid-soluble antioxidants.....	18
4. Photoaging agents.....	20
5. Depigmentation agents.....	24
5-1. Screening tests for depigmentation agents.....	25
6. Fat storage and slimming agents.....	28
7. Research objectives.....	29

<b>II. REAGENT AND INSTRUMENTS</b> .....	<b>30</b>
1. Chemical Reagent.....	30
1-1. Column packing material.....	30
1-2. LC column.....	30
1-3. TLC (Thin Layer Chromatography) plate.....	30
1-4. TLC (Thin Layer Chromatography) visualizing reagent.....	31
1-5. Solvent.....	31
1-6. HPLC additives for analysis solvent and the preprocessing supplies.....	31
1-7. Anti-oxidant assay.....	31
1-8. Anti-inflammatory assay.....	32
1-9. Melanogenesis inhibition assay.....	32
1-10. Anti-obesity assay.....	32
2. Instrument.....	33
<b>III. RESEARCH 1 : <i>Lindera erythrocarpa</i> Makino</b> .....	<b>34</b>
1. General Plants Information.....	34
2. Experimental Methods.....	37
2-1. Plant material.....	37
2-2. Extraction and solvent fractionation.....	37
2-2-1. Extraction from the leaves.....	37
2-2-2. Extraction from the stem barks.....	37
2-3. Isolation and purification.....	38
2-3-1. Isolation produce of methylene chloride fraction from the leaves (LM).....	38
2-3-2. Isolation produce of ethyl acetate fraction from the leaves (LE).....	38
2-3-3. Isolation produce of methylene chloride fraction from the stem barks (SM).....	39
3. Qualitative and Quantitative Determination by LC Analysis.....	42
3-1. HPLC analysis.....	42
3-1-1. Standard solutions for quantitative analysis.....	42
3-1-2. Sample preparation for analysis of quantitative and qualitative.....	42

3-1-3. Determination of HPLC-PDA and ESLD analysis	42
3-1-4. Calibration	44
4. Biological Activity Test	45
4-1. Anti-oxidant assay	45
4-1-1. Preparation of sample	45
4-1-2. DPPH radical scavenging activity assay	45
4-1-3. Superoxide radical scavenging activity assay	46
4-1-4. Xantine oxidase inhibition activity assay	47
4-2. Anti-inflammatory assay	48
4-2-1. Cell culture	48
4-2-2. Cell viability assay by MTT	48
4-2-3. Measurement of NO production	48
4-3. Melanogenesis inhibition activity assay	50
4-3-1. Cell culture	50
4-3-2. Cell viability assay by MTT	50
4-3-3. Measurement of melanin contents	50
4-3-4. Measurement of cell-extracted tyrosinase from cell inhibition activity	51
4-3-5. mRNA preparation and polymerase chain reaction (PCR)	51
4-4. Anti-obesity assay	53
4-4-1. Measurement of yeast $\alpha$ -glucosidase inhibitory activity	53
4-4-2. Cell culture and preadipocyte differentiation	53
4-4-3. Cell viability assay by MTT	54
4-4-4. Cytotoxicity assay (LDH assay)	54
4-4-5. Oil-Red O staining	54
4-5. Statistical analysis	55
5. Results	56
5-1. The structures of the compounds isolated from of <i>L. erythrocarpa</i>	56
5-1-1. Compound <b>1</b>	56
5-1-2. Compound <b>2</b>	59



5-1-3. Compound 3	62
5-1-4. Compound 4	65
5-1-5. Compound 5	68
5-1-6. Compound 6	71
5-1-7. Compound 7	74
5-1-8. Compound 8	77
5-1-9. Compound 9	80
5-1-10. Compound 10	83
5-1-11. Compound 11	86
5-1-12. Compound 12	89
5-1-13. Compound 13	92
5-1-14. Compound 14	99
5-2. Biological activities	102
5-2-1. Antioxidant activity	102
5-2-1-1. Free radical scavenging activity of the solvent fractions	102
5-2-1-2. Free radical scavenging activity of the isolated compounds	105
5-2-2. Anti-inflammatory activity	107
5-2-2-1. Effect on cell viability and LPS-induced NO production	107
5-2-3. Melanogenesis inhibition activity	110
5-2-3-1. Cell viability in B16F10 melanoma cell	110
5-2-3-2. Effect on melanogenesis in B16F10 cells	113
5-2-3-3. Morphological observation of B16F10 melanoma cells	116
5-2-3-4. Inhibition effect on melanin synthetic abilities on cell-extracted tyrosinase activity	117
5-2-3-5. Inhibition effect on the related mRNA expression	120
5-2-4. Anti-obesity activity	121
5-2-4-1. Inhibition effect on <i>α</i> -glucosidase	121
5-2-4-2. Cell viability in mouse 3T3-L1 preadipocytes	123
5-2-4-3. Effects on reducing lipid accumulation in mouse 3T3-L1 preadipocytes	



differentiated adipocytes .....	126
6. Discussion .....	130
<b>IV. RESEARCH 2 : <i>Cornus macrophylla</i> Wall.....</b>	<b>133</b>
1. General Plants Information .....	133
2. Experimental Methods .....	135
2-1. Plant material .....	135
2-2. Solvent fraction of the leaves .....	135
2-3. Isolation and purification .....	135
2-3-1. Isolation produce of ethyl acetate fraction from the leaves (CE) .....	135
3. Results .....	137
3-1. The structures of the compounds isolated from of <i>C. macrophylla</i> .....	137
3-1-1. Compound 1 .....	137
3-1-2. Compound 2 .....	140
3-1-3. Compound 3 .....	143
3-1-4. Compound 4 .....	146
3-1-5. Compound 5 .....	149
3-1-6. Compound 6 .....	150
3-2. Biological activities .....	151
3-2-1. Antioxidant activity .....	151
3-2-1-1. Free radical scavenging activity of the crude 70% EtOH extract and the isolated compounds .....	151
3-2-1-2. Free radical scavenging activity of the isolated compounds .....	152
4. Discussion .....	153
<b>V. RESEARCH 3 : <i>Aster subulatus</i> Michx.....</b>	<b>154</b>
1. General Plants Information .....	154
2. Experimental Methods .....	156
2-1. Plant material .....	156

2-2. Extraction and solvent fractionation	156
2-2-1. Extraction from the whole plant	156
2-3. Isolation and purification	156
2-3-1. Isolation produce of methylene chloride fraction (AM)	156
2-3-2. Isolation produce of ethyl acetate fraction (AE)	157
3. Results	159
3-1. The structures of the compounds isolated from of <i>A. subulatus</i>	159
3-1-1. Compound <b>1</b>	159
3-1-2. Compound <b>2</b>	160
3-1-3. Compound <b>3</b>	162
3-1-4. Compound <b>4</b>	165
3-1-5. Compound <b>5</b>	172
3-1-6. Compound <b>6</b>	175
3-1-7. Compound <b>7</b>	178
3-2. Biological activities	181
3-2-1. Antioxidant activity	181
3-2-1-1. Free radical scavenging activity of the solvent fractions	181
3-2-1-2. Free radical scavenging activity of the isolated compounds	183
3-2-2. Melanogenesis inhibition activity	184
3-2-2-1. Cell viability in B16F10 melanoma cell	184
3-2-2-2. Effect on melanogenesis in B16F10 cells	187
3-2-3. Anti-obesity activity	190
3-2-3-1. Inhibition effect on <i>α</i> -glucosidase	190
3-2-3-2. Cell viability in mouse 3T3-L1 preadipocytes	193
3-2-3-3. Effects on reducing lipid accumulation in mouse 3T3-L1 preadipocytes differentiated adipocytes	194
4. Discussion	195
<b>VI. RESEARCH 4 : <i>Ishige sinicola</i> (Setchell et Gardner) Chihara</b>	<b>197</b>

1. General Plants Information	197
2. Experimental Methods	199
2-1. Plant material	199
2-2. Solvent fraction from the whole sea plant	199
2-3. Isolation and purification	199
2-3-1. Isolation produce of methylene chloride fraction (IM)	199
2-3-2. Isolation produce of ethyl acetate fraction (IE)	200
3. Results	202
3-1. The structures of the compounds isolated from of <i>I. sinicola</i>	202
3-1-1. Compound 1	202
3-1-2. Compound 2	206
3-1-3. Compound 3	209
3-1-4. Compound 4	212
3-1-5. Compound 5	216
3-2. Biological activities	219
3-2-1. Melanogenesis inhibition activity	219
3-2-2-1. Cell viability in B16F10 melanoma cell	219
3-2-3-2. Effect on melanogenesis in B16F10 cells	222
3-2-3. Anti-obesity activity	224
3-2-3-1. Inhibition effect on $\alpha$ -glucosidase	224
3-2-3-2. Cell viability effect in mouse 3T3-L1 preadipocytes	228
3-2-3-3. Effects on reducing lipid accumulation in mouse 3T3-L1 preadipocytes differentiated adipocytes	231
4. Discussion	234
<b>VII. RESEARCH 5 : <i>Dictyota Coriacea</i> (Holmes) Hwang, Kim, et Lee</b>	<b>236</b>
1. General Plants Information	236
2. Experimental Methods	238
2-1. Plant material	238

2-2. Solvent fraction from the whole sea plant	238
2-3. Isolation and purification	238
2-3-1. Isolation produce of methylene chloride fraction (DM)	238
3. Results	241
3-1. The structures of the compounds isolated from of <i>D. coriacea</i>	241
3-1-1. Compound 1	241
3-1-2. Compound 2	244
3-1-3. Compound 3	247
3-2. Biological activities	250
3-2-1. Antioxidant activity	250
3-2-1-1. Free radical scavenging activity of the solvent fractions	250
3-2-2. Anti-inflammation activity	252
3-2-2-1. Effect on cell viability and LPS-induced NO production	252
3-2-3. Melanogenesis inhibition activity	254
3-2-3-1. Cell viability in B16F10 melanoma cell	254
3-2-3-2. Effect on melanogenesis in B16F10 cells	257
4. Discussion	260
<b>VIII. RESEARCH 6 : <i>Styrax obassia</i> Siebold &amp; Zucc</b>	<b>262</b>
1. General Plants Information	262
2. Experimental Methods	264
2-1. Plant material	264
2-2. Solvent fraction of the leaves	264
2-3. Isolation and purification	264
2-3-1. Isolation produce of <i>n</i> -butanol fraction (SB)	264
3. Results	268
3-1. The structures of the compounds isolated from of <i>S. obassia</i>	268
3-1-1. Compound 1	268
3-1-2. Compound 2	273

3-2. Biological activities.....	278
3-2-1. Antioxidant activity.....	278
3-2-1-1. Free radical scavenging activity of the solvent fractions.....	278
3-2-2. Melanogenesis inhibition activity.....	280
3-2-2-1. Cell viability in B16F10 melanoma cell.....	280
3-2-2-2. Effect on melanogenesis in B16F10 cells.....	282
3-2-3. Anti-obesity activity.....	284
3-2-3-1. Inhibition effect on <i>α</i> -glucosidase.....	284
3-2-3-2. Cell viability in mouse 3T3-L1 preadipocytes.....	287
3-2-3-3. Effects on reducing lipid accumulation in mouse 3T3-L1 preadipocytes differentiated adipocytes.....	290
4. Discussion.....	293
<b>IX. Overall Conclusion.....</b>	<b>295</b>
<b>X. References.....</b>	<b>299</b>
<b>Appendix.....</b>	<b>309</b>
<b>Acknowledgments (감사의 글).....</b>	<b>326</b>

## LIST OF PHOTOGRAPHS

Photo 1. The specimen of <i>L. erythrocarpa</i> .....	34
Photo 2. Photograph of the leave of <i>L. erythrocarpa</i> .....	36
Photo 3. Photograph of the stem bark of <i>L. erythrocarpa</i> .....	36
Photo 4. Photograph of the fruit of <i>L. erythrocarpa</i> .....	36
Photo 5. Differentiation of mouse 3T3-L1 preadipocytes to adipocytes before treated samples.....	127
Photo 6. The specimen of <i>C. macrophylla</i> .....	133
Photo 7. Photograph of <i>C. macrophylla</i> .....	134
Photo 8. Photograph of the bark of <i>C. macrophylla</i> .....	134
Photo 9. Photograph of the fruit of <i>C. macrophylla</i> .....	134
Photo 10. The specimen of <i>A. subulatus</i> .....	154
Photo 11. Photograph of the whole plant of <i>A. subulatus</i> .....	155
Photo 12. Photograph of the flower of <i>A. subulatus</i> .....	155
Photo 13. Photograph of the spore of <i>A. subulatus</i> .....	155
Photo 14. The specimen of <i>I. sinicola</i> .....	197
Photo 15. Photograph of <i>I. sinicola</i> .....	198
Photo 16. Photograph of the whole of <i>I. sinicola</i> .....	198
Photo 17. Photograph of the whole of <i>I. sinicola</i> .....	198
Photo 18. The specimen of <i>D. coriacea</i> .....	236
Photo 19. Photograph of the whole of <i>D. coriacea</i> .....	237
Photo 20. Photograph of the whole of <i>D. coriacea</i> .....	237
Photo 21. Photograph of the whole of <i>D. coriacea</i> .....	237
Photo 22. The specimen of <i>S. obassia</i> .....	262
Photo 23. Photograph of the whole plant of <i>S. obassia</i> .....	263
Photo 24. Photograph of the leave of <i>S. obassia</i> .....	263
Photo 25. Photograph of the flower of <i>S. obassia</i> .....	263



## LIST OF SCHEMES

Scheme 1. Extraction and fractionation of the leaves of <i>L. erythrocarpa</i> .....	40
Scheme 2. Extraction and fractionation of the stem barks of <i>L. erythrocarpa</i> .....	41
Scheme 3. Proposed bio-synthetic pathway to 1-(2'-hydroxy-3',4',5',6'-tetramethylphenyl)-1-methoxy-3-phenylpropane ( <b>13</b> ) from kanakugiol ( <b>10</b> ).....	97
Scheme 4. Extraction and fractionation of the leaves of <i>C. macrophylla</i> .....	136
Scheme 5. Extraction and fractionation of the whole of <i>A. subulatus</i> .....	158
Scheme 6. Extraction and fractionation of the whole of <i>I. sinicola</i> .....	201
Scheme 7. Extraction and fractionation of the whole of <i>D. coriacea</i> .....	240
Scheme 8. Extraction and fractionation of the leaves of <i>S. obassia</i> .....	267

## LIST OF TABLES

Table 1. The classification system of the natural product cosmetics.....	2
Table 2. The typical natural raw material item in the Korea Standard of Cosmetic Ingredients (the manor).....	4
Table 3. Comparison between advantage and disadvantage of the natural product cosmetics .....	5
Table 4. Using cosmetic ingredients from nature.....	7
Table 5. The activity by classification.....	11
Table 6. The roles of naturally existing retinoids.....	22
Table 7. Major main depigmentation agents (Kojic acid) production on a pilot scale.....	25
Table 8. Mechanism of melanogenesis inhibition.....	27
Table 9. Instrument condition for HPLC-ELSD.....	43
Table 10. Gradient elution condition for HPLC-PDA/ELSD separation.....	44
Table 11. Free radical scavenging effect of the solvent fractions.....	104
Table 12. Free radical scavenging effect of the isolated compounds on DPPH radical scavenging activity	106
Table 13. Cell viability and effects of the solvent fractions on the production of nitric oxide in LPS-stimulated RAW 264.7 cells.....	108
Table 14. Cell viability and effects of the isolated compounds on the production of nitric oxide in LPS-stimulated RAW 264.7 cells.....	109
Table 15. Inhibition effect of the isolated compounds on yeast $\alpha$ -glucosidase inhibitory assay.....	122
Table 16. DPPH radical scavenging effect of the crude 70% <i>aq.</i> EtOH extract.....	151
Table 17. DPPH radical scavenging effect of the isolated compounds.....	152
Table 18. Free radical scavenging effect of the solvent fractions.....	182
Table 19. Free radical scavenging effect of the isolated compounds.....	183
Table 20. Inhibition effect of the isolated compounds on yeast $\alpha$ -glucosidase inhibitory assay.....	191
Table 21. Inhibition effect of the solvent fractions on yeast $\alpha$ -glucosidase inhibitory assay.....	225
Table 22. Inhibition effect of the isolated compounds on yeast $\alpha$ -glucosidase inhibitory assay.....	227
Table 23. Free radical scavenging effect of the solvent fractions.....	251
Table 24. Cell viability and effects of the solvent fractions on the production of nitric oxide in LPS-stimulated RAW 264.7 cells.....	253
Table 25. Gradient elution condition for prep-HPLC separation.....	265
Table 26. Free radical scavenging effect of the solvent fractions.....	279
Table 27. Inhibition effect of the solvent fractions on yeast $\alpha$ -glucosidase inhibitory assay.....	285



# LIST OF FIGURES

## I. INTRODUCTION

Figure 1. Activation of the antioxidant network by environmental oxidative stressors	14
Figure 2. Radical reaction potentials	15
Figure 3. The network antioxidants in the human cell	16
Figure 4. Chemical Structures of selected antioxidants from nature	17
Figure 5. Layers of the skin including major function tissue	20
Figure 6. Mechanism of photoaging by UV-irradiation	21
Figure 7. Structure of retinoids	23
Figure 8. Chemical Structures of main depigmentation agents	26

## III. RESEARCH 1 : *Lindera erythrocarpa* Makino

Figure 9. <sup>1</sup> H-NMR spectrum of ethyl caffeate (1) in CD <sub>3</sub> OD	57
Figure 10. <sup>13</sup> C-NMR spectrum of ethyl caffeate (1) in CD <sub>3</sub> OD	57
Figure 11. DEPT135 spectrum of ethyl caffeate (1) in CD <sub>3</sub> OD	57
Figure 12. Structure of compound 1; Ethyl caffeate	58
Figure 13. <sup>1</sup> H-NMR spectrum of methyl cinnamate (2) in DMSO- <i>d</i> <sub>6</sub>	60
Figure 14. <sup>13</sup> C-NMR spectrum of methyl cinnamate (2) in DMSO- <i>d</i> <sub>6</sub>	60
Figure 15. Structure of compound 2; Methyl cinnamate	61
Figure 16. <sup>1</sup> H-NMR spectrum of lucidone (3) in CDCl <sub>3</sub>	63
Figure 17. <sup>13</sup> C-NMR spectrum of lucidone (3) in CDCl <sub>3</sub>	63
Figure 18. Structure of compound 3; Lucidone	64
Figure 19. <sup>1</sup> H-NMR spectrum of methyllinderone (4) in CDCl <sub>3</sub>	66
Figure 20. <sup>13</sup> C-NMR spectrum of methyllinderone (4) in CDCl <sub>3</sub>	66
Figure 21. Structure of compound 4; Methyllinderone	67
Figure 22. <sup>1</sup> H-NMR spectrum of β-sitosterol (5) in Acetone- <i>d</i> <sub>6</sub>	69
Figure 23. <sup>13</sup> C-NMR and DEPT135 spectra of β-sitosterol (5) in Acetone- <i>d</i> <sub>6</sub>	69
Figure 24. Structure of compound 5; β-sitosterol	70
Figure 25. <sup>1</sup> H-NMR spectrum of quercetin (6) in CD <sub>3</sub> OD	72
Figure 26. <sup>13</sup> C-NMR spectrum of quercetin (6) in CD <sub>3</sub> OD	72
Figure 27. Structure of compound 6; Quercetin	73
Figure 28. <sup>1</sup> H-NMR spectrum of quercetin-3- <i>O</i> -α- <i>L</i> -rhamnoside (7) in CD <sub>3</sub> OD	75

Figure 29. $^{13}\text{C}$ -NMR spectrum of quercetin-3- <i>O</i> - $\alpha$ -L-rhamnoside ( <b>7</b> ) in $\text{CD}_3\text{OD}$ .....	75
Figure 30. Structure of compound <b>7</b> ; Quercetin-3- <i>O</i> - $\alpha$ -L-rhamnoside (quercitrin).....	76
Figure 31. $^1\text{H}$ -NMR spectrum of quercetin-3- <i>O</i> - $\alpha$ -L-arabinofuranoside ( <b>8</b> ) in $\text{CD}_3\text{OD}$ .....	78
Figure 32. $^{13}\text{C}$ -NMR and DEPT135 spectra of quercetin-3- <i>O</i> - $\alpha$ -L-arabinofuranoside ( <b>8</b> ) in $\text{CD}_3\text{OD}$ .....	78
Figure 33. Structure of compound <b>8</b> ; quercetin-3- <i>O</i> - $\alpha$ -L-arabinofuranoside (avicularin).....	79
Figure 34. $^1\text{H}$ -NMR spectrum of kaempferol-3- <i>O</i> - $\alpha$ -L-rhamnoside ( <b>9</b> ) in $\text{CD}_3\text{OD}$ .....	81
Figure 35. $^{13}\text{C}$ -NMR spectrum of kaempferol-3- <i>O</i> - $\alpha$ -L-rhamnoside ( <b>9</b> ) in $\text{CD}_3\text{OD}$ .....	81
Figure 36. Structure of compound <b>9</b> ; Kaempferol-3- <i>O</i> - $\alpha$ -L-rhamnoside (afzelin).....	82
Figure 37. $^1\text{H}$ -NMR spectrum of kanakugiol ( <b>10</b> ) in $\text{CD}_3\text{OD}$ .....	84
Figure 38. $^{13}\text{C}$ -NMR and DEPT135 spectra of kanakugiol ( <b>10</b> ) in $\text{CD}_3\text{OD}$ .....	84
Figure 39. Structure of compound <b>10</b> ; 2'-Hydroxy-3',4',5',6'-tetramethoxychalcone (kanakugiol).....	85
Figure 40. $^1\text{H}$ -NMR spectrum of methyllicudone ( <b>11</b> ) in $\text{CDCl}_3$ .....	87
Figure 41. $^{13}\text{C}$ -NMR and DEPT135 spectra of methyllicudone ( <b>11</b> ) in $\text{CDCl}_3$ .....	87
Figure 42. Structure of compound <b>11</b> ; Methyllicudone.....	88
Figure 43. Expectative tautomers of methyllicudone ( <b>11</b> ).....	88
Figure 44. $^1\text{H}$ -NMR spectrum of stigmasterol ( <b>12</b> ) in $\text{CDCl}_3$ .....	90
Figure 45. $^{13}\text{C}$ -NMR and DEPT135 spectra of stigmasterol ( <b>12</b> ) in $\text{CDCl}_3$ .....	90
Figure 46. Structure of compound <b>12</b> ; stigmasterol.....	91
Figure 47. Comparison on each olefinic structure of 22, 23-position between $\beta$ -sitosterol and stigmasterol .....	91
Figure 48. $^1\text{H}$ -NMR spectrum of 1-(2'-hydroxy-3',4',5',6'-tetramethylphenyl)-1-methoxy-3-phenylpropane ( <b>13</b> ) in $\text{CDCl}_3$ .....	93
Figure 49. $^{13}\text{C}$ -NMR and DEPT135 spectra of of 1-(2'-hydroxy-3',4',5',6'-tetramethylphenyl)-1-methoxy-3- -phenylpropane ( <b>13</b> ) in $\text{CDCl}_3$ .....	93
Figure 50. HMQC spectrum of 1-(2'-hydroxy-3',4',5',6'-tetramethylphenyl)-1-methoxy-3-phenylpropane ( <b>13</b> ) in $\text{CDCl}_3$ .....	94
Figure 51. HMBC spectrum of 1-(2'-hydroxy-3',4',5',6'-tetramethylphenyl)-1-methoxy-3-phenylpropane ( <b>13</b> ) in $\text{CDCl}_3$ .....	94
Figure 52. NOESY spectrum of 1-(2'-hydroxy-3',4',5',6'-tetramethylphenyl)-1-methoxy-3 -phenylpropane ( <b>13</b> ) in $\text{CDCl}_3$ .....	95
Figure 53. HR FAB MS spectrum of 1-(2'-hydroxy-3',4',5',6'-tetramethylphenyl)-1-methoxy-3-phenyl -propane ( <b>13</b> ) in $\text{CDCl}_3$ .....	95
Figure 54. Important HMBC and NOESY correaltions in 1-(2'-hydroxy-3',4',5',6'-tetramethylphenyl)-1- -methoxy-3-phenylpropane ( <b>13</b> ).....	97
Figure 55. Structure of compound <b>13</b> ; 1-(2'-hydroxy-3',4',5',6'-tetramethylphenyl)-1-methoxy-3-phenyl	

-propane (new compound).....	98
Figure 56. <sup>1</sup> H-NMR spectrum of linderone (14) in CDCl <sub>3</sub> .....	100
Figure 57. <sup>13</sup> C-NMR and DEPT135 spectra of linderone (14) in CDCl <sub>3</sub> .....	100
Figure 58. Structure of compound 14; Linderone.....	101
Figure 59. Expectative tautomers of linderone (14).....	101
Figure 60. Cell viability on B16F10 cells treated with the solvent fractions.....	111
Figure 61. Cell viability on B16F10 cells treated with the isolated compounds.....	112
Figure 62. Melanin contents inhibitory activity of the solvent fractions on B16F10 cells.....	114
Figure 63. Melanin contents inhibitory activity of the isolated compounds on B16F10 cells.....	115
Figure 64. Morphology of control and 1-(2'-hydroxy-3',4',5',6'-tetramethylphenyl)-1-methoxy-3-phenylpropane (new compound) (13) treated B16F10 cells.....	116
Figure 65. Cell viability rate and inhibition effect of the solvent fractions on cell-extracted tyrosinase activity.....	118
Figure 66. Cell viability rate and inhibition effect of the isolated compounds on cell-extracted tyrosinase activity.....	119
Figure 67. Inhibition effects of active three compounds on the tyrosinase and TRP-1, TRP-2 mRNA expression on B16F10 cells.....	120
Figure 68. Inhibition effect of the isolated compounds on yeast α-glucosidase inhibitory assay.....	121
Figure 69. Cell viability of the solvent fractions on mouse 3T3-L1 preadipocytes.....	124
Figure 70. Cell viability of the isolated compounds on mouse 3T3-L1 preadipocytes.....	125
Figure 71. The reduction effects of the solvent fractions on lipid accumulation during differentiation of 3T3-L1 preadipocytes.....	128
Figure 72. The reduction effects of the isolated compounds on lipid accumulation during differentiation of 3T3-L1 preadipocytes.....	129

### III. RESEARCH 2 : *Cornus macrophylla* Wall

Figure 73. <sup>1</sup> H-NMR spectrum of rengyolone (1) in CD <sub>3</sub> OD.....	138
Figure 74. <sup>13</sup> C-NMR spectrum of rengyolone (1) in CD <sub>3</sub> OD.....	138
Figure 75. Structure of compound 1; Rengyolone.....	139
Figure 76. <sup>1</sup> H-NMR spectrum of ethyl gallate (2) in CD <sub>3</sub> OD.....	141
Figure 77. <sup>13</sup> C-NMR spectrum of ethyl gallate (2) in CD <sub>3</sub> OD.....	141
Figure 78. Structure of compound 2; Ethyl gallate.....	142
Figure 79. <sup>1</sup> H-NMR spectrum of (+)-catechin (3) in CD <sub>3</sub> OD.....	144
Figure 80. <sup>13</sup> C-NMR spectrum of (+)-catechin (3) in CD <sub>3</sub> OD.....	144
Figure 81. Structure of compound 3; (+)-catechin.....	145

Figure 82. <sup>1</sup> H-NMR spectrum of ursolic acid (4) in DMSO- <i>d</i> <sub>6</sub> .....	147
Figure 83. <sup>13</sup> C-NMR spectrum of ursolic acid (4) in DMSO- <i>d</i> <sub>6</sub> .....	147
Figure 84. Structure of compound 4; 3β-hydroxy-urs-12-en-28-oic acid (ursolic acid).....	148
Figure 85. Structure of compound 5; Quercetin-3- <i>O</i> - <i>α</i> -L-rhamnoside (quercitrin).....	149
Figure 86. <sup>1</sup> H-NMR and <sup>13</sup> C-NMR spectra of quercetin-3- <i>O</i> - <i>α</i> -L-rhamnoside (5) in CD <sub>3</sub> OD.....	149
Figure 87. Structure of compound 6; Kaempferol-3- <i>O</i> - <i>α</i> -L-rhamnoside (afzelin).....	150
Figure 88. <sup>1</sup> H-NMR and <sup>13</sup> C-NMR spectra of kaempferol-3- <i>O</i> - <i>α</i> -L-rhamnoside (6) in CD <sub>3</sub> OD.....	150

### III. RESEARCH 3 : *Aster subulatus* Michx

Figure 89. Structure of compound 1; stigmasterol.....	159
Figure 90. <sup>1</sup> H-NMR spectrum of stigmasterol (1) in CDCl <sub>3</sub> .....	159
Figure 91. <sup>13</sup> C-NMR and DEPT135 spectra of stigmasterol (1) in CDCl <sub>3</sub> .....	159
Figure 92. Structure of compound 2; Ethyl caffeate.....	160
Figure 93. <sup>1</sup> H-NMR spectrum of ethyl caffeate (2) in CD <sub>3</sub> OD.....	161
Figure 94. <sup>13</sup> C-NMR and DEPT135 spectra of ethyl caffeate (2) in CD <sub>3</sub> OD.....	161
Figure 95. <sup>1</sup> H-NMR spectrum of caffeic acid (3) in CD <sub>3</sub> OD.....	163
Figure 96. <sup>13</sup> C-NMR spectrum of caffeic acid (3) in CD <sub>3</sub> OD.....	163
Figure 97. Structure of compound 3; Caffeic acid.....	164
Figure 98. <sup>1</sup> H-NMR spectrum of 1-[(Butanoyl)phlorogluciny]-β-D-glucopyranoside (4) in CD <sub>3</sub> OD.....	166
Figure 99. <sup>13</sup> C-NMR and DEPT135 spectra of 1-[(Butanoyl)phlorogluciny]-β-D-glucopyranoside (4) in CD <sub>3</sub> OD.....	166
Figure 100. HMQC spectrum of 1-[(Butanoyl)phlorogluciny]-β-D-glucopyranoside (4) in CD <sub>3</sub> OD.....	167
Figure 101. HMBC spectrum of 1-[(Butanoyl)phlorogluciny]-β-D-glucopyranoside (4) in CD <sub>3</sub> OD.....	167
Figure 102. NOESY spectrum of 1-[(Butanoyl)phlorogluciny]-β-D-glucopyranoside (4) in CD <sub>3</sub> OD.....	168
Figure 103. HR FAB MS spectrum of 1-[(Butanoyl)phlorogluciny]-β-D-glucopyranoside (4) in CD <sub>3</sub> OD.....	168
Figure 104. The structure of compound change according to the substitution.....	170
Figure 105. Structure of compound 4; 1-[(Butanoyl)phlorogluciny]-β-D-glucopyranoside (new compound).....	171
Figure 106. <sup>1</sup> H-NMR spectrum of 3,5-di- <i>O</i> -caffeoylquinic acid (5) in CD <sub>3</sub> OD.....	173
Figure 107. <sup>13</sup> C-NMR and DEPT135 spectra of 3,5-di- <i>O</i> -caffeoylquinic acid (5) in CD <sub>3</sub> OD.....	173
Figure 108. Structure of compound 5; 3,5-di- <i>O</i> -caffeoylquinic acid (3,5-DCQA).....	174
Figure 109. <sup>1</sup> H-NMR spectrum of 3,5-di- <i>O</i> -caffeoyl <i>epi</i> -quinic acid (6) in CD <sub>3</sub> OD.....	176
Figure 110. <sup>13</sup> C-NMR spectrum of 3,5-di- <i>O</i> -caffeoyl <i>epi</i> -quinic acid (6) in CD <sub>3</sub> OD.....	176
Figure 111. Structure of compound 6; 3,5-di- <i>O</i> -caffeoyl <i>epi</i> -quinic acid (3,5- <i>e</i> DCQA).....	177
Figure 112. Comparison on each olefinic structure of carbonyl group of quinic acid at 1-position.....	

between 3,5-DCQA (5) and 3,5- <i>e</i> DCQA (6).....	177
Figure 113. <sup>1</sup> H-NMR spectrum of kaempferol-3- <i>O</i> -β-D-glucoside (7) in CD <sub>3</sub> OD.....	179
Figure 114. <sup>13</sup> C-NMR spectrum of kaempferol-3- <i>O</i> -β-D-glucoside (7) in CD <sub>3</sub> OD.....	179
Figure 115. Structure of compound 7; kaempferol-3- <i>O</i> -β-D-glucoside (Astragalin).....	180
Figure 116. Cell viability on B16F10 cells treated with the solvent fractions.....	185
Figure 117. Cell viability on B16F10 cells treated with the isolated compounds.....	186
Figure 118. Melanin contents inhibitory activity of the solvent fractions on B16F10 cells.....	188
Figure 119. Melanin contents inhibitory activity of the isolated compounds on B16F10 cells.....	189
Figure 120. Inhibition effect of the isolated compounds on yeast <i>α</i> -glucosidase inhibitory assay.....	192
Figure 121. Cell viability of the solvent fractions on mouse 3T3-L1 preadipocytes.....	193
Figure 122. The reduction effects of the isolated compounds on lipid accumulation during differentiation of 3T3-L1 preadipocytes.....	194

### III. RESEARCH 4 : *Ishige sinicola* (Setchell et Gardner) Chihara

Figure 123. <sup>1</sup> H-NMR spectrum of linoleic acid (1) in CDCl <sub>3</sub> .....	204
Figure 124. <sup>13</sup> C-NMR spectrum of linoleic acid (1) in CDCl <sub>3</sub> .....	204
Figure 125. Structure of compound 1; 9Z,12Z-octadecadienoic acid (linoleic acid; Telfairic acid).....	205
Figure 126. <sup>1</sup> H-NMR spectrum of 1-linoleoyl glycerol (2) in CD <sub>3</sub> OD.....	207
Figure 127. <sup>13</sup> C-NMR and DEPT135 spectra of 1-linoleoyl glycerol (2) in CD <sub>3</sub> OD.....	207
Figure 128. Structure of compound 2; 1-linoleoyl glycerol (1-LG).....	208
Figure 129. <sup>1</sup> H-NMR spectrum of pyromeconic acid (3) in CDCl <sub>3</sub> .....	210
Figure 130. <sup>13</sup> C-NMR and DEPT135 spectra of pyromeconic acid (3) in CDCl <sub>3</sub> .....	210
Figure 131. Structure of compound 3; 3-hydroxy-4 <i>H</i> -pyrone (pyromeconic acid).....	211
Figure 132. <sup>1</sup> H-NMR spectrum of <i>di</i> -phlorethohydroxycarmalol (4) in CD <sub>3</sub> OD.....	213
Figure 133. <sup>13</sup> C-NMR and DEPT135 spectra of <i>di</i> -phlorethohydroxycarmalol.....	213
Figure 134. Basic units to structure of phlorotannin from brown alga.....	214
Figure 135. Structure of compound 4; <i>di</i> -phlorethohydroxycarmalol (DPHC).....	215
Figure 136. <sup>1</sup> H-NMR spectrum of 1,2-dilinoleoyl glycerol-3- <i>O</i> -D-glucoside (5) in CD <sub>3</sub> OD.....	217
Figure 137. <sup>13</sup> C-NMR and DEPT135 spectra of 1,2-dilinoleoyl glycerol-3- <i>O</i> -D-glucoside (5) in CD <sub>3</sub> OD.....	217
Figure 138. Structure of compound 5; 1,2-dilinoleoyl glycerol-3- <i>O</i> -D-glucoside.....	218
Figure 139. Cell viability on B16F10 cells treated with the solvent fractions.....	220
Figure 140. Cell viability on B16F10 cells treated with the isolated compounds.....	221
Figure 141. Melanin contents inhibitory activity of the solvent fractions on B16F10 cells.....	222
Figure 142. Melanin contents inhibitory activity of the isolated compounds on B16F10 cells.....	223
Figure 143. Inhibition effect of the solvent fractions on yeast <i>α</i> -glucosidase inhibitory assay.....	226

Figure 144. Cell viability of the solvent fractions on mouse 3T3-L1 preadipocytes	229
Figure 145. Cell viability of the isolated compounds on mouse 3T3-L1 preadipocytes	230
Figure 146. The reduction effects of the solvent fractions on lipid accumulation during differentiation of 3T3-L1 preadipocytes	232
Figure 147. The reduction effects of the isolated compounds on lipid accumulation during differentiation of 3T3-L1 preadipocytes	233

### III. RESEARCH 5 : *Dictyota coriacea* (Holmes) Hwang, Kim, et Lee

Figure 148. <sup>1</sup> H-NMR spectrum of D-mannitol (1) in D <sub>2</sub> O with CD <sub>3</sub> OD	242
Figure 149. <sup>13</sup> C-NMR spectrum of D-mannitol (1) in D <sub>2</sub> O with CD <sub>3</sub> OD	242
Figure 150. Structure of compound 1; D(-)mannitol	243
Figure 151. <sup>1</sup> H-NMR spectrum of 1,9-dihydroxycrenulide (2) in CD <sub>3</sub> OD	245
Figure 152. <sup>13</sup> C-NMR spectrum of 1,9-dihydroxycrenulide (2) in CD <sub>3</sub> OD	245
Figure 153. Structure of compound 2; 1,9-dihydroxycrenulide	246
Figure 154. <sup>1</sup> H-NMR spectrum of loliolide (3) in CD <sub>3</sub> OD	248
Figure 155. <sup>13</sup> C-NMR spectrum of loliolide (3) in CD <sub>3</sub> OD	248
Figure 156. Structure of compound 3; Loliolide (calendin)	249
Figure 157. Cell viability on B16F10 cells treated with the solvent fractions	255
Figure 158. Cell viability on B16F10 cells treated with the isolated compounds	256
Figure 159. Melanin contents inhibitory activity of the solvent fractions on B16F10 cells	258
Figure 160. Melanin contents inhibitory activity of the isolated compounds on B16F10 cells	259

### III. RESEARCH 6 : *Styrax obassia* Siebold & Zucc

Figure 161. Prep-HPLC isolation of compound 1 and 2 of SB-V isolated from <i>n</i> -BuOH fraction	266
Figure 162. <sup>1</sup> H-NMR spectrum of Jegosaponin A (1) in CD <sub>3</sub> OD	270
Figure 163. <sup>13</sup> C-NMR and DEPT135 spectra of Jegosaponin A (1) in CD <sub>3</sub> OD	270
Figure 164. Structure of compound 1; Jegosaponin A	272
Figure 165. <sup>1</sup> H-NMR spectrum of Jegosaponin B (2) in CD <sub>3</sub> OD	275
Figure 166. <sup>13</sup> C-NMR spectrum of Jegosaponin B (2) in CD <sub>3</sub> OD	275
Figure 167. Structure of compound 2; Jegosaponin B	277
Figure 168. Cell viability in B16F10 cells treated with the solvent fractions	281
Figure 169. Melanin contents inhibitory activity of the solvent fractions on B16F10 cells	283
Figure 170. Inhibition effect of the solvent fractions on yeast <i>α</i> -glucosidase inhibitory assay	286
Figure 171. Cell viability and cytotoxicity of the solvent fractions on mouse 3T3-L1 preadipocytes	288
Figure 172. Cell viability and cytotoxicity of the isolated compounds on mouse 3T3-L1 preadipocytes	289

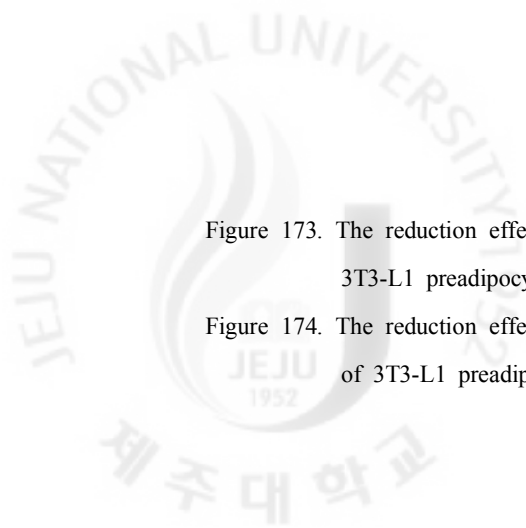


Figure 173. The reduction effects of the solvent fractions on lipid accumulation during differentiation of 3T3-L1 preadipocyte..... 291

Figure 174. The reduction effects of the isolated compounds on lipid accumulation during differentiation of 3T3-L1 preadipocytes..... 292



## LIST OF ABBREVIATIONS

### 1. Plant Name

- *L. erythrocarpa* : *Lindera erythrocarpa* Makino
- *C. macrophylla* : *Cornus macrophylla* Wall
- *A. subulatus* : *Aster subulatus* Michx
- *I. sinicola* : *Ishige sinicola* (Setchell et Gardner) Chihara
- *D. Coriacea* : *Dictyota coriacea* (Holmes) Hwang, Kim, et Lee
- *S. obassia* : *Styrax obassia* Siebold & Zucc

### 2. Experiment Term

- Ext. : extraction, extract
- RP : reverse-phase
- NP : normal-phase
- Fr. : fraction
- *aq.* : aqueous solution
- RC<sub>50</sub> : reduction concentration of 50 percent
- SC<sub>50</sub> : scavenging concentration of 50 percent
- IC<sub>50</sub> : inhibition concentration of 50 percent
- TLC : thin layer chromatography
- CC : column chromatography

### 3. Solvent and Reagent

- MeOH : methanol
- EtOH : ethanol
- *n*-Hex (*n*-Hx) : *n*-hexane
- CH<sub>2</sub>Cl<sub>2</sub> (MC) : methylene chloride
- CHCl<sub>3</sub> : chloroform



- Me<sub>2</sub>CO : acetone
- Et<sub>2</sub>O : diethyl ether
- EtOAc (EA) : ethyl acetate
- *n*-BuOH (*n*-Bu) : *n*-butanol
- H<sub>2</sub>O : water
- CD<sub>3</sub>OD : methanol-*d*<sub>4</sub> (NMR solvent that changed hydrogen to deuterium)
- DPPH : 1,1-diphenyl-2-picryl hydrazyl
- Vit-C : vitamin C
- Arb. : arbutin
- PMSF : phenylmethylsulfonyl fluoride
- MTT : 3-(4,5-dimethyl-2-thiazolyl)-2,5-diphenyl-2H-tetrazolium bromide)
- ACN : acetonitrile
- DMSO : dimethyl sulfoxide

#### 4. Analysis

- UV/VIS : ultraviolet/visible
- NMR : nuclear magnetic resonance
- HR FAB MS : High Resolution Fast Atom Bombardment Mass Spectroscopy
- HPLC-PDA : High Performance Liquid Chromatography-Photo Diode Array Detector
- UPLC-PDA-MS/MS : Ultra Performance Liquid Chromatography-Photo Diode Array Detector-Electrospray Ionization Mass Spectrometry
- ECL : Enhanced chemiluminescence

#### 5. Terms used in Structure Analysis

##### 5-1. NMR

- DEPT : distortionless enhancement by polarization transfer
- COSY : correlation spectroscopy
- HMQC : heteronuclear multiple quantum correlation

- HMBC : heteronuclear multiple bond correlation
- NOESY : nuclear overhauser effect spectroscopy
- 1D : one dimension
- 2D : two dimension
- *J* : coupling constant (Hz)
- *s* : singlet
- *d* : doublet
- *dd* : doublet of doublets
- *ddd* : doublet of doublet of doublets
- *dt* : doublet of triplets
- *t* : triplet
- *dt* : doublet of triplet
- *m* : multiple
- ppm : chemical shift
- int. : integration

## 5-2. HPLC

- LOD : limit of detectin
- LOQ : limit of quantification
- S/N : signal to noise ratio


## 5-3. Etc.

- O.R. : optical rotation
- M.P. : melting point
- M.W. : molecular weight

## 6. Terms used in bio-assay

### 6-1. Anti-oxidant

- DPPH : 1,1-diphenyl-2-picrylhydrazyl

- 
- BHA : butylated hydroxyanisole
  - EDTA : ethylenediaminetetraacetic acid
  - NBT : nitroblue tetrazolium
  - XO : xanthine oxidase

#### 6-2. Anti-inflammatory

- LPS : Lipopolysaccharide
- MTT : 3-(4,5-dimethyl-2-thiazolyl)-2,5-diphenyl-2H-tetrazolium bromide
- DMEM : Dulbecco's Modified Eagle's Medium
- FBS : fetal bovine serum
- PBS : phosphate buffered saline
- NO : nitric oxide

#### 6-3. Anti-melanogenesis

- $\alpha$ -MSH :  $\alpha$ -Melanocyte Stimulating Hormone
- L-DOPA : L-3,4-dihydroxyphenylalanine
- MTT : 3-(4,5-dimethylthiazol-2-yl)-2,5-diphenyltetrazolium bromide
- TRP-1 : Tyrosinase Related Protein-1
- TRP-2 : Tyrosinase Related Protein-2
- PVDF : polyvinylidene fluoride
- SDS-PAGE : SDS-polyacrylamide gel

#### 6-4. Anti-obesity

- PNPG : *p*-nitrophenyl- $\alpha$ -D-glucopyranoside
- LDH : Lactate dehydrogenase



## ABSTRACT (English)

**Title** : Chemical Constituents and Cosmetics-Related Activities  
from Plants in Jeju Island

Ryeo Kyeong Ko

Natural Products Chemistry Major

Doctoral Course in the Graduate School

Jeju National University

In this study, investigation into bioactive substances with *Lindera erythrocarpa* Makino, *Cornus macrophylla* Wall, *Aster subulatus* Michx, *Ishige sinicola* (Setchell et Gardner) Chihara, *Dictyota coriacea* (Holmes) Hwang, Kim, et Lee, and *Styrax obassia* Siebold & Zucc was conducted to develop functional cosmetic materials using Jeju native plants. The dried samples were extracted with 70% *aq.* ethanol and the crude extracts were subjected to solvent fractions according to polarity. Chromatography was carried out for the fractions which showed high biological activities (antioxidant, anti-inflammatory, melanogenesis inhibition, and anti-obesity). Through this process, 37 phytochemicals including 35 known compounds and two new compounds were isolated and identified. Chemical structures of the isolated compounds were identified with analytical data from spectrometers such as HR FAB MS and NMR.

From the extract of *Lindera erythrocarpa* Makino, 14 phytochemicals including one new compound were isolated. The isolated lucidone, methyllinderone,

methyllucidone, 1-(2'-hydroxy-3',4',5',6'-tetramethylphenyl)-1-methoxy-3-phenylpropane (new compound), kanakugiol, and linderone showed high melanogenesis inhibition activity compared with arbutin, the control group, in B16F10 melanoma cell. At the concentration where the activity was appeared, shows activity, the compounds exhibited no cytotoxicity. Furthermore, TRP-1 and tyrosinase *mRNA* expression were inhibited dose dependently in the suppression experiment of *mRNA* expression in melanin synthesis.

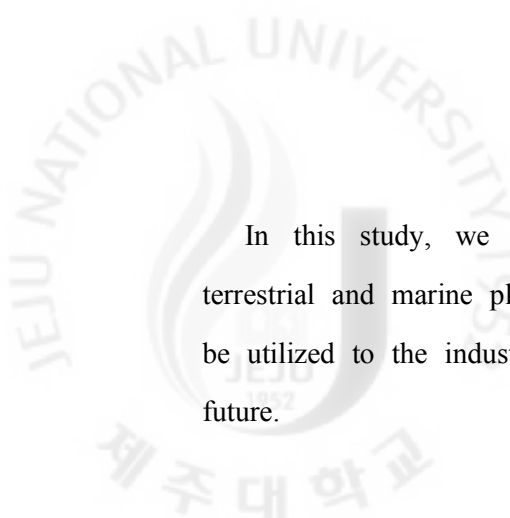
Six phytochemicals were isolated from *Cornus macrophylla* Wall and their structures were identified in the same manner as above mentioned. Among the isolates, ethyl gallate and (+)-catechin had significant free radical scavenging effect.

Seven phytochemicals including one new compound were isolated from *Aster subulatus* Michx. Among the isolates, ethyl caffeate and caffeic acid showed potent melanogenesis inhibition activity without influencing cell toxicities.

*Ishige sinicola* (Setchell et Gardner) Chihara, Ishigeaceae in Phaeophyta of seaweeds, inhabit in the coast of Jeju. Five phytochemicals were isolated from *Ishige sinicola* Chihara ethanol extract. Among the isolates, linoleic acid inhibited melanin synthesis strongly at the lower concentration compared to arbutin. Furthermore, isolated *di*-phlorethohydroxycarmalol showed high enzyme inhibition activity compared to acarbose, the control group of  $\alpha$ -glucosidase inhibition activity experiment for anti-obesity.

Three phytochemicals were isolated from ethanol extract of *Dictyota coriacea* (Holmes) Hwang, Kim, et Lee. Activity screening was conducted using the isolated compounds to investigate melanogenesis inhibition activity and antioxidant effect. As a result, 1,9-dihydroxycrenulide and loliolide showed strong melanogenesis inhibition activity compared to arbutin.

Two Jegasaponins were isolated from ethanol extract of *Styrax obassia* Siebold & Zucc. For the study of anti-obesity screening, they inhibited on reducing lipid accumulation in 3T3-L1 preadipocytes and formation of cellular lipid contents. The compounds did not exhibit cell toxicities by MTT and LDH assay.

The logo of Jeju National University is a circular emblem. It features a stylized flame or flower-like shape in the center, with the year '1952' below it. The text 'JEJU NATIONAL UNIVERSITY' is written in an arc at the top, and '제주대학교' is written in Korean at the bottom.

In this study, we have shown that the natural products isolated from Jeju terrestrial and marine plants possessed various biological activities. These results could be utilized to the industrial applications such as functional cosmetic additives in the future.

**Keywords :** *Lindera erythrocarpa* Makino, *Cornus macrophylla* Wall, *Aster subulatus* Michx, *Ishige sinicola* (Setchell et Gardner) Chihara, *Dictyota coriacea* (Holmes) Hwang, Kim, et Lee, *Styrax obassia* Siebold & Zucc, cosmeceutical ingredient, antioxidant, anti-inflammatory, melanogenesis inhibition, anti-obesity, Jeju island

## 초록 (국문)

제목 : 제주 식물로부터 화장품 관련 유효성분 규명 및  
활성 연구

제주대학교 일반대학원 박사과정  
천연물화학 전공  
고려 경

본 연구에서는 제주 자생식물을 이용한 기능성 화장품 소재 개발을 목표로 비목나무 (*Lindera erythrocarpa* Makino), 곰의말채나무 (*Cornus macrophylla* Wall), 비짜루국화 (*Aster subulatus* Michx), 넓패 (*Ishige sinicola* (Setchell et Gardner) Chihara), 참가죽그물바탕말 (*Dictyota coriacea* (Holmes) Hwang, Kim, et Lee), 쪽동백나무 (*Styrax obassia* Siebold & Zucc)를 이용한 생리활성성분 규명에 관한 연구를 하였다. 본 연구에 사용된 건조 시료는 70% 에탄올 수용액을 통해 추출되었고, 얻어진 추출물은 극성별로 용매 분획되었다. 각각의 분획층은 활성 검색 (항산화, 항염, 멜라닌합성억제, 항비만)에서 높은 활성을 보이는 분획층을 선택하여 크로마토그래피를 수행 하였다. 이 과정을 통해 35종의 기지 화합물과 2종의 신규 화합물을 분리·동정 하였다. 분리 물질의 화학구조 동정은 고분해능 질량분석기(HR-FAB MS)와 핵자기공명분광기(NMR) 등 분광기기를 통하여 얻어진 데이터를 분석하여 이루어졌다.

비목나무를 이용한 연구 결과, 신규 화합물 1종을 포함한 14종의 성분을 추출물로부터 분리하였다. 분리된 루시돈 (luidone), 메틸린더론 (methyllinderone), 메틸루시돈 (methyllucidone), 1-(2'-hydroxy-3',4',5',6'-tetra-methylphenyl)-1-methoxy-3

-phenylpropane (신규 화합물), 카나쿠지올 (kanakugiol), 린더론 (linderone) 화합물이 흑색종 세포(B16F10)에서 대조군으로 사용된 알부틴과 비교 하였을 때 높은 멜라닌 합성 저해 효과를 나타내었다. 활성을 나타내는 농도에서 화합물이 세포 독성에 영향을 나타내지 않음이 확인되었다. 또한, 멜라닌 합성 mRNA 발현 억제 실험에서 TRP-1과 티로시나아제 효소 mRNA 발현 역시 농도 의존적으로 억제하는 것을 확인하였다.

곰의말채나무로부터 6종의 성분을 분리하여 동정하였다. 분리된 화합물 중 에틸갈레이트 (ethyl gallate)와 카테킨 (catechin)이 대조군인 BHA와 비교 하였을 때, 자유 라디칼 소거 활성이 뛰어난 것을 확인하였다.

비짜루국화로 부터 1종의 신규 화합물과 6종의 기지 물질을 분리 하였다. 분리된 화합물 중 에틸카페에이트 (ethyl caffeate)와 카페인산 (caffeic acid)이 멜라닌 합성 저해 실험에서 알부틴과 비교 하였을 때 강하게 멜라닌 합성 저해 효과를 나타내었으며, 활성을 나타내는 농도에서 화합물이 세포 독성에 영향을 나타내지 않음을 확인하였다.

갈조류 패과의 해조식물인 넓패 에탄올 추출물로부터 5종의 성분을 분리 하였고, 분리된 화합물 중 리놀레인산 (linoleic acid)은 적은 농도에서도 강하게 멜라닌 합성 저해 효과를 나타내는 것을 확인 하였다. 그리고 분리된 디플로레토하이드록시카마롤 (di-phlorethohydroxycarmalol)이 항비만 실험 중 알파글루코시아다아제 활성 억제 실험에서 대조군으로 사용된 아카보스 (acarbose)와 비교 하였을 때 높은 효소 활성 저해 효과를 나타냄을 확인하였다.

해양 녹조식물인 참가죽그물바탕말의 에탄올 추출물로부터 3종의 성분을 분리 하였다. 분리된 화합물 중 1,9-디하이드록시크레누라이드(1,9-dihydroxy-crenulide)와 롤리오라이드 (loliolide)가 강하게 멜라닌 합성 저해 효과를 나타내는 것을 확인 하였다.

쪽동백나무 에탄올 추출물로부터 2종의 제고사포닌을 분리하였고, 이들은 항비만 효과 실험에서 지방세포분화 (3T3-L1)를 강하게 억제시켜 지방분화를 강하게 억제 시켰으며, 활성을 나타내는 농도에서 화합물이 세포에 독성을 나타내지 않음이 확인되었다.



기능성 화장품 소재개발이 가능한 제주 자생식물로부터 유효 활성 성분을 분리하였고, 관련 분석 장비를 통해 얻은 자료를 토대로 성분의 구조를 동정하였다. 6종의 육·해상 식물로부터 분리된 성분과 생리 활성 연구 결과는 기능성 화장품 소재를 개발하는데 중요한 자료로 활용 될 것이다. 본 연구결과를 통해 총 10건의 국내외 특허를 출원 하였고, SCI급 논문 4편, SCIE급 논문 3편을 등재하였다. 앞으로 본 연구결과를 토대로 심도 깊은 천연물 화학 연구를 계속 진행한다면 더욱 다양한 결과물을 도출할 수 있을 것이라 사료된다.

**주요단어** : 비목나무, 곰의말채나무, 비짜루국화, 넓죽, 참가죽그물바탕말, 쪽동백나무, 기능성화장품 소재, 항산화, 항염, 멜라닌합성저해, 항비만, 제주



# I . INTRODUCTION

## 1. Natural product and cosmetics

### 1-1. Need for cosmeceuticals from nature

With the development of modern medicine, average life span increased. And with aging society, desire for the duration of healthy and beautiful years increased, and demand for products that can meet this is also increasing. Along with these social changes, with the improvement of income by economic growth and the increased women's social activities, cosmetics industry rapidly increased so that it forms a large domestic market with the size of about 10 trillion won. Currently, it is an industry that forms a large market following that of medicines and grows by 10 ~ 15% annually. In Korea, as 'Cosmetic Act' was enforced (July 2007) and 'Guideline for Efficacy Evaluation of Functional Cosmetics' was established (September 2001), the concept of disease prevention using beauty products was introduced. Therefore not only as effective as medicines but also safe functional cosmetics such as whitening, anti-wrinkle, UV-Block, anti-inflammatory, and anti-obesity etc. are required. Also according to a report of the British 'Director Club,' women absorb about 2 kg of chemical substances for a year while they make themselves up everyday. Many people make themselves look beautiful using more than 20 kinds of beauty products daily. The synthetic stuff contained in cosmetics cause dermatitis, stimulates aging and have a danger of side effects like the onset of cancer. It is not accurately understood what reactions would take place in human bodies if all chemical substances used for skin have been mixed up. Thus, with the increased danger and damage of synthetic stuff in cosmetics, as the issue of safety of the ingredients of cosmetics are on the rise. In

response to such demands from consumers, cosmetics industry based on natural substances will be positioned to a cutting-edge industry in the future.<sup>1-9)</sup>

Table 1. The classification system of the natural product cosmetics

Large classification	Intermediate
Functional cosmetic	Whitening agents
	Wrinkle care agents
The pimple, anti-inflammation and skin improvement-related cosmetics	Ultraviolet or UV protecting agents
	Anti-acne agents
	Anti-inflammatory agents
	Skin care agents
The skin hydration, exfoliating and the others	Humectants or moisturizing agents
	Corneocyte desquamating agents
	Others natural cosmetic

## 1-2. Botanical extract and cosmetic uses

Natural extracts, whether from animal, botanical or mineral origin, have been used as "active ingredients" of cosmetics for as long as human history can go. Oils, butter, honey, beeswax, lead and lemon juice were common ingredients of the beauty recipes from ancient Egypt. People in Japan have long cared their skin with rice bran oil (米糠) or sponge gourd water while those in China have already used herbs as cosmetics as written in ‘外台秘要’, ‘千金翼方’, and ‘千金美容方’. Many botanical extracts are used today in traditional medicine and large pharmaceutical companies are rediscovering them. The major differences between the drug and the cosmetic approach rely on the intent as well as how the extract is considered. In the cosmetic

industry, the botanical extract is the active ingredient. It may contain hundreds of chemical structures and it has a proven activity. In the drug industry, you need to know the chemical structure of the active ingredient within the extract. Total extracts are most common in the cosmetics industry, but they are used in drugs. They are generally known from traditional usage, which has a long history. Their activity is often empirical and their active ingredients are not always identified, but their benefits are very often without possible doubt. Their mode of preparation can be found in traditional pharmacopeas (China, India, Africa, Europe, and America). Very often, plants are blended in order to better control or synergize their effects, but sometimes also to preserve the secret of the active ingredient.<sup>10)</sup>

Table 2. The typical natural raw material item in the Korea Standard of Cosmetic Ingredients (the manor)

Guar gum	Chrysanthemum extract	Mink oil
Oyster extract	The strawberry extract	The denaturation edible starch
Grape seed oil	Rosemarinus officinalis extract	The Bipidus extract
The grapefruit extract	Locust bean gum	The yarn flower oil
Green tea extract	Macadamia nut oil	The cortex mori radiceis extract
The chicken comb extract	The matricaria extract	Sage extract
Carrot extract	Cottonseed oil	Luffa extract
Swertia herb extract	Mineral oil	Squalene
Camellia oil	Wax	The vegetability squalene
Sweet flag extract	Wheat starch	The silk dust
The Cnidium Rhizome extract	The perm freedom	Brown algae extract
Gardeniae fructus extract	The hypericum extract	Potato starch
Karaya gums	The henna extract	Glycyrrhiza extract
Carene Dura extract	The horsetail extract	Extract from sophora flavescenes
Coconut oil	Jojoba oil	Capsicum tincture
Kaolin dust	Mixed plant extract	Honey
Soybean oil	The flowerpot extract	Evening primrose oil
The parsley extract	Yellow soil	The sesame oil
Rice starch Artemisia extract	The yeast extract	Ginseng extract
Almond oil	The egg oil	Peony extract
Avocado oil	Corn starch	Oil-soluble licorice extract
The aibi extract	Olive oil	Adlay extract
Acacia	The milk protein extract	The aloe extraction powder
The aloe vera gel	Curcuma longa extract	Aloe extract

### 1-3. Characteristics of the phytochemical component used for the cosmetics

The purposes of the mix of natural substances are divided broadly into manufacture and functional efficacy. Manufacture includes a variety of vegetable oil and sugars while various materials are used as active components. Raw materials of cosmetics are usually 20 to 30 kinds of materials depending on the products such as toner and lotion, etc., and cosmetics of which the main raw materials are medicinal herbs or natural herbs do not have smooth supply of raw materials, so they have the greatest weak points of difficult mass production and high price. Recently as the research and development and commercialization of natural cosmetics get active, technological development that overcomes such issues takes place.<sup>1-9)</sup>

Table 3. Comparison between advantage and disadvantage of the natural product cosmetics

<b>Advantage</b>	<b>disadvantage</b>
<ul style="list-style-type: none"><li>· The side effect is small</li><li>· The effect is mild and it is continued</li><li>· The refractory components or reverse components with the assistant ingredient</li><li>· The effect is brought with the effect of being contrary the effective component and assistant ingredient</li><li>· Good image from nature origin</li><li>· Be High biodegradable and eco-friendly</li></ul>	<ul style="list-style-type: none"><li>· The content of the effective component is not fixed</li><li>· Effective component or pharmacological activity is not clarified</li><li>· It is made and the hour hangs long.</li><li>· Being imitation or fake products.</li><li>· The storage is difficult</li><li>· It is not suitable for the mass production</li></ul>

Among the natural substances used for cosmetics, there are a lot of herb medicines that exhibit efficacy on living bodies, and its key substance is the mixture of various chemical substances. The herb medicinal components apply for the purpose of protecting skin or hair and nourishing hair as well as decoration for beauty, typically a

variety of vegetable oil that protect and shine skin, *Trichosanthes kirilowii* powder, sponges, aloe, *pleuropterus multiflorus* and safflower used as pigment. Since usually herb medicines are natural substances and collected only once a year, wild products as well as cultivated ones are also used. Also, as the climate or soil environment of the habitat differs, there are differences of quality by the producing area or harvest time, and also there are much differences in quality by the various processing methods carried out for the purpose of preservation, improvement of quality, removal or increase of a particular ingredient, so there is a difficulty in treatment of the selection of the standards of extracts to be used as cosmetics with a constant quality. Natural substances used for cosmetics are often mixed with extracts containing various substances as well as refined ones. The main ingredients are fat and oil, fatty acids, sugars, amino acids, proteins and organic acids while helping ingredients are active components that can show efficacy including vitamins. This is the typical natural substance items listed on the standard of raw materials for cosmetics (Tab. 4).<sup>1-9)</sup>

Table 4. Using cosmetic ingredients from nature

Using Part	Item
Oil and fatty acid	Olive oil, camellia oil, sesame oil, canola oil, cottonseed oil, palm oil, soybean oil, nature wax, lecithin from the yolk of an egg
Sugars	aloe vera, seaplant extract, trehalose, hyaluronic from fermentation using microbial, chitin chitosan, pectin, carrageenan, locust bean gum
Amino acid	glutamine acid, aspartic acid, glycine, D,L-allanine, N-methyl- $\beta$ -allanine, N-methyltaurine, threonine, sarcosine, lysine, arhinine, PCA, tri-methyl glycine
Organic acid	$\alpha$ -hydroxy acid (lactic acid), citric acid (fruits)
Vitamins	vitamin C, acerola, rosehip oil, $\beta$ -carotene (provitaminA; nature pigment), vitamin E, biotin (vitamin H; yolk egg, liver)
Shikimic acid type	flavonoid, tannin, phenylpropanoid, coumaric acid (fragrance)
Mevalonic acid type	monoterpenoid (fragrance), diterpene, triterpene (surfactant)
Quinoid	shikonin, Arbutin, Kojic acid
Alkaloid	morphine, atropine, ephedrine, berberine (antiinflammatory, antibacterial and effect of absorb UV ray)
Vegetable wax	carnauba wax, rice wax, candelilla wax, jojoba wax
Vegetability pigment	carotinoid, anthocyanin, anthraquinone, flavonoid, porphyrin, deketone, $\beta$ -cyanin



## 2. Trend of development of functional cosmetics ingredients

### 2-1. The natural product and functional cosmetic

As the development of functional cosmetics for whitening and anti-aging using natural substances became active, extracts from plants kingdom have been proven to be attractive as ingredients of cosmetics. With the recent nature-oriented and environment-friendly market trend, natural substances originating from plants or animals are mixed and used in cosmetic formulations. Especially, on the wind of naturalism, the development of cosmetics using terrestrial and marine raw materials are carried out, and the golden age of functional cosmetics using natural materials is coming. Functional cosmetics broadly for whitening, wrinkle care, the improvement of skin, the depression of acne, the moisture of skin, atopic dermatitis and hair restorer are the targets of development. Various materials with active components for this purpose are mixed and used. The greatest problem of skin aging are ultraviolet rays and impacts of sunlight. Measures against blackening by ultraviolet rays, oxidative impairment by radical caused by infection or UV, the degeneration of the skin elastic fibers and DNA disorder, etc. are required. For this, the beneficial action, Tea (茶), extracted gold solution, and  $\gamma$ -Oryzanol that is the ultraviolet ray absorbing effect, comfrey, peony root, licorice root extract that have anti-inflammation effect, gold, ginseng extract that is the light ray suppression effect also attract attention. Also recently with the increase of the demand for treatment of atopic diseases, comfrey, peony, moutan, salvia and the basewood with anti-allergic effect come into the spotlight. To maintain elastic skin, collagen-related raw materials and chlorella, and placenta extract with the activation effect of fibroblast can be used. For moisturizing effect, hyaluronic acid, derivatives of chitin, a polysaccharide or fat and oil are used. For whitening, tyrosinase inhibition effects and assessment by melanoma cell culture are carried out for which arbutin, kojic acid, morus bark and the root of an arrowroot are used.<sup>1-9)</sup>

## 2-2. The overseas technology trend

In developed countries, with the outbreak of mad cow disease, most animal-derived cosmetics materials are getting rapidly replaced by plant-derived materials. As plant-derived cosmetics materials, water soluble ingredients containing olive oil, palm oil and saponin, wheat oil, rice oil, amino acids, peptide, sugars, the surface active component including the phospholipid, and etc. are being used as moisturizer, encapsulant and skin protectant. Materials possessing the activities of the MMP-1 (Matrix Metalloproteinase-1) and elastase inhibition, the synthesis of hyaluronic acid, free radical scavenging, keratinocyte proliferation, fibroblast proliferation and melanogenesis inhibition are being studied as the raw materials for moisturizing, anti-aging and whitening cosmetics. The development of edible cosmetics is also active. Japanese companies such as *Kanebo* or *Shiseido* release brands named 'beauty food.' The new concept eating cosmetics mainly consisting of vegetables, fruits and tea expect the indigestion of anti-oxidant or other activities in the body. In addition to plants, recently, studies on discovering physiologically active substances from the ocean are actively carried out. Currently, the bio active substances from the ocean exceeded 7,000 species, and product development using spa, deep ocean water and caviar are carried out. Thalasso-therapy products are gaining fame already in other countries and a variety of cosmetic on thalasso-therapy based on marine plants, ocean water and sea mud are being released.<sup>1-9)</sup>

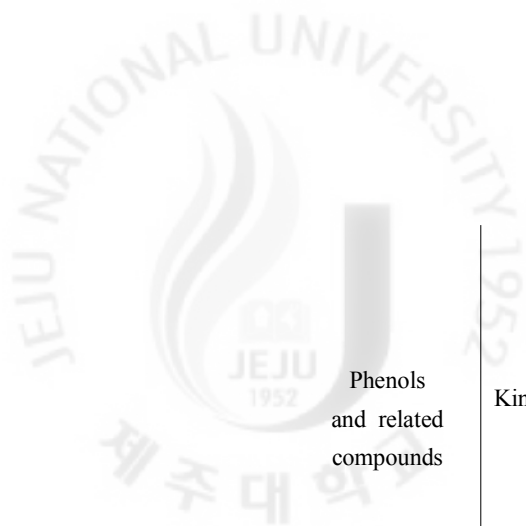
## 2-3. The domestic technology trend

At the end of the 2000s, the size of the market of functional cosmetics for whitening, wrinkle care, sun screens is estimated at 312.5 billion won. The market size of each of the three domains is estimated 100 billion won in whitening, 60 billion in anti-wrinkle, and 58 billion in sun block. The search for new whitening products using natural plants is the field on which domestic businesses especially

focus. Products having whitening effects and anti-aging function together is expected. The history for using herb medicines with efficacy for beauty is as long as human life. But the first direct use of them for cosmetics in Korea was that Amore Pacific released 'Ginseng Sammi' with Ginseng as the main raw material in 1973. Later, it used actively for the development of cosmetics by extracting active components from various plant resources such as wild ginseng, red ginseng, licorice, mung-bean, black-bean, maple leaf, bamboo, paper mulberry, yew (朱木), mandarin tree, acanthopanax, palm tree, ginger, mushroom, green tea, burdock, mulberry tree, and constant material developments take place. The development of cosmetics materials and products applying domestic natural plants focuses its R&D on skin engineering concepts excluding chemical raw materials as possible. It is based on oriental medicines, which stimulate the functionalities of the organs of human body and the cycle of vitality and blood. Recently, not only cosmetics businesses but also oriental medical clinics, bio-venture companies and pharmaceutical companies are active in the development of cosmetics using natural substances. Collagen, an animal raw material has been used for cosmetics and food; however, with the outbreak of mad cow disease, questions has been raised around its safety and the use of collagen extracted from land animals are prohibited worldwide. Therefore the development of alternative materials from natural marine raw materials are carried out: e.g. safely extracting and industrializing it from starfish. The future domestic cosmetics industry, emphasizing not only aesthetic functions but also efficacies will lead subsequent cosmetics industry. It will be centered around 'cosmeceutical' implying the concept of pharmacological activity; 'phytocosmetic' implying natural healing power concept using naturally sprouting plants; 'organic cosmetic' mainly using organic materials not polluted by heavy metals and chemically hazardous substances. In order to meet all of these concepts, new natural substances, new technologies are further required.<sup>1-9)</sup>

Table 5. The activity by classification<sup>11-12)</sup>

Type	Item
Lipid	<p>Kind of compounds</p> <p>fatty acid, alcohols, aldehyde, long hydrocarbon chain, other complex lipids</p> <p>Biological activities</p> <p>skin moisturizing, smoothing lubrication, antieczema, anti-inflammation, arthritis, smoothing of sunburn, healing of wounds, ulcers</p> <p>- EFAs (Essential fatty acids)</p> <p>i Ricinoleic acid (skin dryness, acne and baldness)</p> <p>ii linoleic acid (eczema, hair loss, reduced wound healing and circulatory defects)</p>
Terpenoids	<p>Kind of compounds</p> <p>monoterpenes, iridoids, sesquiterpenes, saponin, retinoids</p> <p>Biological activities</p> <p>i Iridoids (rheumatologic conditions, aucubin, allergic inflammations)</p> <p>ii Sesquiterpenes (dermatological conditions, skin revitalization; ursolic acid, skin aging)</p> <p>iii Saponin (cytotoxic, antitumor, antifungal, immunoregulatory, hypoglycemic, cardiovascular properties, antioxidant, anti-aging)</p> <p>iv Carotenoids (antioxidants, cell proliferation)</p> <p>v Retinoids (activation of tumor suppressor genes, epithelial growth, renewal of the epidermal layer, anti-bacterial, anti-inflammation, psoriasis, ichthyoses, keratodermas, melanoma, non-melanoma skin cancers)</p> <p>vi Tocopherols (erythema, wrinkling, sagging, tumor incidence, photodamage, antioxidant)</p>



Phenols  
and related  
compounds

Kind of compounds

Biosynthetic is through shikimic acid, aromatic amino acid

Biological activities

- i Curcumin (antibacterial, antiparasitic, anti-HIV, cicatrizing, antitumor, antioxidant, anti-inflammatory, eczema, psoriasis, acne, wound and burn healing, aging)
- ii Phenylpropanoid (hair loss, acne, anticancer drugs, anogenital warts)
- iii Coumarins (fragrances, skin-whitening)
- iv Anthranoids (antimicrobial, anticancer, antipsoriatic)

Flavonoids

Kind of compounds

Polyphenolic acmpounds,

Biological activities

Anticancer, antioxidant, antiproliferative, antiangiogenic, antithrombogenic, antiallergic, antiviral, antiaging, leg heaviness, cramps, pain, edema

- i Apigenin (anticancer, skin aging)
- ii Isoflavones (activity of estradiol, phytoestrogens, aging)
- iii Anthocyanosides (increasing in rhodopsin photoreception)

Alkaloids

Kind of compounds

Heterogeneous group of natural organic bases, basic nitrogen is inserted in a heterocyclic ring

Biological activities

inhibiting microtubule disassembly, cancer chemotherapy, psoriasis, treatment of skin infections



Carbohydrates	<p>i Caffeien (dihydrotestosterone on hair follicles, helpful to combat androgenic alopecia)</p> <p>Kind of compounds</p> <p>Dimers and polymeric forms of various lengths, termed polysaccharides.</p>
Glycosides	<p>Biological activities</p> <p>i Glucans (film formers, humectants, skin moisturizers)</p> <p>ii Carragenans (protect against UV, activate collagen protein moisturize , smoothe irritated skin)</p> <p>iii Gums and mucilages (antioxidant, emollient properties, oral cavity)</p> <p>Kind of compounds</p> <p>Glycosidic moieties of terpenes, flavonoids, polyketides and alkaloids</p> <p>Biological activities</p> <p>Glycosides are natural pro-drugs whose pharmaceutical usefulness is realated to their stability and solubility in the liquids of the guman body. This allows a proper release of the active aglycone to its reactive center.</p> <p>The most useful classification for biochemical and pharmacological purposes concerns the type of aglycone.</p>
Hydroxy acids	<p>Kind of compounds</p> <p>This group of <math>\alpha</math>-hydroxy acids (AHAs), as fruit acids, glycolic, citric, malic, lactic acids</p> <p>Biological activities</p> <p>A main role in skin care and dermatological therapy (cell renewal, collagen synthesis)</p>

### 3. Antioxidants

As the outermost organ of the body, the skin is frequently and directly exposed to a prooxidative environment, including ultraviolet radiation, drugs and air pollutants (tobacco, stress).<sup>13)</sup> Besides external inducers of oxidative attack, the skin has to cope with endogenous generation of reactive oxygen species (ROS) and other free radicals, which are continuously produced during physiological cellular metabolism. To counteract the harmful effects of ROS, the skin is equipped with antioxidant systems, which maintain an equilibrium between prooxidants and antioxidants. In the course of skin evolution, a variety of primary (preventive, *e.g.*, vitamin C) and secondary (interceptive, *e.g.*, vitamin E) antioxidant mechanisms have been developed, which form an "antioxidative network" of closely interlinked components (Fig. 1).

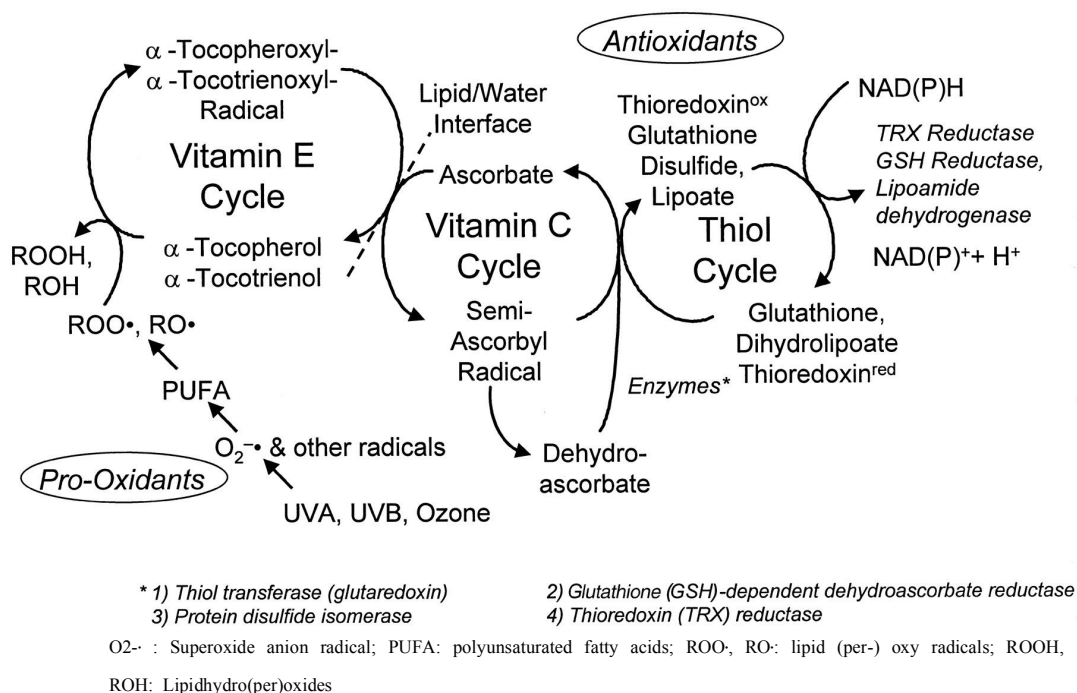


Figure 1. Activation of the antioxidant network by environmental oxidative stressors

Antioxidants intervene at different levels of oxidative processes: (1) scavenging free radicals; (2) scavenging lipid peroxy radicals; (3) binding metal ions or removing

oxidatively damaged biomolecules.<sup>14)</sup> The antioxidant defense in cutaneous tissues can be overwhelmed either by an increased exposure to exogenous (*e.g.*, UV exposure) or endogenous (*e.g.*, inflammatory disorders) sources of ROS, or by a primarily depleted antioxidant defense (*e.g.*, malnutrition) facing a normal level of prooxidative challenge. Such a disturbance of the prooxidant/antioxidant valance may result in oxidative damage of biomolecules, such as lipids, proteins and DNA and has been termed 'oxidative stress'.<sup>14-15)</sup> In skin, the induction of oxidative damage by environmental stimuli such as UVA, UVB and ozone was demonstrated to occur in lipids,<sup>17-19)</sup> proteins,<sup>20)</sup> and DNA.<sup>21-22)</sup> Currently available knowledge on the presence and physiological distribution of natural antioxidants in skin their response to oxidative environmental stressors and the photoprotective potential of topically applied antioxidants. Free radicals can be listed by one-electron reduction potentials in milli Volts (mV) at pH 7.0. The reduced form of each radical is capable of neutralizing (reducing) free radicals having a higher potential. As can be seen from the table, the hydroxyl radical ( $\cdot\text{OH}$ ) has the highest potential and is the most destructive (reactive) of biological free radicals.<sup>20)</sup>

Radical	mV	Radical	mV
$\cdot\text{OH}$ (hydroxyl)	+ 2300	$\cdot\text{HU}^-$ (urate)	+ 590
$\cdot\text{LO}$ (alkoxyl)	+ 1600	$\cdot\text{Toc}$ (tocopherol)	+ 480
$\text{LOO}\cdot$ (peroxyl)	+ 1000	$\cdot\text{Asc}^-$ (ascorbate)	+ 282
$\cdot\text{GS}$ (glutathione)	+ 920	$\text{Fe}^{3+}\text{-EDTA}$	+ 120

Figure 2. Radical reaction potentials



### 3-1. Water-soluble antioxidants

Vitamin C (ascorbate, AscH<sup>-</sup>), for example, can donate a hydrogen atom to a free radical molecule (R·) thereby neutralizing the free radical while becoming an ascorbate radical itself (·Asc<sup>-</sup>, or Asc·<sup>-</sup>, in different notation). But the ·Asc<sup>-</sup> free radical is very stable because of its resonance structure. Moreover, AscH<sup>-</sup> is readily regenerated from ·Asc<sup>-</sup> with NADH or NADPH-dependent reductases.<sup>11)</sup> Vitamin C can not only neutralize hydroxyl (·OH), alkoxyl (·OL) and peroxy (LOO·) radicals by hydrogen donation, ascorbate can also neutralize the radical form of other antioxidants, such as glutathione (·GS) and Vitamin E (tocopherol) (·Toc):

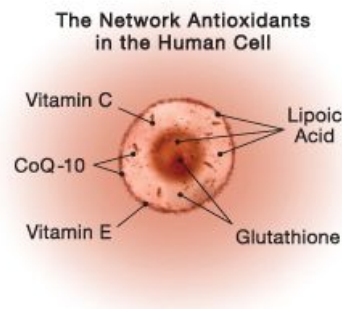
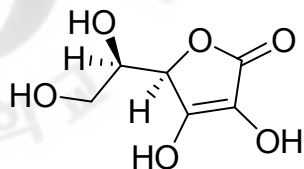
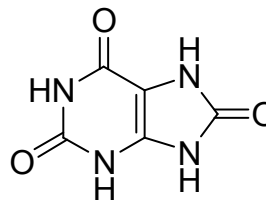


Figure 3. The network antioxidants in the human cell

1. L-ascorbic acid ( $176.1 \text{ g mol}^{-1}$ )



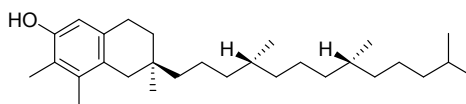
2. Uric acid ( $168.1 \text{ g mol}^{-1}$ )



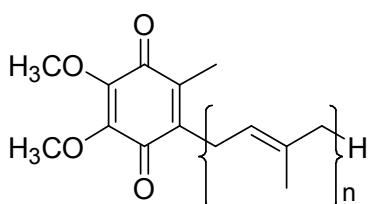
3. D-*a*-lipoic acid ( $206.3 \text{ g mol}^{-1}$ )



4. tocopherols ( $416.7 \text{ g mol}^{-1}$ )



5. ubiquinone ( $n = 9$ ,  $795.3 \text{ g mol}^{-1}$ )



6. vitamin A (all-*trans*-retinol:  $286.5 \text{ g mol}^{-1}$ )

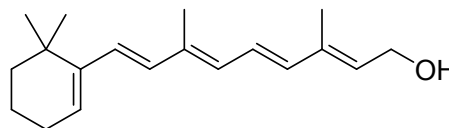


Figure 4. Chemical structures of selected antioxidants from nature

Glutathione ( $\gamma$ -glutamyl-cysteinyl-glycine; GSH), present intracellularly at millimolar concentrations, is an important water soluble antioxidant and reducing compound. Oral GSH is absorbed and is not required to be provided by dietary intake.<sup>10)</sup>

Uric acid (deprotonated form: urate) is a small water-soluble molecule (Fig. 4) that accumulates in human tissues as the endproduct of purine metabolism. In blood plasma, urate has been shown to be a powerful scavenger of singlet oxygen, peroxy-, and hydroxyl radicals.<sup>10)</sup>

### 3-2. Lipid-soluble antioxidants

Vitamin E is the major lipophilic antioxidant in plasma, membranes and tissues. The term 'vitamin E' collectively refers to the eight naturally occurring molecules (four tocopherols and four tocotrienols), which exhibit vitamin E activity. Tocotrienols differ from tocopherols in forms of tocopherols and tocotrienols differ in the number of methyl groups on the chromanol nucleus. In humans,  $\alpha$ -tocopherol is the most abundant vitamin E homologue, followed by  $\gamma$ -tocopherol. Vegetable oils rich in tocopherols and tocotrienols.  $\alpha$ -Tocopherol contributes directly to cell membrane structure by stabilizing it and allowing for proper functioning of membrane enzymes. Wheat germ oil and palm oil are particularly rich in tocopherols and  $\alpha$ -,  $\beta$ -,  $\gamma$ -tocotrienols. The terms 'coenzyme Q' as well as 'ubiquinone' are commonly used for the redox couple ubiquinol/ubiquinone (Fig. 4). Ubiquinones are lipid-soluble quinone derivatives with an isoprenoid side chain. In nature, ubiquinone homologues containing 1 to 12 isoprene units occur. Dietary vitamin A is available in the form of pro-vitamin A compounds (*e.g.*,  $\alpha$ - and  $\beta$ -carotene and cryptoxanthin) or directly from animal food (liver, milk, egg and fish). Carotenoids, such as  $\beta$ -carotene, found in plants or in part of plants exposed to the sun. Of particular interest is a unicellular microalgae, *Dunaliella*. Under normal conditions of light, temperature, or salt, these algae are green, However, under extreme conditions (high salinity, low pH, high sunlight, lack of nitrogen or phosphorus), they protect themselves by multiplying their  $\beta$ -carotene concentration by 10. The ponds become red, and the  $\beta$ -carotene concentration can reach 14% of their dry weight. SOD is an enzyme that deactivates free radicals. Its concentration decreases with age. It has been possible to obtain *Bifidus* extracts that are rich in SOD. Flavonoids, rich extracts from *Gingko*, *Fagopyrum* (buckwheat), *Eucalyptus sambucus* (European elder), or *Sophora japonica* are used for their antioxidant and

anti-free radical properties. *Rosmarinus* (rosemary) extracts, rich in carnosic acid, are very potent antioxidants, used to protect food. *Syzygium aromaticum* or *Germanium thumberhii* extracts can be used to protect collagenase activity and ECM from free radicals.<sup>10)</sup>

#### 4. Photoaging agents

The epidermis, the top most layer of skin, consist of keratinocytes. They protect from outer stress and environment. And the basal cell layer contains melanocytes, specialized cells that produce melanin to protect the skin against sun damage. Rate of melanin production determines skin color. In dermis, beneath the epidermis, fibroblasts which were respond to stimuli produce fiber proteins (Fig. 5). Among them collagen is the main component of extracellular matrix (ECM) and supports the epidermis.

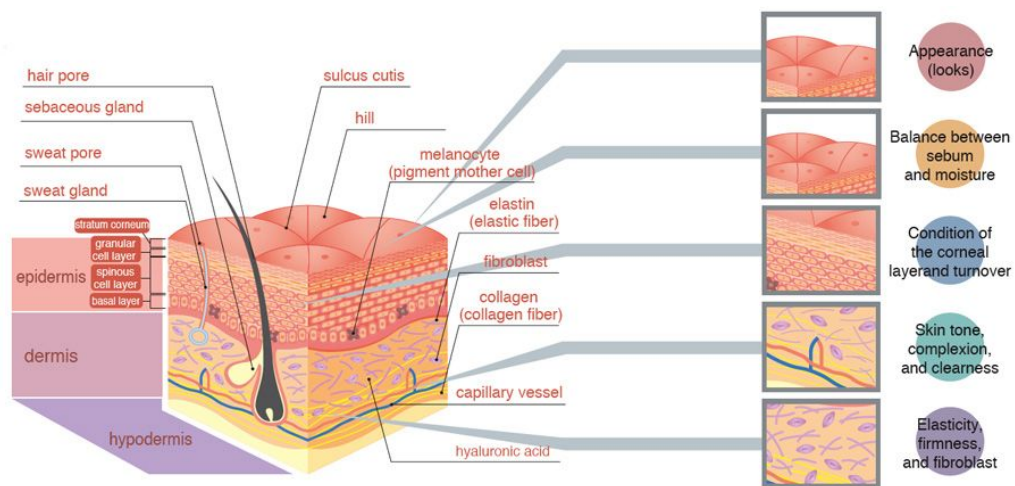


Figure 5. Layers of the skin including major function tissue

ECM maintains the durability, flexibility and elasticity. Growth factors by keratinocytes, inflammation cells and dermal fibroblasts themselves affect the fibroblasts. Fibroblasts are also stimulated by their surrounding milieu and ECM molecules. The process of skin aging in humans is complex and induced by multiple factors, including genetic and various environment. Skin aging is classified into time-dependant intrinsic aging by decrease in anti-oxidant defence mechanism and photo-aging by chronic irradiation of ultraviolet (UV) rays. Both cases induce

production of reactive oxygen species (ROS), accumulation of DNA mutation and stimulation of signal transduction pathway. Photo-aging of the skin is a complex biological process affecting various layers of the skin with the major damage seen in the connective tissue of the dermis (Fig. 6). Clinically, photo-aging is characterized by wrinkles, pigmentation, blister formation and impaired wound healing. By contrast, intrinsically aged skin is thin, smooth and is reduced elasticity. Numerous inherent defense mechanisms protect the skin against UV radiation. These include increased epidermal thickness, pigmentation, DNA repair mechanisms, apoptosis and antioxidative defences. Apoptotic mechanisms and endogenous antioxidants are thought to decline with age.<sup>10)</sup>

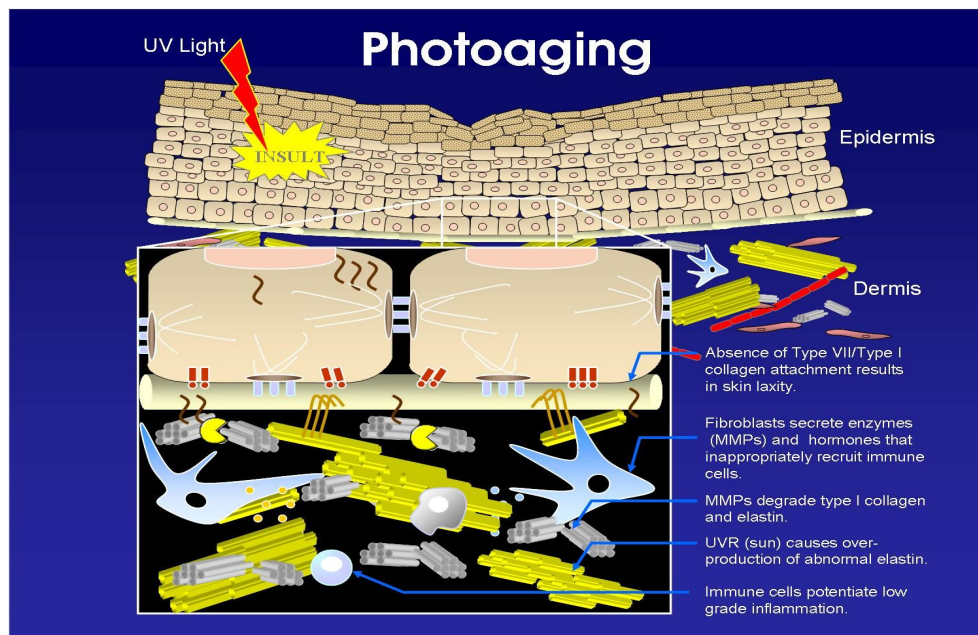


Figure 6. Mechanism of photoaging by UV-irradiation

The retinoids are a diverse class of pharmacological compounds, consisting of vitamin A (retinol) and its naturally occurring and synthetic derivatives, which possess biological vitamin A activity (Tab. 6). The major forms of retinoids that may

be of significant interest to the cosmeceutical industry are retinol, retinal and possible, retinoic acid. The main role of retinoids in cosmeceuticals are in extrinsic aging (photoaging). Currently, topical retinoid acid is FDA-approved for the treatment of acne and in the adjunct treatment of fine skin wrinkling, skin roughness and hyperpigmentation due to photoaging as well as reducing the number of senile lentigines (liver spots). At present, retinol is becoming an increasingly utilized ingredient in cosmetic preparations, such as moisturizers and hair products. Retinol is a necessary dietary nutrient, required for growth and bone development, vision, reproduction and the integrity of mucosal and epithelial surfaces (Fig. 7).<sup>10)</sup>

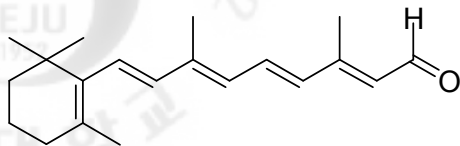
Table 6. The roles of naturally existing retinoids

<b>Retinoid</b>	<b>Role</b>
Retinol	Growth promotion
	Differentiation/maintenance of epithelia
	Reproduction
Retinal	Vision
Retinoid acid	Growth promotion
	Differentiation/maintenance of epithelia

---

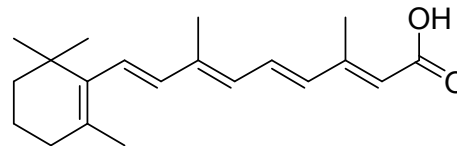
1. all-trans retinal

---



2. all-trans retinoic acid

---



3. all-trans retinol

---

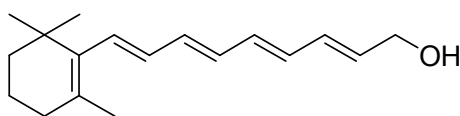


Figure 7. Structure of retinoids

Ascorbic acid is a key element in collagen synthesis. It stimulates the production of RNA coding for collagen and contributes to the synthesis of hydroxproline and hydroxylysine. Apigenin, extracted from *Chamomile* and its derivatives and rutin from *Fagopyrum* have anti-inflammatory properties (by inhibiting histamine release). Saponins, a huge family of compounds, whether of a steroidal or triterpenic structure, are known for their detergent activity. They probably have other activities, which are yet to be established. Constant research shows that saponins, present in botanical extracts, have tremendous pharmacological and metabolic properties.

- i *Ginseng* and *bupleurum*: stimulate biosynthesis of proteins, RNA, cholesterol or lipogenesis
- ii *Centella asiatica* (asiaticosides): stimulates synthesis of collagen and fibronectin
- iii *Hedera, ficaria* (hederagenin): inhibits proteases<sup>10)</sup>



## 5. Depigmentation agents

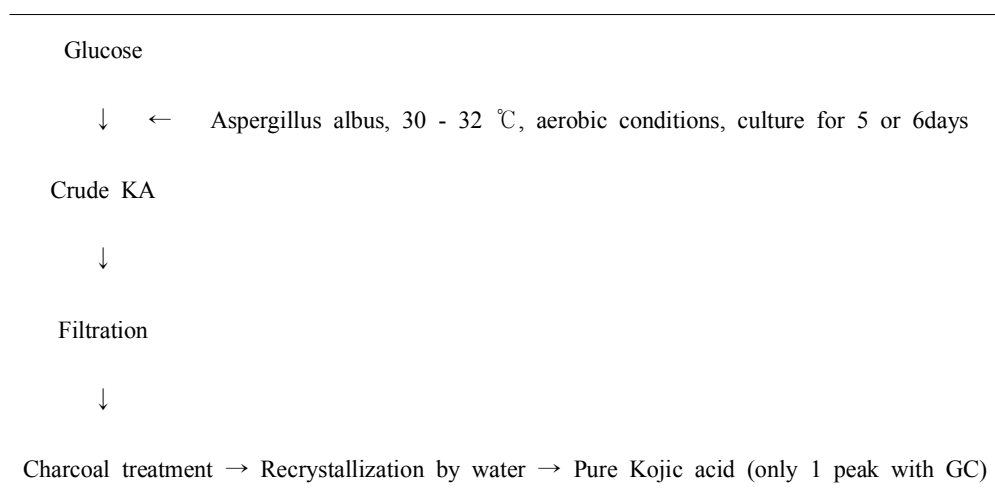
There are a variety of facial pigmentary disorders. Among such disease, malignant tumors should be diagnosed and treated properly because some of them are quick to develop, destructive, or fatal. Hyperpigmentation of the face of middle aged women, is most commons however, it is benign, and if diagnosed and treat early, it can be prevented in the future. Melasama is commonly observed among middle-aged women (average age of 43) and is rare in men. It is a diffuse or well-circumscribed noninflammatory brown hyperpigmentation that frequently occurs around the eyes, mouth, cheeks, and forehead. Subjective symptoms such as itching or irritation are lacking. Melasma is present in middle age, but is rare in women over the age of 70. The main cause of melasma is considered to be an increase in progesterone (P4) in the serum at luteal phases and other hormones, such as estradiol, follicle stimulating hormone, luteinizing hormone, prolactin, androstendione, and cortisol, showed no differences between groups during the ovarial and luteal phases. The increase in plasma progesterone may be attributed to the fact that melasma is exacebated by pregnancy where plasma progesterone is increased or by contraceptive pills that occasionally contained progesterone; there is gradual decline of melasma after climacterium by 70 years of age. Histopathology of melasma shows an increase in melanin pigments in the epidermal cells especially in the supranuclear region of the basal cells. The number of epidermal melanocytes has not increased and therefore, the hyperpigmentation of melasma is considered to be functional and reversible.<sup>10)</sup>

### 5-1. Screening test for depigmentation agent

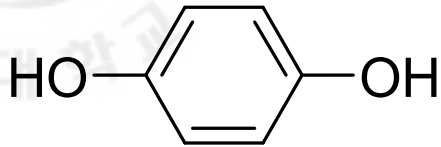
A standard method for screening depigmentation agents is the isolated tyrosinase inhibition test. Mushroom tyrosinase has been commonly used, and the suppression of tyrosinase could be demonstrated when dose-dependent inhibition was demonstrated with hydroquinone as an effective control. Another kind of tyrosinase assay is non-inhibitory or non-suppressive-type reactions of melanogenesis. By extension, cultured B-16 melanoma cells have been used in this field and are useful in demonstrating several new mechanisms of melanogenesis inhibition:

Glycosylation turned out to be another process of the production, along with maturation of melanogenesis. Its inhibition also decreased the amount of melanin, and depigmentation agents were also found. Tyrosinase activities in ribosomes and the production of premelanosomes can also be targets for melanin production inhibition. There are two melanins eumelanin (black to brown) and pheomelanin (yellow or red), and eumelanin production inhibition is usually considered with depigmentation agents.<sup>10)</sup>

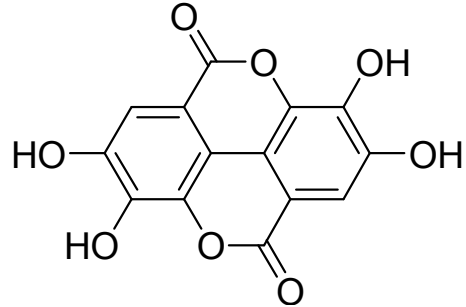
Table 7. Major main depigmentation agents (Kojic acid) production on a pilot scale



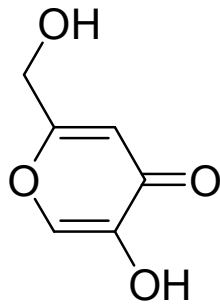
1. Hydroquinone



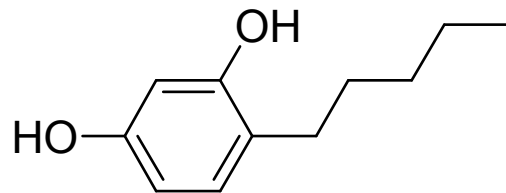
2. Ellagic acid



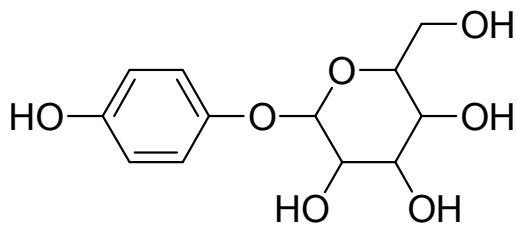
3. Kojic acid



4. Rucinol (4-n-Butylresorcino)



5. Arbutin



6. N-Ac-4-S CAP (N-2,4-acetoxyphenyl thioethyl acetamid)

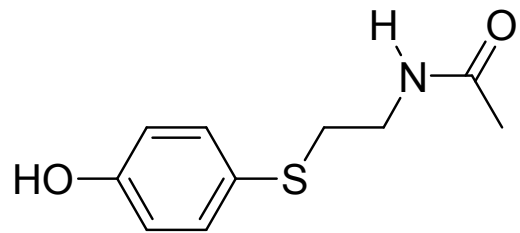


Figure 8. Chemical Structures of main depigmentation agents

Table 8. Mechanism of melanogenesis inhibition

Mechanisms	Example
1. Suppression of tyrosinase	Kojic acid
	Hydroquinone
	Ascorbic acid
	Arbutin
	Ellagic acid
2. Other mechanisms	
a. Decrease in tyrosinase synthesis	Biomein <sup>®</sup>
b. Decrease in tyrosinase transfer	Glucosamine
	Tunicamycin
c. Cytotoxicity to melanocytes	Hydroquinone monobenzylether
	APTA <sup>a</sup>

<sup>a</sup> n-2,4-Acetoxyphenyl thioethyl acetamide.

## 6. Fat storage and slimming agents

Recently using botanical extracts with very specific actions that act at various levels of adipocyte metabolism.

- *Garcinia cambodgia* decreases the transformation of sugars into fat.
- Extracts of *Guarana*, tea, coffee, cocoa, which are rich in methylxantines (caffeine, theobromin) are cAMP-phosphodiesterase inhibitors and thus accelerate lipid degradation.
- Flavonoids, like quercetin or its derivatives, are also inhibitors of this enzyme and could lead to a 40% increase in cAMP.
- Methylxantines of the same plants will act on lipoprotein lipase (LPL), reducing the passage of fatty acids into the adipocyte.
- Reducing the passage of fatty acids into the adipocyte.
- Phytosterols from plant oils are being investigated for their potential action on fat storage or degradation, on adipocyte differentiation<sup>10)</sup>

## 7. Research objectives

As mentioned above, cosmetics market would like to demand various and powerful functional ingredients safe to skin from natural substances, and consumers would also continue to prefer cosmetics applying them. Thus, in the various fields of dermatology, studies on naturally bioactive materials will continue to be carried out, which shows the necessity of the continuous development of natural substances. Jeju Island has a bio-diversity environment and is a clean nature preservation district. The Island is a volcanic island having a geological environment different from other regions centering around Mt. *Halla* in the middle and has subtropical climate, so it abundantly has diverse and peculiar natural terrestrial and marine biological resources required to develop the materials of functional cosmetics. The aim of this study is to develop materials of functional cosmetics using Jeju Island's natural substances. Therefore, research was conducted to isolate and identify active components using *Lindera erythrocarpa* Makino, *Cornus macrophylla* Wall, *Aster subulatus* Michx, *Ishige sinicola* (Setchell et Gardner) Chihara, *Dictyota coriacea* (Holmes) Hwang, Kim, et Lee, and *Styrax obassia* Siebold & Zucc with excellent activities in pre-biological *in-vitro* activity test (antioxidant, anti-inflammatory, melanogenesis inhibition, anti-obesity). to identify active materials and their new physiological activation by that, and to actively develop the materials of functional cosmetics using natural substances naturally growing in Jeju Island.



## II. REAGENT AND INSTRUMENTS

### 1. Chemical Reagent

Following chemicals and reagents were used in this research work.

#### 1-1. Column packing material

- Celite (Celite 545, Celite Korea Ltd.)
- Silica gel 60 (0.063-0.200 mm, Merck Co.)
- Silica gel 60 (0.040-0.063 mm, Merck Co.)
- Silica gel 60H (15  $\mu$ m, Merck Co.)
- Silica gel 100 (RP-18, 230-400 mesh, Merck Co.)
- YMC-gel (ODS-A, AA12S75, S75  $\mu$ m, 12 nm, 500 g)
- Sephadex LH-20 (0.1 mm-0.025 mm)
- Silica gel 60 (0.040-0.063 mm, Merck Co.)

#### 1-2. LC column

- MPLC : (Normal phase) Si 40+M2146-1, 25+M2126-2, 12+M2136-1  
(Reverse phase) C18HS 12+M1946-3 (Biotage Co.)
- HPLC : XTerra<sup>®</sup> C<sub>18</sub> 100  $\times$  4.6 mm, I.D. 3.5  $\mu$ m (Waters Co. Ltd. USA)

#### 1-3. TLC (Thin Layer Chromatography) plate

- Precoated silica gel aluminium sheet (Silicagel 60 F<sub>254</sub>, 2.0 mm, Merck Co.)
- Precoated silica gel aluminium sheet (RP-18 Silica gel F<sub>254</sub>, 2.0 mm, Merck Co.)

1-4. TLC (Thin Layer Chromatography) visualizing reagent

- $\text{KMnO}_4$  solution
- 1% Anisaldehyde-MeOH
- 2%  $\text{FeCl}_3$ -MeOH

1-5. Solvent

- Column Chromatography : General laboratory grade solvents were used in the experiments which were procured from commercial grade used.
- HPLC Analysis : Used HPLC grade solvent (Merk Co., Fisher Co.)
- NMR Analysis : Used only for NMR solvent by Merck Co. (USA)
  - $\text{CD}_3\text{OD}$ ,  $\text{D}_2\text{O}$ ,  $\text{CDCl}_3$ ,  $\text{DMSO-}d_6$ ,  $\text{Pyridine-}d_6$  and the chemical shift values were referenced relative to the corresponding residual solvent signals.

1-6. HPLC additives for analysis solvent and the preprocessing supplies

- Acetic acid : Used HPLC grade solvent (Merck Co., USA)
- Formic acid : Used HPLC grade solvent (Merck Co., USA)
- Syringe filter : Advantec Tokyo Roshi kaisha Ltd., DISMIC<sup>R</sup>-13<sub>JP</sub>, Japan

1-7. Anti-oxidant assay

- DPPH : Sigma Co., USA (D9132)
- BHA : Sigma Co., USA (B1253)
- Allopurinol : Sigma Co., USA (A8003)
- Xanthine oxidase : Sigma Co., USA (X1875)
- EDTA : Sigma Co., USA (ED)
- NBT : Sigma Co., USA (N6639)



1-8. Anti-inflammatory assay

- DMEM : Gibco Life Technol. Laboratories (Auckland, N.Z.)
- FBS : Gibco Life Technol. Laboratories (Auckland, N.Z.)
- PBS : Gibco Life Technol. Laboratories (Auckland, N.Z.)
- MTT : BIO BASIC INC.
- DMSO : AMERESCO ACS grade (0231)
- LPS : Sigma Co., USA (L7770)
- Griess reagent : Sigma Co., USA (G4410)
- 24 and 48-well plate (SPL, Pocheon, Korea)
- 24-well plate (SPL, Pocheon, Korea)

1-9. Melanogenesis inhibition assay

- B16F10 mouse melanoma cell : ATCC (American Type Culture collection)
- Theophylline : Sigma Co., USA
- Mushroom tyrosinase : Sigma Co., USA (T3824)
- L-tyrosine : Sigma Co., USA (T3754)
- Arbutin : Bio-Land Co., Korea
- PVDF membrane (BIO-RAD, HC, USA)
- Western blotting detection kit (Amersham Pharmacia Biotech., NY, USA)
- Secondary antibody (Amersham Pharmacia Biotech, Little Chalfont, UK)

1-10. Anti-obesity assay

- *a*-glucosidase : Sigma Co., USA (G5003)
- *p*-nitrophenyl-*a*-D-glucopyranoside (PNPG) : Sigma Co., USA (N1377)
- Acarbose : Sigma Co., USA (A8980)
- Oil-Red O stock solution : MUTO (4049)
- Ez-CyTox cell viability assay kit. (DAEIL LAB SERVICE Co, Korea)
- Cytotoxicity Detection kit (Roche, Swiss)
- triglyceride assay kit (Triglyzyme-V, Eiken Chemical, Tokyo, Japan)

## 2. Instrument

- Polarimeter : P-1030 (Jasco, Used solvents MeOH and H<sub>2</sub>O, *Ref.* sucrose)
- UV/VIS spectrometer : LibraS22 (Biochrom Co.)
- Determined Melting points : 12-142T (Fisher scientific Co.)
- HRFAB-MS spectral data were obtained from the Korea Basic Science Institute (Seoul)
- NMR : AVANCE III (Bruker Co., 500 MHz)
- HPLC : Alliance 2695 system with AMDS and ELSD (Waters Co. USA)
- MPLC : SP1 system with dual UV spectrometer (Biotage Co.)
- Microplate reader :  $\mu$ Quant (USA)
- Microscope : Olympus (Japan)

### III. RESEARCH 1 : *Lindera erythrocarpa* Makino

#### 1. General Plants Information

- **Scientific name** *Lindera erythrocarpa* Makino
- **Korean name** 비목나무
- **Nickname** 보안목, 백목
- **Family name** Lauracea
- **Distribution** South Korea, China, Japan
- **Flowering** April - May
- **Fruiting** September
- **Usage** Timber for furniture
- **Folk medicinal use**

alleviation of neuralgia (fruit), stomachache<sup>24)</sup>



Photo 1. The specimen of *L. erythrocarpa*

#### • **Identified constituents in the literature**

terpenes (caryophyllene, geranyl acetate,  $\alpha$ -pinene, camphene,  $\beta$ -pinene, limonene, bornyl acetate),<sup>25)</sup> cyclopentenediones (methyllucidone, linderone, methyllinderone, lucidone),<sup>26)</sup> unsaturated fatty acids,<sup>27)</sup> lignans,<sup>24)</sup> 5,6,7,8-tetramethoxyflavone-5,6,7,8-tetramethoxy-3',4'-methylenedioxyflavone, lucidin<sup>28)</sup>

#### • **Biological activities in the literature**

anti-tumor,<sup>29)</sup> anti-fungus,<sup>30)</sup> anti-inflammation,<sup>31)</sup> cytotoxicity,<sup>32)</sup> anti-cancer,<sup>33)</sup> anti-chitin synthase II<sup>34)</sup>

• **Research objective**

Standard material : 70% *aq.* EtOH extract of *L. erythrocarpa*

For ingredient of cosmeceutical (whitening, anti-wrinkle and sliming product)

1. Antioxidant activity : DPPH radical scavenging test ( $RC_{50} = 16.8 \mu\text{g/mL}$ )

2. Melanogenesis inhibition activity

: In 100  $\mu\text{g/mL}$ , the 59.8% melanin contents inhibitory activity on B16F10 cell  
(the cytotoxin none)

3. Anti-obesity activity

• In 100  $\mu\text{g/mL}$ , the 30.0% lipid accumulation reduction on 3T3-L1 preadipocytes  
(the cytotoxin none)



Photo 2. Photograph of the leaf of *L. erythrocarpa*



Photo 3. Photograph of the stem bark of *L. erythrocarpa*



Photo 4. Photograph of the fruit of *L. erythrocarpa*



## 2. Experimental Methods

### 2-1. Plant material

The whole plant of *L. erythrocarpa* was collected from Jeju Island in August 2004. A voucher specimen (06-105) is deposited at Extraction Bank of Bio-Conversion Center, Jutechnopark (JTP), Jeju, Korea.

### 2-2. Extraction and solvent fractionation

#### 2-2-1. Extraction from the leaves

The fresh leaves of *L. erythrocarpa* were washed and dried by hot blast at 40 °C for three days. The powder of the leaves (200 g) was extracted with 70% *aq.* ethanol in glass jar at room temperature under stirring for three days. The extract was filtered to remove the insoluble residue and the filtrate was concentrated to afford a gummy residue (50 g). A part of the residue (42 g) was suspended in water, and successively partitioned to give *n*-hexane (8.5 g), methylene chloride (2.5 g), ethyl acetate (4.1 g), *n*-butanol (10.2 g) and water (14.5 g) fractions (Scheme 1).

#### 2-2-2. Extraction from the stem barks

The fresh stem barks of *L. erythrocarpa* were washed in the same manner as described above. The dried material (560 g) was pulverized by a mill and extracted with 70% *aq.* ethanol at room temperature under stirring for three days. The extract was filtered to remove the insoluble residue and the filtrate was concentrated to afford a gummy residue (68.2 g). The residue was suspended in water, and successively partitioned to give *n*-hexane (5.0 g), methylene chloride (7.0 g), ethyl

acetate (12.0 g), *n*-butanol (18.4 g) and water (29.6 g) fractions (Scheme 2).

### 2-3. Isolation and purification

#### 2-3-1. Isolation produce of methylene chloride fraction from the leaves (LM)

The methylene chloride fraction (2.5 g) was fractionated by VLC (vacuum liquid column chromatography) over silica gel eluting with stepwise gradient solvents of *n*-Hex/EtOAc (0 ~ 100%) and then a total of 12 fractions were collected (LM-I ~ XII). The LM-II (80.3 mg) was applied to recrystallization and provided the compound **5** (2.3 mg). Subjection of LM-V to silica gel CC with CHCl<sub>3</sub>/MeOH (10/1) provided the compound **1** (37.2 mg). The LM-VI (244.6 mg) was applied to recrystallization and provided the compound **3** (20.8 mg) and the LM-VII was provided compound **2** (3.3 mg). Finally, Compound **4** (8.7 mg) was separated from the LM-VIII (69.7 mg) by silica gel CC using CHCl<sub>3</sub>/MeOH (10/1) as eluents (Scheme 1).

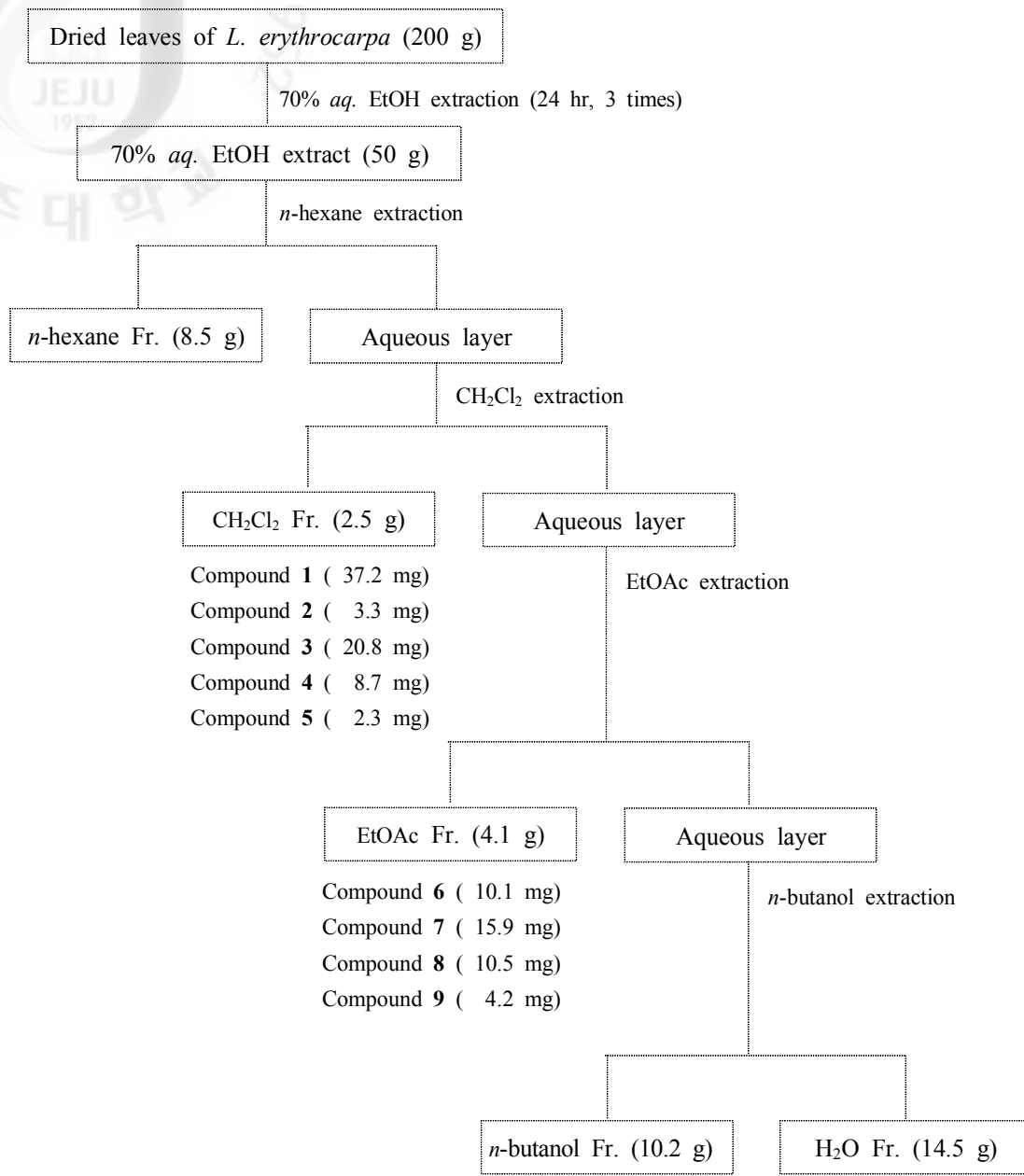
#### 2-3-2. Isolation produce of ethyl acetate fraction from the leaves (LE)

The EtOAc fraction (4.1 g) was chromatographed over celite with CH<sub>2</sub>Cl<sub>2</sub>, Et<sub>2</sub>O, EtOAc, acetone successively. The obtained Et<sub>2</sub>O fraction was chromatographed over silica gel CC with CHCl<sub>3</sub>/MeOH (9/2) to provided 5 fractions (LE-I ~ V). The LE-IV was further purified by preparative HPLC (Alliance 2695) on an ODS-18 column (Sunfire<sup>TM</sup> C<sub>18</sub> 250 × 4.6 mm, i.d. 5 μm) with mobile phase of 30% *aq.* methanol (flow rate: 1.5 mL/min; detection: 280 nm) to give compound **8** (10.5 mg) and compound **9** (4.2 mg). Finally, the LE-V (66.9 mg) was chromatographed by silica gel CC with CHCl<sub>3</sub>/MeOH (7/2) provide the compound **6** (10.1 mg) and compound **7** (15.9 mg) (Scheme 1).

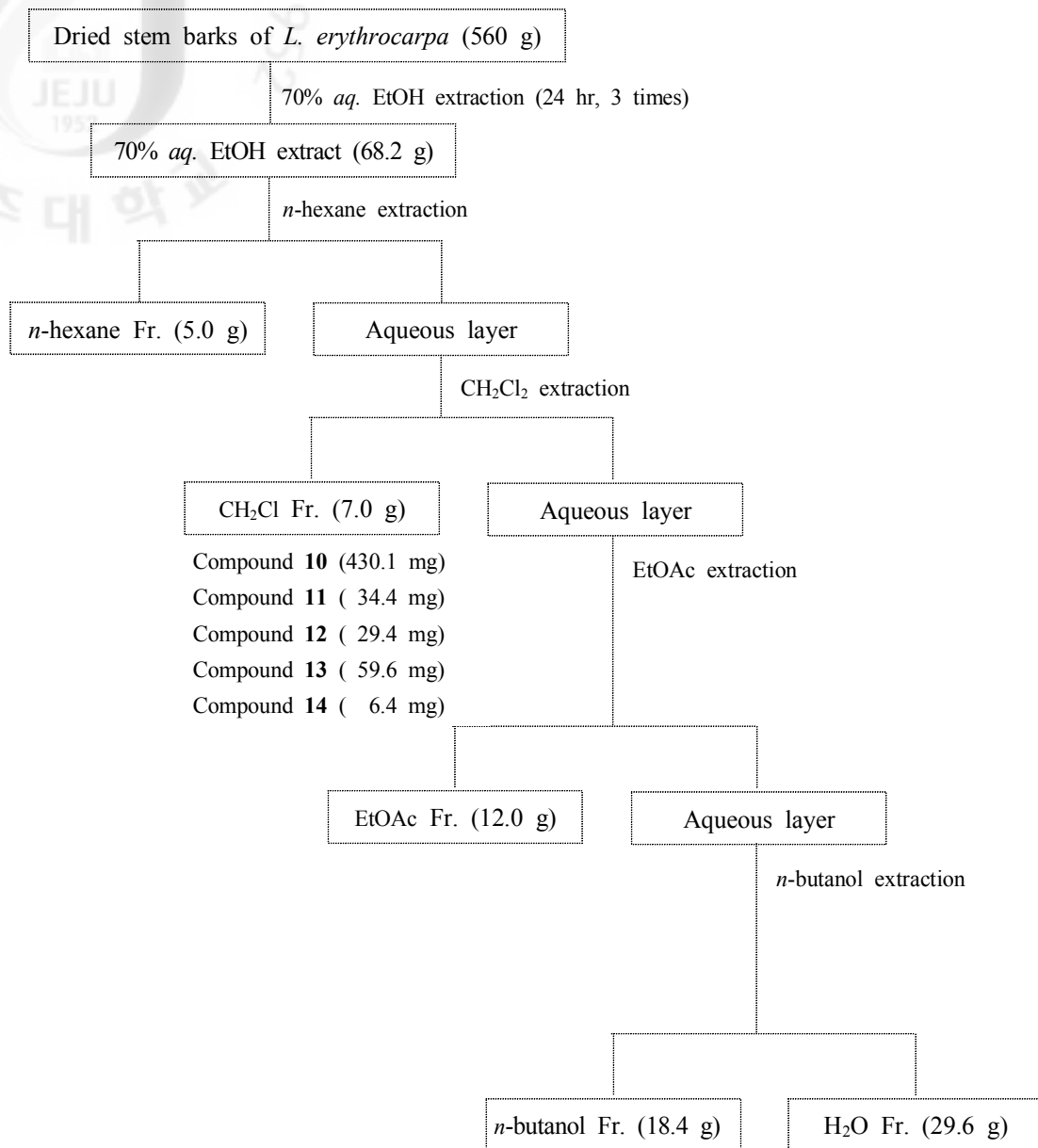
2-3-3. Isolation produce of methylene chloride fraction from the stem barks (SM)

The methylene chloride fraction (7.0 g) was subjected to further purification by silica gel with stepwise gradient solvents of *n*-Hex/EtOAc to afford eight fractions (SM-I ~ VIII). The SM-I (557.7 mg) was applied to silica gel CC with *n*-Hex/EtOAc (3/1) to give three fractions (SM-I-1 ~ 3). Subjection of SM-I-2 to silica gel CC with CHCl<sub>3</sub>/MeOH (40/1) provided the compound **10** (430.1 mg) and compound **12** (29.4 mg). The compound **13** (59.6 mg) was separated from the SM-II (975.4 mg) by silica gel CC using *n*-Hex/EtOAc (3/2) as eluents. The SM-III was partitioned with MeOH to obtain MeOH-soluble fraction (641.3 mg) and insoluble fraction (34.4 mg). This insoluble fraction from SM-III was identified to be compound **11** (34.4 mg). The MeOH-soluble fraction was further chromatographed by silica gel CC with *n*-Hex/EtOAc (1/1) to provide the compound **14** (6.4 mg) (Scheme 2).





Scheme 1. Extraction and fractionation of the leaves of *L. erythrocarpa*



Scheme 2. Extraction and fractionation of the stem barks of *L. erythrocarpa*

### 3. Qualitative and Quantitative Determination by LC Analysis

#### 3-1. HPLC analysis

##### 3-1-1. Standard solutions for quantitative analysis

All purified compounds were stored at low temperature, protected from light and humidity. The standard stock solution of the isolated compounds was prepared by dissolving accurately weighted standards in MeOH, transferring it to a 2 mL volumetric flask and then adding MeOH to make up the volume. A series of working standard solutions with gradient concentration was obtained by diluting the stock solution. All the solutions were stored in a refrigerator at -4 °C.

##### 3-1-2. Sample preparation for analysis of quantitative and qualitative

Powdered dried plant materials (200 mg) were sonicated in 10 mL of MeOH for 15 min. After centrifugation for 10 min at 3,000 rpm, the solution was decanted. MeOH was used to dilute the concentrated solution under sonication and the volume was made up to exactly 2 mL. Prior to use, all samples were filtered through 0.45 µm PTFE (polytetrafluoroethylene) syringe filter.

##### 3-1-3. Determination of HPLC-PDA and ESLD analysis

The HPLC analysis was performed using Alliance 2695 system (Waters Co., USA) with a photodiode-array detector (PDA 2998) and Electron liquid spray detector (ELSD 2420). The used ODS-18 column was XTerra<sup>®</sup> C<sub>18</sub> with 100 × 4.6 mm, I.D. 3.5 µm (Waters Co. Ltd. USA). The solvents were mixture of A (aqueous 0.5% acetic acid) and B (0.5% acetic acid in ACN). The mobile phase was filtered

through a 0.45  $\mu\text{m}$  pore size cellulose acetate and PTFE membrane filter (Sartorius) and degassed by sonicating for 10 min. The elution system was described in Table 10. The HPLC system was operated at a flow rate of 1 mL/min and the injection volume 10  $\mu\text{L}$  with a column temperature at 35  $^{\circ}\text{C}$ . The analysis was monitored at 254.0, 280.0, 320.0 and 363.9 nm by PDA. And ELSD condition was performed according as Table 9. The content of pure compounds in extraction of each plant was determined from the corresponding calibration curves. Each standards were injected for the HPLC analysis and peaks were assigned by comparing their retention times (Rt.) and absorption of UV spectrum with those of each reference compound.

Table 9. Instrument condition for HPLC-ELSD

Item	ELSD (W2420)
Gas Pressure (psi)	50.0
Gas type	Nitrogen ( $\text{N}_2$ )
Gain	50
Time Constant (sec)	1.0
Nebulizer Heater (%)	80
Drift tube temperature ( $^{\circ}\text{C}$ )	70.0

Table 10. Gradient elution condition for HPLC-PDA/ELSD separation

Time (min)	Flow (mL/min)	(%) A	(%)B	Curve
	1.0	95.0	5.0	6
5.00	1.0	95.0	5.0	6
7.00	1.0	90.0	10.0	6
9.00	1.0	80.0	20.0	6
15.00	1.0	80.0	20.0	6
18.00	1.0	70.0	30.0	6
24.00	1.0	70.0	30.0	6
27.00	1.0	50.0	50.0	6
33.00	1.0	50.0	50.0	6
35.00	1.0	10.0	90.0	6
40.00	1.0	10.0	90.0	6
42.00	1.0	95.0	5.0	6
45.00	1.0	95.0	5.0	6

#### 3-1-4. Calibration

Calibration curves were plotted as the peak area ratio vs the amount of each analyte. The linearity was evaluated by linear regression analysis calculated by the least squares regression method. The LOD and LOQ were determined on the basis of response at a S/N of 3 or 10, respectively.

## 4. Biological Activity Test


### 4-1. Antioxidant assay

#### 4-1-1. Preparation of sample

The powder *n*-Hex and CH<sub>2</sub>Cl<sub>2</sub> layer extraction were eluted sequentially with 100% EtOH and *n*-BuOH and water solvent fractions were eluted with 100% EtOH and 1 × PBS (pH 7.4) (1:1, v/v). The sample solution was filtered through a syringe filter.

#### 4-1-2. DPPH radical scavenging activity assay

The free radical scavenging activity assay was evaluated by DPPH radical scavenging activity assay. The hydrogen atom content or electron donation ability of the corresponding extracts as well as some pure compounds were measured based on bleaching of the purple-colored DPPH methanol solution. Determined electron donating ability was determined according to the method described in 'Blois' method with some modifications.<sup>35)</sup> The samples were dissolved in MeOH and diluted at various concentrations (0 ~ 1000 mg/mL). 100 μL Diluted compounds and 100 μL 0.4 mM DPPH solution in ethanol were transferred to a 96-well plate. Then, the plates were incubated at room temperature for 10 min in dark place. Absorbance was measured at 517 nm by using microplate reader. The same mixture, Except for the samples were used as a control. And diluted samples except for DPPH solution were used a sample blank. Total reaction mixture was 200 μL and contained DMSO less than 0.1% (v/v) BHA was used for a positive control. Each treatment was replicated thrice. The percent scavenging of DPPH was calculated as follows.


$$(\%) \text{ Scavenging activity} = [1 - (Abs_s - Abs_b) / Abs_c] \times 100$$

$Abs_s$  = The absorbance of the experimental sample

$Abs_c$  = The absorbance of the control

$Abs_b$  = The absorbance of using solvent

The concentration of samples at which 50% of the scavenging activity was inhibited ( $SC_{50}$  value) was obtained by linear curve fitting.

#### 4-1-3. Superoxide radical scavenging activity assay

Superoxide radical scavenging activity was assayed using the NBT reduction method.<sup>36)</sup> The assay mixture consisted of 200 mM phosphate buffer (pH 7.5), 0.5 mM xanthine, 0.5 mM NBT and 1 mM EDTA in the presence or absence of the samples. The reaction was initiated by the addition of 50 mU/mL xanthine oxidase. The increase in absorbance at 550 nm was read using a microplate reader. Allopurinol was used for a positive control and each treatment was replicated thrice. The superoxide radical scavenging activity was expressed by the decrease in the NBT reduction of the test group compared to that of the control group and calculated using the following equation:

$$(\%) \text{ Scavenging activity} = [1 - (Abs_c - Abs_s) / Abs_c] \times 100$$

$Abs_s$  = The absorbance of the experimental sample

$Abs_c$  = The absorbance of the control

The  $SC_{50}$  values were defined as the concentration be able to scavenge 50% of the radicals produced, and calculated using average value from thrice experiments.

#### 4-1-4. Xantine oxidase inhibition activity assay

The effect of the lyophilized infusion on the xanthine oxidase activity was evaluated by measuring the formation of uric acid from xanthine, using a spectrophotometer at room temperature. The reaction mixtures contained the same proportion of components as in the enzymatic assay for the superoxide radical scavenging activity, except for the NBT, in a final volume of 500  $\mu$ L. The absorbance was measured at 290 nm for 5 min. The IC<sub>50</sub> values were calculated from five test concentrations using the following equation:

$$(\%) \text{ Inhibition activity} = [(Abs_{\text{control}} - Abs_{\text{blank}}) - (Abs_{\text{sample}} - Abs_{\text{blank of sample}})] / (Abs_{\text{con}} - Abs_{\text{blank}}) \times 100$$

$Abs_{\text{sample}}$  = The absorbance of the sample with enzyme

$Abs_{\text{control}}$  = The absorbance of enzyme without sample

$Abs_{\text{blank}}$  = The absorbance of using solvent

$Abs_{\text{blank of sample}}$  = The absorbance of sample without enzyme



## 4-2. Anti-inflammatory assay

### 4-2-1. Cell culture

The mouse macrophage RAW264.7 was purchased from Korean Cell Line Bank (KCLB) and cultured in DMEM supplemented with 10% (v/v) heat-activated FBS, streptomycin (100  $\mu\text{g}/\text{mL}$ ) and penicillin (100 U/mL) at 37  $^{\circ}\text{C}$  atmosphere and 5%  $\text{CO}_2$ .<sup>37-40)</sup>

### 4-2-2. Cell viability by MTT

MTT assay was performed to estimate cellular viability. RAW264.7 cells were seeded onto a 48-well plate at a density of  $2.0 \times 10^5$  cell/mL. After 24 hr incubation, the cells were treated with various concentrations of samples. At the end of incubation time, the cells were incubated in a PBS containing 0.2 mg/mL MTT for 2 hr at 37  $^{\circ}\text{C}$ . Then, removed supernatant and the attached purple formazan crystal products were dissolved in DMSO. Absorbance was measured at 570 nm by using microplate reader.<sup>37-40)</sup>

### 4-2-3. Measurement of NO production

After pre-incubation of RAW264.7 cells ( $2.0 \times 10^5$  cell/mL) on 48 well-plate for 18 hr, the various concentrations (0 ~ 100  $\mu\text{g}/\text{mL}$ ) of sample with LPS (1  $\mu\text{g}/\text{mL}$ ) were incubated for 24 hr. Nitrite in culture supernatant was measured by adding 100  $\mu\text{L}$  of Griess reagent (1% (W/V) sulfanilamide and 0.1% N-[1-naphthyl]-ethylene -diamine dihydrochloride in 2.5% (V/V) phosphoric acid) to 100  $\mu\text{L}$  samples of medium. To quantify nitrite concentration, standard nitrite solutions were prepared and absorbance of the mixture was determined with a microplate at 540 nm. All measurements were performed in triplicate. The

concentration of  $\text{NO}_2^-$  was calculated by comparison with a standard curve prepared using  $\text{NaNO}_2$ .<sup>41)</sup>

### 4-3. Melanogenesis inhibition activity assay

#### 4-3-1. Cell culture

The B16F10 melanoma cells (mouse melanoma cells) were obtained from the ATCC and cultured in DMEM supplemented with 10% (v/v) heat-activated FBS, 1% Antibiotic-Antimycotic in 5% CO<sub>2</sub> humidified atmosphere incubator at 37 °C.<sup>42-44)</sup>

#### 4-3-2. Cell viability assay by MTT

The cell viability assay activity on B16F10 was measured as described previously with some modifications.<sup>42-44)</sup> B16F10 melanoma cells were seeded in a 24-well plate at a density of  $2 \times 10^4$  cell/well. After 24 hr incubation under 5% CO<sub>2</sub> humidified atmosphere incubator at 37 °C. The cells were treated with various concentrations (12.5, 25, 50 and 100 µg/mL) of sample for 72 hr. Then, medium were removed and replaced by adding 200 µL MTT solution (2 mg/mL). Absorbance was measured at 570 nm by using microplate reader.

#### 4-3-3. Measurement of melanin contents

The mealnogenesis inhibitory activity was measured as described previously with some modifications.<sup>42-44)</sup> B16F10 melanoma cells were seeded in a 24-well plate at a density  $2 \times 10^4$  cell/well and were allowed to attach for 24 hr at 5% CO<sub>2</sub> humidified atmosphere incubator at 37 °C. Then the cells were incubated in a fresh medium containing various concentrations (12.5, 25, 50 and 100 µg/mL) of samples adding  $\alpha$ -MSH for 3 days. And then, the remaining medium were removed, the plate was washed with PBS on 2 times. Cells were harvested by trypsinization. The harvested cells were centrifuged, and then solubilized by 100 µL of 1 N NaOH in 56 °C for 30 min .to dissolve melanins. The relative quantity of intracellular melanin

contents was estimated by the absorbance at 405 nm using microplate reader. The results are expressed as fold of stimulation compared to the control conditions. Arbutin was used for positive control.

#### 4-3-4. Measurement of cell-extracted tyrosinase from cell inhibition activity

The cells were divided up in a 24-well plate ( $2 \times 10^4$  cells/well), and the cells were grown at 37 °C, 5% CO<sub>2</sub> in the incubator for 24 h. After the cells were washed with PBS, lysis buffer (0.1 M sodium phosphate buffer, 0.2 mM PMSF, 1% Triton X-100) was put into the culture dish and the cells were dissolved, and transferred to an e-tube and fixed in ice. They were agitated after 60 min for 2 ~ 3 seconds, then centrifuged and each protein was obtained which was mixed with reaction solution (12.5 mM L-Dopa, 1.5 mM L-tyrosine, 67 mM sodium phosphate buffer (pH 6.8)). Then the mixture was left for 1 hr at 37 °C. After than, the absorbance of reaction solution was measured at 405 nm using an microplate reader.<sup>42-48)</sup>

#### 4-3-5. mRNA preparation and polymerase chain reaction (PCR)

Total RNA was isolated from B16F10 cells using the TRIzol reagent (Invitrogen, USA) according to the manufacturer's instructions. Reverse transcription and PCR amplification were performed using an Access RT-PCR system as recommended by the manufacturer. The primer sequence, designed according to literature,<sup>42-48)</sup> were as follows: Tyrosinase, 5'-GGC CAG CTT TCA GGC AGA GGT-3' (forward), 5'-TGG TG TTC ATG GGC AAA ATC-3' (reverse); TRP-1, 5'-GCT GCAGGA GCC TTC TTT CTC-3' (forward), 5'-AAG ACG CTG CAC TGC TGG TCT-3' (reverse); TRP-2, 5'-GGA TGA CCG TGA GCA ATG GCC-3' (forward), 5'-CGG TTG TGA CCA ATG GGT GGC-3' (reverse); and  $\beta$ -actin, 5'-TGG AAT CCT GTG GCA TCC ATG AAA C-3' (forward), 5'-TAA AAC GCA GCTCAG TAACAG TCC G-3'

(reverse). PCR was performed for 20 ~ 25 cycles of 94 °C for 30 sec, 50 ~ 55 °C for 45 sec and 72 °C for 45 sec in a DNA thermal cycler (Perkin-Elmer Co., USA). PCR products were analyzed on 1.2% agarose gels and visualized using ethidium bromide staining. Band intensity was calculated using a gel imaging system.

#### 4-4. Anti-obesity assay

##### 4-4-1. Measurement of yeast $\alpha$ -glucosidase inhibitory activity

The yeast  $\alpha$ -glucosidase inhibitory activity was measured as described previously with some modifications.<sup>51-53)</sup> The yeast  $\alpha$ -glucosidase was prepared with 50 mM sodiumphosphate buffer (pH 6.8) and PNPG was diluted as same enzyme dilution solution. Sample and  $\alpha$ -glucosidase of 0.2 U/mL was mixed. And then, The test mixture was incubated for 10 min at 37 °C and the absorption due to the formation of PNP was measured at 405 nm. The same mixture, except for the plant extract was used as the control and acarbose was used as positive control. Each treatment was replicated twice. The percent inhibition of  $\alpha$ -glucosidase activity was calculated as follows:

$$(\%) \text{ Inhibition} = 1 - [(Abs_{\text{sample}} - Abs_{\text{blank}}) / Abs_{\text{control}}] \times 100$$

$Abs_{\text{sample}}$  = The absorbance of the experimental sample

$Abs_{\text{control}}$  = The absorbance of the control

$Abs_{\text{blank}}$  = The absorbance of using solvent

The concentration of a samples at which 50% of the enzyme activity was inhibited ( $IC_{50}$  value) was obtained by linear curve fitting.

##### 4-4-2. Cell culture and preadipocyte differentiation

The preadipocytes cells (Mouse 3T3-L1 cells) were obtained from the ATCC. It were grown in DMEM with 10% BS, 100 U/mL penicillin and 100  $\mu$ g/mL streptomycin at 37 °C in a humidified atmosphere of 5%  $CO_2$ . At 2 days

post-confluence (designated “day 0”), cell differentiation was induced with a mixture of isobutylmethylxanthine (0.5 mM), dexamethasone (1  $\mu$ M) and insulin (10  $\mu$ g/mL) in DMEM containing 10% FBS. After 48 hr (day 2), the induction medium was removed and replaced with DMEM containing 10% FBS supplemented with insulin (10  $\mu$ g/mL). This medium was changed every 2 days. Various sample was administered to the culture medium from day 0 to day 8.

#### 4-4-3. Cell viability assay by MTT

The 3T3-L1 preadipocytes cells were seeded onto a 96-well plate for 24 hr. The cells were treated with Ez-CyTox cell viability assay kit. and than after 3 hr incubation under 5% CO<sub>2</sub> humidified atmosphere incubator at 37 °C. Absorbance was measured at 570 nm by using microplate reader.

#### 4-4-4. Cytotoxicity assay (LDH assay)

The 3T3-L1 preadipocytes cells were seeded onto a 96-well plate for 24 hr. The cells were treated with various concentrations (0 ~ 500  $\mu$ g/mL) of sample for 48 hr. Then, LDH was measured using Cytotoxicity Detection kit. at 490 to 690 nm by microplate reader.

#### 4-4-5. Oil-Red O staining

For Oil-Red O staining, cells were washed with PBS, fixed with 10% fresh formaldehyde in PBS for 1 hr at room temperature, and stained with filtered 0.6% Oil-Red O solution for at least 1 hr. After staining, the Oil-Red O staining solution was removed and the plates were rinsed with water and dried. Images of lipid droplets in 3T3-L1 adipocytes were collected by a microscope. Finally, dye retained in the cells was eluted with 4% NP-40 in isopropanol and quantified by measuring

optical absorbance at 520 nm using a microplate reader.

#### 4-5. Statistical analysis

The student's *t*-test and one-way ANOVA were used to determine the statistical significance of differences between values for a variety of experimental and control groups. Data are expressed as means  $\pm$  standard deviation (SD) of at least three independent experiments performed in triplicate. *p*-values of 0.05 or less were considered statistically.



## 5. Results

5-1. The structures of the compounds isolated from of *L. erythrocarpa*

### 5-1-1. Compound 1

- Compound Name ethyl (*E*)-3-(3,4-dihydroxyphenyl)prop-2-enoate ; ethyl caffeate
- Synonym(s) caffeic acid ethyl ester, caffeoyl ethyl ester
- CAS Registry Number 102-37-4
- Appearance colorless powder
- Chemical Formula  $C_{11}H_{12}O_4$
- Molecular Weight (g/mol) 208.21
- Melting Point ( $^{\circ}C$ ) 148 - 152
- $^1H$ -NMR (500 MHz,  $CD_3OD$ )  
 $\delta$ : 7.54 (1H, *d*,  $J = 16.0$  Hz, H-7), 7.03 (1H, *d*,  $J = 2.0$  Hz, H-6), 6.93 (1H, *dd*,  $J = 8.0, 2.0$  Hz, H-2), 6.78 (1H, *d*,  $J = 8.0$  Hz, H-5), 6.25 (1H, *d*,  $J = 16.0$  Hz, H-8), 4.21 (2H, *q*,  $J = 7.5$  Hz, H-10), 1.30 (3H, *t*,  $J = 7.0$  Hz, H-11)
- $^{13}C$ -NMR (125 MHz,  $CD_3OD$ )  
 $\delta$ : 169.4 (C-9), 149.6 (C-4), 146.9 (C-7), 146.8 (C-3), 127.9 (C-1), 123.0 (C-6), 116.6 (C-5), 115.4 (C-2), 115.2 (C-8), 61.5 (C-10), 14.7 (C-11)
- Biological activities in the literature  
antioxidant, anti-inflammation, antifibrotic, ACE inhibitory activity
- Other data in the literature
  1. Biological Source: Occurs in wine

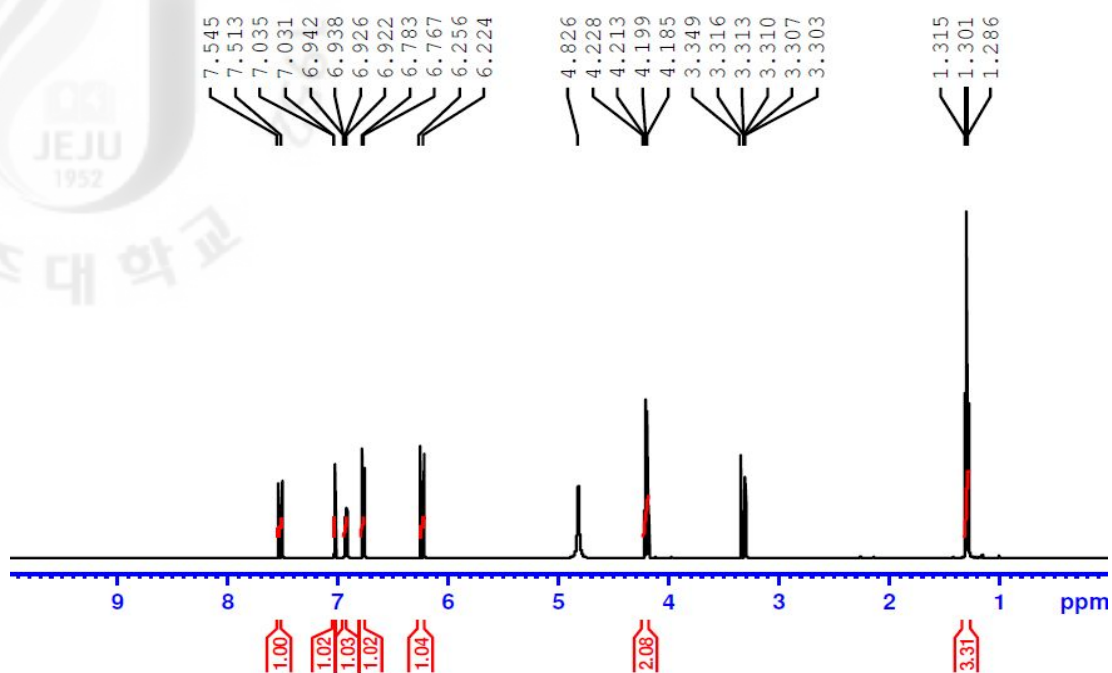


Figure 9.  $^1\text{H-NMR}$  spectrum of ethyl caffeate (**1**) in  $\text{CD}_3\text{OD}$

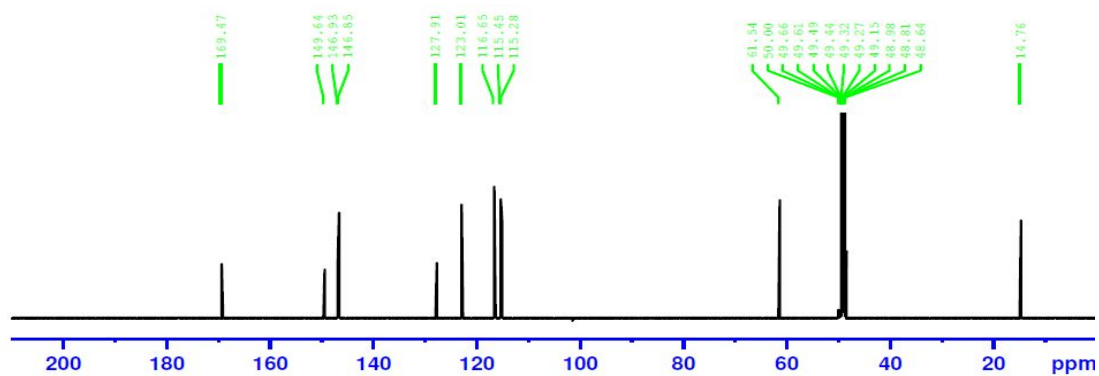


Figure 10.  $^{13}\text{C-NMR}$  spectrum of ethyl caffeate (**1**) in  $\text{CD}_3\text{OD}$

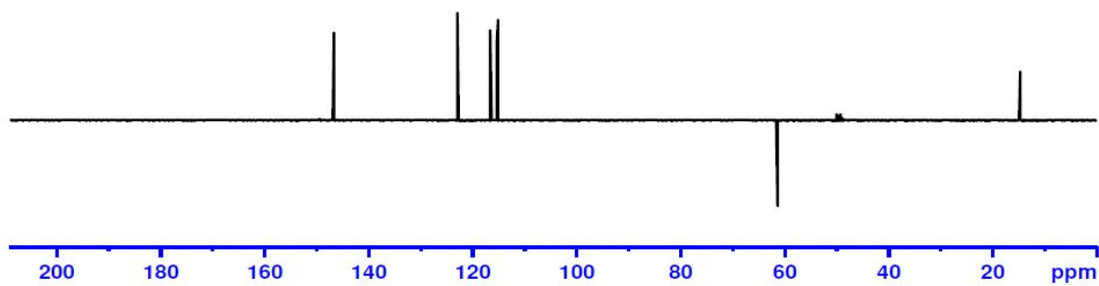


Figure 11. DEPT135 spectrum of ethyl caffeate (**1**) in  $\text{CD}_3\text{OD}$

Compound **1** was isolated as colorless powder. The  $^1\text{H-NMR}$  spectrum of compound **1** showed three aromatic protons at  $\delta_{\text{H}}$  7.03 (1H, *d*,  $J = 2.0$  Hz, H-6), 6.93 (1H, *dd*,  $J = 8.0, 2.0$  Hz, H-2), 6.78 (1H, *d*,  $J = 8.0$  Hz, H-5), two olefinic protons at  $\delta_{\text{H}}$  7.54 (1H, *d*,  $J = 16.0$  Hz, H-7), 6.25 (1H, *d*,  $J = 16.0$  Hz, H-8) and one ethyl group  $\delta_{\text{H}}$  4.21 (2H, *q*,  $J = 7.5$  Hz, H-10), 1.30 (3H, *t*,  $J = 7.0$  Hz, H-11) (Fig. 9). The  $^{13}\text{C-NMR}$  spectrum of compound **1** was showed eleven carbon signals including five carbon signals of benzene rings at  $\delta_{\text{C}}$  149.6 (C-4), 146.8 (C-3), 127.9 (C-1), 123.0 (C-6), 116.6 (C-5), 115.4 (C-2), two olefinic carbons at  $\delta_{\text{C}}$  146.9 (C-7), 115.2 (C-8), one ethyl group at  $\delta_{\text{C}}$  61.5 (C-10), 14.7 (C-11) and one carbonyl group at  $\delta_{\text{C}}$  169.4 (C-9) (Fig. 10-11). Thus, the structure of compound **1** was determined as ethyl caffeate by comparison of its spectral data with those in the literature (Fig. 12).<sup>55,74)</sup>

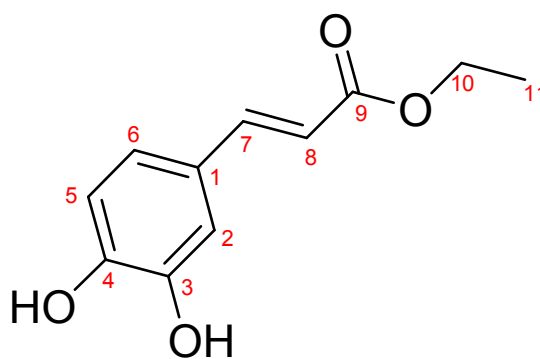


Figure 12. Structure of compound **1**; Ethyl caffeate

## 5-1-2. Compound 2

- Compound Name methyl (*E*)-3-Phenylprop-2-enoate; methyl cinnamate
- Synonym(s) cinnamic acid methyl ester
- CAS Registry Number 103-26-4
- Appearance colorless needle
- Chemical Formula  $C_{10}H_{10}O_2$
- Molecular Weight (g/mol) 162.06
- Melting Point ( $^{\circ}C$ ) 36
- $^1H$ -NMR (500 MHz,  $DMSO-d_6$ )  
 $\delta$ : 7.74 (1H, *d*,  $J = 15.6$  Hz, H-7), 7.68 (2H, *dd*,  $J = 7.4, 2.4$  Hz, H-2, 6),  
7.47 (3H, *m*, H-3, 4, 5), 7.47 (1H, *d*,  $J = 15.6$  Hz, H-8), 3.93 (3H, *s*,  
H-10)
- $^{13}C$ -NMR (125 MHz,  $DMSO-d_6$ )  
 $\delta$ : 166.5 (C-9), 141.8 (C-7), 134.4 (C-1), 129.2 (C-3, 4, 5), 128.3 (C-2, 6),  
109.5 (C-8), 59.2 (C-10)
- Biological activities in the literature  
antioxidant, anti-microbial
- Other data in the literature
  1. Hazard and toxicity:  $LD_{50}$  (rat, orl) 2,610 mg/kg
  2. Biological Source: Occurs in essential oils *e. g.* from *Ocimum*

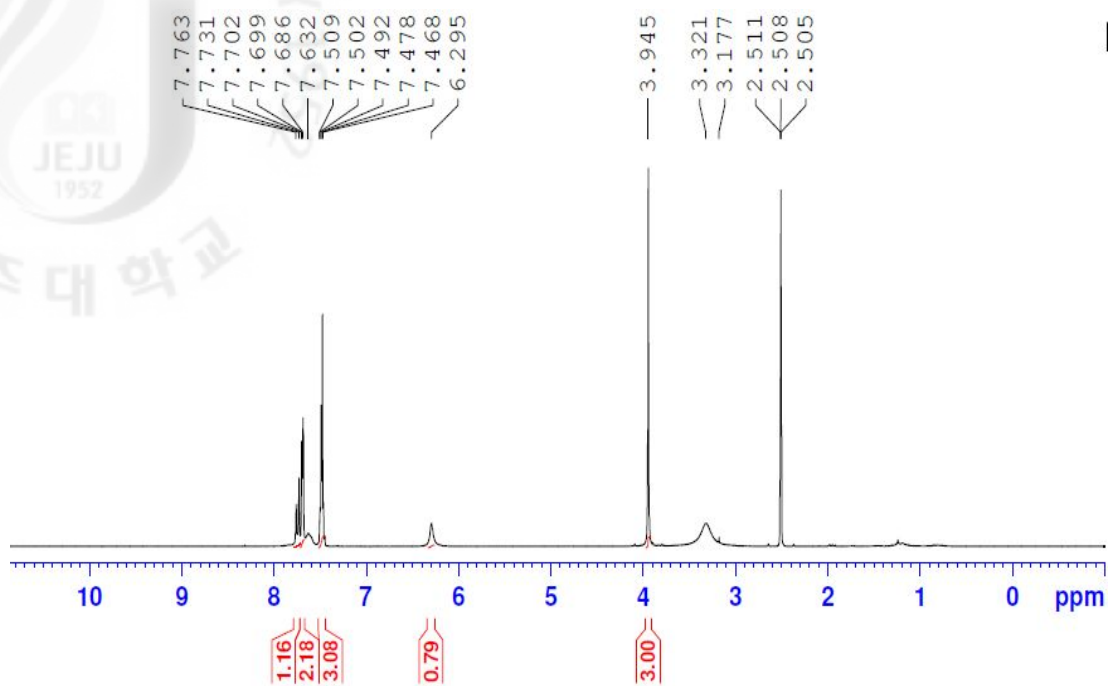


Figure 13.  $^1\text{H-NMR}$  spectrum of methyl cinnamate (2) in  $\text{DMSO-}d_6$

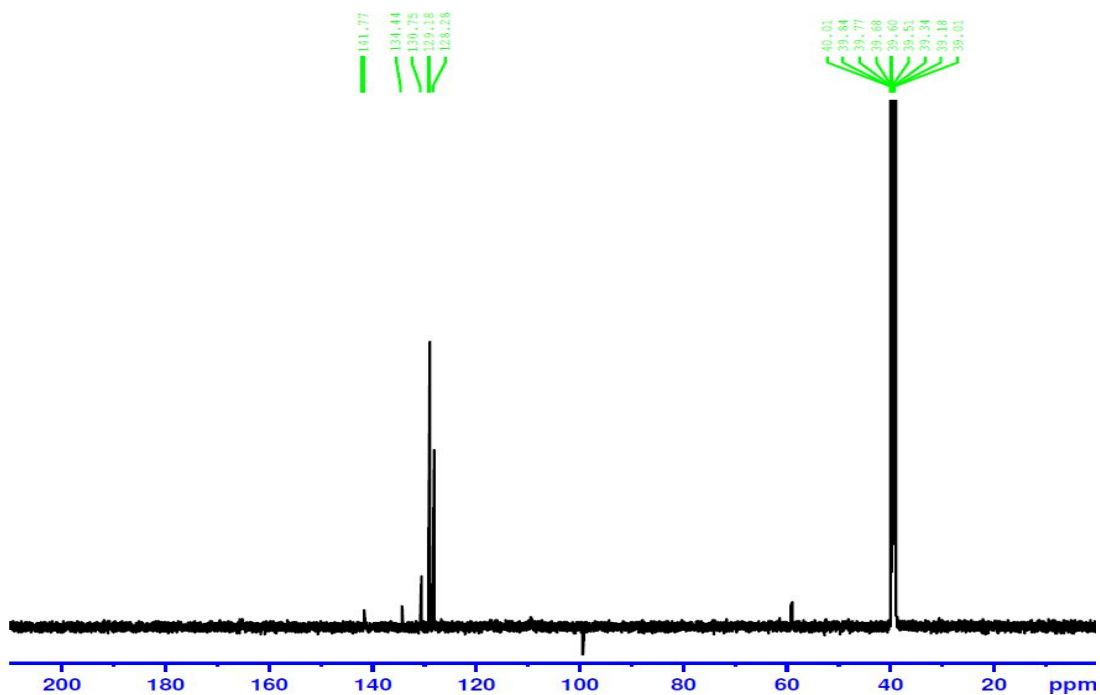


Figure 14.  $^{13}\text{C-NMR}$  spectrum of methyl cinnamate (2) in  $\text{DMSO-}d_6$

Compound **2** was isolated as colorless needle. The  $^1\text{H-NMR}$  spectrum of compound **2** showed five aromatic protons at  $\delta_{\text{H}}$  7.68 (2H, *dd*,  $J = 7.4, 2.4$  Hz, H-2, 6) and 7.47 (3H, *m*, H-3, 4, 5), two olefinic protons at  $\delta_{\text{H}}$  7.74 (1H, *d*,  $J = 15.6$  Hz, H-7), 7.47 (1H, *d*,  $J = 15.6$  Hz, H-8) and one methyl ester 3.93 (3H, *s*, H-10) (Fig. 13). The  $^{13}\text{C-NMR}$  spectrum of compound **2** showed ten carbon signals including three carbon signals of benzene rings at  $\delta_{\text{C}}$  134.4 (C-1), 129.2 (C-3, 4, 5), 128.3 (C-6), two olefinic carbons at  $\delta_{\text{C}}$  141.8 (C-7) and 109.5 (C-8), one methoxy group at  $\delta_{\text{C}}$  59.2 (C-10) and one carbonyl group at  $\delta_{\text{C}}$  166.5 (C-9) (Fig. 14). Thus, the structure of compound **2** was determined as methyl cinnamate by comparison of its spectral data with those in the literature (Fig. 15).<sup>56)</sup>

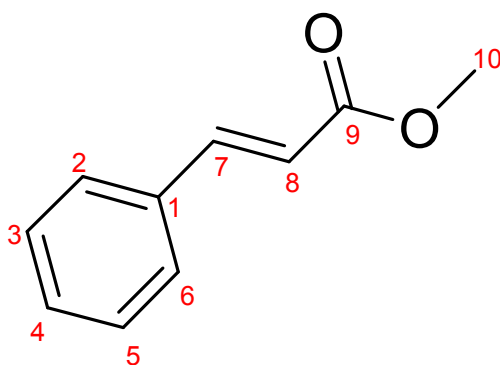


Figure 15. Structure of compound **2**; Methyl cinnamate

### 5-1-3. Compound 3

- Compound Name lucidone
- Synonym(s) 2-(1-Hydroxy-3-phenyl-2-propenylidene)-4-methoxy-4-cyclopentene-1,3-dione
- CAS Registry Number 19956-53-7
- Appearance yellow crystal
- Chemical Formula  $C_{15}H_{12}O_4$
- Molecular Weight (g/mol) 256.07
- Melting Point ( $^{\circ}C$ ) 164.5 - 165.5
- $^1H$ -NMR (500 MHz,  $CDCl_3$ )  
 $\delta$ : 7.74 (1H, *d*,  $J = 16.0$  Hz, H-7), 7.64 (1H, *d*,  $J = 16.0$  Hz, H-8), 7.61 (2H, *dd*,  $J = 7.5, 3.0$  Hz, H-2, 16), 7.39 (1H, *m*, H-3), 7.39 (1H, *m*, H-3, 4, 5), 7.39 (1H, *m*, H-5), 5.82 (1H, *s*, H-4'), 3.94 (3H, *s*, H-6')
- $^{13}C$ -NMR (125 MHz,  $CDCl_3$ )  
 $\delta$ : 198.9 (C-5'), 185.0 (C-2'), 171.2 (C-3'), 168.4 (C-9), 143.2 (C-7), 135.0 (C-1), 130.9 (C-4), 129.2 (C-2, 6), 128.9 (C-5), 117.8 (C-8), 111.8 (C-3), 108.1 (C-4'), 103.1 (C-1'), 59.0 (C-6')
- Biological activities in the literature  
melanogenesis inhibition, anti-cancer, anti-inflammation, anti-microbial
- Other data in the literature
  1. UV (EtOH)  $\lambda_{max}nm$ : 243 and 355

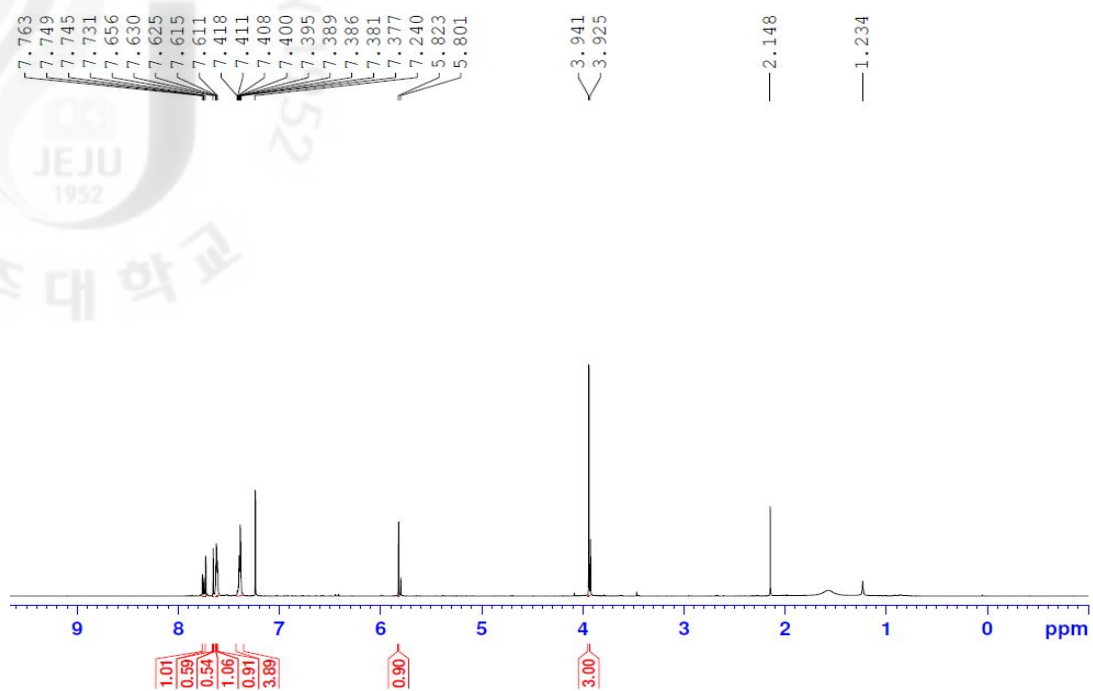


Figure 16.  $^1\text{H}$ -NMR spectrum of lucidone (**3**) in  $\text{CDCl}_3$

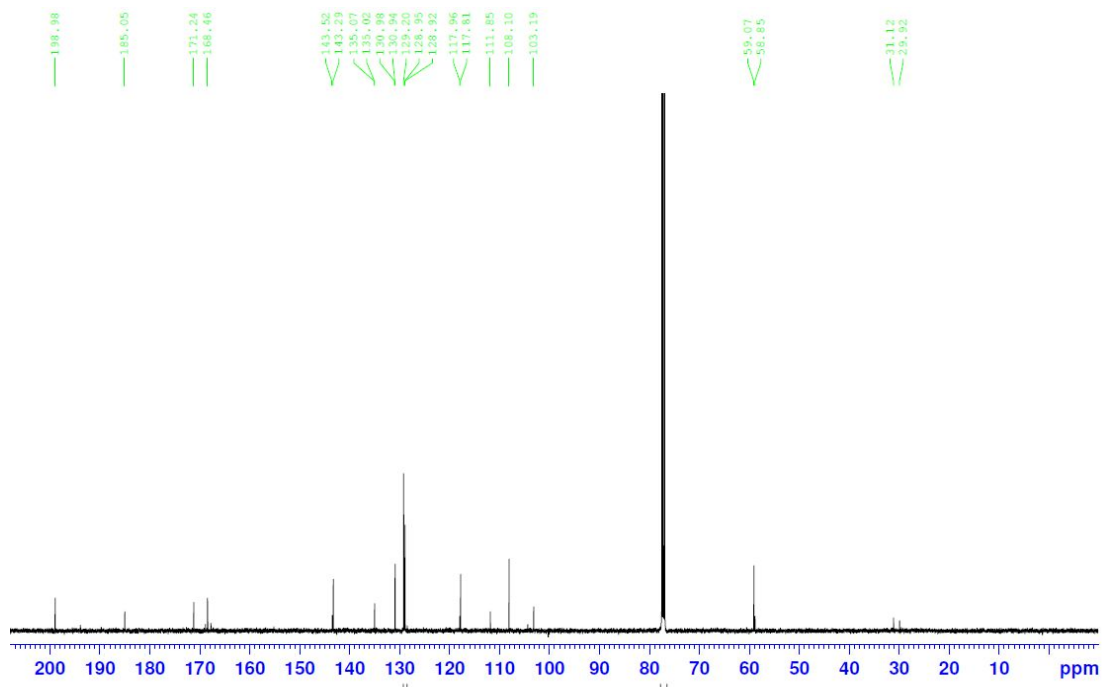


Figure 17.  $^{13}\text{C}$ -NMR spectrum of lucidone (**3**) in  $\text{CDCl}_3$



Compound **3** was isolated as yellow solid. The  $^1\text{H-NMR}$  spectrum of compound **3** was showed five aromatic protons at  $\delta_{\text{H}}$  7.61 (1H, *dd*,  $J = 7.5, 3.0$  Hz, H-2), 7.61 (1H, *dd*,  $J = 7.5, 3.0$  Hz, H-6), 7.39 (1H, *m*, H-3), 7.39 (1H, *m*, H-4), 7.39 (1H, *m*, H-5), two olefinic protons at  $\delta_{\text{H}}$  7.74 (1H, *d*,  $J = 16.0$  Hz, H-7), 7.64 (1H, *d*,  $J = 16.0$  Hz, H-8) and one singlet peak  $\delta_{\text{H}}$  5.82 (1H, *s*, H-4') (Fig. 16). The  $^{13}\text{C-NMR}$  spectrum of **3** showed carbon signals including five of benzene ring at  $\delta_{\text{C}}$  135.0 (C-1), 130.9 (C-4), 129.2 (C-6), 129.2 (C-2), 128.9 (C-5), 111.8 (C-3), two olefinic carbons at  $\delta_{\text{C}}$  143.2 (C-7), 117.8 (C-8), one methoxyl group 59.0 (C-6') and two keto group at  $\delta_{\text{C}}$  198.9 (C-2'), 185.0 (C-5') (Fig. 17). Thus, the structure of **3** was determined as lucidone by comparison of its spectral data with those in the literature (Fig. 18).<sup>33)</sup>

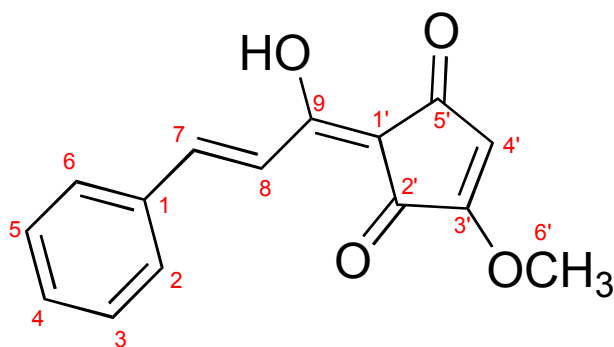


Figure 18. Structure of compound **3**; Lucidone

#### 5-1-4. Compound 4

- Compound Name 4,5-dimethoxy-2-(1-methoxy-3-phenyl-allylidene)-cyclopent-4-ene-1,3-dione; methyllinderone
- Synonym(s) -
- CAS Registry Number KMP39-Y
- Appearance yellow solid
- Chemical Formula  $C_{17}H_{16}O_5$
- Molecular Weight (g/mol) 300.09
- Melting Point ( $^{\circ}C$ ) 84 - 85
- $^1H$ -NMR (500 MHz,  $CDCl_3$ )  
 $\delta$ : 7.92 (1H, *d*,  $J = 16.0$  Hz, H-7), 7.92 (1H, *d*,  $J = 16.0$  Hz, H-8), 7.58 (1H, *dd*,  $J = 7.7, 1.5$  Hz, H-2), 7.58 (1H, *dd*,  $J = 7.7, 1.5$  Hz, H-6), 7.35 (3H, *m*, H-3, 4, 5), 4.17 (6H, *s*, H-6', 7'), 4.08 (3H, *s*, H-10)
- $^{13}C$ -NMR (125 MHz,  $CDCl_3$ )  
 $\delta$ : 187.4 (C-5'), 184.9 (C-2'), 165.6 (C-9), 149.1 (C-4'), 148.0 (C-3'), 141.4 (C-7), 135.8(C-1), 130.2 (C-4), 129.1 (C-3), 129.1 (C-5), 128.5 (C-2), 128.5 (C-6), 121.4 (C-8), 109.6 (C-1'), 64.5 (C-10), 60.1 (C-6'), 60.1 (C-7')
- Biological activities in the literature  
anti-cancer, anti-inflammation, anti-microbial, human chymase inhibitor
- Other data in the literature  
1. UV (EtOH)  $\lambda_{max}nm$ : 248 and 364

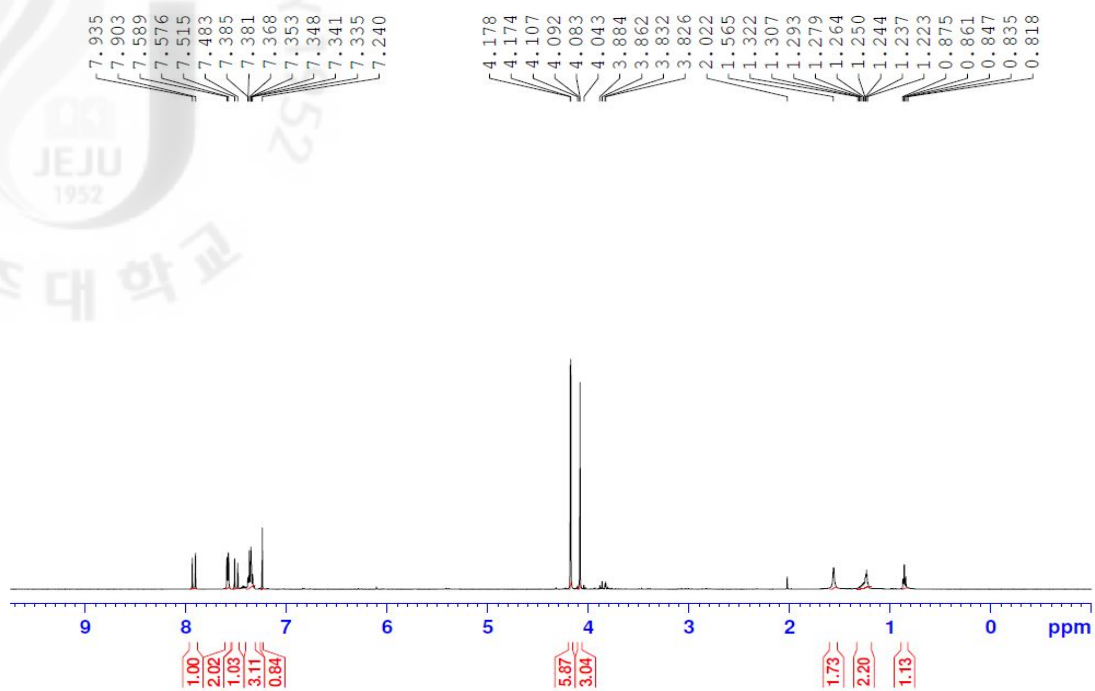


Figure 19.  $^1\text{H}$ -NMR spectrum of methylindrone (**4**) in  $\text{CDCl}_3$

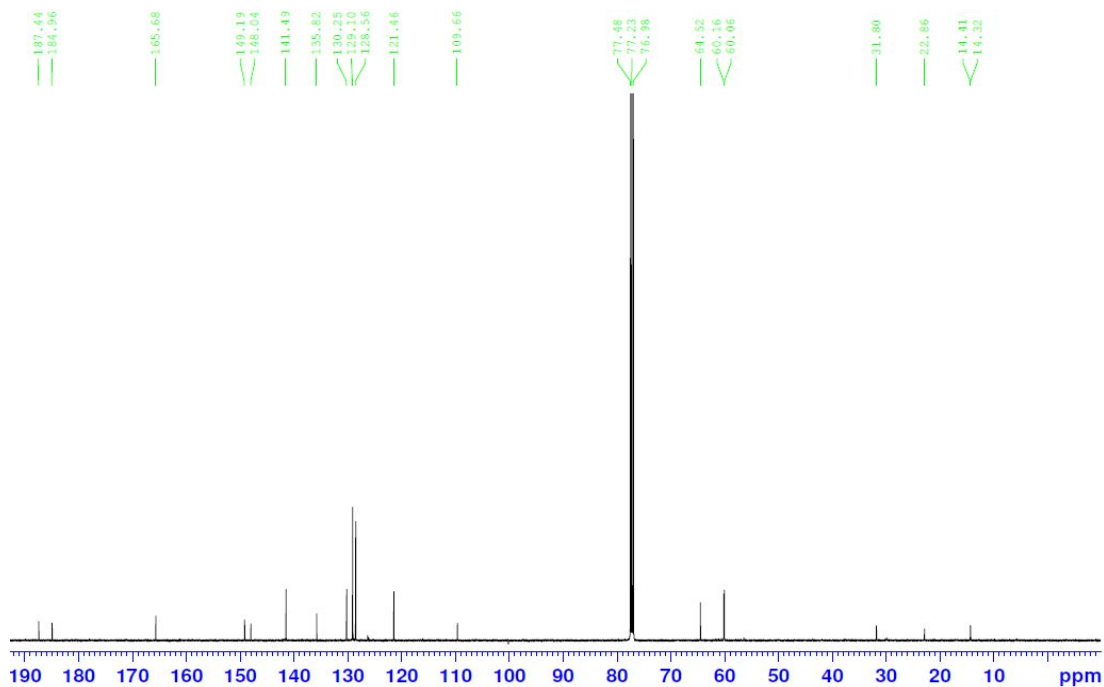


Figure 20.  $^{13}\text{C}$ -NMR spectrum of methylindrone (**4**) in  $\text{CDCl}_3$

Compound **4** was isolated as yellow solid. The  $^1\text{H}$  and  $^{13}\text{C}$ -NMR spectrum of compound **4** was showed  $\delta_{\text{H}}$  7.92 (2H, *d*,  $J = 16.0$  Hz, H-7, 8), 187.4 (C-2') were indicative of H- $\alpha$  and H- $\beta$ , respectively (Fig. 20).  $^1\text{H}$ -NMR spectrum indicated five aromatic protons including mono substituted benzenering coupling pattern at 7.58 (1H, *dd*,  $J = 7.7, 1.5$  Hz, H-2) and 7.35 (3H, *m*, H-3, 4, 5), three methoxyl groups at 4.17 (6H, *s*, H-6', 7') and 4.08 (3H, *s*, H-10) (Fig. 19). In addition,  $\delta_{\text{C}}$  165.6 (C-9), 149.1 (C-3'), 148.0 (C-4') and 141.4 (C-8) were assumed as four aromatic carbon signals on  $^{13}\text{C}$ -NMR spectrum (Fig. 20). Thus, the structure of **4** was determined to be 4,5-dimethoxy-2-(1-methoxy-3-phenyl-allylidene)-cyclopent-4-ene-1,3-dione (methyllinderone) (Fig. 21). This was confirmed by a spectral data comparison with those of published data.<sup>57-58,61)</sup>

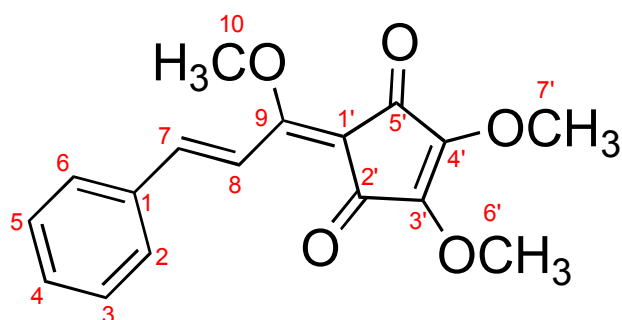


Figure 21. Structure of compound **4**; Methyllinderone

### 5-1-5. Compound 5

- Compound Name stigmast-5-en-3-ol; (3 $\beta$ ,24R)-form;  $\beta$ -sitosterol
- Synonym(s) nimbosterol, cupreol, quebrachol, rhamnol, cinchol
- CAS Registry Number 83-46-5
- Appearance colorless needle
- Chemical Formula C<sub>29</sub>H<sub>50</sub>O
- Molecular Weight (g/mol) 414.38
- Melting Point (°C) 136 - 137
- <sup>1</sup>H-NMR (500 MHz, Acetone-*d*<sub>6</sub>)  
 $\delta$ : 5.35 (1H, *m*, H-6), 3.97 (1H, *m*, H-3), 1.00 (3H, *d*, *J* = 7.2 Hz, Me-21), 0.94 (3H, *s*, Me-19), 0.89 (9H, *m*, Me-26, Me-27, Me-29), 0.67 (3H, *s*, Me-18)
- <sup>13</sup>C-NMR (125 MHz, Acetone-*d*<sub>6</sub>)  
 $\delta$ : 140.7 (C-5), 121.7 (C-6), 71.8 (C-3), 56.7 (C-14), 55.9 (C-17), 50.5 (C-9), 45.7 (C-24), 42.2 (C-13), 39.7 (C-12), 37.2 (C-1), 36.5 (C-10), 36.1 (C-20), 33.8 (C-22), 31.8 (C-7), 31.8 (C-8), 31.6 (C-2), 29.1 (C-25), 28.2 (C-16), 25.9 (C-23), 24.2 (C-15), 22.9 (C-28), 21.0 (C-11), 19.8 (C-26), 19.4 (C-19), 18.9 (C-27), 18.7 (C-21), 12.2 (C-29), 11.8 (C-18)
- Biological activities in the literature  
anti-hypercholesterolaemic, estrogenic, hypolipidaemic agent, anti-microbial, anti-fungal
- Hazard and Toxicity  
1. Optical Rotation :  $[\alpha]_{22}^D = -35$  (CHCl<sub>3</sub>)

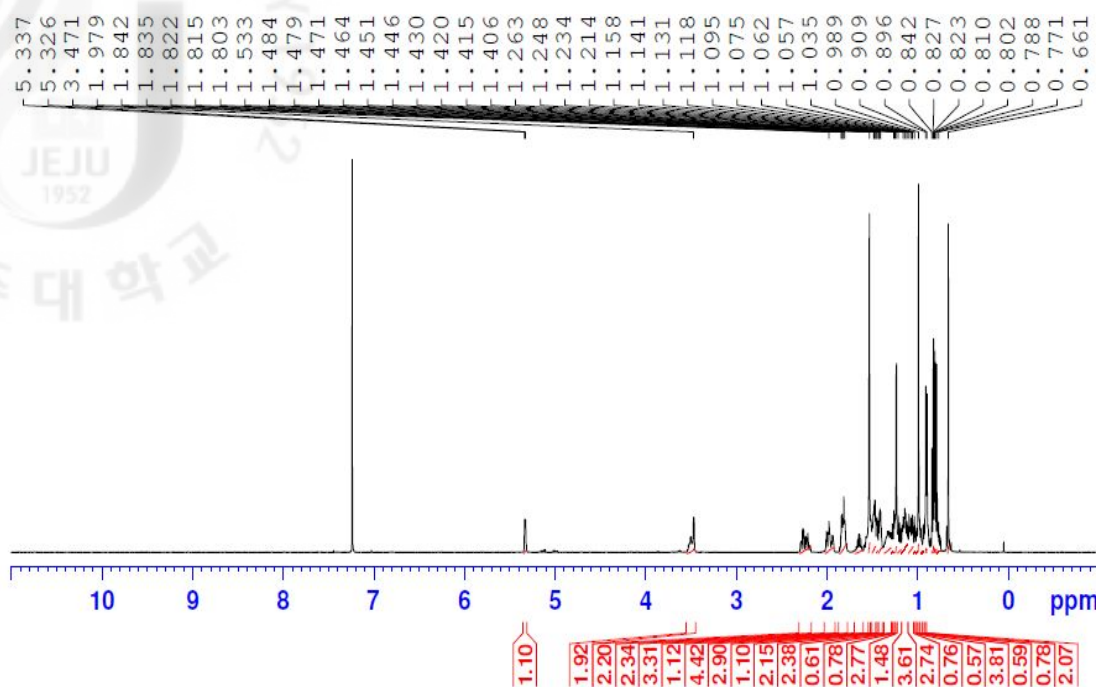


Figure 22.  $^1\text{H}$ -NMR spectrum of  $\beta$ -sitosterol (**5**) in Acetone- $d_6$

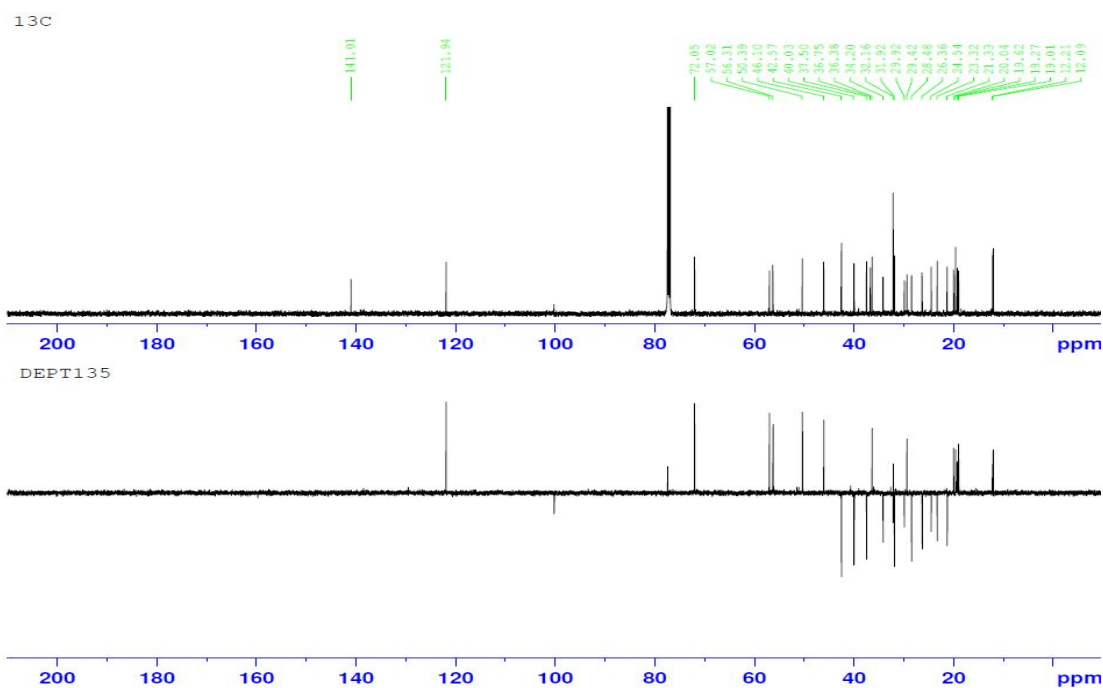


Figure 23.  $^{13}\text{C}$ -NMR and DEPT135 spectra of  $\beta$ -sitosterol (**5**) in Acetone- $d_6$

Compound **5** was isolated as colorless needle. The  $^1\text{H-NMR}$  spectrum of compound **5** in acetone- $d_6$  was showed two angular methyl singlet signals at  $\delta_{\text{H}}$  0.67 (3H, *s*, Me-18), 0.94 (3H, *s*, Me-19). The peak of olefinic proton showed at  $\delta_{\text{H}}$  5.35 (1H, *m*, H-6) (Fig. 22). The  $^{13}\text{C-NMR}$  spectrum of **5** was showed twenty-nine carbon signals including two olefinic carbons at  $\delta_{\text{C}}$  140.7 (C-5), 121.7 (C-6), six methyl group 19.8 (C-26), 19.4 (C-19), 18.9 (C-27), 18.7 (C-21), 12.2 (C-29), 11.8 (C-18) (Fig. 23). Thus, the structure of compound **5** was determined as  $\beta$ -sitosterol by comparison of its spectral data with those in the literature (Fig. 24).<sup>59)</sup>

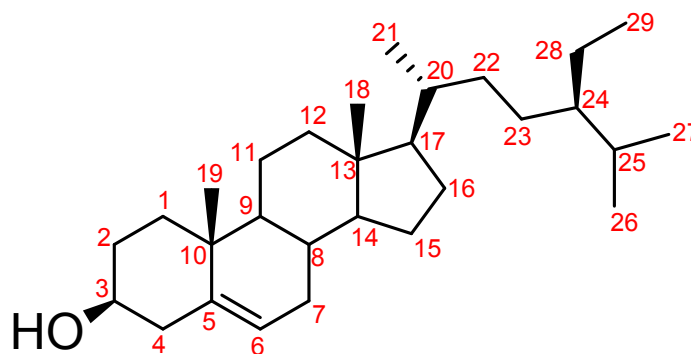


Figure 24. Structure of compound **5**;  $\beta$ -sitosterol

#### 5-1-6. Compound 6

- Compound Name 3,3',4',5,7-pentahydroxyflavone; quercetin
- Synonym(s) 3',4',5,7-tetrahydroxyflavonol, meletin, sophoretin
- CAS Registry Number 117-39-5
- Appearance amorphous yellow powder
- Chemical Formula  $C_{15}H_{10}O_7$
- Molecular Weight (g/mol) 302.04
- Melting Point ( $^{\circ}C$ ) 313 - 314
- $^1H$ -NMR (500 MHz,  $CD_3OD$ )  
 $\delta$ : 7.63 (1H, *d*,  $J = 2.0$  Hz, H-2'), 7.63 (1H, *dd*,  $J = 8.5, 2.0$  Hz, H-6'), 6.89 (1H, *d*,  $J = 8.5$  Hz, H-5'), 6.38 (1H, *d*,  $J = 2.0$  Hz, H-8), 6.17 (1H, *d*,  $J = 2.0$  Hz, H-6)
- $^{13}C$ -NMR (125 MHz,  $CD_3OD$ )  
 $\delta$ : 177.4 (C-4), 166.1 (C-7), 162.6 (C-9), 158.4 (C-5), 148.9 (C-4'), 148.0 (C-2), 146.3 (C-3'), 137.3 (C-3), 124.3 (C-1'), 121.8 (C-6'), 116.1 (C-2'), 116.3 (C-5'), 104.5 (C-10), 99.5 (C-6), 94.6 (C-8)
- Biological activities in the literature  
anti-carcinogenic, anti-tumour, algicide, free radical scavenger, anti-HIV
- Other data in the literature
  1. Hazard and toxicity:  $LD_{50}$  (mus, orl) 159 mg/kg. Exp. reprod. effect
  2. UV (EtOH)  $\lambda_{maxnm}$ : 258 and 375



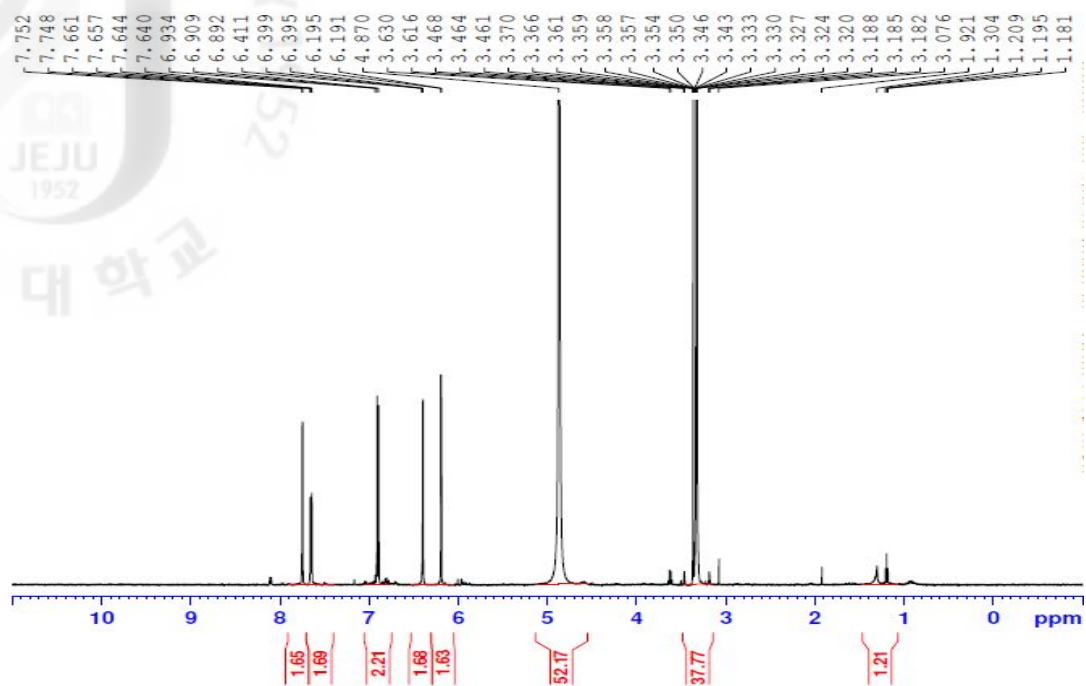


Figure 25.  $^1\text{H}$ -NMR spectrum of quercetin (6) in  $\text{CD}_3\text{OD}$

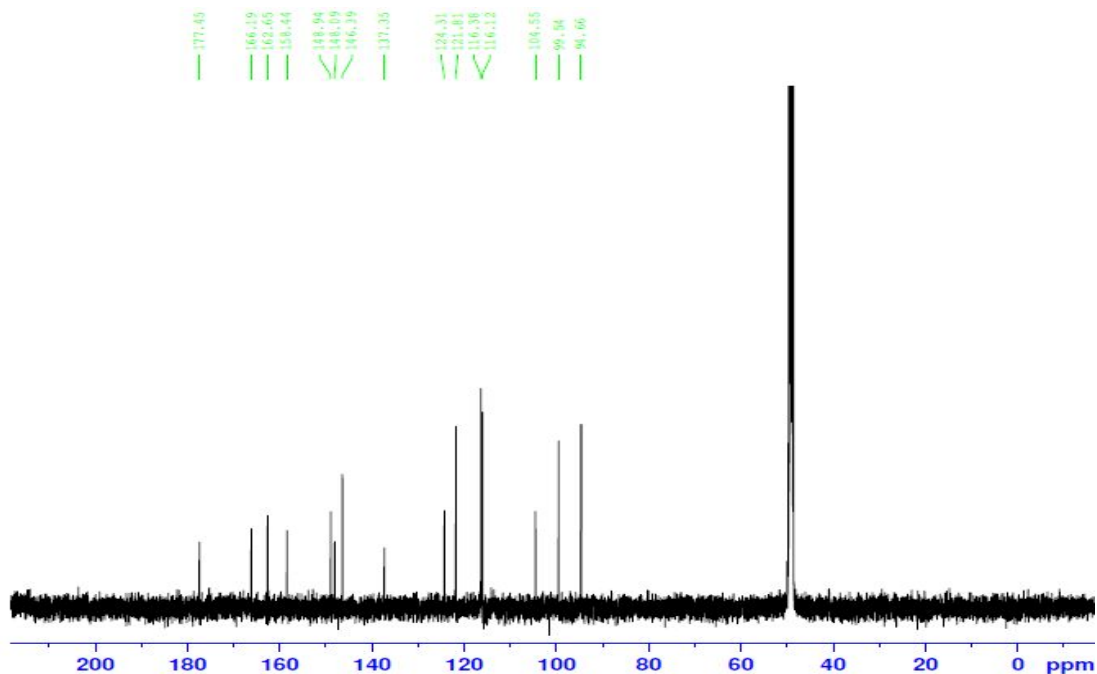


Figure 26.  $^{13}\text{C}$ -NMR spectrum of quercetin (6) in  $\text{CD}_3\text{OD}$

Compound **6** was isolated as amorphous yellow powder. The  $^1\text{H-NMR}$  spectrum of compound **6** in  $\text{CD}_3\text{OD}$  indicated a 5,7-dihydroxylated pattern for ring A (two *meta*-coupled doublets at  $\delta_{\text{H}}$  6.38 (1H, *d*,  $J = 2.0$  Hz, H-8), 6.17 (1H, *d*,  $J = 2.0$  Hz, H-6) and a 3,4-dihydroxylation pattern for ring B [ABX system signals at  $\delta_{\text{H}}$  7.63 (1H, *d*,  $J = 2.0$  Hz, H-2'), 7.63 (1H, *dd*,  $J = 8.5, 2.0$  Hz, H-6'), 6.89 (1H, *d*,  $J = 8.5$  Hz, H-5')] (Fig. 25), The  $^{13}\text{C-NMR}$  spectrum of compound **6** showed fifty carbon signals including one keto carbonyl group at  $\delta_{\text{C}}$  177.4 (C-4) and specific peaks which C-ring of flavonoid at  $\delta_{\text{C}}$  166.1 (C-7), 162.6 (C-9), 158.4 (C-5) (Fig. 26). Thus, the structure of compound **6** was determined as quercetin by comparison of its spectral data with those in the literature (Fig. 27).<sup>60</sup> Quercetin was reported for the first time from this plant.

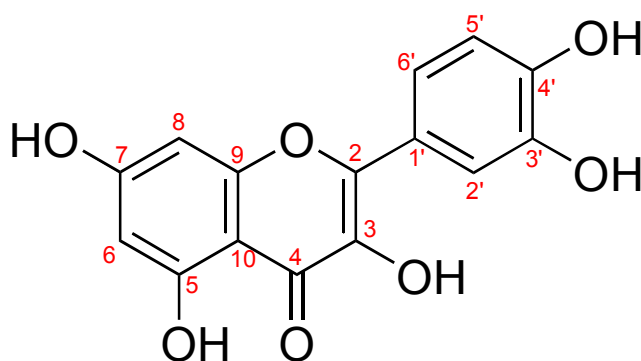


Figure 27. Structure of compound **6**; Quercetin

### 5-1-7. Compound 7

- Compound Name quercetin-3-*O*- $\alpha$ -L-rhamnoside; quercitrin
- Synonym(s) quercetin 3-rhamnoside, quercitroside, quercitronic acid
- CAS Registry Number 22324-77-2
- Appearance amorphous yellow powder
- Chemical Formula  $C_{21}H_{20}O_{11}$
- Molecular Weight (g/mol) 448.10
- Melting Point ( $^{\circ}C$ ) 182 - 185
- $^1H$ -NMR (500 MHz,  $CD_3OD$ )  
 $\delta$ : 7.33 (1H, *d*,  $J = 2.6$  Hz, H-2'), 7.30 (1H, *dd*,  $J = 8.5, 2.0$  Hz, H-6'), 6.91 (1H, *d*,  $J = 8.5$  Hz, H-5'), 6.36 (1H, *d*,  $J = 2.0$  Hz, H-8), 6.20 (1H, *d*,  $J = 2.0$  Hz, H-6), 5.35 (1H, *d*,  $J = 1.5$  Hz, H-1"), 0.94 (3H, *d*,  $J = 6.0$  Hz, H-6')
- $^{13}C$ -NMR (125 MHz,  $CD_3OD$ )  
 $\delta$ : 179.8 (C-4), 166.0 (C-7), 163.3 (C-9), 159.4 (C-5), 158.7 (C-4'), 149.9 (C-2), 146.5 (C-3'), 136.4 (C-3), 123.1 (C-1'), 123.0 (C-6'), 117.1 (C-5'), 116.5 (C-2'), 106.0 (C-10), 103.7 (C-1"), 99.9 (C-6), 94.8 (C-8), 73.4 (C-4"), 72.2 (C-3"), 72.1 (C-2"), 72.0 (C-5"), 17.8 (C-6")
- Biological activities in the literature  
  
anti-viral, anti-spasmodic, diuretic, possesses vasopressor props.
- Other data in the literature
  1. Optical Rotation:  $[\alpha]_{15}^D = -158$  ( $c$  0.61 in MeOH)
  2. UV (MeOH)  $\lambda_{max}nm$ : 257 and 356

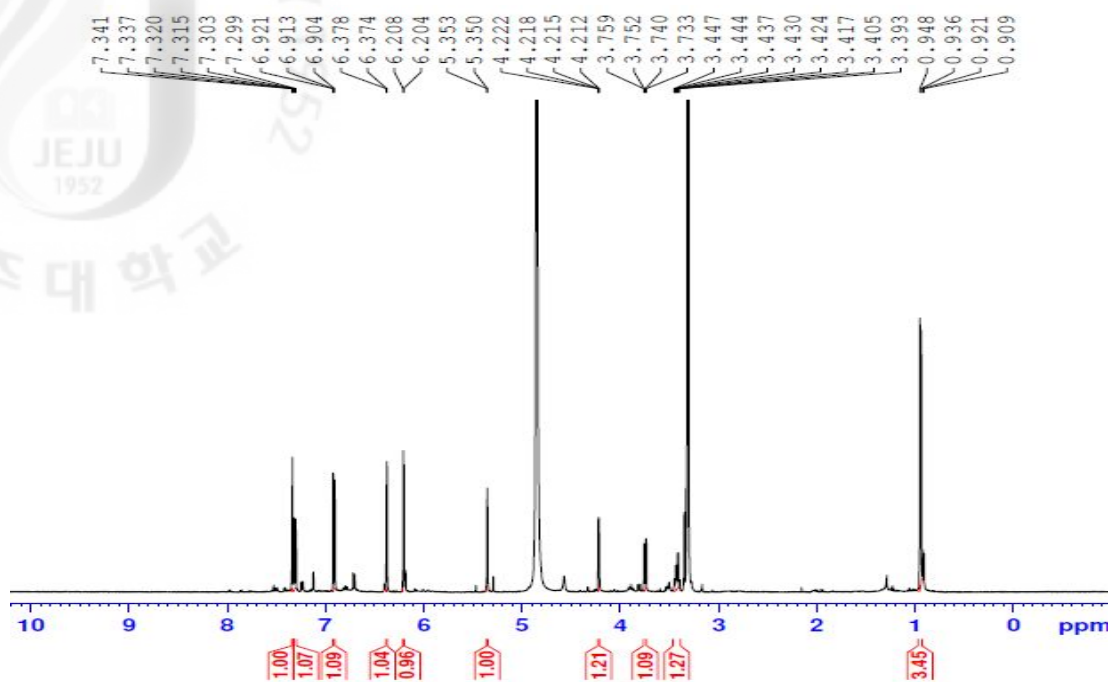


Figure 28.  $^1\text{H-NMR}$  spectrum of quercetin-3-*O*- $\alpha$ -L-rhamnoside (7) in  $\text{CD}_3\text{OD}$

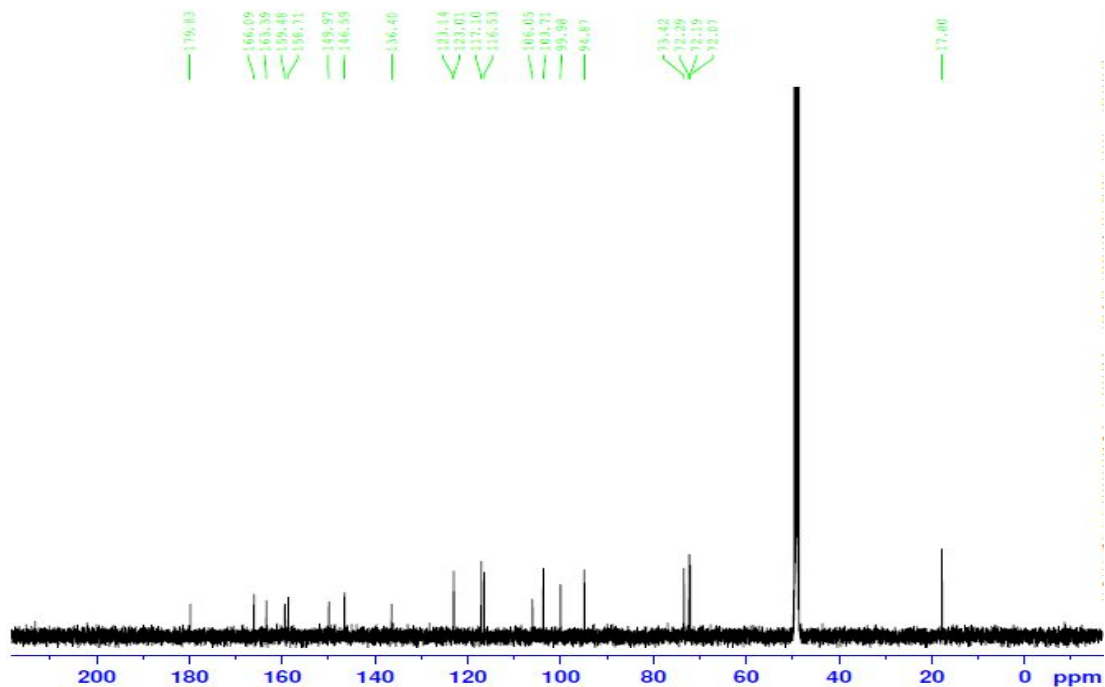


Figure 29.  $^{13}\text{C-NMR}$  spectrum of quercetin-3-*O*- $\alpha$ -L-rhamnoside (7) in  $\text{CD}_3\text{OD}$

Compound **7** was isolated as amorphous yellow powder. The  $^1\text{H-NMR}$  spectrum of compound **7** in  $\text{CD}_3\text{OD}$  indicated a 5,7-dihydroxylated pattern for ring A (two *meta*-coupled doublets at  $\delta_{\text{H}}$  6.36 (1H, *d*,  $J = 2.0$  Hz, H-8), 6.20 (1H, *d*,  $J = 2.0$  Hz, H-6) and a 3,4-dihydroxylation pattern for ring B [ABX system signals at  $\delta_{\text{H}}$  7.33 (1H, *d*,  $J = 2.6$  Hz, H-2'), 7.30 (1H, *dd*,  $J = 8.5, 2.0$  Hz, H-6'), 6.91 (1H, *d*,  $J = 8.5$  Hz, H-5')] (Fig. 28), The  $^{13}\text{C-NMR}$  spectrum of compound **7** was showed twenty-one carbon signals including one keto carbonyl group at  $\delta_{\text{C}}$  179.8 (C-4) and specific peaks which C-ring of flavonoid at  $\delta_{\text{C}}$  166.0 (C-7), 163.3 (C-9), 159.4 (C-5) (Fig. 29). Analysis of the chemical shifts, signal multiplicities, absolute values of the coupling constants, and their magnitude in the  $^1\text{H}$  and  $^{13}\text{C-NMR}$  spectrum indicated the presence of one rhamnosyl residue with *a*-configuration with the anomeric proton at  $\delta_{\text{H}}$  5.35 (1H, *d*,  $J = 1.5$  Hz, H-1''). The HMBC spectrum showed a correlation between the anomeric rhamnoside proton and quercetin carbon at the C-3, giving the attachment site of the rhamnose on quercetin. The compound **7** was identified as quercetin-3-*O-a*-L-rhamnoside (quercitrin) (Fig. 30).<sup>61-62</sup> Quercitrin was reported for the first time from this plant.

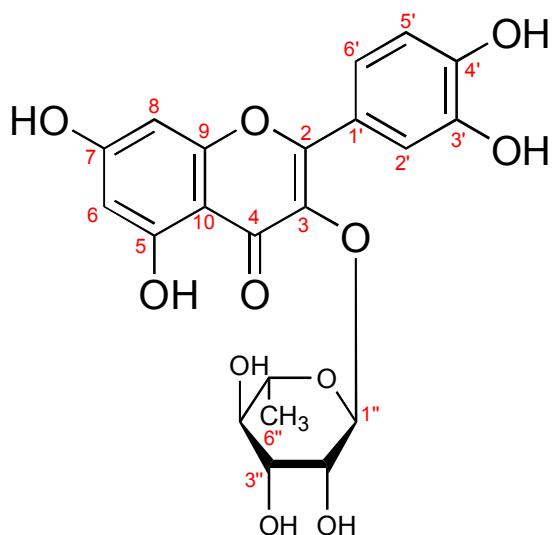


Figure 30. Structure of compound **7**; Quercetin-3-*O-a*-L-rhamnoside (quercitrin)

#### 5-1-8. Compound 8

- Compound Name quercetin-3-*O*-*α*-L-arabinofuranoside; avicularin
- Synonym(s) fenicularin, avicularoside
- CAS Registry Number 119786-64-0

• Appearance amorphous yellow powder

• Chemical Formula  $C_{20}H_{18}O_{11}$

• Molecular Weight (g/mol) 434.08

• Melting Point (°C) 217

•  $^1H$ -NMR (500 MHz,  $CD_3OD$ )

$\delta$ : 7.52 (1H, *d*,  $J = 2.0$  Hz, H-2'), 7.48 (1H, *dd*,  $J = 2.0, 8.0$  Hz, H-6'), 6.90 (1H, *d*,  $J = 8.5$  Hz, H-5'), 6.38 (1H, *d*,  $J = 2.0$  Hz, H-6), 6.20 (1H, *d*,  $J = 2.0$  Hz, H-8), 5.46 (1H, *s*, H-1"), 4.33 (1H, *m*, H-4"), 3.91 (1H, *m*, H-2"), 3.87 (1H, *m*, H-3"), 3.50 (2H, *m*, H-5")

•  $^{13}C$ -NMR (125 MHz,  $CD_3OD$ )

$\delta$ : 180.0 (C-4), 166.3 (C-7), 163.1 (C-9), 159.3 (C-5), 158.6 (C-4'), 149.8 (C-2), 146.4 (C-3'), 134.9 (C-3), 123.1 (C-1'), 122.9 (C-6'), 116.8 (C-5'), 116.4 (C-2'), 109.5 (C-1"), 105.7 (C-10), 99.9 (C-6), 94.8 (C-8), 88.0 (C-4"), 83.3 (C-2"), 78.7 (C-3"), 62.5 (C-5")

• Biological activities in the literature

analgesic, anti-inflammation, protective cell death from oxidative stress

• Other data in the literature

1. Optical Rotation:  $[\alpha]_{22}^D = -241$

2. UV (EtOH)  $\lambda_{max}nm$ : 260 and 360

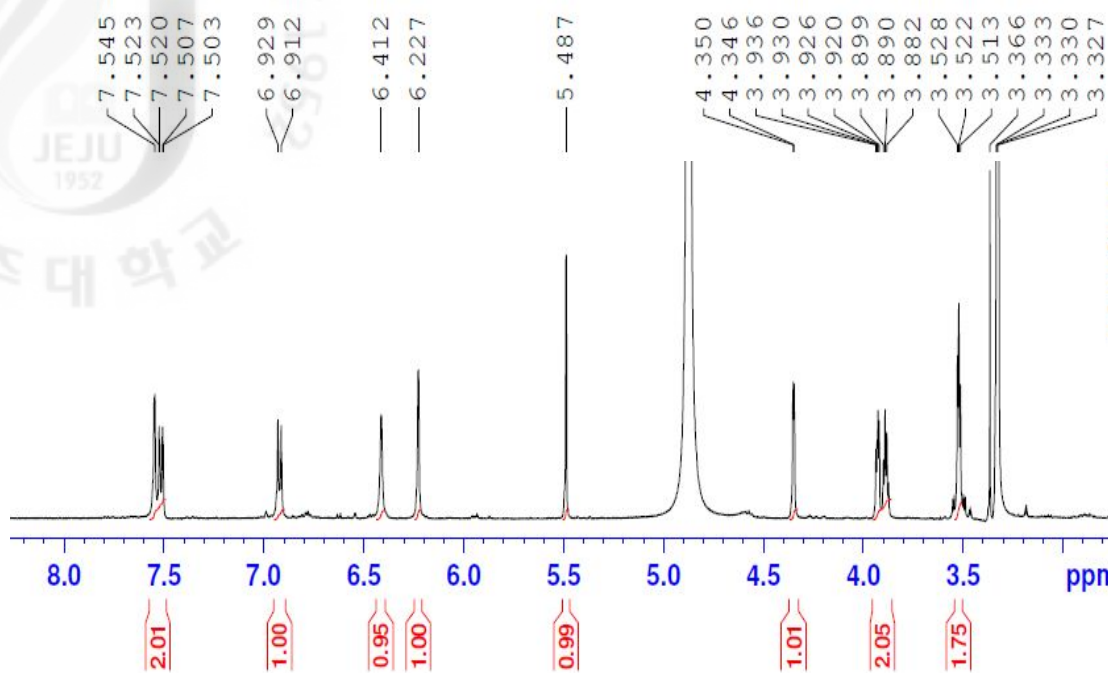


Figure 31.  $^1\text{H-NMR}$  spectrum of quercetin-3-*O*- $\alpha$ -L-arabinofuranoside (**8**) in  $\text{CD}_3\text{OD}$

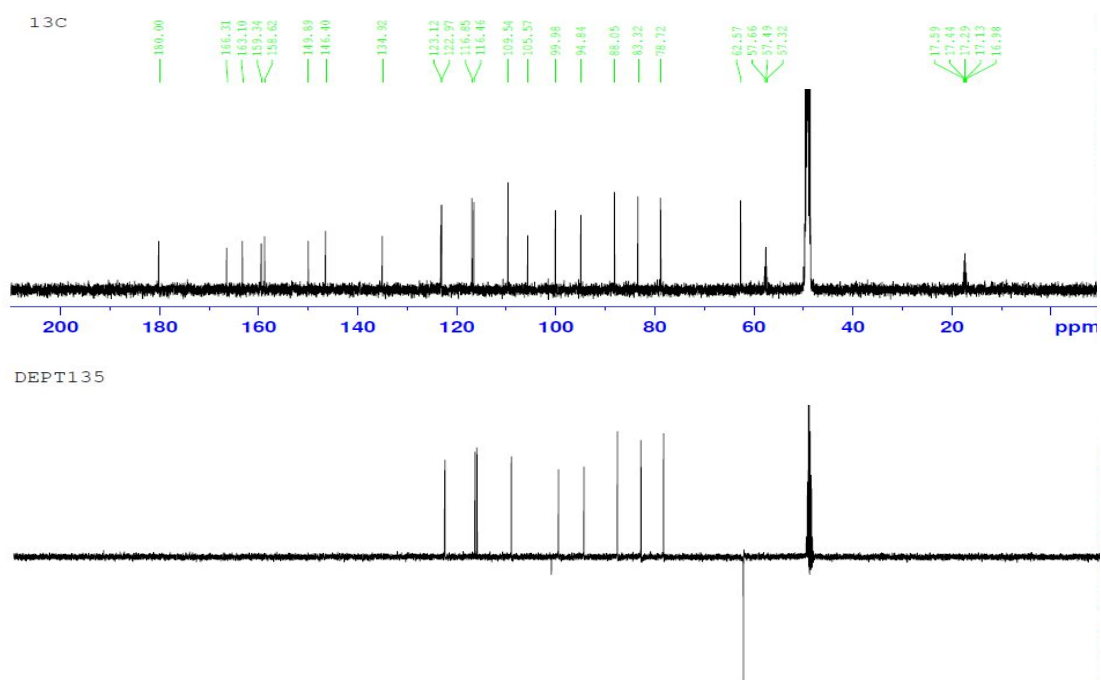


Figure 32.  $^{13}\text{C-NMR}$  and DEPT135 spectra of quercetin-3-*O*- $\alpha$ -L-arabinofuranoside (**8**) in  $\text{CD}_3\text{OD}$

Compound **8** was isolated as amorphous yellow powder. The  $^1\text{H}$  and  $^{13}\text{C}$ -NMR spectra of compound **8** in  $\text{CD}_3\text{OD}$  was similar to those of compound 7 except for moiety of sugar (Fig. 30). Analysis of the chemical shifts, signal multiplicities, absolute values of the coupling constants, and their magnitude in the  $^1\text{H}$  and  $^{13}\text{C}$ -NMR spectrum indicated the presence of one arabinofuranosyl residue with  $\alpha$ -configuration with the anomeric proton at  $\delta_{\text{H}}$  5.46 (1H, *s*, H-1'') (Fig. 31-32). The HMBC spectrum showed a correlation between the H-1'' and C-3. The compound **8** was identified as quercetin-3-*O*- $\alpha$ -L-arabinofuranoside (avicularin) (Fig. 33).<sup>61-62,64</sup> Avicularin was reported for the first time from this plant.

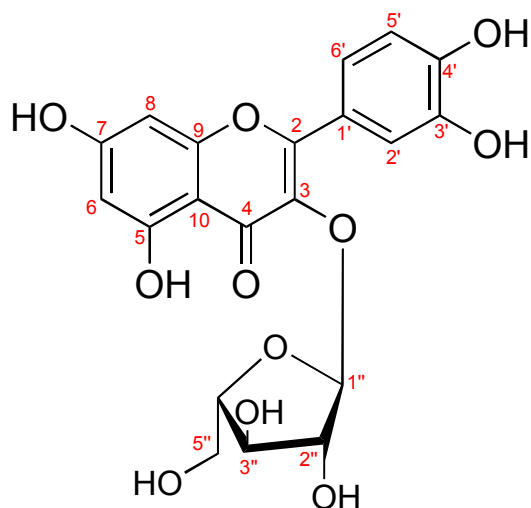


Figure 33. Structure of compound **8**; quercetin-3-*O*- $\alpha$ -L-arabinofuranoside (avicularin)



### 5-1-9. Compound 9

- Compound Name kaempferol-3-*O*- $\alpha$ -L-rhamnoside; Afzelin
- Synonym(s) kaempferol 3-rhamnoside, afzeloside, kaempferin
- CAS Registry Number 482-39-3
- Appearance amorphous yellow powder
- Chemical Formula  $C_{21}H_{20}O_{11}$
- Molecular Weight (g/mol) 432.10
- Melting Point ( $^{\circ}C$ ) 172 - 174
- $^1H$ -NMR (500 MHz,  $CD_3OD$ )  
 $\delta$ : 7.77 (2H, *d*,  $J = 9.0$  Hz, H-2', 6'), 6.93 (2H, *d*,  $J = 9.0$  Hz, H-3', 5'), 6.37 (1H, *d*,  $J = 2.0$  Hz, H-6), 6.20 (1H, *d*,  $J = 2.0$  Hz, H-8), 5.37 (1H, *d*,  $J = 1.5$  Hz, H-1"), 4.21 (1H, *dd*,  $J = 1.5, 3.0$  Hz, H-2"), 3.70 (1H, *dd*,  $J = 3.0, 9.0$  Hz, H-3"), 0.92 (3H, *d*,  $J = 5.5$  Hz, H-6")
- $^{13}C$ -NMR (125 MHz,  $CD_3OD$ )  
 $\delta$ : 179.7 (C-4), 166.4 (C-7), 163.3 (C-5), 161.7 (C-4'), 159.4 (C-9), 158.7 (C-2), 136.3 (C-3), 132.0 (C-6'), 132.0 (C-2'), 122.8 (C-1'), 116.6 (C-3'), 116.6 (C-5'), 105.9 (C-10), 103.6 (C-1"), 100.1 (C-6), 95.0 (C-8), 73.3 (C-4"), 72.2 (C-3"), 72.1 (C-2"), 72.0 (C-5"), 17.8 (C-6")
- Other data in the literature
  1. Biological Source: Isol. from *Afzelia* sp. heartwood and many other plant spp. incl. ferns

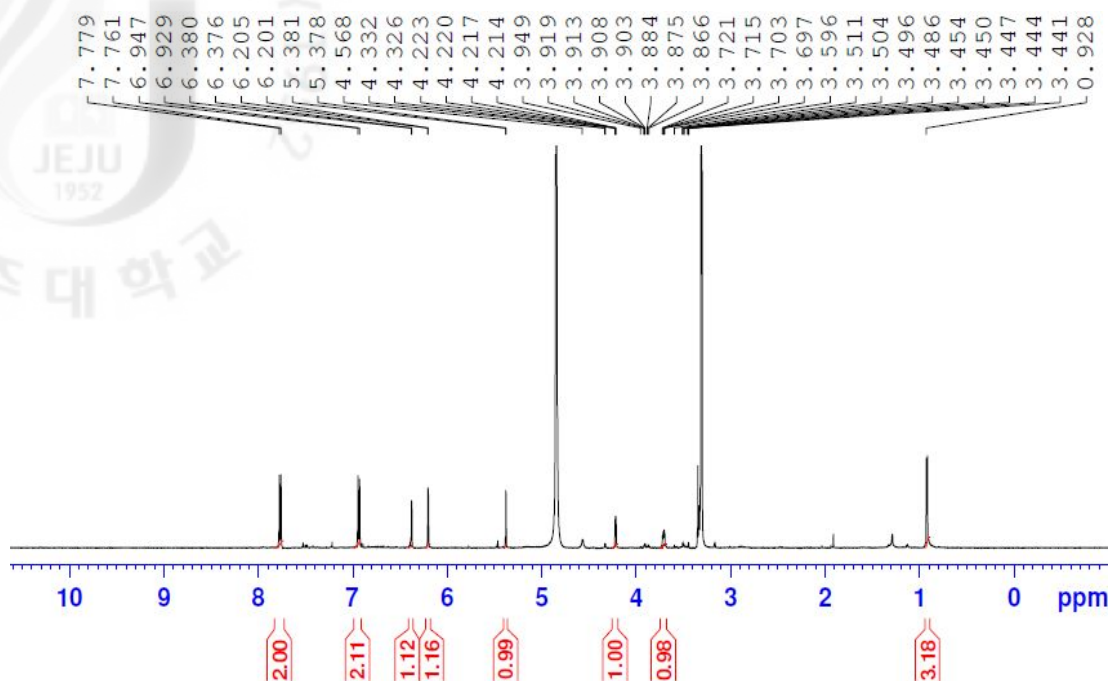


Figure 34.  $^1\text{H-NMR}$  spectrum of kaempferol-3-*O*- $\alpha$ -L-rhamnoside (9) in  $\text{CD}_3\text{OD}$

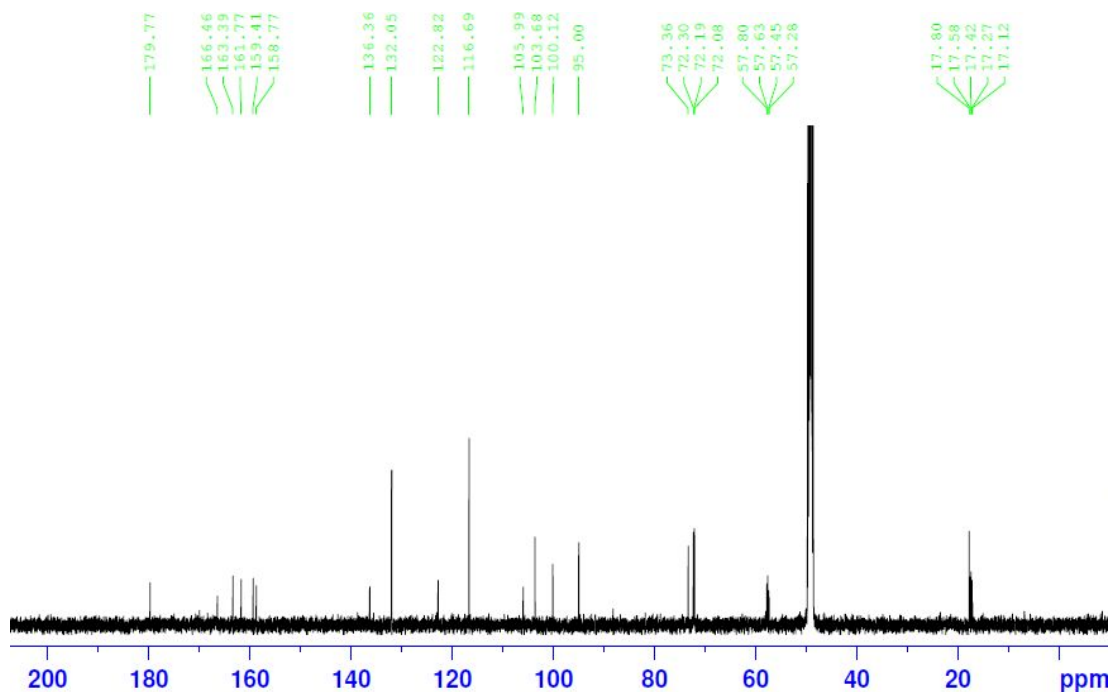


Figure 35.  $^{13}\text{C-NMR}$  spectrum of kaempferol-3-*O*- $\alpha$ -L-rhamnoside (9) in  $\text{CD}_3\text{OD}$

Compound **9** was isolated as amorphous yellow powder. The  $^1\text{H}$  and  $^{13}\text{C}$ -NMR spectra of compound **9** in  $\text{CD}_3\text{OD}$  was eventually identified by NMR by comparison with literature data.<sup>61-62</sup> The  $^1\text{H}$  and  $^{13}\text{C}$ -NMR spectroscopic data of compound **9** exhibited a characteristic pattern of kaempferol aglycone with a sugar attached at 3 position (Fig. 34-35). The signal of anomeric proton at  $\delta_{\text{H}}$  5.37 appeared as a  $J = 1.5$  Hz doublet, along with the downfield shift of the carbon resonance ( $\delta_{\text{C}}$  103.6), indicated a  $\alpha$ -configuration. The sugar moiety was completely elucidated as rhamnoside thus allowing this compound to be identified as kaempferol-3- $O$ - $\alpha$ -L-rhamnoside (afzelin) (Fig. 36).<sup>61-62,63</sup> Afzelin was reported for the first time from this plant.

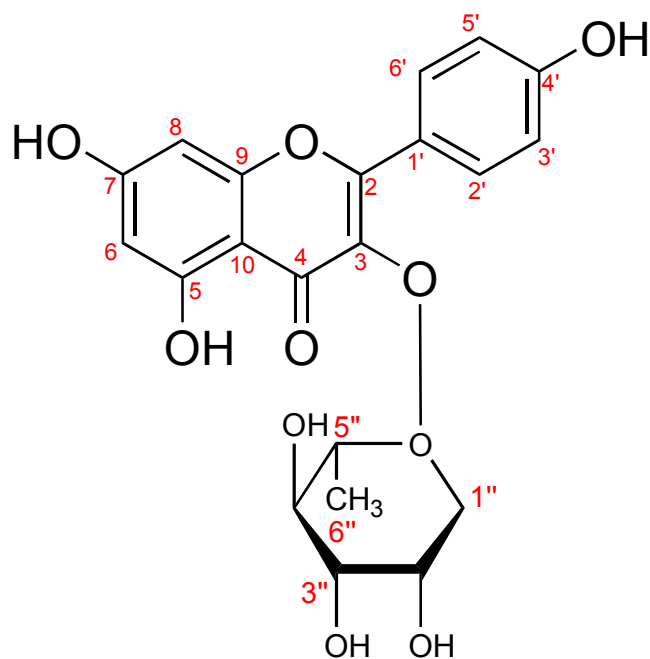


Figure 36. Structure of compound **9**; Kaempferol-3- $O$ - $\alpha$ -L-rhamnoside (afzelin)

5-1-10. Compound **10**

- Compound Name 2'-Hydroxy-3',4',5',6'-tetramethoxychalcone;  
2',3,4',5',6'-pentahydroxychalcone;2',3',4',5'-Tetra-Me ether;  
kanakugiol
- Synonym(s) 1-(2-Hydroxy-3,4,5,6-tetramethoxyphenyl)-3-phenyl-2-propen-1-one, 2'-Hydroxy-3',4',5',6'-tetramethoxychalcone.
- CAS Registry Number 57499-44-2
- Appearance yellow oil
- Chemical Formula  $C_{19}H_{20}O_6$
- Molecular Weight (g/mol) 344.12
- Melting Point ( $^{\circ}C$ ) -
- $^1H$ -NMR (500 MHz,  $CD_3OD$ )  
 $\delta$ : 7.68 and 7.62 (2H, *d*,  $J_{AB} = 15.0$  Hz, H-2 and H-3), 7.66 (2H, *m*, H-2" and H-6"), 7.43 (3H, *m*, H-3", H-4" and H-5"), 4.03 (3H, *s*, 6'-OMe), 3.86 (3H, *s*, 3'-OMe), 3.84 (3H, *s*, 5'-OMe), 3.83 (3H, *s*, 4'-OMe)
- $^{13}C$ -NMR (125 MHz,  $CD_3OD$ )  
 $\delta$ : 195.6 (C-1), 153.5 (C-6'), 152.4 (C-5'), 151.3 (C-2'), 145.7 (C-3), 140.3 (C-4'), 138.7 (C-3'), 136.5 (C-1"), 131.8 (C-2), 130.2 (C-2", 6"), 129.7 (C-3", 5"), 128.4 (C-4"), 114.5 (C-1'), 62.7 (C-6'-OMe), 62.0 (C-3'-OMe), 61.9 (C-5'-OMe), 61.6 (C-4'-OMe)
- Biological activities in the literature  
antifungal, inhibition of chitin synthase 2
- Other data in the literature
  1. Biological Source: Isol. from *Didymocarpus pedicellata* and *Popowia cauliflor*
  2. UV (MeOH)  $\lambda_{max}nm$ : 208 and 314

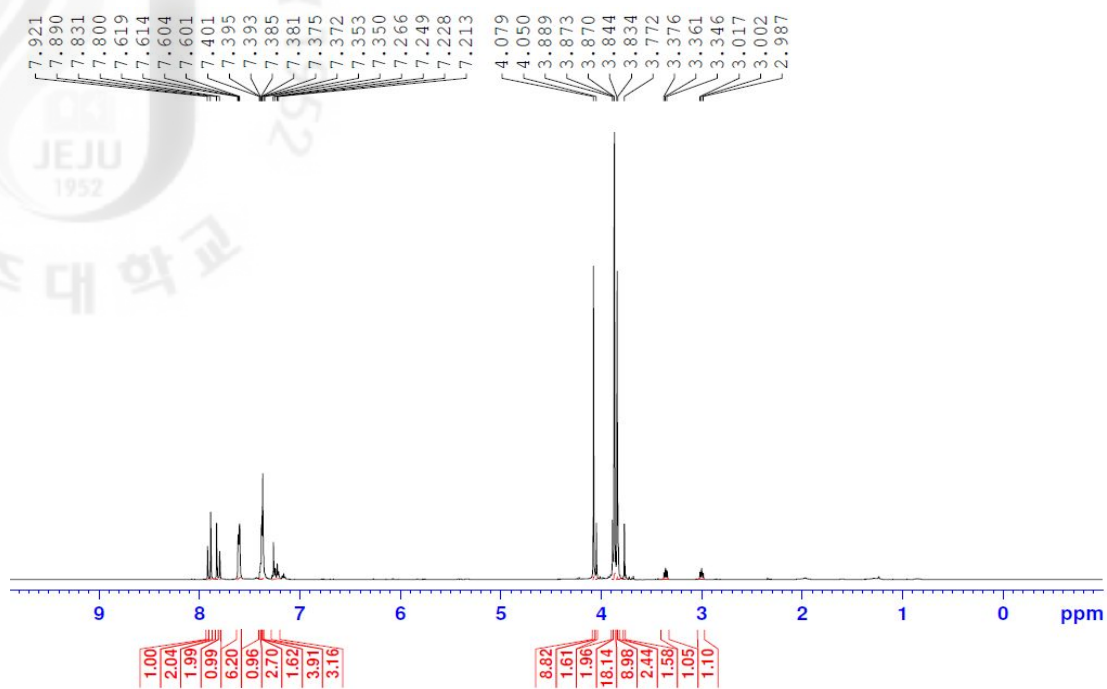


Figure 37.  $^1\text{H-NMR}$  spectrum of kanakugiol (**10**) in  $\text{CD}_3\text{OD}$

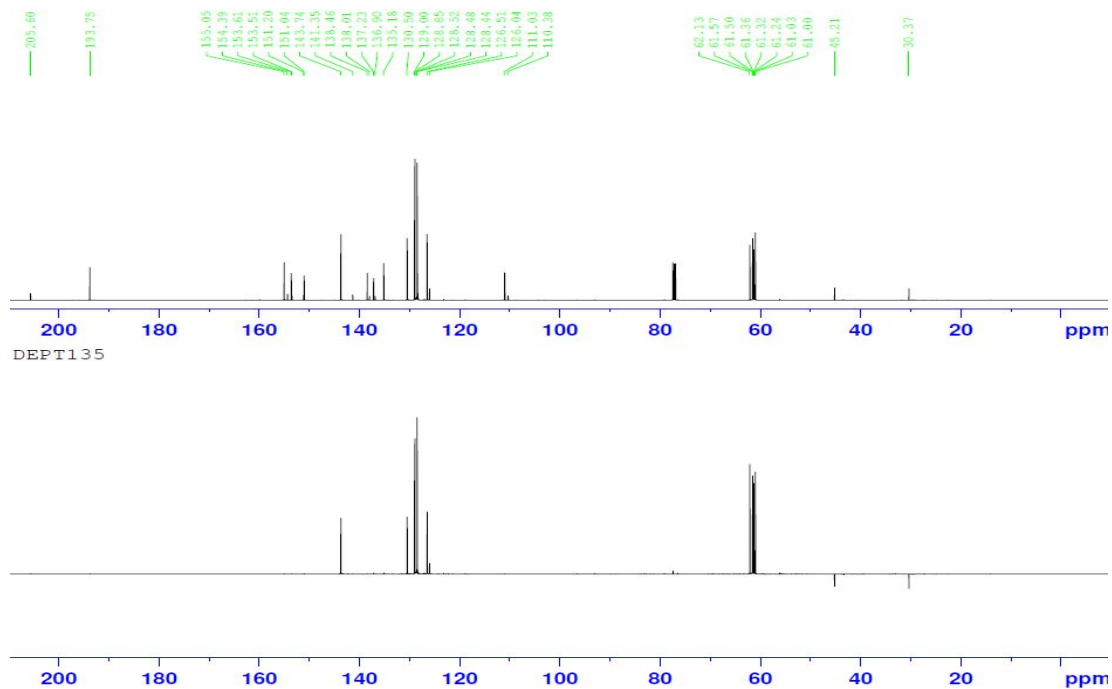


Figure 38.  $^{13}\text{C-NMR}$  and DEPT135 spectra of kanakugiol (**10**) in  $\text{CD}_3\text{OD}$

Compound **10** was isolated as yellow oil. The  $^1\text{H}$  and  $^{13}\text{C}$ -NMR spectra of compound **10** showed a keto group peak at  $\delta_{\text{C}}$  195.6 (C-1), four methoxyl carbons at  $\delta_{\text{C}}$  62.7 (C-6'-OMe), 62.0 (C-3'-OMe), 61.9 (C-5'-OMe) and 61.6 (C-4'-OMe) (Fig. 38), and  $\delta_{\text{H}}$  4.03 (3H, *s*, 6'-OMe), 3.86 (3H, *s*, 3'-OMe), 3.84 (3H, *s*, 5'-OMe) and 3.83 (3H, *s*, 4'-OMe) (Fig. 37). The mono substituted aromatic hydrogen peaks appear at  $\delta_{\text{H}}$  7.66 (2H, *m*, H-2'' and H-6'') and 7.43 (3H, *m*, H-3'', H-4'' and H-5'') (Fig. 37). The twelve aromatic carbon peaks appear  $\delta_{\text{C}}$  153.5 (C-6'), 152.4 (C-5'), 151.3 (C-2'), 145.7 (C-3), 140.3 (C-4'), 138.7 (C-3'), 136.5 (C-1''), 131.8 (C-2), 130.2 (2C, C-2''/6''), 129.7 (2C, C-3''/5''), 128.4 (C-4'') and 114.5 (C-1') (Fig. 38). Especially, 131.8 (C-2) and 145.7 (C-3) correlated to 7.68 and 7.62 (2H, *d*,  $J_{\text{AB}} = 15.0$  Hz, H-2 and H-3) in HMQC spectrum (Data did not shown). Thus, the structure of **10** was determined to be 2'-Hydroxy-3',4',5',6'-tetramethoxychalcone (kanakugiol) (Fig. 39). This was confirmed by spectral data comparison with published data.<sup>61,66)</sup>

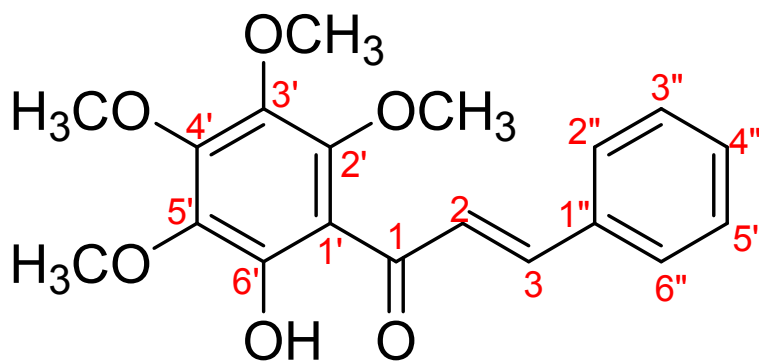


Figure 39. Structure of compound **10**; 2'-Hydroxy-3',4',5',6'-tetramethoxychalcone (kanakugiol)

5-1-11. Compound **11**

• Compound Name                    methyllucidone

• Synonym(s)                            -

• CAS Registry Number            19956-54-8

• Appearance                         yellow solid

• Chemical Formula                 $C_{16}H_{14}O_4$

• Molecular Weight (g/mol)    270.07

• Melting Point (°C)                126 - 128

•  $^1H$ -NMR (500 MHz,  $CDCl_3$ )

$\delta$ : 7.96 (1H, *d*,  $J = 12.8$  Hz, H-7), 7.57 (3H, *m*, H-2, 6, 8), 7.34 (3H, *m*, H-3, 4, 5), 5.90 (1H, *s*, H-4'), 4.16 (3H, *s*, 3'-OMe), 3.89 (3H, *s*, 9-OMe)

•  $^{13}C$ -NMR (125 MHz,  $CDCl_3$ )

$\delta$ : 191.8 (C-2'), 188.4 (C-5'), 170.1 (C-3'), 169.1 (C-9), 143.0 (C-8), 135.5 (C-1), 130.5 (C-4), 129.1 (C-3, 5), 128.8 (C-2, 6), 121.6 (C-7), 112.3 (C-4'), 109.6 (C-1'), 65.1 (3'-OMe), 58.7 (9-OMe)

• Biological activities in the literature

farnesyl protein transferase inhibitor, anti-tumor

• Other data in the literature

1. Biological Source: Isol. from *Lindera* spp.

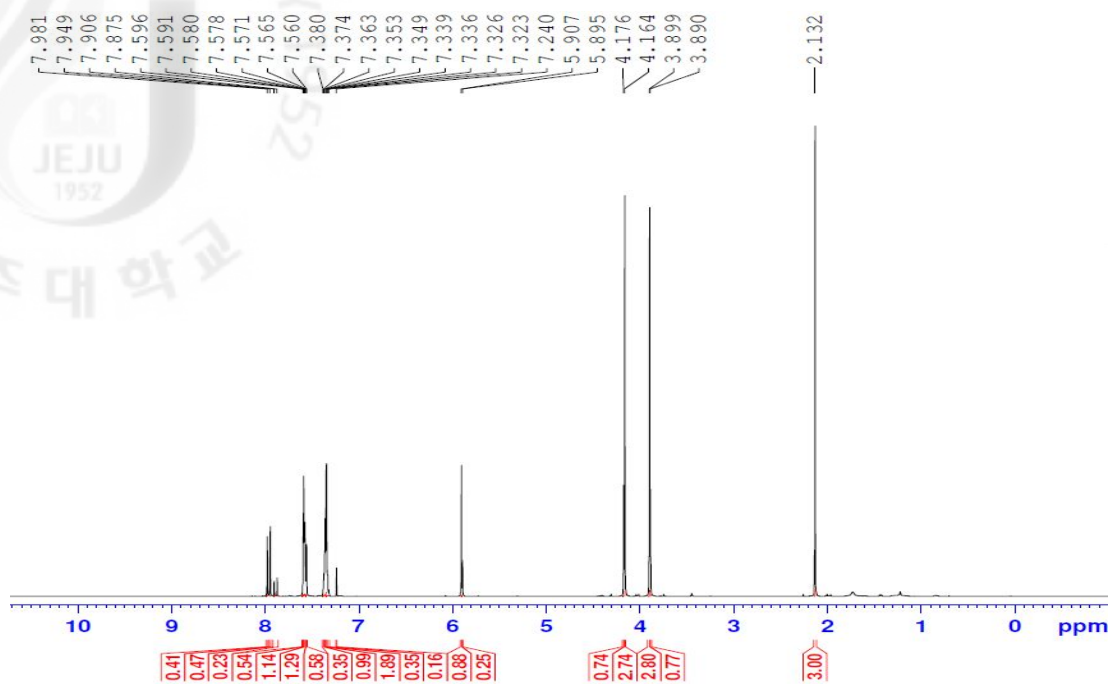


Figure 40.  $^1\text{H}$ -NMR spectrum of methyl lucidone (**11**) in  $\text{CDCl}_3$

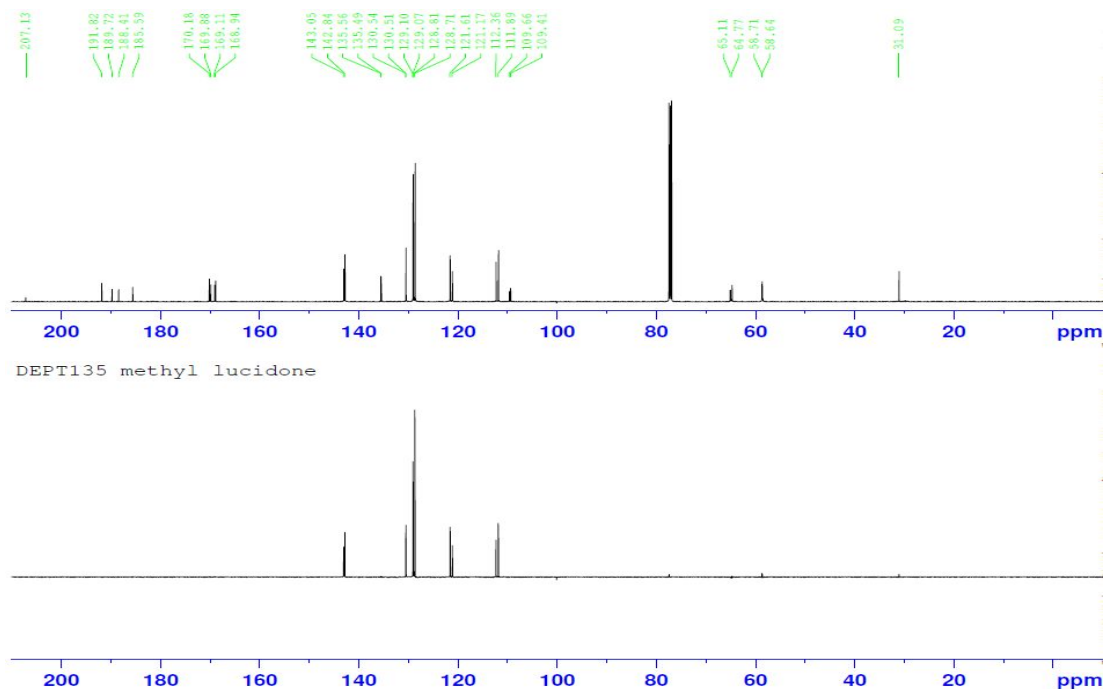


Figure 41.  $^{13}\text{C}$ -NMR and DEPT135 spectra of methyl lucidone (**11**) in  $\text{CDCl}_3$



Compound **11** was isolated as yellow solid. The  $^1\text{H}$  and  $^{13}\text{C}$ -NMR spectra of compound **11** in  $\text{CDCl}_3$  was similar to those of compound **3** except for a substituent on  $\delta_{\text{H}}$  3.89 (3H, *s*, 9-OMe) and  $\delta_{\text{C}}$  58.7 (9-OMe) (Fig. 16, 17, 40, 41). Thus, the structure of **11** was determined as methyllicudone by comparison of its spectral data with those in the literature (Fig. 42).<sup>66)</sup>

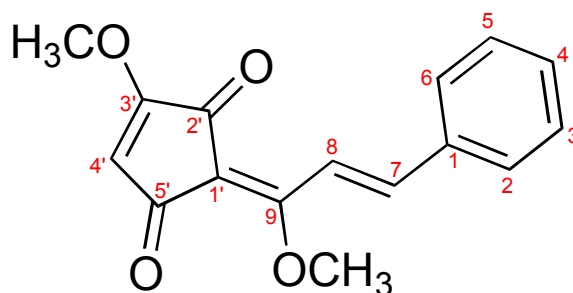


Figure 42. Structure of compound **11**; Methyllicudone

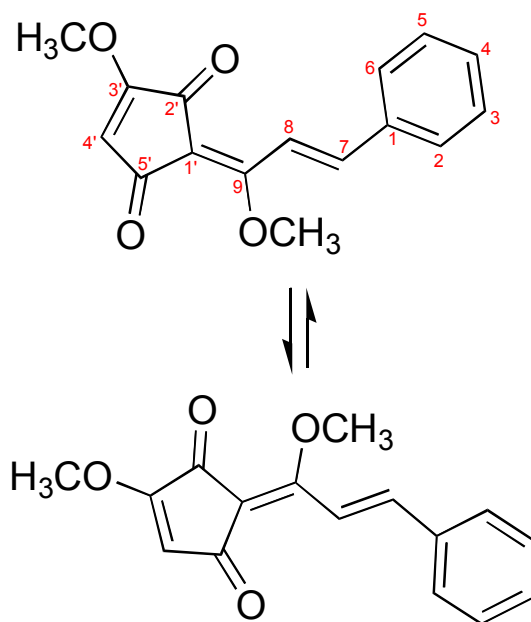


Figure 43. Expectative tautomers of methyllicudone (**11**)

5-1-12. Compound 12

- Compound Name stigmastera-5,22-dien-3-ol; (3 $\beta$ ,22*E*,24*S*)-form; stigmasterol
- Synonym(s) serposterol
- CAS Registry Number 83-48-7

• Appearance colorless needle

• Chemical Formula C<sub>29</sub>H<sub>48</sub>O

• Molecular Weight (g/mol) 412.69

• Melting Point (°C) 156 - 157

• <sup>1</sup>H-NMR (500 MHz, CDCl<sub>3</sub>)

$\delta$ : 5.13 (1H, *m*, H-6), 5.13 (1H, *dd*, *J* = 9.0, 15.0 Hz, H-22), 4.99 (1H, *dd*, *J* = 5.0, 15.0 Hz, H-23), 3.58 (1H, *m*, H-3), 1.23 (3H, *s*, Me-19), 1.00 (3H, *d*, *J* = 6.5 Hz, H-21), 0.82 (3H, *t*, *J* = 7.5 Hz, H-29), 0.82 (3H, *d*, *J* = 6.0 Hz, H-26), 0.78 (3H, *d*, *J* = 4.0 Hz, H-27), 0.51 (3H, *s*, Me-18)

• <sup>13</sup>C-NMR (125 MHz, CDCl<sub>3</sub>)

$\delta$ : 139.8 (C-5), 138.4 (C-22), 129.6 (C-23), 117.6 (C-6), 71.3 (C-3), 56.1 (C-14), 55.3 (C-17), 51.4 (C-24), 49.69 (C-9), 43.5 (C-13), 41.0 (C-4), 40.5 (C-20), 39.8 (C-12), 39.7 (C-1), 37.0 (C-10), 34.4 (C-8), 32.1 (C-7), 31.7 (C-25), 29.8 (C-2), 28.7 (C-16), 25.6 (C-28), 23.3 (C-15), 21.7 (C-11), 21.6 (C-26), 21.3 (C-21), 19.2 (C-19), 13.2 (C-26), 12.4 (C-29), 12.2 (C-18)

• Biological activities in the literature

anti-mutagenic, anti-hyperlipidemic

• Other data in the literature

1. Optical Rotation:  $[\alpha]_D^{22} = -57$  (CHCl<sub>3</sub>)

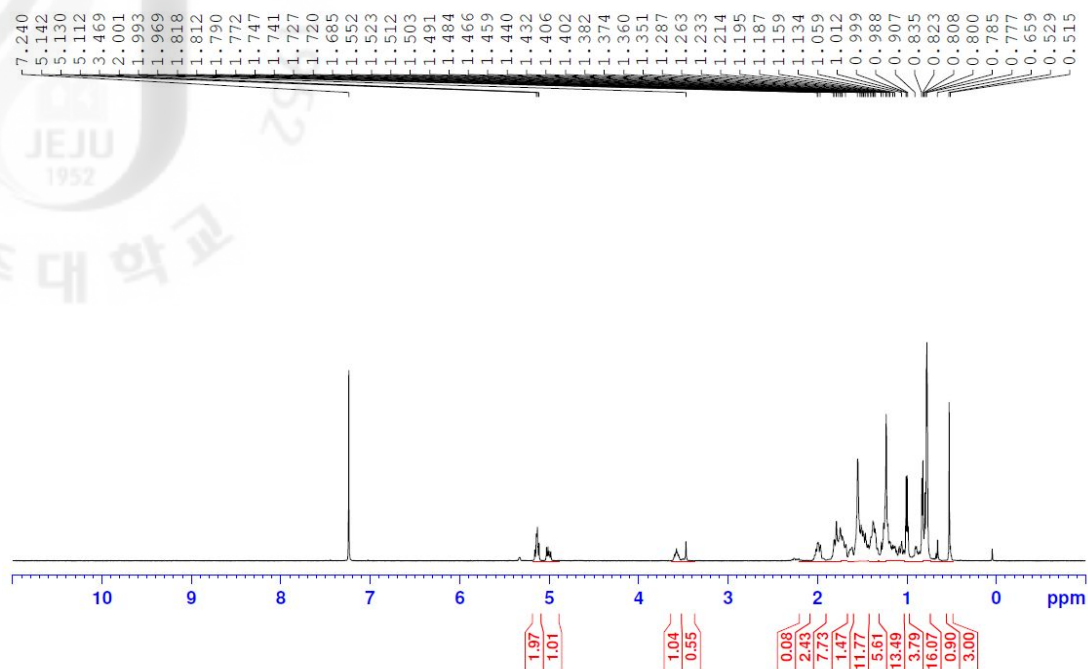


Figure 44.  $^1\text{H}$ -NMR spectrum of stigmasterol (**12**) in  $\text{CDCl}_3$

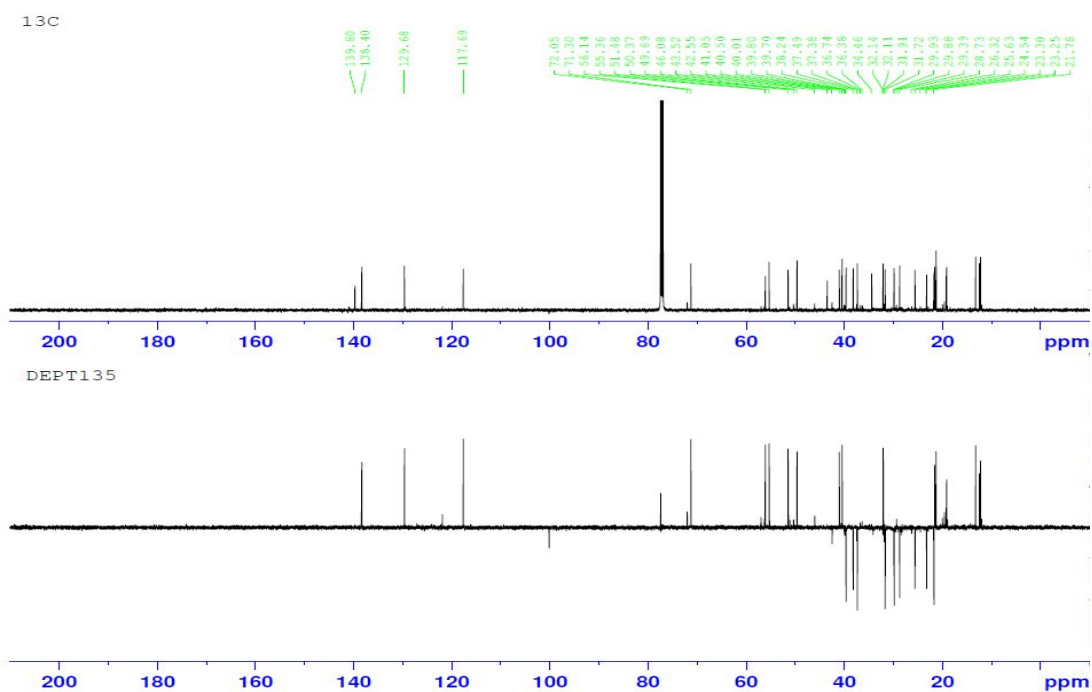


Figure 45.  $^{13}\text{C}$ -NMR and DEPT135 spectra of stigmasterol (**12**) in  $\text{CDCl}_3$

Compound **12** isolated as colorless needle. The  $^1\text{H-NMR}$  spectrum of compound **12** in  $\text{CDCl}_3$  showed two methyl singlet signals at  $\delta_{\text{H}}$  1.23 (3H, *s*, Me-19), 0.51 (3H, *s*, Me-18). The peak of olefinic proton showed at  $\delta_{\text{H}}$  5.13 (1H, *m*, H-6), 5.13 (1H, *dd*,  $J = 9.0, 15.0$  Hz, H-22), and 4.99 (1H, *dd*,  $J = 5.0, 15.0$  Hz, H-23). Three methyl doublets at  $\delta_{\text{H}}$  1.00 (3H, *d*,  $J = 6.5$  Hz, H-21), 0.82 (3H, *d*,  $J = 6.0$  Hz, H-26), 0.78 (3H, *d*,  $J = 4.0$  Hz, H-27), a methyl triplet at  $\delta_{\text{H}}$  0.82 (3H, *t*,  $J = 7.5$  Hz, H-29) were appeared (Fig. 44). A comparison with  $\beta$ -sitosterol suggested that both compounds had the same side chain (Fig. 47), while the presence of the olefinic protons identified its structure. Thus, the structure of compound **12** was determined as stigmasterol by comparison its spectral data with those of literature (Fig. 46).<sup>68,69</sup>

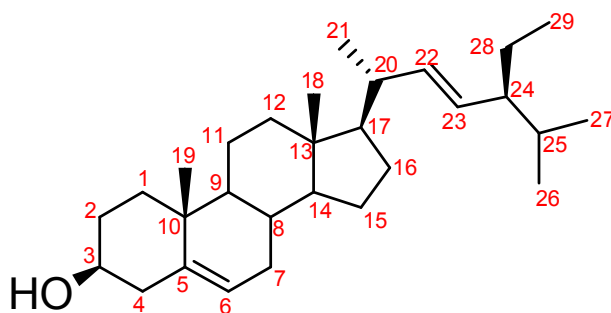


Figure 46. Structure of compound **12**; stigmasterol

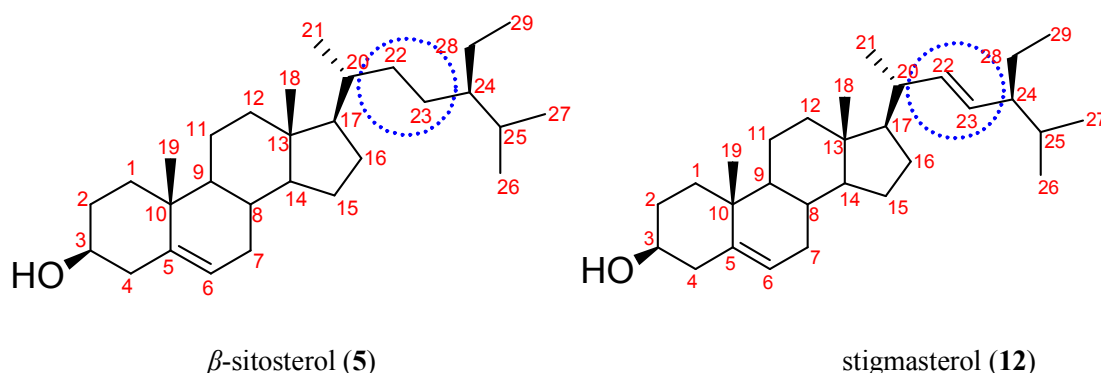


Figure 47. Comparison on each olefinic structure of 22, 23-position between  $\beta$ -sitosterol and stigmasterol

5-1-13. Compound **13**

- Compound Name 1-(2'-hydroxy-3',4',5',6'-tetramethylphenyl)-1-methoxy-3-phenylpropane
- Synonym(s)
- CAS Registry Number - (new compound)
- Appearance greenish viscous oil
- Chemical Formula  $C_{20}H_{26}O_6$
- Molecular Weight (g/mol) 362. 1629
- Melting Point ( $^{\circ}C$ ) -
- $^1H$ -NMR (500 MHz, Acetone- $d_6$ )  
 $\delta$ : 8.8 (1H, *s*, 2'-OH), 7.27 (2H, *t*,  $J = 7.5$  Hz, H-3'', 5''), 7.22 (2H, *d*,  $J = 7.5$  Hz, H-2'', 6''), 7.16 (1H, *t*,  $J = 7.5$  Hz, H-4''), 4.71 (1H, *dd*,  $J = 8.5, 4.5$  Hz, H-1), 3.87 (3H, *s*, 5'-OCH<sub>3</sub>), 3.78 (3H, *s*, 3'-OCH<sub>3</sub>), 3.76 (3H, *s*, 4'-OCH<sub>3</sub>), 3.72 (3H, *s*, 6'-OCH<sub>3</sub>), 3.34 (3H, *s*, 1-OCH<sub>3</sub>), 2.82 (1H, *ddd*,  $J = 15.0, 9.5, 4.0$  Hz, H-3 $\beta$ ), 2.65 (1H, *ddd*,  $J = 15.0, 9.0, 7.5$  Hz, H-3 $\alpha$ ), 2.26 (1H, *m*, H-2 $\beta$ ), 1.98 (1H, *m*, H-2 $\alpha$ )
- $^{13}C$ -NMR (125 MHz, Acetone- $d_6$ )  
 $\delta$ : 146.5 (C-2'), 142.8 (C-1''), 138.6 (C-3'), 148.4 (C-6'), 148.0 (C-5'), 140.3 (C-4'), 129.4 (C-2'', 6''), 129.2 (C-3'', 5''), 126.6 (C-4''), 115.3 (C-1'), 78.9 (C-1), 61.4 (3'-OCH<sub>3</sub>), 61.4 (4'-OCH<sub>3</sub>), 61.5 (5'-OCH<sub>3</sub>), 61.1 (6'-OCH<sub>3</sub>), 57.5 (1-OCH<sub>3</sub>), 37.8 (C-2), 32.8 (C-3)
- Other data
  1. HR-FAB MS :  $m/z$  385.1629 [M+Na] $^+$  (calcd. for  $C_{20}H_{26}O_6Na$  385.1627,  $\Delta + 0.2$  *mamu*)
  2. UV (MeOH)  $\lambda_{max}nm$ : 216 and 285
  3. Optical Rotation :  $[\alpha]_D^{22} = + 4.49^{\circ}$  (*c* 0.025, MeOH)

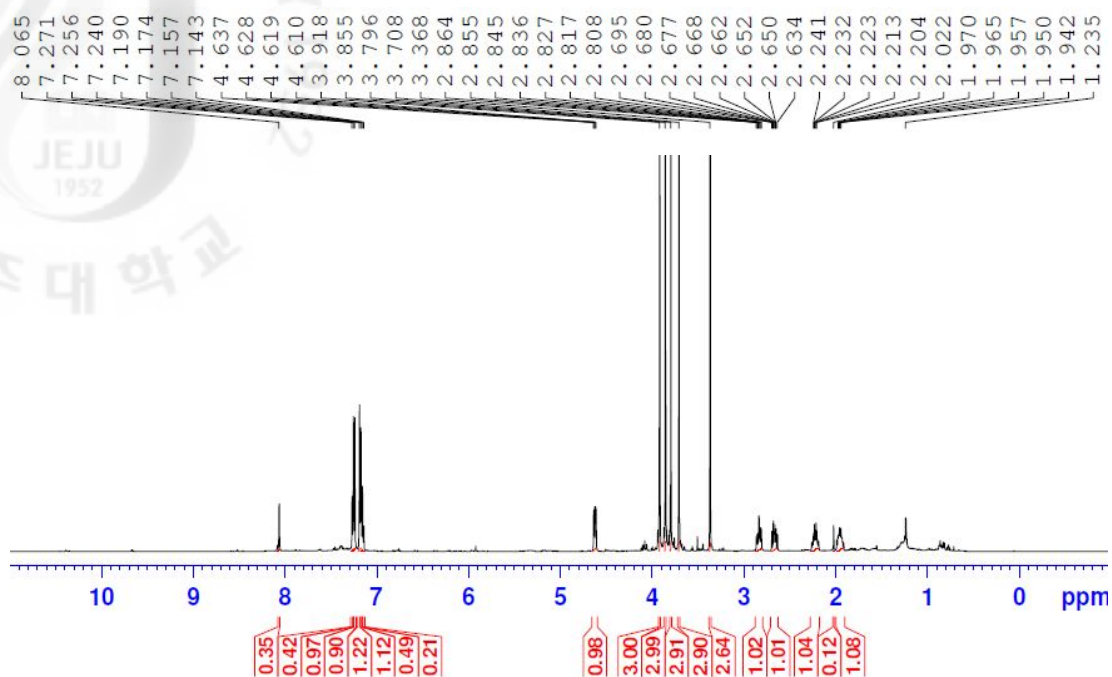


Figure 48.  $^1\text{H-NMR}$  spectrum of 1-(2-(2'-hydroxy-3',4',5',6'-tetramethylphenyl)-1-methoxy-3-phenylpropane (**13**) in  $\text{CDCl}_3$

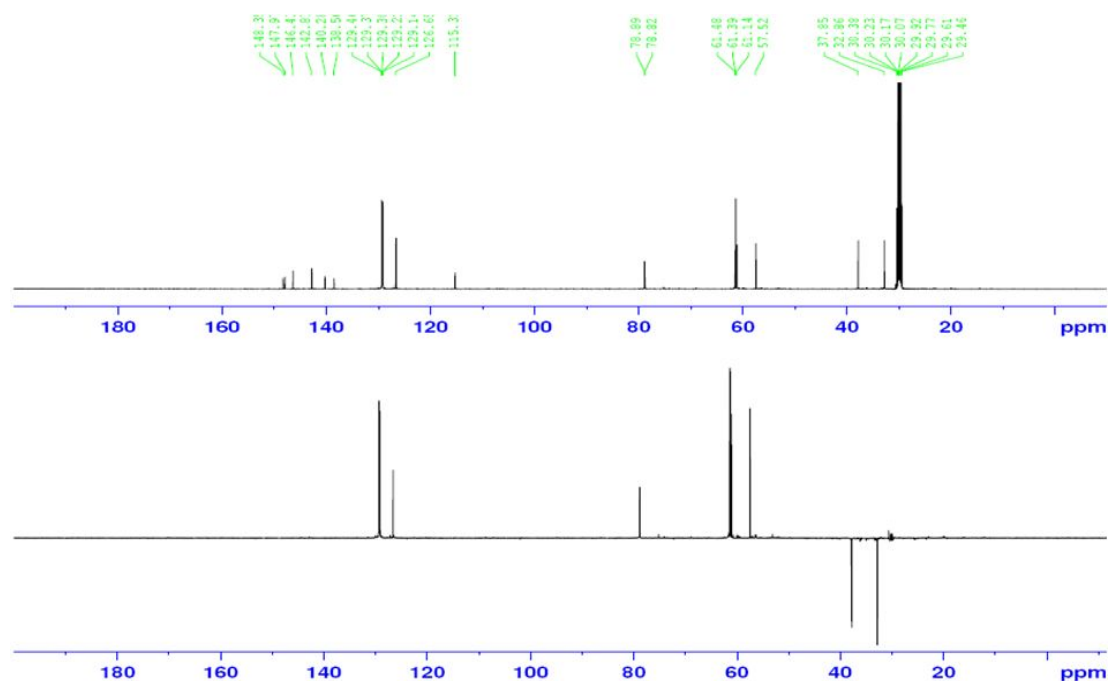


Figure 49.  $^{13}\text{C-NMR}$  and DEPT135 spectra of 1-(2-(2'-hydroxy-3',4',5',6'-tetramethylphenyl)-1-methoxy-3-phenylpropane (**13**) in  $\text{CDCl}_3$

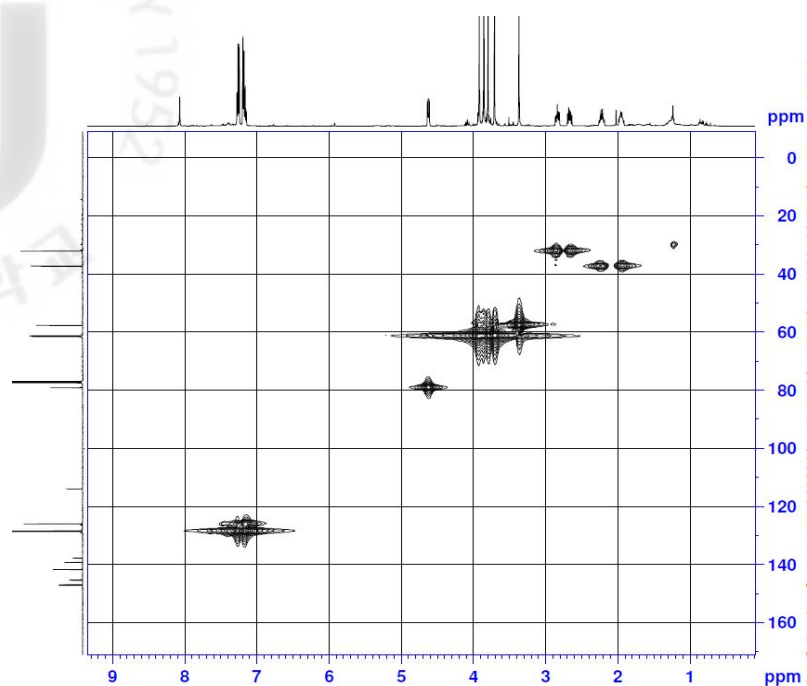


Figure 50. HMQC spectrum of 1-(2'-hydroxy-3',4',5',6'-tetramethylphenyl)-1-methoxy-3-phenylpropane (**13**) in  $\text{CDCl}_3$

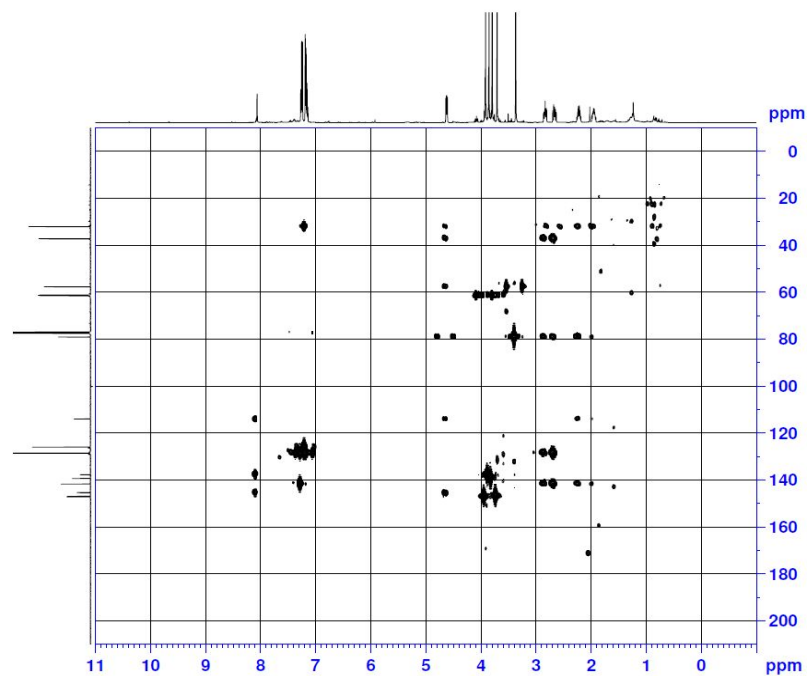


Figure 51. HMBC spectrum of 1-(2'-hydroxy-3',4',5',6'-tetramethylphenyl)-1-methoxy-3-phenylpropane (**13**) in  $\text{CDCl}_3$

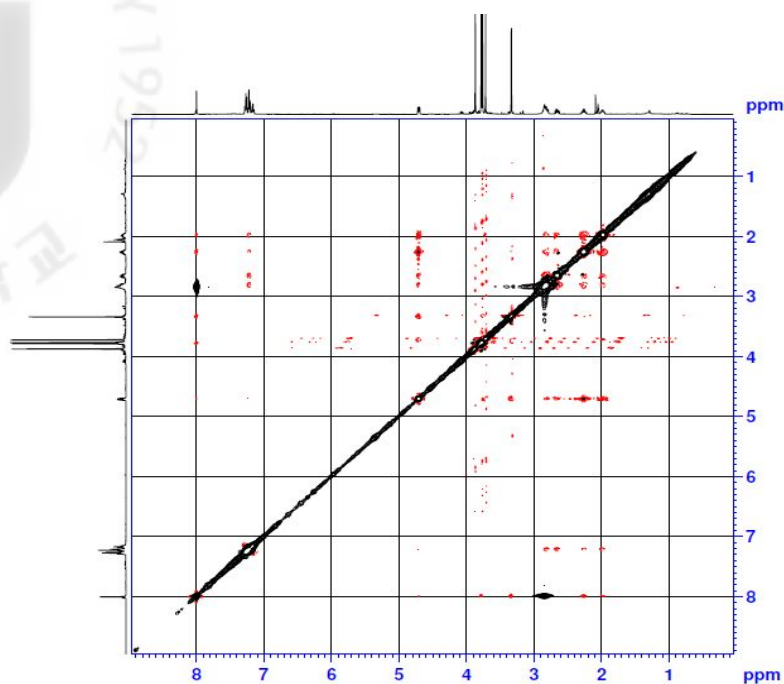


Figure 52. NOESY spectrum of 1-(2'-hydroxy-3',4',5',6'-tetramethylphenyl)-1-methoxy-3-phenylpropane (**13**) in  $\text{CDCl}_3$

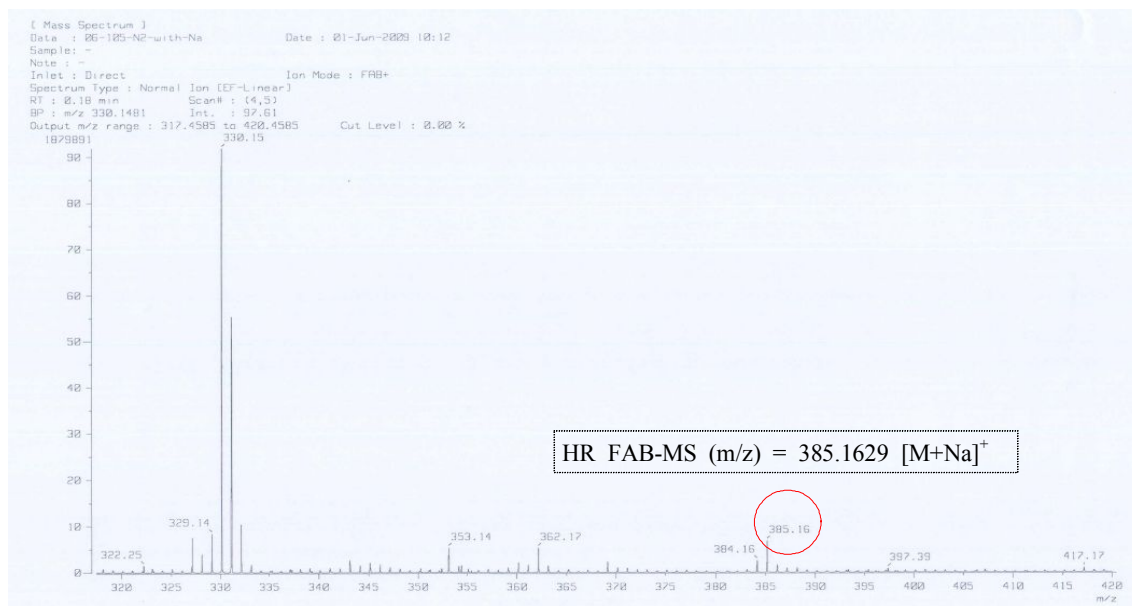


Figure 53. HR FAB MS spectrum of 1-(2'-hydroxy-3',4',5',6'-tetramethylphenyl)-1-methoxy-3-phenylpropane (**13**) in  $\text{CDCl}_3$



Compound **13** was obtained as a greenish viscous oil. It showed an  $[M+Na]^+$  peak at  $m/z$  385.1629 (calcd  $m/z$  385.1627) in the HR-FAB MS, consistent with the molecular formula  $C_{20}H_{26}O_6$  (eight unsaturations) (Fig. 53). Inspection of  $^{13}C$  and DEPT NMR spectra identified 18 signals accounting for ten aromatic carbons, five methoxy carbons, two methylene carbons and one oxygen-bearing methine carbon (Fig. 49). The presence of aromatic ring(s) were also supported by the UV absorption maxima at 216 and 285 nm (Data did not shown). One of the aromatic rings is inferred as phenyl group based on the observation of its typical  $^{13}C$  NMR peaks at  $\delta_C$  126.6, 129.2, 129.4 and 142.8 coupled with  $^1H$  NMR signals at  $\delta_H$  7.16 (1H, *t*,  $J = 7.5$  Hz), 7.22 (2H, *d*,  $J = 7.5$  Hz) and 7.27 (2H, *t*,  $J = 7.5$  Hz) (Fig. 50). It was evident that the other aromatic ring is fully substituted benzene as six quaternary  $sp^2$  carbon signals were identified in DEPT experiment. Besides the above-mentioned two aromatic rings, a linear  $C_3$  chain (-CH-CH<sub>2</sub>-CH<sub>2</sub>-) was also characterized by  $^1H$ ,  $^{13}C$  and COSY NMR data. The connection of these subunits were established using HMBC (heteronuclear multiple bond correlations) as well as NOESY NMR experiments (Fig. 54). The methine carbon ( $\delta$  78.9, C-1) in the propyl chain is connected to a methoxy group at  $\delta_H$  3.34, which was confirmed by its HMBC cross peak. The observation of  $^2J$  HMBC correlation between H-1 ( $\delta$  4.71) and C-1' ( $\delta$  115.3) indicated that ring A is attached to C-1. In the ring A, a hydroxy group is assigned to at C-6' as its proton ( $\delta$  8.0) showed correlations with C-1', C-5' and C-6' in HMBC spectrum. This hydroxy proton has NOESY correlations with neighboring protons in methoxy groups attached at C-1 and C-5', which also supports its position at C-6'. The other four methoxy groups were assigned to the remaining positions (C-2', C-3', C-4' and C-5') in the benzene ring A, which was further verified by each methoxy proton's  $^3J$  HMBC correlations with respective aromatic carbons (Fig. 52). Finally, the phenyl group was placed to the end of propyl carbon (C-3), which was corroborated by the HMBC cross peak between C-3 ( $\delta$  32.8) and H-2" ( $\delta$  7.22) in ring B (Fig. 51). From the above spectral data, compound **13** was identified as 1-(2'-hydroxy-3',4',5',6'-tetramethoxyphenyl)propane.

ylphenyl)-1-methoxy-3-phenylpropane (Fig. 55).<sup>70-73)</sup>

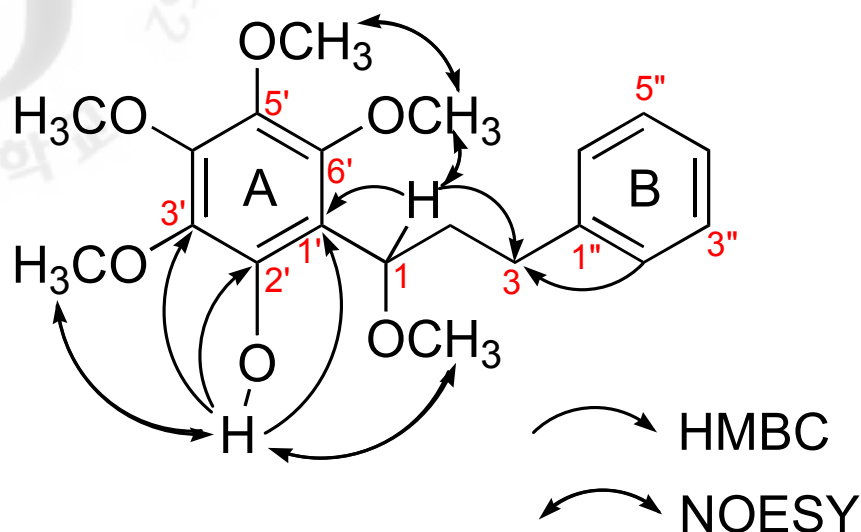
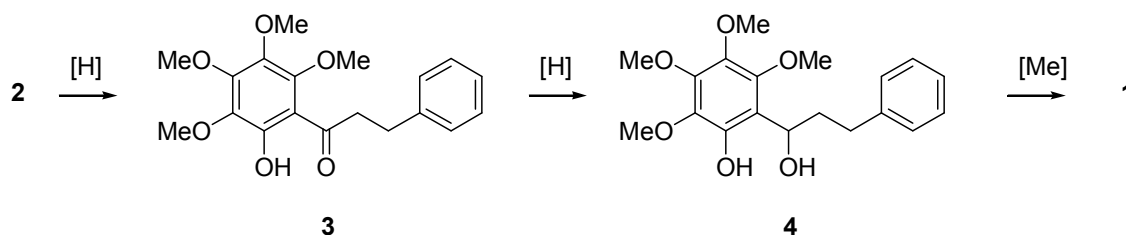


Figure 54. Important HMBC and NOESY correlations in 1-(2'-hydroxy-3',4',5',6'-tetramethylphenyl)-1-methoxy-3-phenylpropane (**13**)

The isolated 1-(2'-hydroxy-3',4',5',6'-tetramethylphenyl)-1-methoxy-3-phenylpropane (**13**) has the same molecular skeleton with kanakugiol (**10**), which was also isolated in this experiment. The kanakugiol (**10**) has previously been identified from this plant,<sup>61-62)</sup> and considered to be biosynthesized by polyketide condensation.



Scheme. 3. Proposed bio-synthetic pathway to 1-(2'-hydroxy-3',4',5',6'-tetramethylphenyl)-1-methoxy-3-phenylpropane (**13**) from kanakugiol (**10**)

It is interesting to suggest that the 1-(2'-hydroxy-3',4',5',6'-tetramethylphenyl)-1-methoxy-3-phenylpropane (**13**) is biologically induced from kanakugiol (**10**). As seen in the scheme 3, consecutive reductions of the enone **2** to the corresponding alcohol **4** and the following methylation should lead to the 1-(2'-hydroxy-3',4',5',6'-tetramethylphenyl)-1-methoxy-3-phenylpropane (**13**).

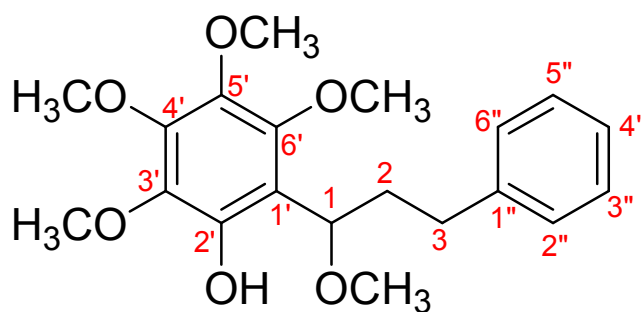


Figure 55. Structure of compound **13**; 1-(2'-hydroxy-3',4',5',6'-tetramethylphenyl)-1-methoxy-3-phenylpropane (new compound)

5-1-14. Compound **14**

- Compound Name linderone
- Synonym(s) 4,5-Dimethoxy-2-(1-oxo-3-phenyl-2-propenyl)-4-cyclopentene-1,3-dione
- CAS Registry Number 1782-79-2
- Appearance yellow solid
- Chemical Formula  $C_{16}H_{14}O_5$
- Molecular Weight (g/mol) 286.27
- Melting Point ( $^{\circ}C$ ) 92 - 93.5
- $^1H$ -NMR (500 MHz,  $CDCl_3$ )  
 $\delta$ : 7.63 (1H, *d*,  $J = 10.5$  Hz, H-7), 7.62 (1H, *d*,  $J = 10.5$  Hz, H-8), 7.43 - 7.38 (5H, *m*, H-2, 3, 4, 5, 6), 4.23 (3H, *s*, 4'-OMe), 4.18 (3H, *s*, 5'-OMe)
- $^{13}C$ -NMR (125 MHz,  $CDCl_3$ )  
 $\delta$ : 193.4 (C-2'), 184.9 (C-5'), 164.8 (C-9), 148.4 (C-3'), 145.6 (C-4'), 141.7 (C-7), 135.2 (C-1), 130.5 (C-4), 130.2 (C-3, 5), 129.1 (C-2, 6), 118.0 (C-8), 102.0 (C-1'), 60.1 (4'-OMe), 60.1 (5'-OMe)
- Biological activities in the literature  
anti-diabetic, anti-inflammation, chitin synthase 2 inhibitor, antifungal, anti-tumor
- Other data in the literature
  1. Hazard and toxicity:  $LD_{50}$  (mus, orl) 159 mg/kg. Exp. reprod. effect
  2. Biological Source: Isol. from roots of *Lindera pipericarpa* and *Lindera erythrocarpa*

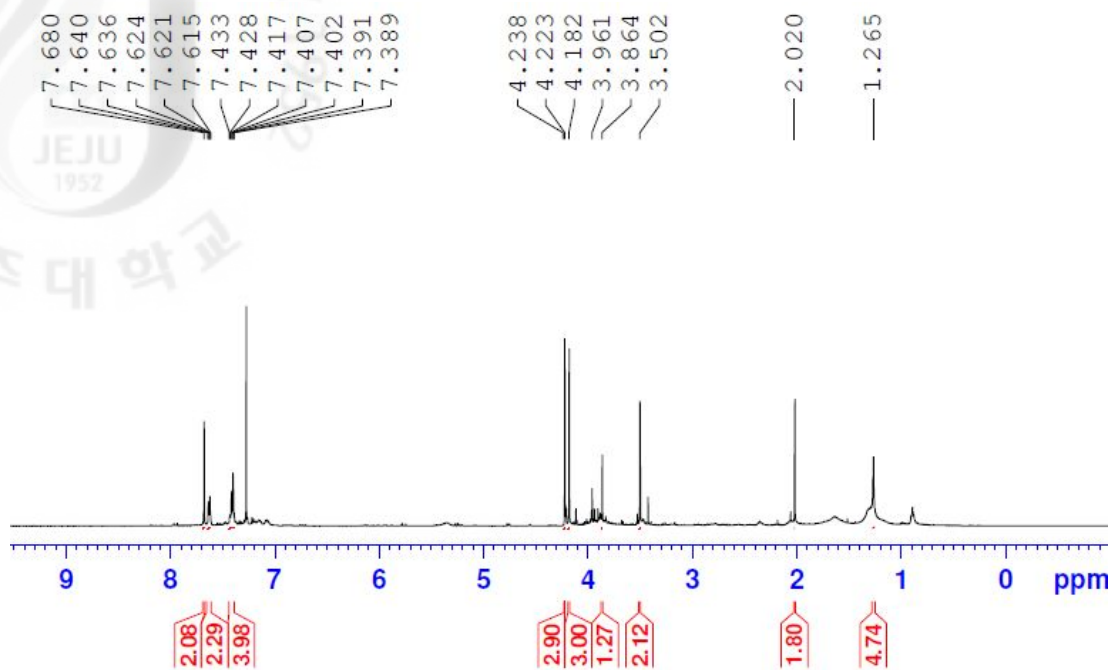


Figure 56.  $^1\text{H-NMR}$  spectrum of linderone (**14**) in  $\text{CDCl}_3$

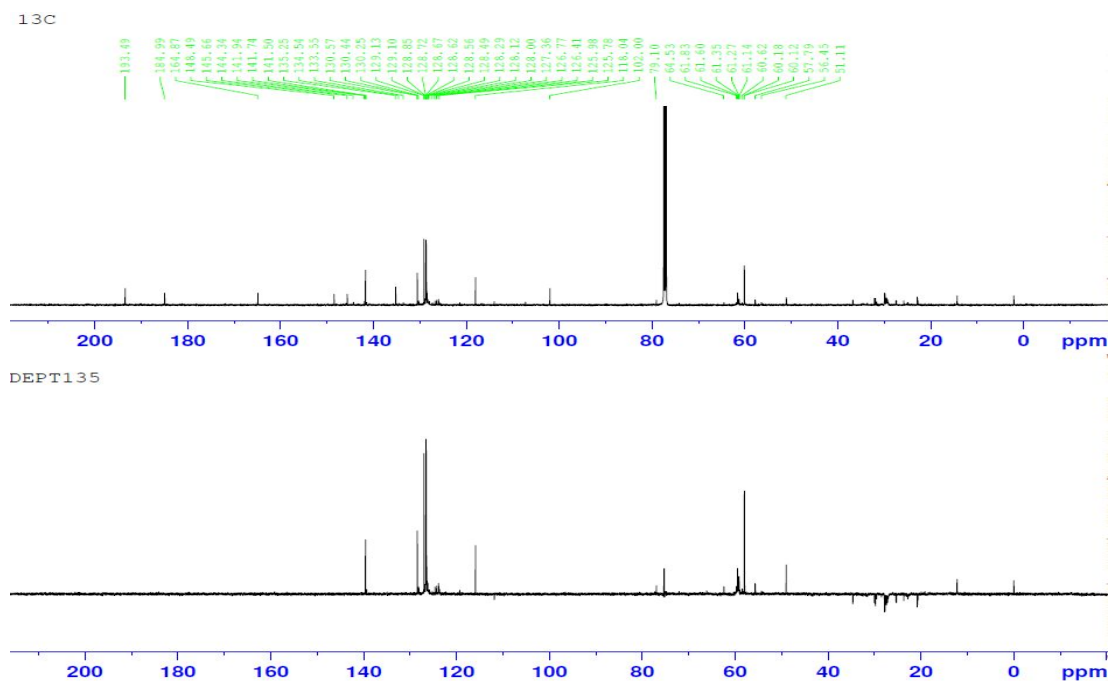


Figure 57.  $^{13}\text{C-NMR}$  and DEPT135 spectra of linderone (**14**) in  $\text{CDCl}_3$

Compound **14** was isolated as a yellow solid. The  $^1\text{H-NMR}$  spectrum of compound **14** was showed  $\delta_{\text{H}}$  7.63 (1H, *d*,  $J = 10.5$  Hz) and 7.63 (1H, *d*,  $J = 10.5$  Hz) indicating of H-7 and H-8, respectively.  $^1\text{H-NMR}$  spectrum indicated five aromatic protons including mono substituted coupling pattern at  $\delta_{\text{H}}$  7.60 (5H, *m*, H-2, 3, 4, 5, 6), two methoxyl groups signals appear at  $\delta_{\text{H}}$  4.23 (3H, *s*, 4'-OMe), 4.18 (3H, *s*, 5'-OMe) (Fig. 56). Thus, the structure of **14** was determined to be 4,5-dimethoxy-2-(3-phenyl-acryloyl)-cyclopent-4-ene-1,3-dione (linderone) (Fig. 59). This was confirmed by a spectral data comparison with published data.<sup>32,61)</sup>

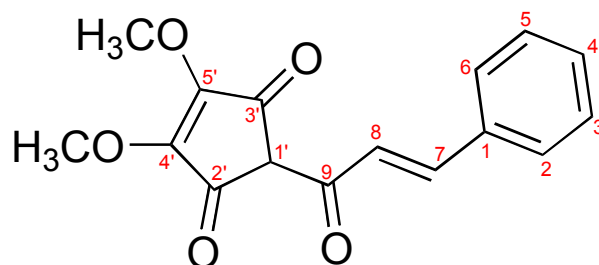


Figure 58. Structure of compound **14**; Linderone

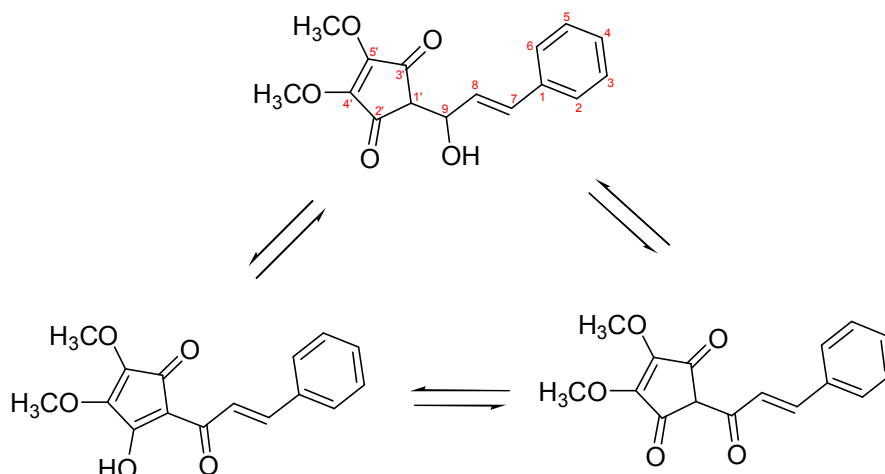


Figure 59. Expectative tautomers of linderone (**14**)

## 5-2. Biological activities

### 5-2-1. Antioxidant activity

#### 5-2-1-1. Free radical scavenging activity of the solvent fractions

Antioxidative activity was determined by 3 types of free radical scavenging activity assays. DPPH is relatively stable radical compared to the superoxide and hydroxyl species that are primarily responsible for oxidative damage in biological systems. DPPH is widely used to test the ability of compound acting as free radical scavengers or hydrogen donors. The odd electron in the DPPH radical gives a strong absorption maximum at 517 nm (purple color). The color turns from purple to light yellow when the add electron of the DPPH radical becomes paired with a hydrogen from an antioxidant to form the reduced DPPH-H. The antioxidant activity of various natural products can be determined conveniently and rapidly using DPPH. The DPPH radical scavenging activity of the crude 70% *aq.* EtOH extract and its solvent fractions of *L. erythrocarpa* were showed in Table 11. The 70% *aq.* EtOH extract, *n*-Hex, CH<sub>2</sub>Cl<sub>2</sub>, EtOAc, *n*-BuOH and water solvent fractions exhibited DPPH radical scavenging activities dose-dependently. The activity increased in the following order : *n*-Hex fraction < CH<sub>2</sub>Cl<sub>2</sub> fraction < H<sub>2</sub>O fraction < *n*-BuOH fraction < EtOAc fraction. Among them, EtOAc solvent fraction exhibited higher scavenging activity compared to other fractions with dose-dependent behavior.

The superoxide anion radical is generated by *in vivo* oxidative enzymes such as xanthine oxidase, which converts hypoxanthine to xanthine. Many polyphenols have been shown to be effective xanthine oxidase inhibitors and superoxide radical scavengers. In the present study, to avoid the unclear determination on superoxide anion scavenging activity of antioxidant in the xanthine/xanthine oxidase system, we employed the riboflavin-light-NBT system to generate superoxide anion radicals. The superoxide anion scavenging activities of the samples were measured based on the

NBT-reduction by photochemically generated  $O_2^{\cdot -}$  in the presence of riboflavin-light-NBT. The decrease of absorbance at 550 nm by the antioxidative fractions indicated the consumption of superoxide anion. The superoxide anion scavenging activity of the crude 70% *aq.* EtOH extract and its solvent fractions were shown in Table 11. EtOAc fraction showed a highly superoxide anion scavenging activity with  $IC_{50} = 16.8 \mu\text{g/mL}$ . But, *n*-Hex,  $CH_2Cl_2$  and  $H_2O$  fractions did not show antioxidant activity as compared to crude extract and other solvent fractions. This results showed that EtOAc and *n*-BuOH solvent fractions should be the major fractions containing active constituents for the free radical scavenging activity of *L. erythrocarpa*.



Table 11. Free radical scavenging effect of the solvent fractions

Samples	RC <sub>50</sub> (µg/mL)		
	DPPH radical scavenging activity	Xanthine oxidase inhibitory activity	Superoxide radical scavenging activity
70% <i>aq.</i> EtOH ext.	16.8 ± 0.20	5.5 ± 0.12	63.5 ± 0.01
<i>n</i> -Hex Fr.	> 1000	> 1000	> 1000
CH <sub>2</sub> Cl <sub>2</sub> Fr.	410.4 ± 10.87	86.2 ± 4.68	806.7 ± 17.14
EtOAc Fr.	7.4 ± 0.73	5.5 ± 2.29	16.8 ± 0.09
<i>n</i> -BuOH Fr.	18.5 ± 2.01	5.6 ± 0.18	58.5 ± 4.01
H <sub>2</sub> O Fr.	66.7 ± 2.01	9.7 ± 0.33	270.7 ± 3.93
Positive control (BHA) <sup>1)</sup>	7.4 ± 0.07	N/A	N/A
Positive control (Allopurinol)	N/A	2.1 ± 0.03	3.8 ± 1.06

Primarily radical scavenging activity was determined at 0 to 1000 µg/mL concentration of samples. Scavenging concentration for 50% of free radical (RC<sub>50</sub>) was calculated from logarithmic regression equation obtained from the values of at least five dilutions of the primary concentration. Values represent mean ± SDs (n = 3); in parentheses is RC<sub>50</sub> value of respective sample

N/A. not assay; BHA. butylated hydroxyanisole<sup>1)</sup>; >. out of range

#### 5-2-1-2. Free radical scavenging activity of the isolated compounds

The DPPH radical scavenging activities of the isolated compounds from *L. erythrocarpa* were shown in Table 12. Among the isolated compounds, ethyl caffeate (**1**), quercetin (**6**), and avicularin (**8**) had more potent radical scavenging activity than activity the positive control (BHA,  $RC_{50} = 11.0 \mu\text{g/mL}$ ) (Tab. 12). This result showed that phenolic compounds containing NH or many OH functional groups have a strong hydrogen donation or radical scavenging ability, and the methylation and glycosylation of hydroxyl group in polyphenols cause a decrease in activity.

Table 12. Free radical scavenging effect of the isolated compounds on DPPH radical scavenging activity

Samples	RC <sub>50</sub> (µg/mL)		
	DPPH radical scavenging activity		
Compound 1 ethyl cafferate	3.3	±	0.3
Compound 2 methyl cinnamate	>		250
Compound 3 lucidone	>		250
Compound 4 methyllinderone	>		250
Compound 5 β-sitosterol	>		250
Compound 6 quercetin	6.5	±	0.6
Compound 7 quercitrin	42.6	±	4.4
Compound 8 avicularin	3.7	±	0.2
Compound 9 afzelin	21.6	±	0.9
Compound 10 kanakugiol	>		250
Compound 11 methyllucidone	>		250
Compound 12 stigmasterol	N/A		
Compound 13 new compound	>		250
Compound 14 linderone	>		250
Positive control (BHA) <sup>1)</sup>	11.0	±	0.7

Primarily radical scavenging activity was determined at 0 to 250 µg/mL concentration of samples. Scavenging concentration for 50% of free radical (RC<sub>50</sub>) was calculated from logarithmic regression equation obtained from the values of at least five dilutions of the primary concentration. Values represent mean ± SDs (n = 3); in parentheses is RC<sub>50</sub> value of respective sample

N/A. not assay; BHA. butylated hydroxylanisole<sup>1)</sup>; >. out of range

## 5-2-2. Anti-inflammation activity

### 5-2-2-1. Effect on cell viability and LPS-induced NO production

NO production by activated macrophages is involved in various harmful responses including tissue injury, septic shock, and apoptosis.<sup>67)</sup> Stimulation of RAW 264.7 macrophage with LPS for 24 hr increased the NO production in the medium compared to cells treated with vehicle alone. We first examined the suppressive effects of crude 70% *aq.* EtOH extract with solvent fractions and isolated compounds on LPS-induced NO production at 0 to 100  $\mu\text{g/mL}$ . Among them,  $\text{CH}_2\text{Cl}_2$  solvent fraction significantly inhibited NO production compared to other solvent fractions with dose-dependent behavior of  $\text{IC}_{50} = 68.9 \mu\text{g/mL}$  and did not affect cell viability at the concentration of 100  $\mu\text{g/mL}$  on MTT assay (Tab. 13). Ethyl cafferate (**1**), methyl cinnamate (**2**), lucidone (**3**), methyllinderone (**4**) and kanakugiol (**10**) showed NO production inhibitory activity. However, They showed strong toxicity in RAW264.7 cells (Tab. 14). On the other hand, Quercetin (**6**) and avicularin (**8**) isolated from EtOAc fraction showed the good inhibition effect of NO production and it did not affect the cell viability in the RAW264.7 cell. They should be the major constituents responsible for the anti-inflammation activity of *L. erythrocarpa*.

Table 13. Cell viability and effects of the solvent fractions on the production of nitric oxide in LPS-stimulated RAW264.7 cells

Samples	Anti-inflammatory activity		
	TC <sub>50</sub> <sup>1)</sup> (μg/mL)	IC <sub>50</sub> <sup>2)</sup> (μg/mL)	Selectivity index <sup>3)</sup>
70% <i>aq.</i> EtOH ext.	> 100	> 100	> 1.00
<i>n</i> -Hex Fr.	> 100	> 100	> 1.00
CH <sub>2</sub> Cl <sub>2</sub> Fr.	> 100	68.9	> 1.45
EtOAc Fr.	> 100	94.0	> 1.06
<i>n</i> -BuOH Fr.	> 100	> 100	> 1.00
H <sub>2</sub> O Fr.	> 100	> 100	> 1.00

Primarily, It was determined at 0 to 100 μg/mL concentration of samples. Inhibition concentration for 50% of NO production (IC<sub>50</sub>) was calculated from logarithmic regression equation obtained from the values of at least five dilutions of the primary concentration. Values represent mean ± SD (n = 3); in parentheses is IC<sub>50</sub> value of respective sample

N/A. not assay; >. out of range

<sup>1)</sup> TC<sub>50</sub> is the concentration producing 50% toxicity in RAW264.7 cells.

<sup>2)</sup> IC<sub>50</sub> is the concentration producing 50% inhibition of NO production in RAW264.7 cells.

<sup>3)</sup> Selectivity Index = TC<sub>50</sub> / IC<sub>50</sub>

Table 14. Cell viability and effects of the isolated compounds on the production of nitric oxide in LPS-stimulated RAW264.7 cells

Samples	Anti-inflammatory activity		
	TC <sub>50</sub> <sup>1)</sup> (µg/mL)	IC <sub>50</sub> <sup>2)</sup> (µg/mL)	Selectivity index <sup>3)</sup>
Compound 1 ethyl cafferate	32.8	4.0	> 8.1
Compound 2 methyl cinnamate	44.9	4.6	> 9.6
Compound 3 lucidone	74.9	5.6	> 13.3
Compound 4 methyllinderone	25.8	4.5	> 5.6
Compound 5 β-sitosterol	N/A	N/A	N/A
Compound 6 quercetin	> 100	15.9	> 6.2
Compound 7 quercitrin	> 100	> 100	> 1.0
Compound 8 avicularin	> 100	24.0	> 4.1
Compound 9 afzelin	> 100	> 100	> 1.0
Compound 10 kanakugiol	18.9	5.3	> 3.5
Compound 11 methylucidone	N/A	N/A	N/A
Compound 12 stigmasterol	N/A	N/A	N/A
Compound 13 new compound	N/A	N/A	N/A
Compound 14 linderone	N/A	N/A	N/A

Primarily, It was determined at 0 to 100 µg/mL concentration of samples. Inhibition concentration for 50% of NO production (IC<sub>50</sub>) was calculated from logarithmic regression equation obtained from the values of at least five dilutions of the primary concentration. Values represent mean ± SD (n = 3); in parentheses is IC<sub>50</sub> value of respective sample

N/A. not assay; >. out of range

<sup>1)</sup> TC<sub>50</sub> is the concentration producing 50% toxicity in RAW264.7 cells.

<sup>2)</sup> IC<sub>50</sub> is the concentration producing 50% inhibition of NO production in RAW264.7 cells.

<sup>3)</sup> Selectivity Index = TC<sub>50</sub> / IC<sub>50</sub>

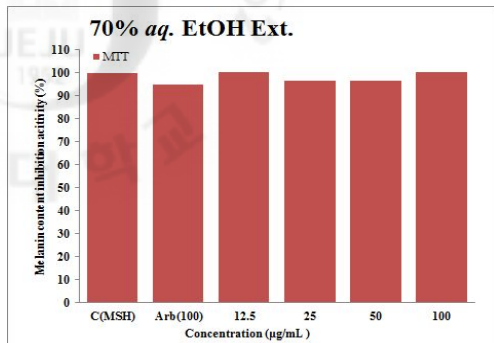
### 5-2-3. Melanogenesis inhibition activity

#### 5-2-3-1. Cell viability in B16F10 melanoma cell

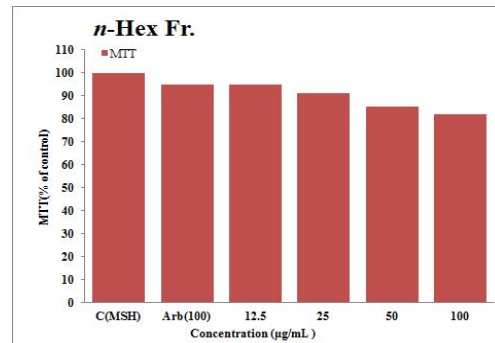
The study on the melanogenesis inhibition activity was conducted using murine melanoma B16F10 cells stimulated by  $\alpha$ -MSH. The cell line has been widely used for this purpose probably because they are relatively easy to culture *in-vitro*. Treatment of  $\alpha$ -MSH induced cellular melanogenesis, as shown by extracellular melanin content and cell pigmentation. When the cells were pretreated with the crude extract of *L. erythrocarpa*, the cellular melanogenesis significantly reduced (Fig. 62). *L. erythrocarpa* crude extract was further fractionated into *n*-Hex, CH<sub>2</sub>Cl<sub>2</sub>, EtOAc, *n*-BuOH and H<sub>2</sub>O solvent fractions. The five solvent fractions were treated for the cell viability rates at the concentration of 12.5, 25, 50 and 100  $\mu$ g/mL by MTT assay. As shown in Fig. 60, all solvent fractions together with crude extract did not show the big difference of cell viability rate in comparison with the positive control group.

Also, B16F10 cells were treated with isolated compounds for cell viability. Based on MTT assay, the treated all compounds did not affect on the cell viability in the concentration of 10  $\mu$ g/mL (Fig. 61).

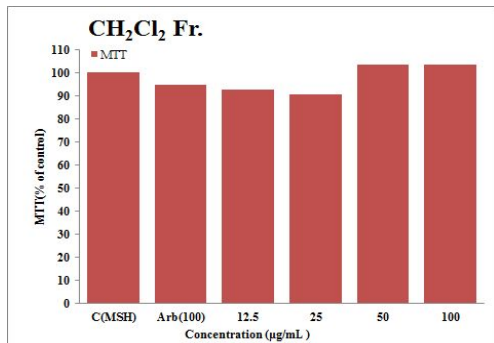
(A)



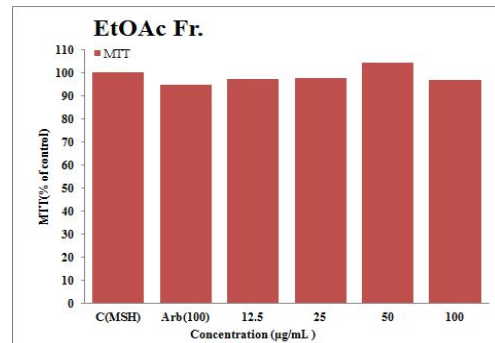
(B)



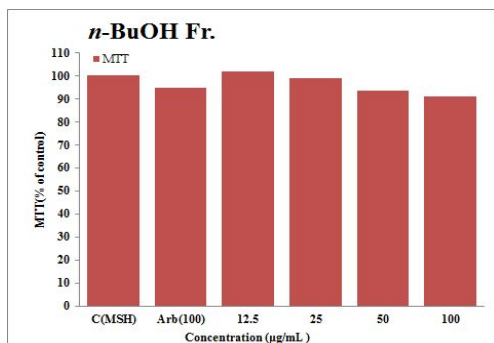
(C)



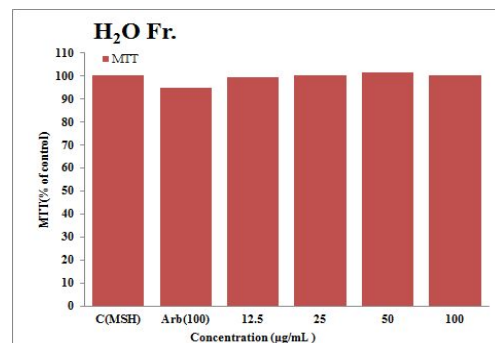
(D)



(E)



(F)



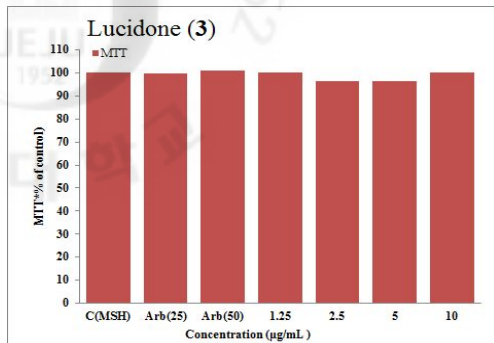
Values are mean ± SD of 3 replicates

(A) 70% aq. EtOH Ext. (B) n-Hex Fr. (C) CH<sub>2</sub>Cl<sub>2</sub> Fr. (D) EtOAc Fr. (E) n-BuOH Fr. (F) H<sub>2</sub>O Fr.

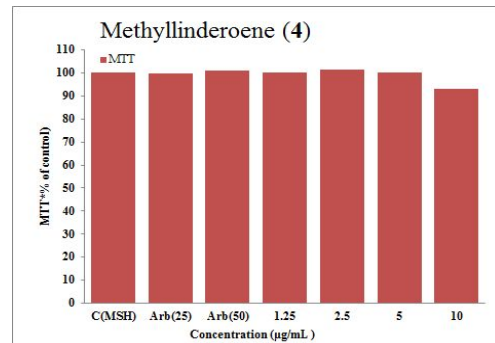
Figure 60. Cell viability on B16F10 cells treated with the solvent fractions



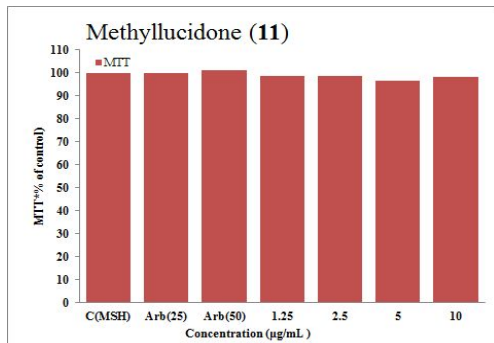
(A)



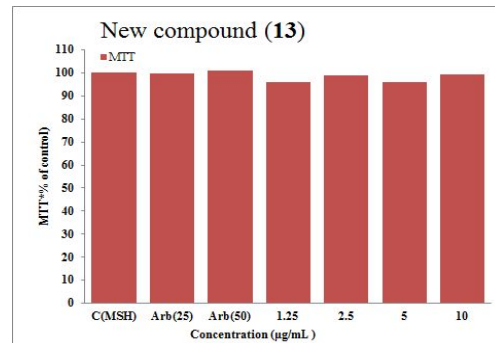
(B)



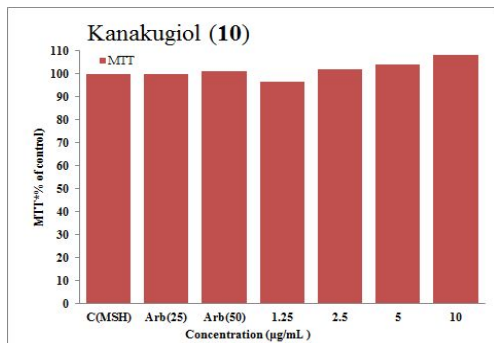
(C)



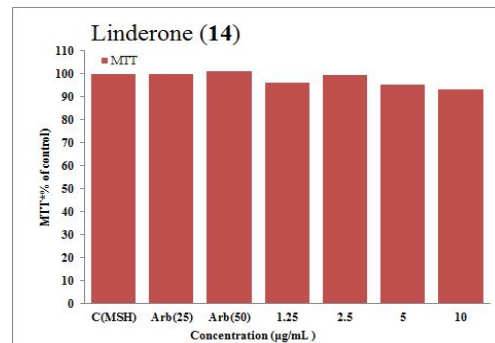
(D)



(E)



(F)



Values are mean  $\pm$  SD of 3 replicates

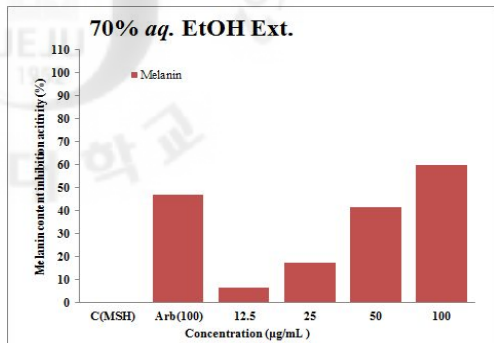
(A) Lucidone (B) Methyllinderoene (C) Methyllucidone (D) New compound (E) Kanakugiol (F) Linderone

Figure 61. Cell viability on B16F10 cells treated with the isolated compounds

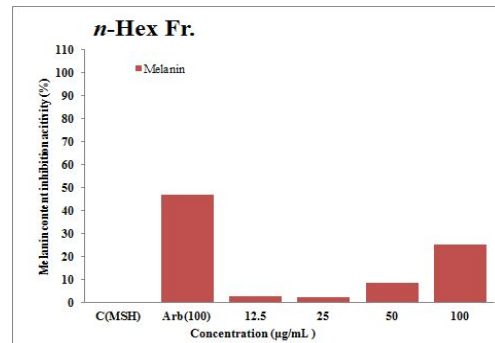
#### 5-2-3-2. Effect on melanogenesis in B16F10 cells

We examined the melanin contents inhibitory activity using B16F10 melanoma cells. As shown in Figure 62, the 70% *aq.* EtOH extract of *L. erythrocarpa* clearly showed melanin contents inhibitory activity in a dose-dependent manner. In comparison with the positive control group, the melanin contents of the CH<sub>2</sub>Cl<sub>2</sub> fraction was significantly reduced by 47.4% in concentration of 100 µg/mL (Fig. 62). Activity-guided isolation was carried out using the CH<sub>2</sub>Cl<sub>2</sub> solvent fraction and column chromatography led to isolations of six compounds. Lucidone (**3**), methyllinderone (**4**), methyllucidone (**11**) new compound (**13**), kanakugiol (**10**), and linderone (**14**) inhibited melanin contents in a dose-dependent manner at 10 µg/mL concentration by 53.6, 62.1, 46.1, 40.7, 40.3 and 38.9% respectively (Fig. 63). Among the six isolates, lucidone (**3**), methyllucidone (**11**), and new compound (**13**) had the melanin content inhibitory activity stronger than arbutin.

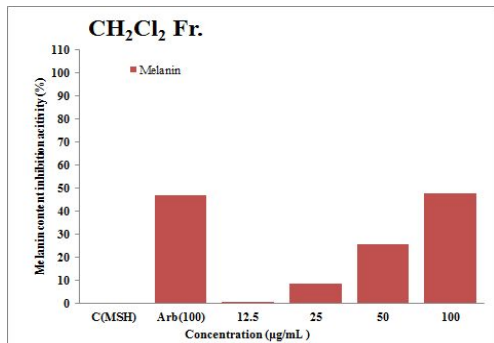
(A)



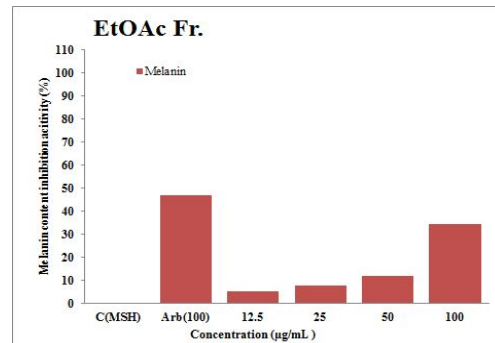
(B)



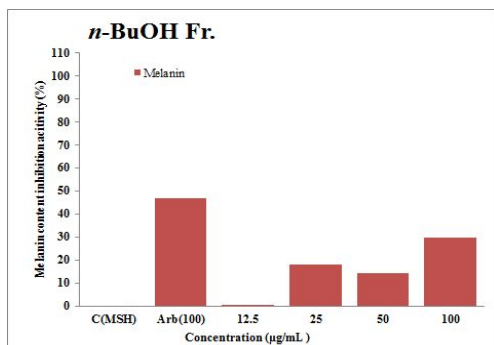
(C)



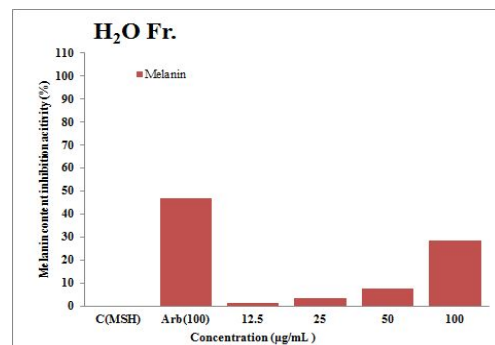
(D)



(E)



(F)

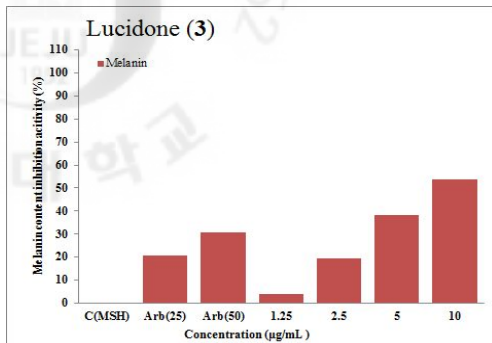


Values are mean  $\pm$  SD of 3 replicates

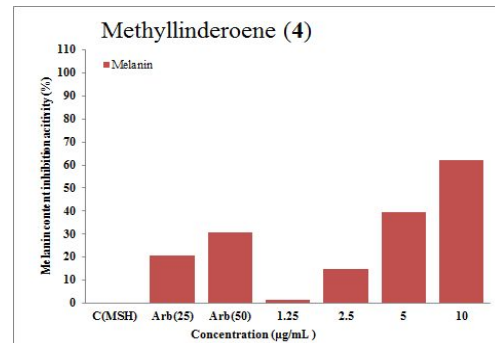
(A) 70% aq. EtOH Ext. (B) *n*-Hex Fr. (C) CH<sub>2</sub>Cl<sub>2</sub> Fr. (D) EtOAc Fr. (E) *n*-BuOH Fr. (F) H<sub>2</sub>O Fr.

Figure 62. Melanin contents inhibitory activity of the solvent fractions on B16F10 cells

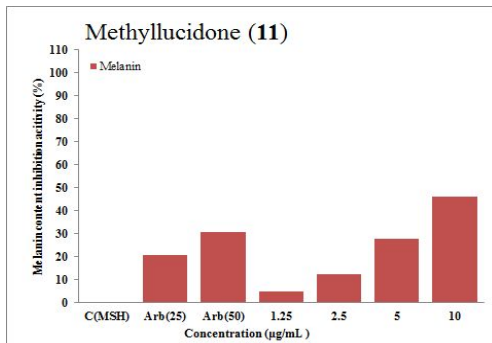
(A)



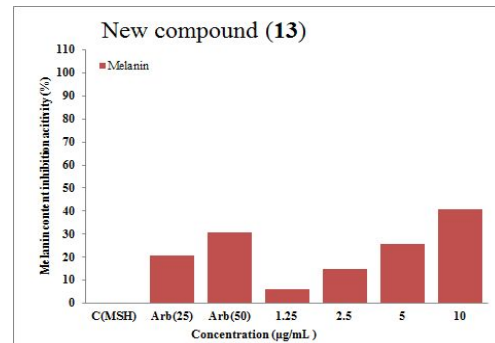
(B)



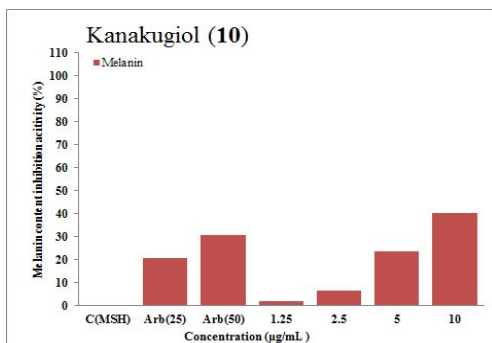
(C)



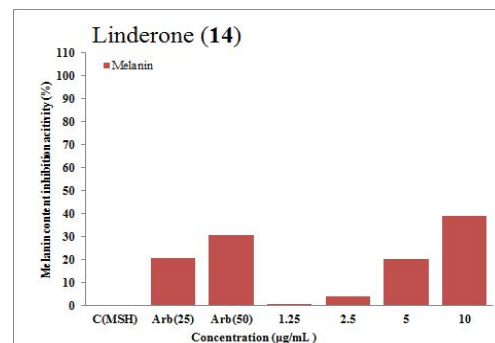
(D)



(E)



(F)



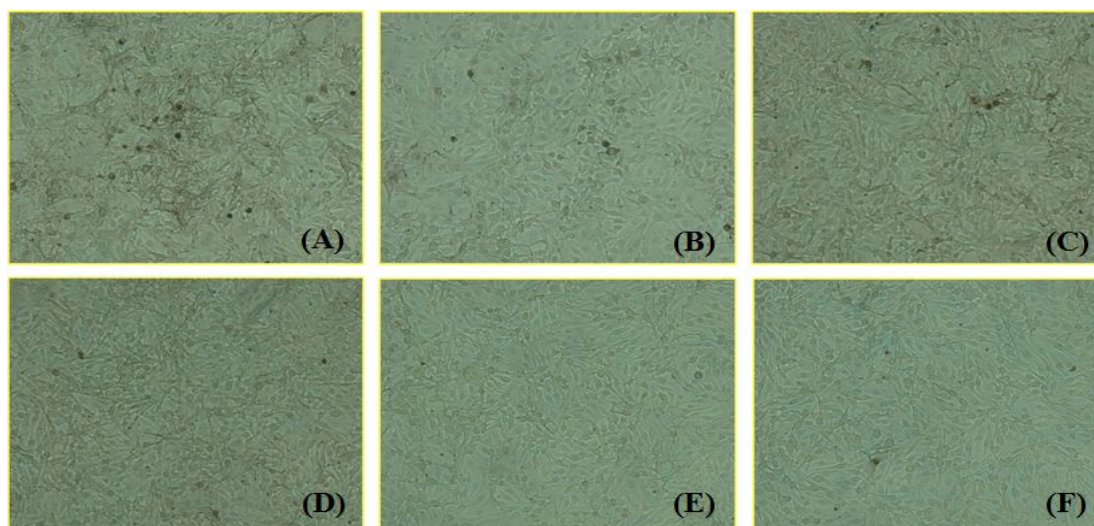
Values are mean ± SD of 3 replicates

(A) Lucidone (B) Methyllinderone (C) Methyllucidone (D) New compound (E) Kanakugiol (F) Linderone

Figure 63. Melanin contents inhibitory activity of the isolated compounds on B16F10 cells

### 5-2-3-3. Morphological observation of B16F10 melanoma cells

B16F10 melanoma cells were stimulated by  $\alpha$ -MSH with 5, 10, 20 and 30  $\mu\text{g}/\text{mL}$  concentrations of new compound (**13**) for 3 days. 50  $\mu\text{g}/\text{mL}$  Arbutin and respectively concentration of new compound (**13**) were observed compared with the inverted microscope (Fig. 64). The control group showed a lot of melanocyte dendrites and of black precipitate induced by melanin synthesis. However, in the groups which treated in 20  $\mu\text{g}/\text{mL}$  of new compound (**13**) the melanin synthesis was inhibited and the dendron was reduced in a dose-dependent way more strongly than 50  $\mu\text{g}/\text{mL}$  of arbutin (Fig. 64).



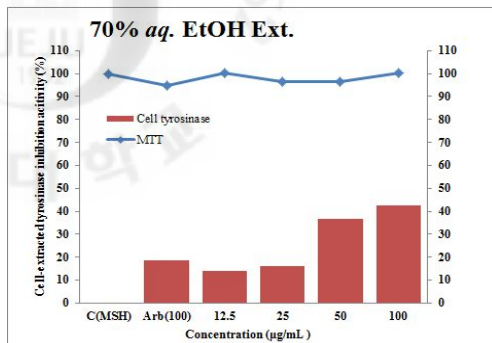
(A) control (B) arbutin (positive control; 50  $\mu\text{g}/\text{mL}$ ), (C), (D), (E) and (F) cells treated with 5, 10, 20 and 30  $\mu\text{g}/\text{mL}$  new compound (**13**), respectively

Figure 64. Morphology of control and 1-(2'-hydroxy-3',4',5',6'-tetramethylphenyl)-1-methoxy-3-phenyl-propane (new compound) (**13**) treated B16F10 cells

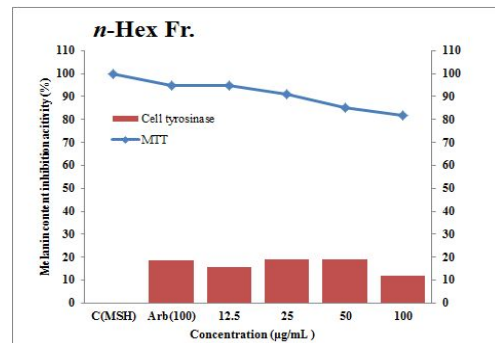
5-2-3-4. Inhibition effect on melanin synthetic abilities on cell-extracted tyrosinase activity

We examined the cell tyrosinase inhibitory activity using B16F10 melanoma cell. As shown in Figure 65, the 70% *aq.* EtOH extract clearly showed cell tyrosinase inhibitory activity in a dose-dependent manner. Among the five solvent fractions, EtOAc and *n*-BuOH fractions exhibited higher inhibitory activity than other solvent fractions, and these significantly inhibited at 100  $\mu\text{g/mL}$  by 40.4 and 41.1% (Fig. 65). And among the isolated compounds, lucidone (**3**) inhibited tyrosinase activity in a dose-dependent manner with 15.4% inhibition at 1.25  $\mu\text{g/mL}$  (Fig. 66).

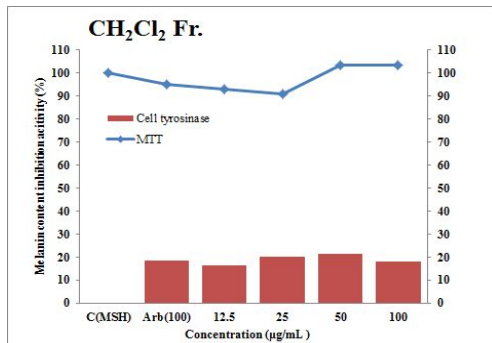
(A)



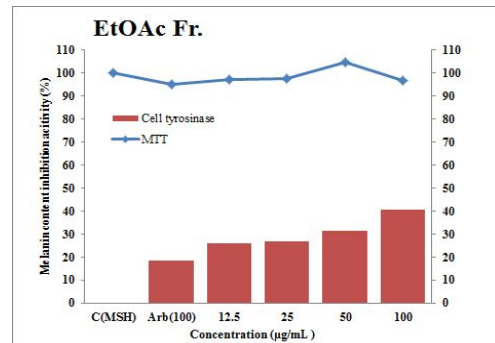
(B)



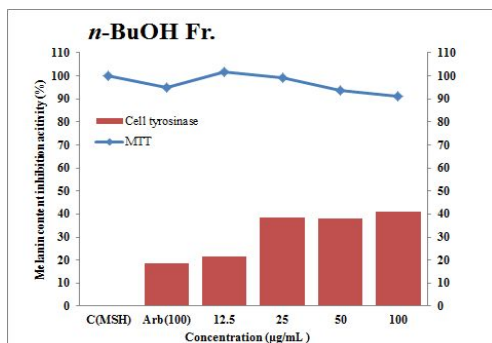
(C)



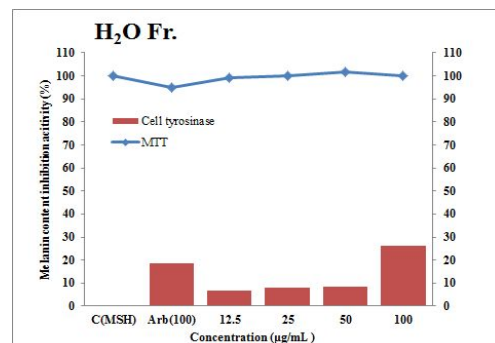
(D)



(E)



(F)

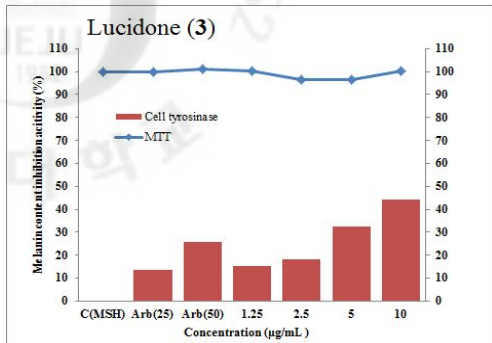


Values are mean ± SD of 3 replicates

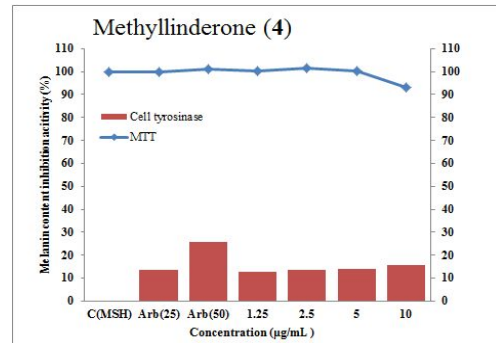
(A) 70% aq. EtOH Ext. (B) *n*-Hex Fr. (C) CH<sub>2</sub>Cl<sub>2</sub> Fr. (D) EtOAc Fr. (E) *n*-BuOH Fr. (F) H<sub>2</sub>O Fr.

Figure 65. Cell viability rate and inhibition effect of the solvent fractions on cell-extracted tyrosinase activity

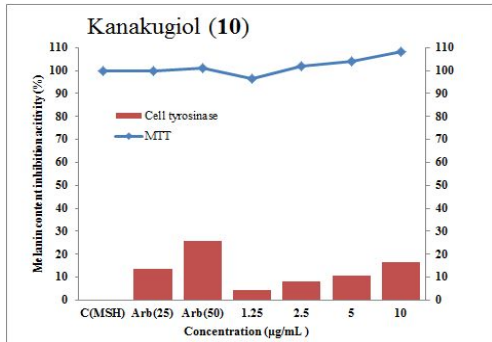
(A)



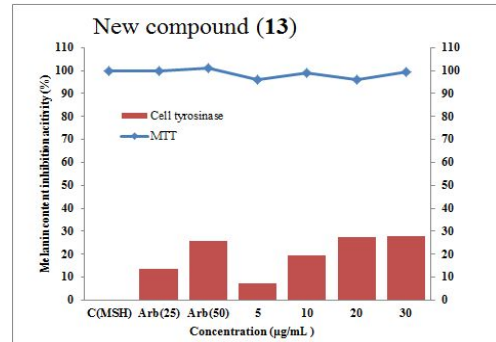
(B)



(C)



(D)



Values are mean ± SD of 3 replicates

(A) Lucidone (B) Methyllinderone (C) Kanakugiol (D) New compound

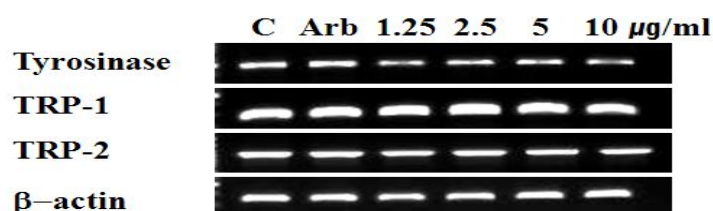
Figure 66. Cell viability rate and inhibition effect of the isolated compounds on cell-extracted tyrosinase activity



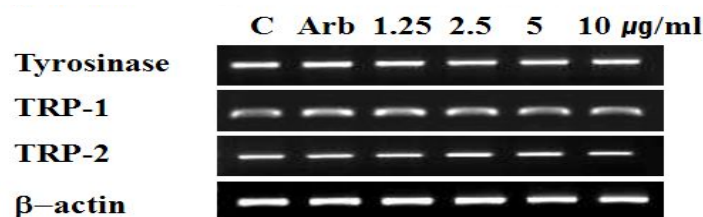
5-2-3-5. Inhibition effect on the related *mRNA* expression

In order to ascertain the effects of lucidone (**3**), methyllinderone (**4**) and new compound (**13**) on related *mRNA* expression, RT-PCR analysis was done. In comparison with the control group, TRP-1 and tyrosinase expression was reduced by all of these compounds, and showed inhibitory effects in a dose-dependent manner (Fig. 67).

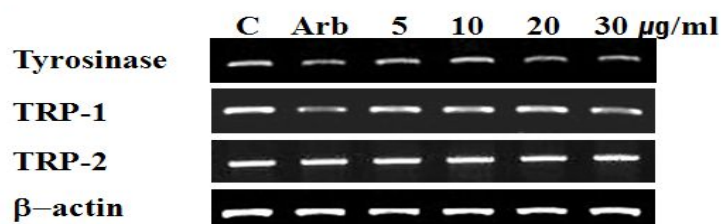
(A)



(B)



(C)



B16F10 cells were cultured for 72 hr inducing melanogenesis with  $\alpha$ -MSH. When it passed for 24 hr, media was exchanged and samples were retreated. Total RNA was subjected to RT-PCR.

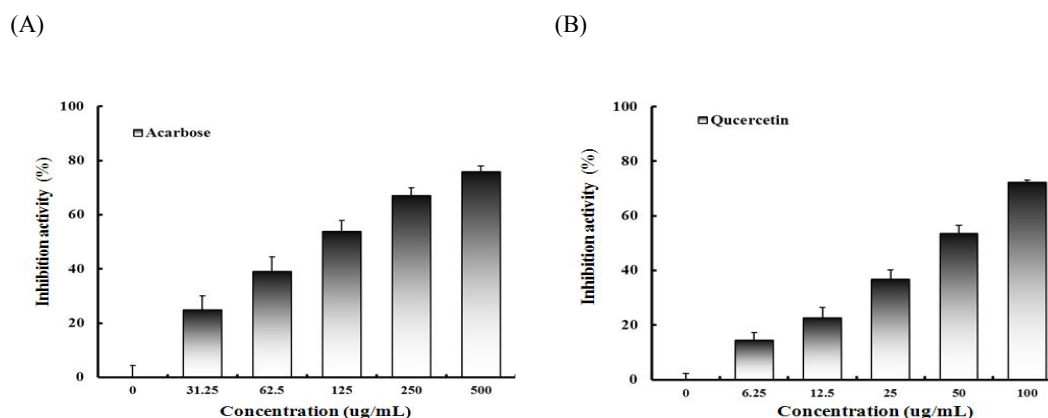
(A) Lucidone (B) Methyllinderone (C) New compound

Figure 67. Inhibition effects of active three compounds on the tyrosinase and TRP-1, TRP-2 *mRNA* expression on B16F10 cells

#### 5-2-4. Anti-obesity activity

##### 5-2-4-1. Inhibition effect on $\alpha$ -glucosidase

$\alpha$ -Glucosidase inhibition activity was determined using yeast  $\alpha$ -glucosidase. The results were shown in Table 15. Inhibition activity was presented by percentage. Various concentrations of the isolated compounds from EtOAc fraction showed  $\alpha$ -glucosidase inhibitory activity in a dose-dependent manner (Data did not shown). According to Figure 68, quercetin (**5**) has good activities on yeast  $\alpha$ -glucosidase inhibitory activity assay.  $IC_{50}$  values of quercetin (**5**) was 43.5  $\mu\text{g/mL}$ . This value showed that yeast  $\alpha$ -glucosidase inhibitory activity is higher than the acarbose (positive control,  $IC_{50} = 104.4 \mu\text{g/mL}$ ) (Tab. 15) (Fig. 68).



Values are mean  $\pm$  SD of 3 replicates

(A) Acarbose (Positive control) (B) Quercetin

Figure 68. Inhibition effect of the isolated compounds on yeast  $\alpha$ -glucosidase inhibitory assay

Table 15. Inhibition effect of the isolated compounds on yeast  $\alpha$ -glucosidase inhibitory assay

Samples	IC <sub>50</sub> (uM)	
	yeast $\alpha$ -glucosidase inhibitory activity	
Compound 1 ethyl cafferate	N/A	
Compound 2 methyl cinnamate	N/A	
Compound 3 lucidone	>	100
Compound 4 methyl linderone	>	100
Compound 5 $\beta$ -sitosterol	N/A	
Compound 6 quercetin	43.5	± 6.25
Compound 7 quercitrin	>	100
Compound 8 avicularin	>	100
Compound 9 afzelin	>	100
Compound 10 kanakugiol	>	100
Compound 11 methyl lucidone	>	100
Compound 12 stigmasterol	N/A	
Compound 13 new compound	N/A	
Compound 14 linderone	N/A	
Positive control (Acarbose)	104.4	± 27.08

Primarily enzyme inhibition activity was determined at 0 to 100 uM concentration of samples. Inhibition concentration for 50% of enzyme inhibition (IC<sub>50</sub>) was calculated from logarithmic regression equation obtained from the values of at least five dilutions of the primary concentration. Values represent mean ± SDs (n = 3); in parentheses is IC<sub>50</sub> value of respective sample

N/A. not assay; >. out of range

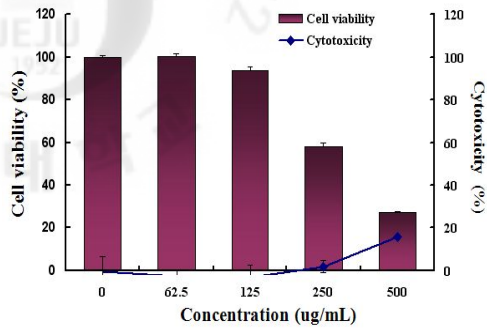
#### 5-2-4-2. Cell viability in mouse 3T3-L1 preadipocytes

Pre-confluent 3T3-L1 preadipocytes were cultured in the presence and absence of various concentrations (0 to 500  $\mu\text{g/mL}$ ) of the solvent fractions. MTT assay was conducted and expressed as % cell viability compared with the control. As shown in Figure 69, the solvent fractions with 25  $\mu\text{g/mL}$  concentration did not show any kind of big difference when comparing to the cell viability with the control group. And isolated compounds also did not affect the cell viability at the concentration of 25  $\mu\text{M}$  based on MTT assay (Fig. 70).

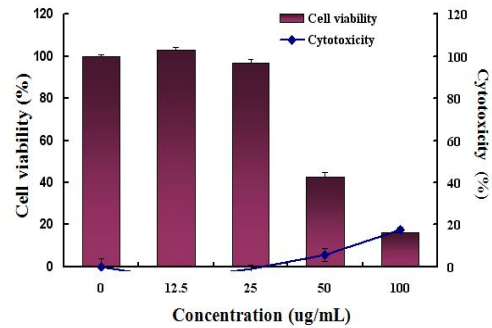
The amount of released LDH into the culture medium was measured in order to evaluate the influence of cell injuries of 3T3-L1 preadipocytes. As shown in Figure 69,  $\text{CH}_2\text{Cl}_2$  solvent fraction in which the active compounds was isolated from *L. erythrocarpa* did not show any cytotoxicity in LDH activity in culture medium of 3T3-L1 preadipocytes. And the isolated several compounds at 50  $\mu\text{M}$  on LDH assay did not show any cytotoxicity as well (Fig. 70).

In this results of LDH assays indicated that few cytotoxicity effects of *L. erythrocarpa* might play a role in the inhibition of cell population of 3T3-L1 preadipocytes.

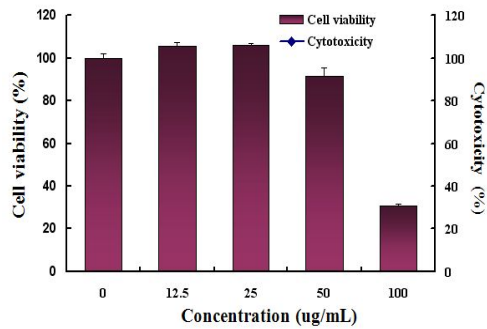
(A)



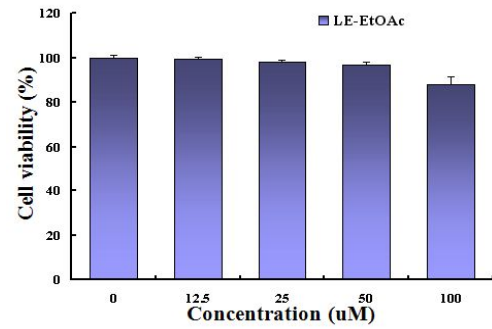
(B)



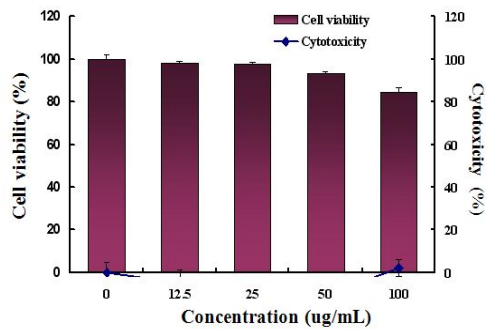
(C)



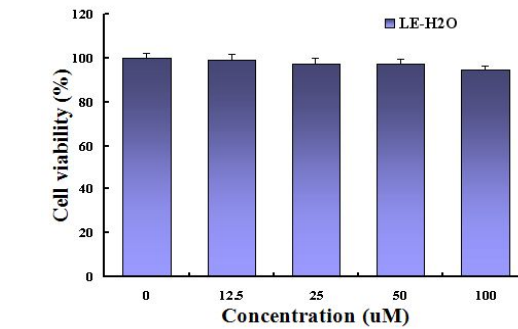
(D)



(E)



(F)

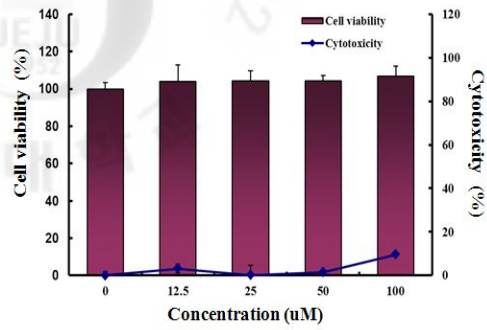


Values are mean ± SD of 3 replicates

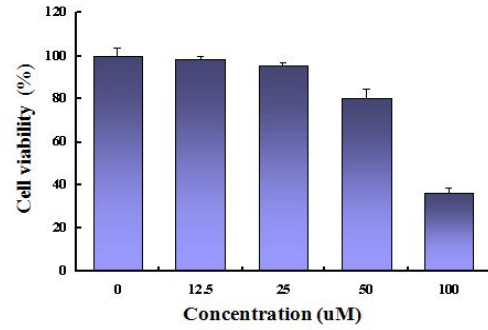
(A) 70% aq. EtOH Ext. (B) *n*-Hex Fr. (C) CH<sub>2</sub>Cl<sub>2</sub> Fr. (D) EtOAc Fr. (E) *n*-BuOH Fr. (F) H<sub>2</sub>O Fr.

Figure 69. Cell viability of the solvent fractions on mouse 3T3-L1 preadipocytes

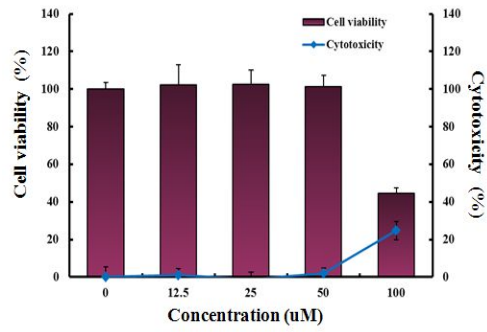
(A)



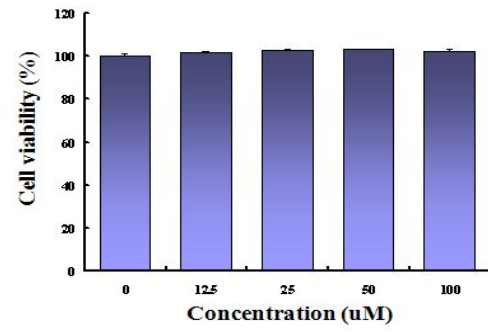
(B)



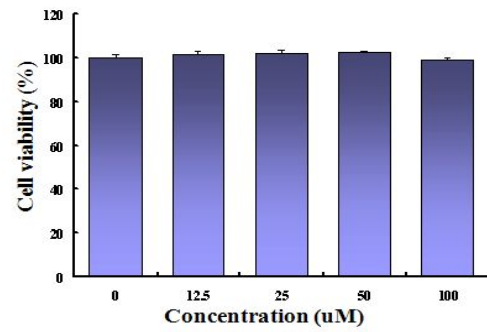
(C)



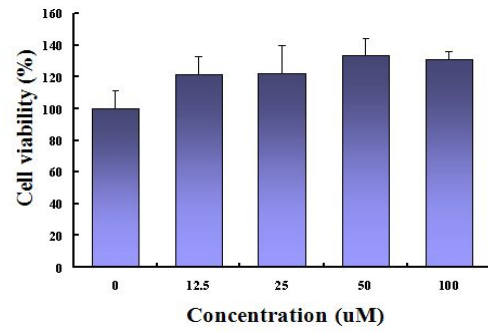
(D)



(E)



(F)



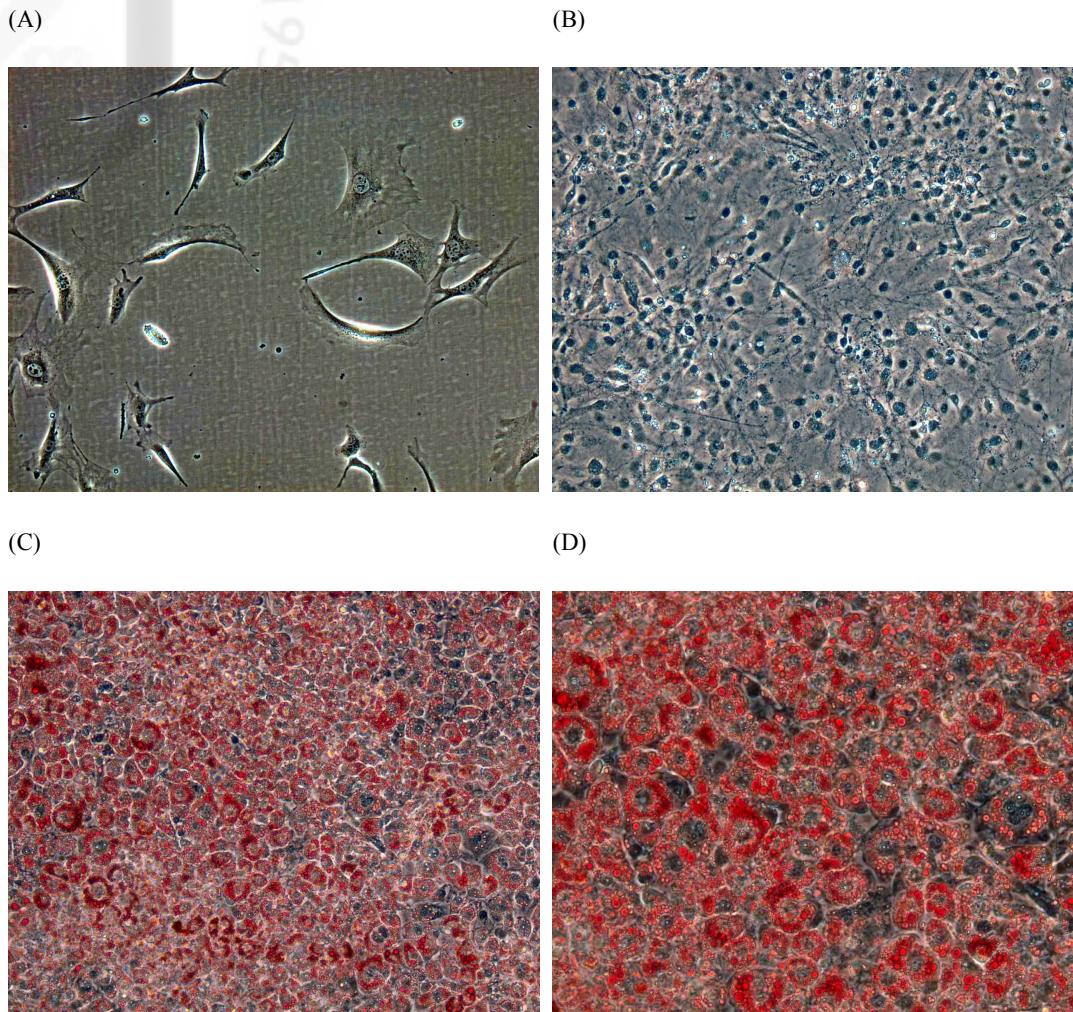
Values are mean  $\pm$  SD of 3 replicates

(A) Lucidone (B) Methyllinderone (C) Methyllucidone (D) New compound (E) Kanakugiol (F) Linderone

Figure 70. Cell viability of the isolated compounds on mouse 3T3-L1 preadipocytes

5-2-4-3. Effects on reducing lipid accumulation in mouse 3T3-L1 preadipocytes differentiated adipocytes

All samples was treated to 3T3-L1 preadipocytes to investigate the effects of *L. erythrocarpa* on obesity. The accumulated lipid droplets were visualized by Oil Red O staining and triglyceride accumulation was quantified in differentiated 3T3-L1 preadipocytes. During differentiation the cells were treated with various concentrations of solvent fractions (0 to 200  $\mu\text{g/mL}$ ) at 0 days with adipogenic hormone mixture and further exchanged culture medium every 3 days for 9 days (Photo 4). As shown in the Figure 71, solvent fractions from *L. erythrocarpa* decreased intracellular lipid droplets in a dose-dependent manner, as indicated by the decrease in Oil Red O incorporation. As shown in Figure 72, each graphs showed that the isolated several compounds were effective to reduce lipid accumulation. Methyllinderone (**4**) and methyllucidone (**11**) have potent effects on reducing lipid accumulation on mouse 3T3-L1 preadipocytes. Particularly, they reduced the lipid content as dose-dependent manner. From these results, methyllinderone (**4**) and methyllucidone (**11**) from *L. erythrocarpa* were effective to decrease lipid accumulation in differentiated 3T3-L1 preadipocytes.

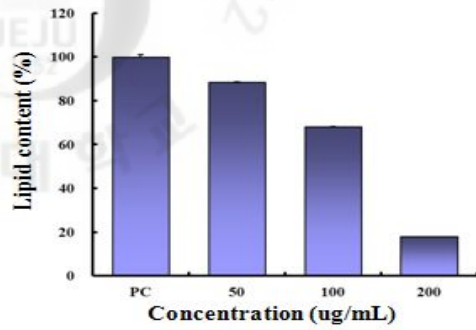


(A) 3T3-L1 preadipocyte, (B) 3T3-L1 preadipocyte after postconfluence, (C) differentiated 3T3-L1 adipocytes after 8 days from pre-confluence were observed by light microscope at a magnification of 100 X. (D) Differentiated 3T3-L1 adipocytes were observed at a magnification of 200 X. Under the optimized differentiation condition, 3T3-L1 fibroblasts were well differentiated to adipocytes. The differentiated cells have changed morphology and they are shown brightly. The lipid drops were observed in the differentiated adipocytes when the magnification was doubled.

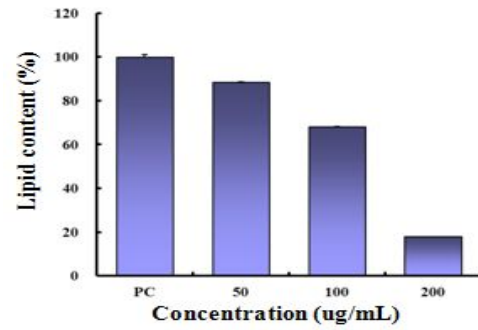
Photo 5. Differentiation of mouse 3T3-L1 preadipocytes to adipocytes before treated samples



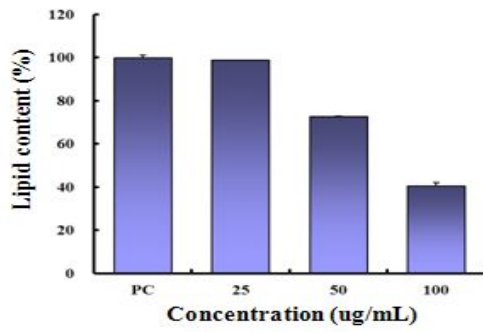
(A)



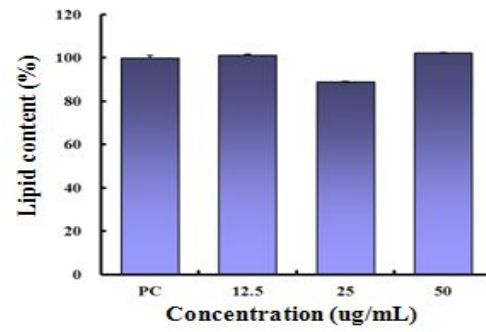
(B)



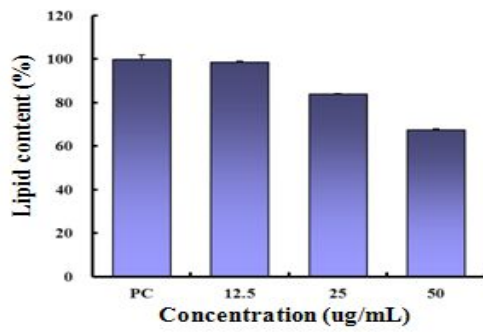
(C)



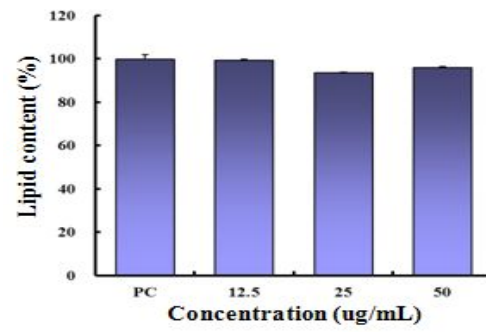
(D)



(E)



(F)

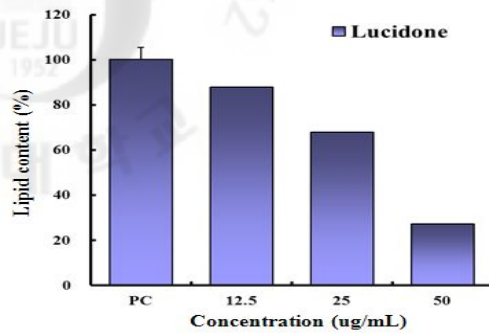


Values are mean  $\pm$  SD of 3 replicates

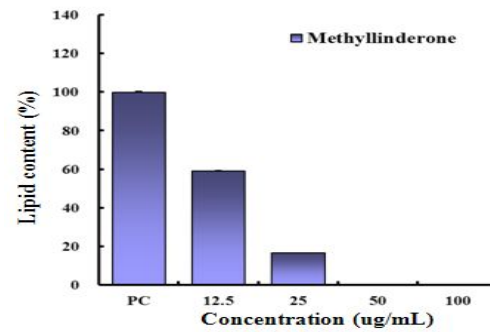
(A) 70% aq. EtOH Ext. (B) *n*-Hex Fr. (C) CH<sub>2</sub>Cl<sub>2</sub> Fr. (D) EtOAc Fr. (E) *n*-BuOH Fr. (F) H<sub>2</sub>O Fr.

Figure 71. The reduction effects of the solvent fractions on lipid accumulation during differentiation of 3T3-L1 preadipocytes

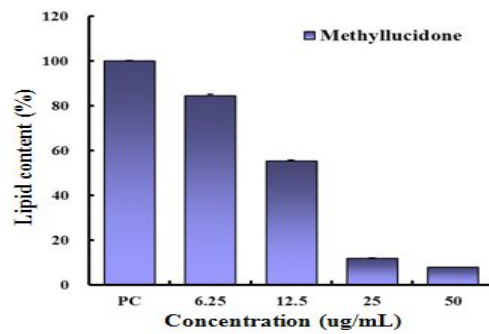
(A)



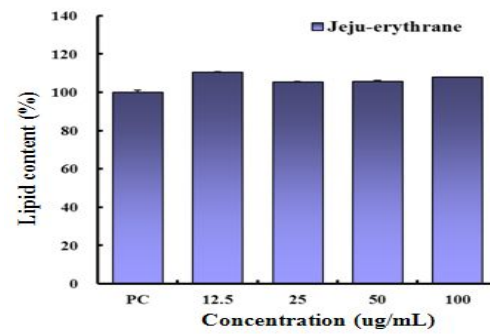
(B)



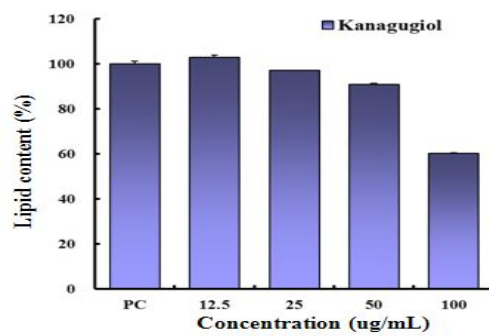
(C)



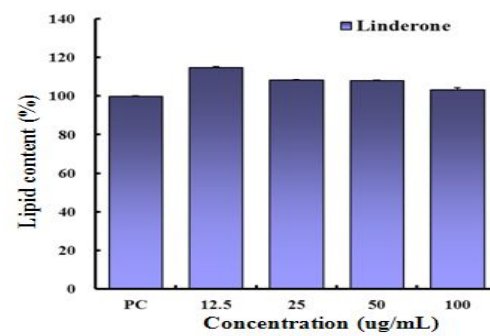
(D)



(E)



(F)



Values are mean  $\pm$  SD of 3 replicates

(A) Lucidone (B) Methyllinderone (C) Methyllucidone (D) New compound (E) Kanakugiol (F) Linderone

Figure 72. The reduction effects of the isolated compounds on lipid accumulation during differentiation of 3T3-L1 preadipocytes

## 6. Discussion

In this study, *L. erythrocarpa* was evaluated for the activities on antioxidant, anti-inflammatory, melanogenesis inhibition activity, anti-obesity. The active constituents were identified following activity-guided isolation with chromatography.

1. The dried leaves and the stem barks of *L. erythrocarpa* were extracted with 70% *aq.* EtOH at room temperature. This extract was partitioned successively into five solvent fractions. These fractions were tested for their inhibitory effects;
  - DPPH and superoxide radical scavenging activity test, xanthine oxidase inhibition activity test for the antioxidant activity
  - The effect of LPS-induced NO production on RAW264.7 cell for the anti-inflammatory activity
  - The effect of melanin contents inhibitory activity on B16F10 cells for the melanogenesis inhibition activity
  - The effect of reducing lipid accumulation in 3T3-L1 preadipocytes for the anti-obesity activity

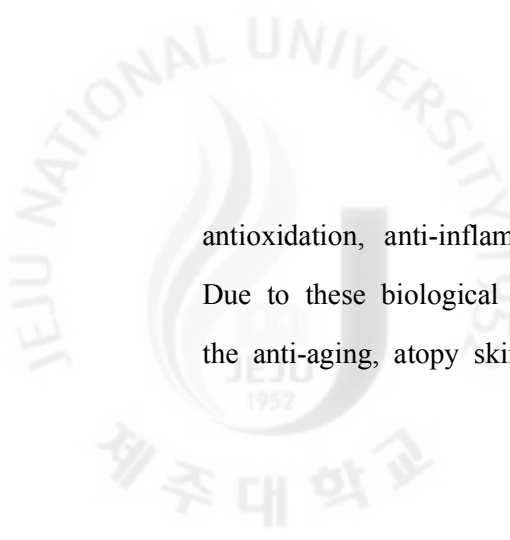
As the CH<sub>2</sub>Cl<sub>2</sub> and EtOAc solvent fractions indicated good activity, this fractions were investigated extensively to find activities compounds.

2. The CH<sub>2</sub>Cl<sub>2</sub> and EtOAc solvent fractions of *L. erythrocarpa* was subjected to a series of chromatographic separations and led to the isolation of fourteen compounds. Among them, 1-(2'-hydroxy-3',4',5',6'-tetramethylphenyl)-1-methoxy-3-phenylpropane (**13**) was isolated for the first time in the nature. The structures of thirteen known compounds and a new compound were determined by the spectroscopic methods (UV/VIS, HRFABMS, and 1D and 2D NMR);
  - ethyl caffeate (**1**), methyl cinnamate (**2**), lucidone (**3**), methylindrone (**4**),  $\beta$ -sitosterol (**5**), quercetin (**6**), quercitrin (**7**), avicularin (**8**), afzerin (**9**),

kanakugiol (**10**), methyllicudone (**11**), stigmasterol (**12**), 1-(2'-hydroxy-3',4',5',6'-tetramethylphenyl)-1-methoxy-3-phenylpropane (new compound) (**13**), and linderone (**14**)

3. In DPPH radical scavenging activity studies ethyl cafferate (**1**) ( $RC_{50} = 3.3 \mu\text{g/mL}$ ), quercetin (**6**) ( $RC_{50} = 6.5 \mu\text{g/mL}$ ), and avicularin (**8**) ( $RC_{50} = 3.7 \mu\text{g/mL}$ ) had more potent radical scavenging activity higher than activity value of positive control (BHA,  $RC_{50} = 11.0 \mu\text{g/mL}$ )
4. In anti-inflammatory activity studies ethyl cafferate (**1**) ( $IC_{50} = 4.0 \mu\text{g/mL}$ ), methyl cinnamate (**2**) ( $IC_{50} = 4.6 \mu\text{g/mL}$ ), lucidone (**3**) ( $IC_{50} = 5.6 \mu\text{g/mL}$ ), methyllicudone (**4**) ( $IC_{50} = 4.5 \mu\text{g/mL}$ ), and kanakugiol (**10**) ( $IC_{50} = 5.3 \mu\text{g/mL}$ ) had more good activity of NO inhibition in RAW264.7 cells when comparing with the control group
5. In melanogenesis inhibition activity studies lucidone (**3**), methyllicudone (**4**), methyllicudone (**11**) new compound (**13**), kanakugiol (**10**), and linderone (**14**) exhibited good activities at  $2.5 \mu\text{g/mL}$  concentration by 19.6, 14.7, 12.3, 14.7, 6.5 and 3.8% inhibition when comparing with positive control group (In  $50 \mu\text{g/mL}$ , Arbutin has inhibition activity abilities in 30.8%). lucidone (**3**), methyllicudone (**4**), and new compound (**13**) isolated from *L. erythrocarpa* were clearly reduced TRP-1 and tyrosinase mRNA expression in a dose-dependent manner
6. In anti-obesity activity studies methyllicudone (**4**) with  $25 \mu\text{M}$  concentration has good effects of 87.0% reduction on lipid accumulation in 3T3-L1 preadipocytes. Lucidone (**3**) and methyllicudone (**11**) were inhibited adipocyte differentiation in dose-dependent manner and lipid synthesis during induced adipocyte.

In conclusion, the extracts and isolated compounds from *L. erythrocarpa* provided

The image contains a large, faint watermark of the Jeju National University logo. The logo is circular, featuring a stylized flame or sunburst in the center. The text "JEJU NATIONAL UNIVERSITY" is written in an arc at the top, and "제주대학교" is written in Korean at the bottom. The year "1952" is visible in the center of the logo.

antioxidation, anti-inflammatory, melanogenesis inhibition activity, anti-obesity effect.  
Due to these biological activities, this plant could be a potential source applicable as  
the anti-aging, atopy skin improvement and slimming cosmetics material.

### III. RESEARCH 2 : *Cornus macrophylla* Wall

#### 1. General Plants Information

- **Scientific name** *Cornus macrophylla* Wall
- **Korean name** 곰의말채나무
- **Nickname** 응수목
- **Family Name** Cornaceae
- **Distribution** Korea, Japan, Taiwan, China
- **Flowering** June - Aug
- **Fruiting** October
- **Usage** Timber for furniture, gardening tree
- **Folk medicinal use**

bleeding, cleaning blood, dactylalgia

- **Identified constituents in the literature**

No data available

- **Biological activities in the literature**

aldose reductase,<sup>77)</sup> Melanogenesis inhibition,<sup>78)</sup> anti-cancer,<sup>79)</sup> immune-modulatory activities,<sup>79)</sup> antioxidation,<sup>80)</sup> anti-diabetic ( $\alpha$ -amylase inhibition)<sup>80)</sup>

- **Research objective**

Standard material : 70% aq. EtOH extract of *C. macrophylla*

For ingredient of cosmeceutical (anti-wrinkle product)

1. Antioxidant : DPPH radical scavenging test ( $RC_{50} = 9.8 \mu\text{g/mL}$ )



Photo 6. The specimen of *C. macrophylla*



Photo 7. Photograph of *C. macrophylla*



Photo 8. Photograph of the bark of *C. macrophylla*



Photo 9. Photograph of the fruit of *C. macrophylla*

## 2. Experimental Methods

### 2-1. Plant material

The whole plant of *C. macrophylla* was collected from Jeju Halla botanical garden in 2006.

### 2-2. Solvent fraction of the leaves

The extract of *C. macrophylla* (10.4 g) leaves was suspended in water (1.0 L) and successively partitioned with *n*-hexane, ethyl acetate and *n*-butanol to give *n*-hexane (0.9 g), ethyl acetate (3.7 g), *n*-butanol (3.0 g) and water (3.4 g) fractions (Scheme 4).

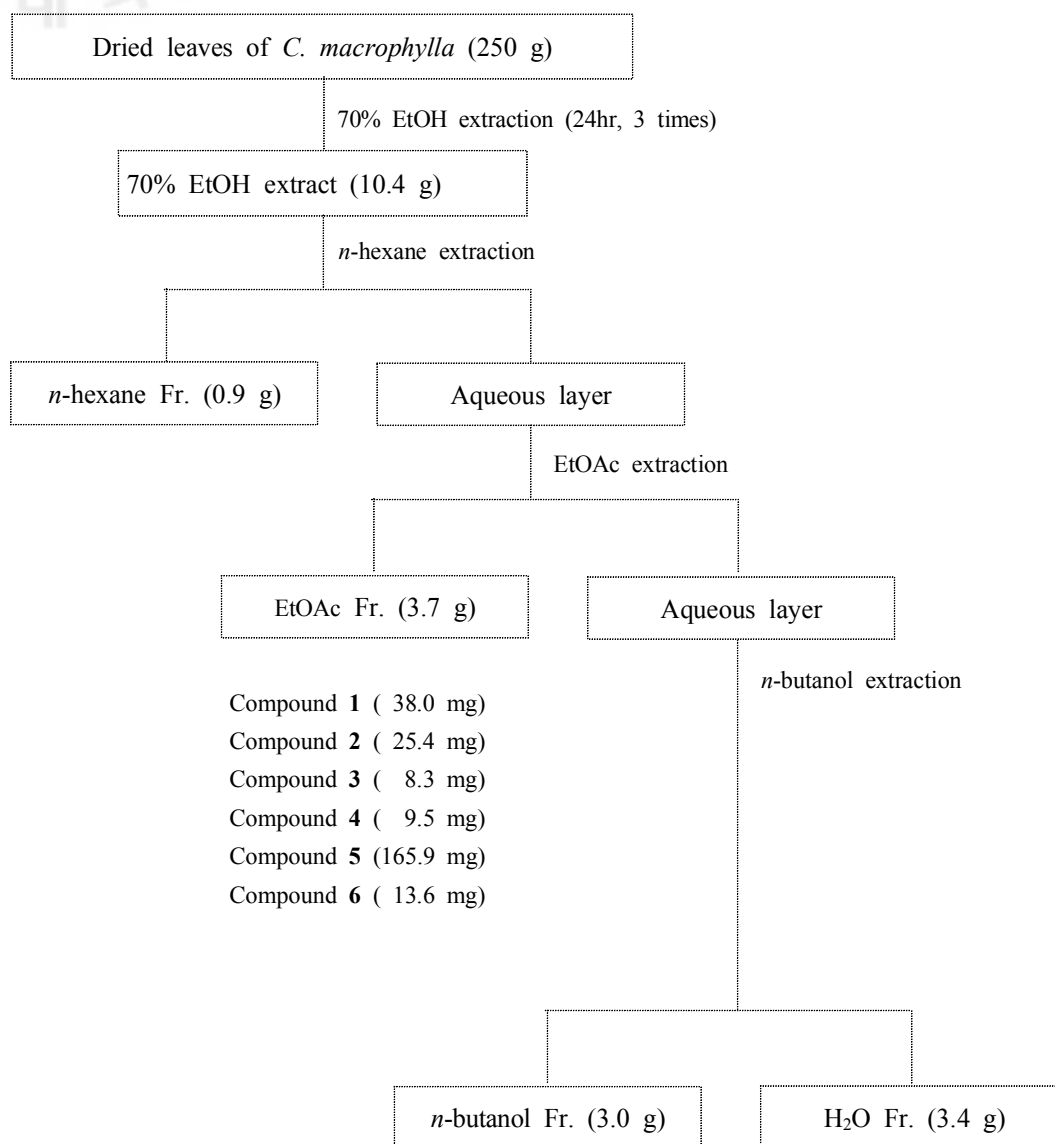
### 2-3. Isolation and purification

#### 2-3-1. Isolation produce of ethyl acetate fraction from the leaves (CE)

The EtOAc fraction (3.7 g) was chromatographed over celite with  $\text{CHCl}_3$ ,  $\text{Et}_2\text{O}$ , EtOAc, and  $\text{Me}_2\text{CO}$  successively. The obtained  $\text{CHCl}_3$  fraction (90.4 mg) was applied to recrystallization and provided the compound **1** (38.0 mg). It was further chromatographed over silica gel CC with  $\text{CHCl}_3/\text{MeOH}$  (7/2) to provided 4 fractions (CE-I ~ IV), and CE-IV was identified as the compound **2** (25.4 mg). The obtained  $\text{Et}_2\text{O}$  fraction (1.8 g) was subjected to reversed-phase silica gel column chromatography using step gradient solvents (water and methanol) to give 10 fractions (CE- I ~ XVI). The CE-IV was chromatographed over silica gel CC with  $\text{CHCl}_3/\text{MeOH}$  (7/1) to provided 3 fractions (CE-IV-1~3), CE-IV-2 and CE-IV-3 were respectively identified as the compound **3** (8.3 mg) and **4** (9.5 mg). Other subsection of CE-VII was chromatographed over silica gel CC with  $\text{CHCl}_3/\text{MeOH}$  (3/1) to



provided 3 fractions, and CE-VII-3 provided the compound **5** (165.8 mg). Finally, the CE-VIII fraction was purified by short silica gel column with CHCl<sub>3</sub>/MeOH (4/1) to give the compound **6** (13.6 mg) (Scheme 4).



Scheme 4. Extraction and fractionation of the leaves of *C. macrophylla*

### 3. Results

3-1. The structures of the compounds isolated from of *C. macrophylla*

#### 3-1-1. Compound 1

- Compound Name renyolone; cleroindicin F
- Synonym(s) 3,3*a*,7,7*a*-Tetrahydro-3*a*-hydroxy-6(2*H*)-benzofuranone
- CAS Registry Number 93675-87-7
- Appearance colorless oil
- Chemical Formula  $C_8H_{10}O_3$
- Molecular Weight (g/mol) 154.16
- Melting Point (°C) -
- $^1H$ -NMR (400 MHz,  $CD_3OD$ )  
 $\delta$ : 6.78 (1H, *dd*,  $J = 1.6, 10.2$  Hz, H-6), 5.96 (1H, *dd*,  $J = 0.5, 10.2$  Hz, H-5), 4.14 (1H, *ddd*,  $J = 1.6, 4.3, 4.5$  Hz, H-2), 3.99 (1H, *dd*,  $J = 5.8, 8.4$  Hz, H-8*a*), 3.85 (1H, *ddd*,  $J = 7.2, 7.8, 8.5$  Hz, H-8 $\beta$ ), 2.77 (1H, *dd*,  $J = 4.0, 16.8$  Hz, H-3 $\beta$ ), 2.56 (1H, *dd*,  $J = 4.0, 16.8$  Hz, H-3*a*), 2.27 (1H, *ddd*,  $J = 7.2, 8.2, 12.7$  Hz, H-7*a*), 2.19 (1H, *ddd*,  $J = 5.6, 7.8, 12.7$  Hz, H-7 $\beta$ )
- $^{13}C$ -NMR (100 MHz,  $CD_3OD$ )  
 $\delta$ : 199.5 (C-4), 151.0 (C-6), 129.1 (C-5), 82.6 (C-2), 75.9 (C-1), 67.4 (C-8), 40.9 (C-3), 40.7 (C-7)
- Other data in the literature
  1. Optical Rotation:  $[\alpha]_{22}^D = -2.7$  ( $c$  0.02 in MeOH)
  2. Racemic (small opt. rotns. reported)

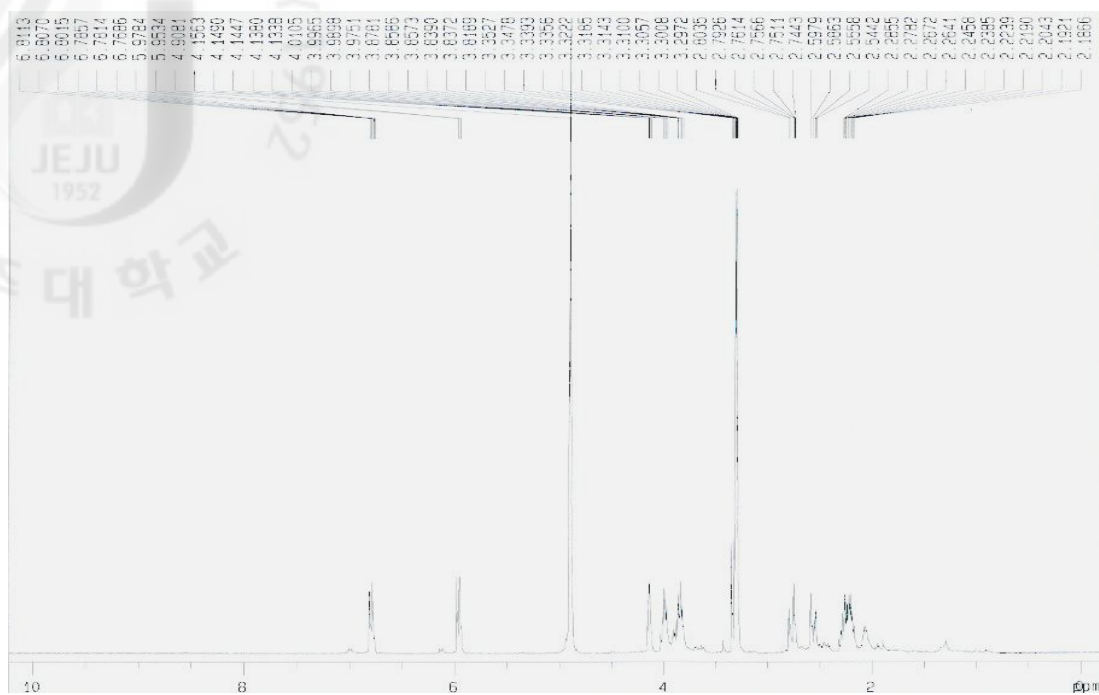


Figure 73.  $^1\text{H-NMR}$  spectrum of renylone (**1**) in  $\text{CD}_3\text{OD}$

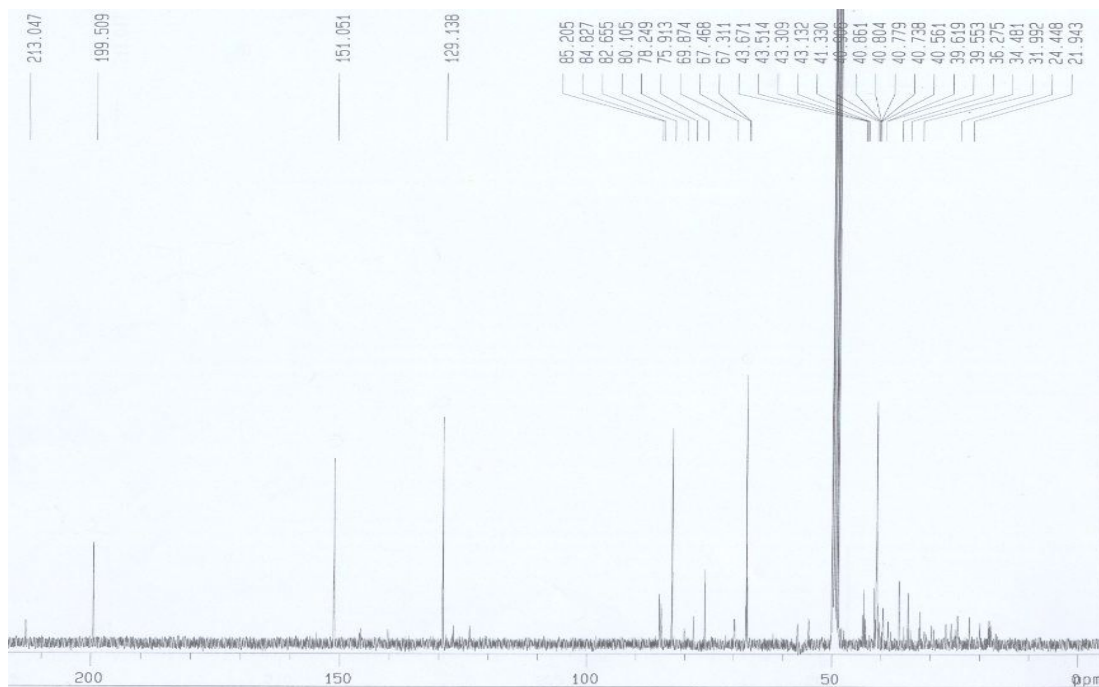


Figure 74.  $^{13}\text{C-NMR}$  spectrum of renylone (**1**) in  $\text{CD}_3\text{OD}$

Compound **1** was isolated as colorless oil. The  $^{13}\text{C}$  and DEPT NMR spectrum in  $\text{CD}_3\text{OD}$  of compound **1** were detected eight peaks at  $\delta_{\text{C}}$  151.0 (C-5), 129.1 (C-6), 82.6 (C-2), 75.9 (C-1), 67.4 (C-3), 40.9 (C-8) and 40.7 (C-7) including one keto group at  $\delta_{\text{C}}$  199.5 (C-4) (Fig. 74). The molecular formula of compound **1** was determined  $\text{C}_8\text{H}_{10}\text{O}_3$  by several NMR datas (Data did not shown). The structure of compound **1** was identified rengyolone by comparison of its spectral data with those in the literature (Fig. 75).<sup>81-85</sup> Rengyolone was reported for the first time from this plant.

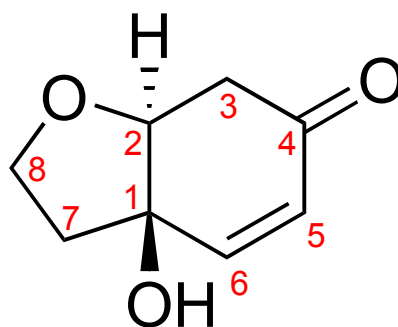


Figure 75. Structure of compound **1**; Rengyolone

### 3-1-2. Compound 2

- Compound Name 3,4,5-trihydroxybenzoic acid; Et ester
- Synonym(s) Ethyl gallate, Phyllemblin, Ethyl 3,4,5-trihydroxybenzoate
- CAS Registry Number 831-61-8
- Appearance white powder
- Chemical Formula  $C_9H_{10}O_5$
- Molecular Weight (g/mol) 198.17
- Melting Point ( $^{\circ}C$ ) 197 - 198
- $^1H$ -NMR (400 MHz,  $CD_3OD$ )  
 $\delta$ : 7.03 (2H, *s*, H-2, 6), 4.27 (2H, *q*,  $J = 7.0$  Hz, H-8), 1.34 (3H, *t*  $J = 7.0$  Hz, H-9)
- $^{13}C$ -NMR (100 MHz,  $CD_3OD$ )  
 $\delta$ : 168.6 (C-7), 146.6 (C-3,5), 139.8 (C-4), 121.8 (C-1), 110.1 (C-2,6), 61.8 (C-8), 14.7 (C-9)
- Biological activities in the literature  
anti-inflammation, antioxidant, antibiotic
- Other data in the literature
  1. Biological Source: Occurs in *Acacia* spp. and Indian gooseberry (*Phyllanthus emblica*)

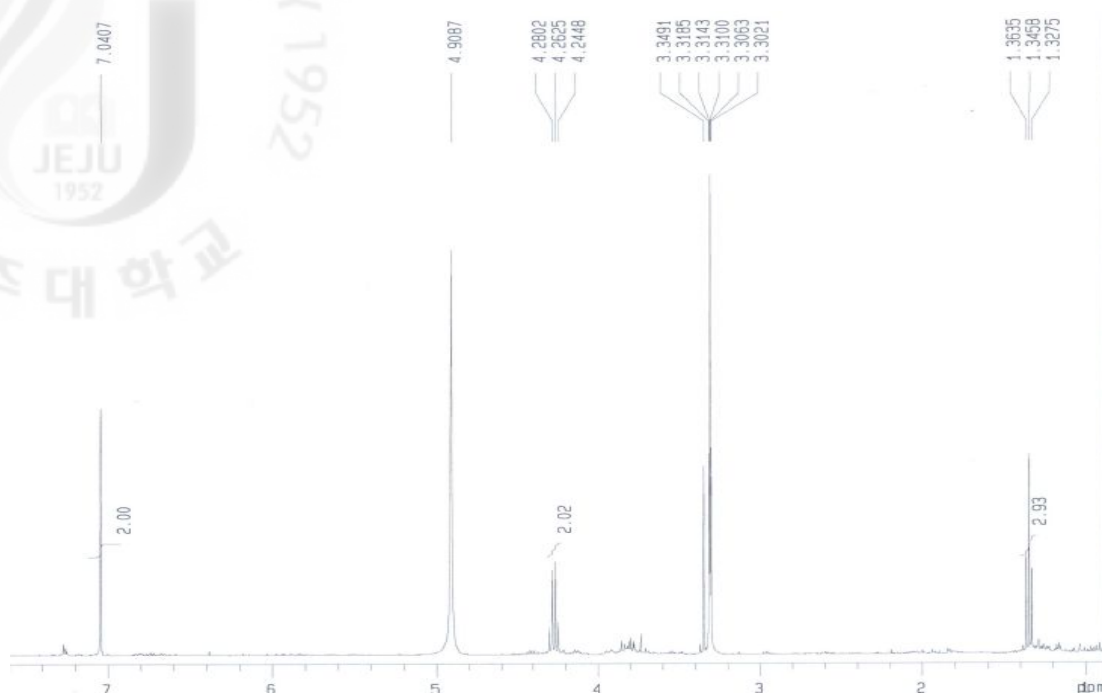


Figure 76.  $^1\text{H-NMR}$  spectrum of ethyl gallate (**2**) in  $\text{CD}_3\text{OD}$

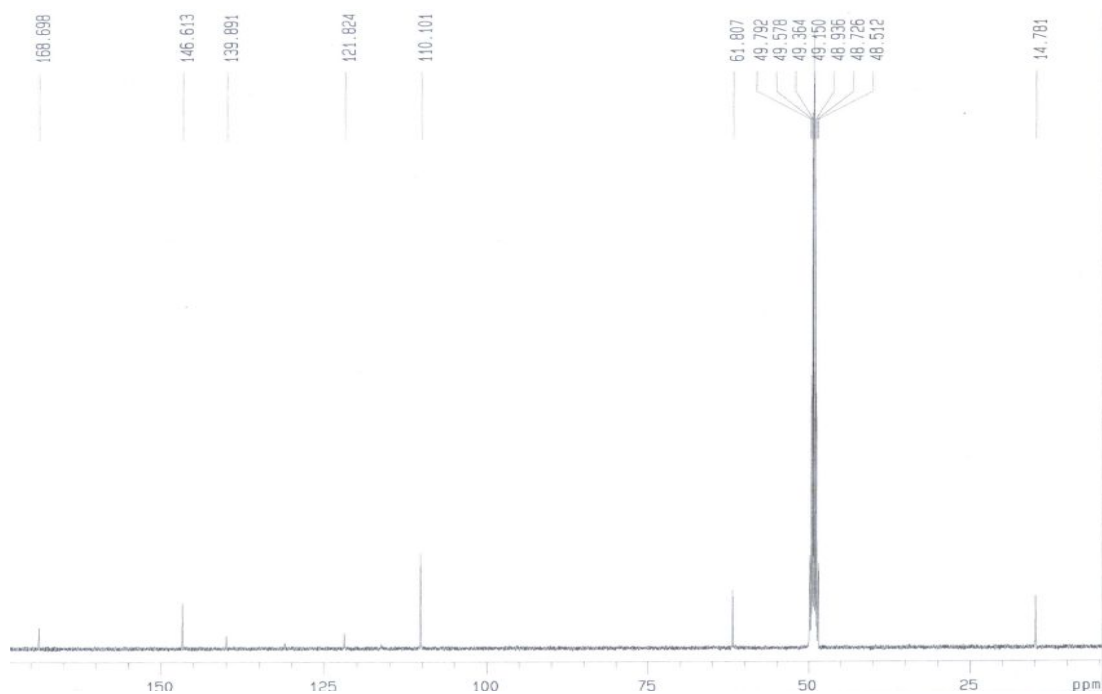


Figure 77.  $^{13}\text{C-NMR}$  spectrum of ethyl gallate (**2**) in  $\text{CD}_3\text{OD}$

Compound **2** was isolated as white powder and phenolic compound with the ester carbonyl group. Its NMR spectrum in CD<sub>3</sub>OD of compound **2** was showed indicating the presence of the 3,4,5-trisubstitued pattern with one symmetry peak at  $\delta_{\text{H}}$  7.03 (2H, *s*, H-2, 6) and one ethyl group  $\delta_{\text{H}}$  4.27 (2H, *q*,  $J = 7.0$  Hz, H-8), 1.34 (3H, *t*  $J = 7.0$  Hz, H-9) (Fig. 76). The <sup>13</sup>C-NMR spectrum of compound **2** was showed nine carbon signals including six signals of aromatic ring(s) at  $\delta_{\text{C}}$  139.8 (C-4), 121.8 (C-1) including symmetry peaks at  $\delta_{\text{C}}$  146.6 (2C, C-3,5), 110.1 (2C, C-2,6) with one ester group at  $\delta_{\text{C}}$  168.6 (C-7) (Fig. 77). Thus, the structure of compound **2** was determined as ethyl gallate by comparison of its spectral data with those in the literature (Fig. 78).<sup>86-89</sup> Ethyl gallate was reported for the first time from this plant.

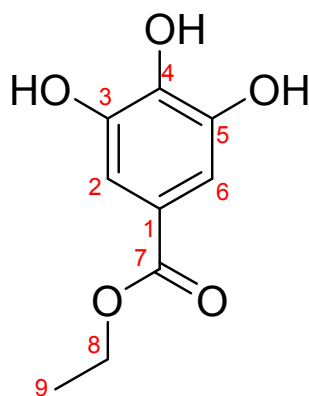


Figure 78. Structure of compound **2**; Ethyl gallate

### 3-1-3. Compound 3

- Compound Name 3,3',4',5',7-pentahydroxyflavan; (2*R*,3*S*)-form
- Synonym(s) (+)-*trans*-form. Catechin, Catechol, Cianidanol, Catechuic acid.
- CAS Registry Number 154-23-4
- Appearance yellow powder
- Chemical Formula  $C_{15}H_{14}O_6$
- Molecular Weight (g/mol) 290.26
- Melting Point ( $^{\circ}C$ ) 93 - 96
- $^1H$ -NMR (400 MHz,  $CD_3OD$ )  
 $\delta$ : 6.83 (1H, *d*,  $J = 1.9$  Hz, H-6'), 6.76 (1H, *d*,  $J = 8.0$  Hz, H-5'), 6.71 (1H, *dd*,  $J = 1.7, 8.0$  Hz, H-2'), 5.92 (1H, *d*,  $J = 2.4$  Hz, H-8), 5.85 (1H, *d*,  $J = 2.2$  Hz, H-6), 4.56 (1H, *d*,  $J = 7.6$  Hz, H-2), 3.96 (1H, *m*, H-3), 2.84 (1H, *dd*,  $J = 5.3, 16.4$  Hz, H-4a), 2.50 (1H, *dd*,  $J = 8.0, 16.0$  Hz, H-4b)
- $^{13}C$ -NMR (100 MHz,  $CD_3OD$ )  
 $\delta$ : 157.9 (C-5), 157.7 (C-7), 157.0 (C-9), 146.4 (C-4'), 146.3 (C-5'), 132.3 (C-1'), 120.1 (C-6'), 116.2 (C-3'), 115.3 (C-2'), 100.9 (C-10), 96.3 (C-6), 95.6 (C-8), 82.9 (C-2), 68.9 (C-3), 28.6 (C-4)
- Biological activities in the literature  
anti-ulcer, treatment of hepatic disorders, antioxidant, anti-inflammation, anti-diabetic
- Other data in the literature  
1. Optical Rotation:  $[\alpha]_D^{22} = + 17 (CHCl_3)$





Figure 79.  $^1\text{H}$ -NMR spectrum of (+)-catechin (**3**) in  $\text{CD}_3\text{OD}$

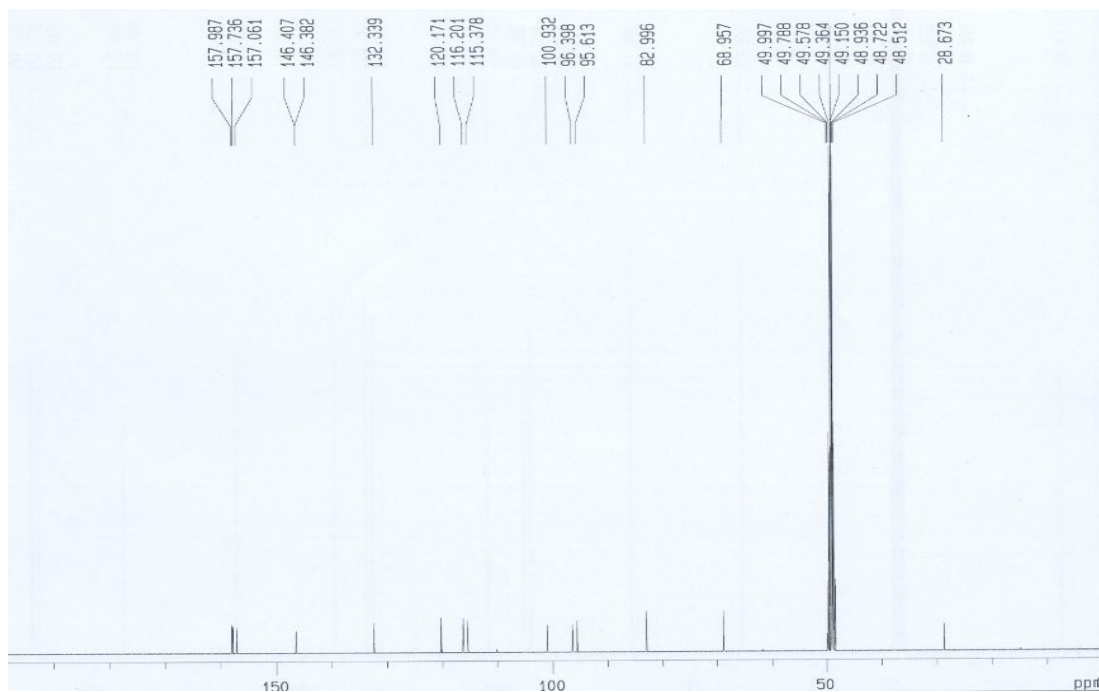


Figure 80.  $^{13}\text{C}$ -NMR spectrum of (+)-catechin (**3**) in  $\text{CD}_3\text{OD}$

Compound **3** was isolated as yellow powder. The  $^1\text{H-NMR}$  spectra of compound **1** in  $\text{CD}_3\text{OD}$  indicated a 5,7-dihydroxylated pattern for ring A (two *meta*-coupled doublets at  $\delta_{\text{H}}$  5.92 (1H, *d*,  $J = 2.4$  Hz, H-8), 5.85 (1H, *d*,  $J = 2.2$  Hz, H-6) and a 3,4-dihydroxylation pattern for ring B [ABX system signals at  $\delta_{\text{H}}$  6.83 (1H, *d*,  $J = 1.9$  Hz, H-6'), 6.76 (1H, *d*,  $J = 8.0$  Hz, H-5'), 6.71 (1H, *dd*,  $J = 1.7, 8.0$  Hz, H-2')], showed flavan-3-ols pattern like a catechin and *epi*-catechin at  $\delta_{\text{H}}$  2.84 (1H, *dd*,  $J = 5.3, 16.4$  Hz, H-4a) and 2.50 (1H, *dd*,  $J = 8.0, 16.0$  Hz, H-4b) (Fig. 79). The  $^{13}\text{C-NMR}$  spectrum of compound **3** showed fifty carbon signals including twelve carbon signals of aromatic rings at  $\delta_{\text{C}}$  157.9 (C-5), 157.7 (C-7), 157.0 (C-9), 146.4 (C-4'), 146.3 (C-5'), 132.3 (C-1'), 120.1 (C-6'), 116.2 (C-3'), 115.3 (C-2'), 100.9 (C-10), 96.3 (C-6), 95.6 (C-8) (Fig. 80). Thus, the structure of compound **3** was determined as (+)-catechin by comparison of its spectral data with those in the literature (Fig. 81).<sup>90)</sup>

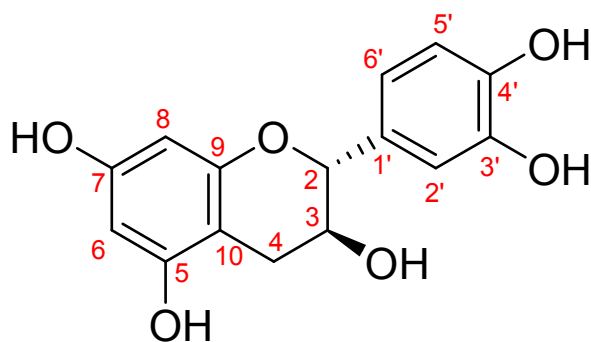


Figure 81. Structure of compound **3**; (+)-catechin

### 3-1-4. Compound 4

- Compound Name 3-Hydroxy-12-ursen-28-oic acid; 3 $\beta$ -form; ursolic acid
- Synonym(s) micromerol, formosolic acid, forucosolic acid, bungeolic acid
- CAS Registry Number 77-52-1
- Appearance white needle crystal
- Chemical Formula C<sub>30</sub>H<sub>48</sub>O<sub>3</sub>
- Molecular Weight (g/mol) 456.70
- Melting Point (°C) 291
- <sup>1</sup>H-NMR (400 MHz, DMSO-*d*<sub>6</sub>)  
 $\delta$ : 5.12 (1H, *t*, *J* = 4.1 Hz, H-12), 4.30 (1H, *dd*, *J* = 5.1, 8.4 Hz, H-3), 2.20 (1H, *brd*, *J* = 11.0 Hz, H-18), 1.03 (3H, *s*, Me-26), 0.91 (3H, *d*, *J* = 6.1 Hz, Me-30), 0.89 (3H, *s*, Me-23), 0.86 (3H, *s*, Me-27), 0.81 (3H, *d*, *J* = 6.1 Hz, Me-29), 0.74, 0.67 (3H each, *s*, Me-24 and Me-25)
- <sup>13</sup>C-NMR(100MHz, DMSO-*d*<sub>6</sub>)  
 $\delta$ : 178.3 (C-28), 138.2 (C-13), 124.5 (C-12), 76.8 (C-3), 54.7 (C-5), 52.3 (C-18), 47.0 (C-17), 46.8 (C-9), 41.6 (C-14), 38.5 (C-8), 38.4 (C-19), 38.3 (C-1, 4), 38.2 (C-20), 38.3 (C-20), 38.3 (C-20), 36.7 (C-22, 10), 32.7 (C-7), 30.1 (C-21), 28.2 (C-15), 27.5 (C-23), 27.0 (C-27), 23.8 (C-2), 23.2 (C-16), 22.8 (C-29), 21.1 (C-30), 18.0 (C-6), 17.0 (C-26), 16.9 (C-11), 16.1 (C-25), 15.2 (C-24)
- Biological activities in the literature  
anti-neoplastic, anti-ulcer, angiogenesis inhibition, anti-HIV, skin tumourigenesis, protein kinase C inhibition, HIV-1 protease inhibitor, anti-wrinkle
- Other data in the literature  
1. Optical Rotation:  $[\alpha]_D^{22} = + 66$  (EtOH)



Figure 82.  $^1\text{H-NMR}$  spectrum of ursolic acid (**4**) in  $\text{DMSO-}d_6$

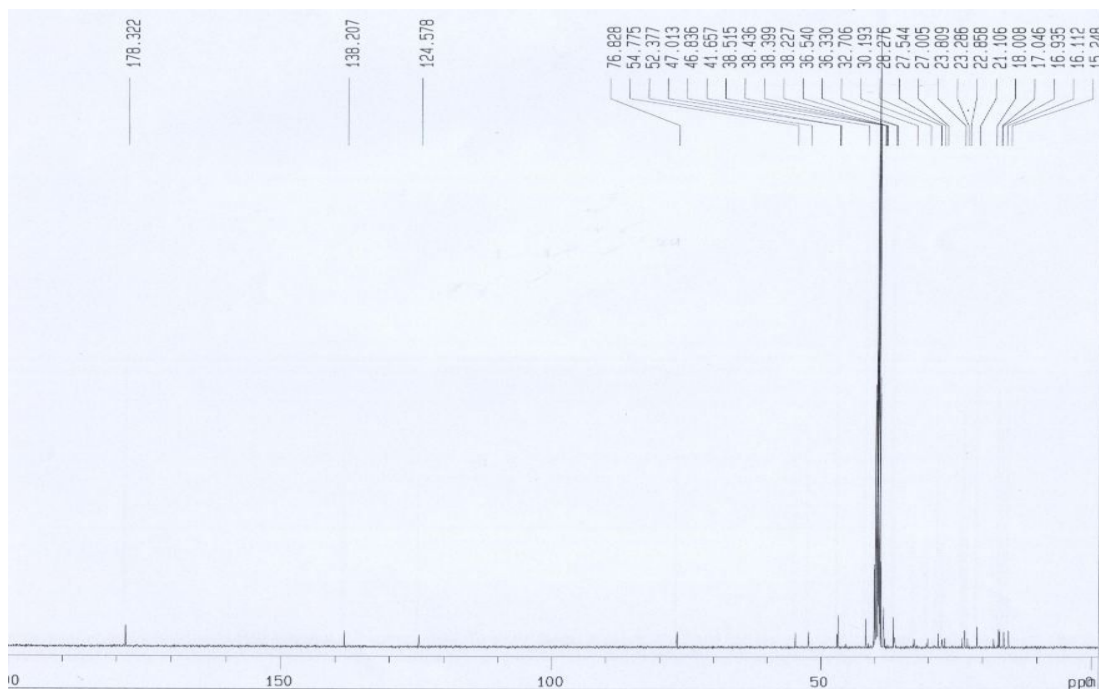


Figure 83.  $^{13}\text{C-NMR}$  spectrum of ursolic acid (**4**) in  $\text{DMSO-}d_6$

Compound **4** was isolated as white needle crystal and whole pattern of NMR spectra suggested the presence of a triterpenoid skeleton. The  $^1\text{H-NMR}$  spectrum of compound **4** in  $\text{DMSO-}d_6$  was indicated five angular methyl group at  $\delta_{\text{H}}$  1.03 (3H, *s*, Me-26), 0.89 (3H, *s*, Me-23), 0.86 (3H, *s*, Me-27), 0.74, 0.67 (3H each, *s*, Me-24 and Me-25), two secondary methyl group at 0.91 (3H, *d*,  $J = 6.1$  Hz, Me-30) and 0.81 (3H, *d*,  $J = 6.1$  Hz, Me-29), two doublets at  $\delta_{\text{H}}$  4.30 (1H, *dd*,  $J = 5.1, 8.4$  Hz, H-3), 2.20 (1H, *brd*,  $J = 11.04$  Hz H-18) and a triplet at  $\delta_{\text{H}}$  5.12 (1H, *t*,  $J = 4.1$  Hz, H-12) due to H-12 and by the chemical shifts at  $\delta_{\text{C}}$  124.5 (C-12) and 138.2 (C-13) and that of 28-COOH at  $\delta_{\text{C}}$  178.3 in the  $^{13}\text{C-NMR}$  spectrum (Fig. 82-83). The compound **4** was identified as  $3\beta$ -hydroxy-urs-12-en-28-oic acid (ursolic acid) (Fig. 84).<sup>91)</sup> Ursolic acid was reported for the first time from this plant.

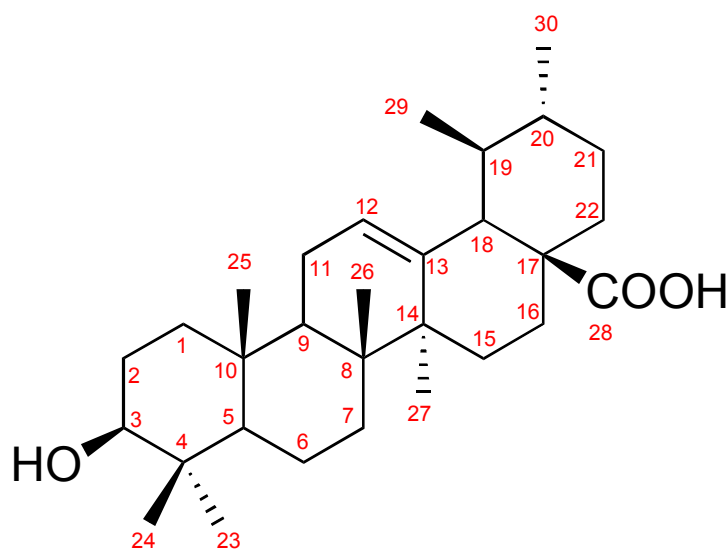


Figure 84. Structure of compound **4**;  $3\beta$ -hydroxy-urs-12-en-28-oic acid (ursolic acid)

3-1-5. Compound 5

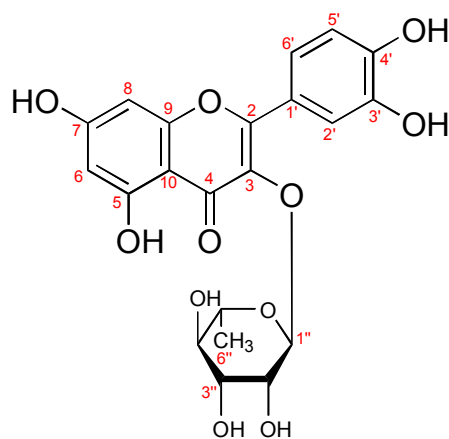


Figure 85. Structure of compound 5; Quercetin-3-*O*- $\alpha$ -L-rhamnoside (quercitrin)<sup>60)</sup>

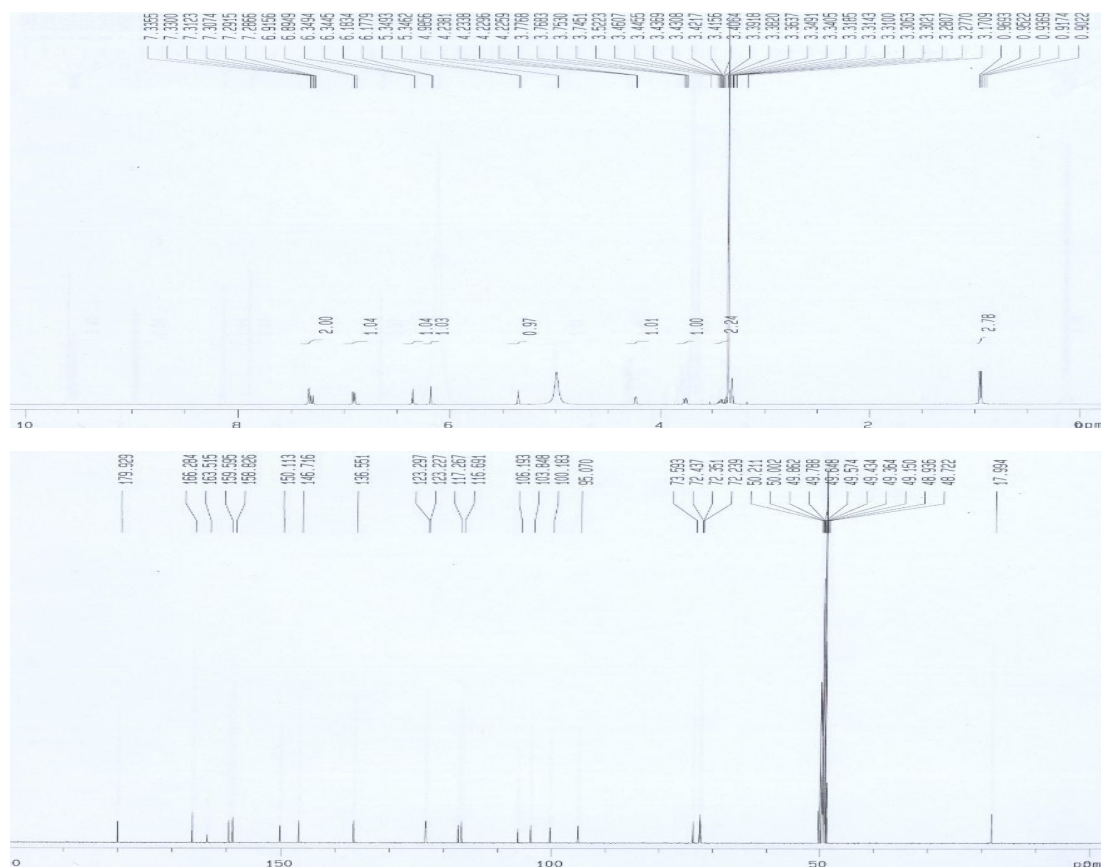


Figure 86. <sup>1</sup>H-NMR and <sup>13</sup>C-NMR spectra of quercetin-3-*O*- $\alpha$ -L-rhamnoside (5) in CD<sub>3</sub>OD

3-1-6. Compound 6

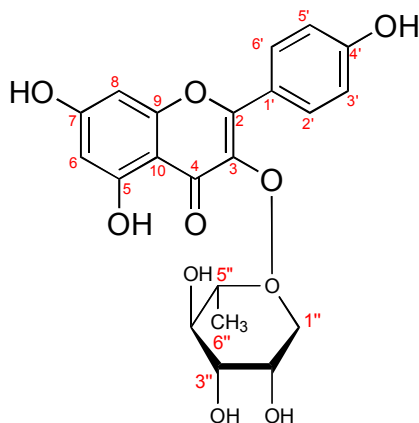


Figure 87. Structure of compound 6; Kaempferol-3-*O*- $\alpha$ -L-rhamnoside (afzelin)<sup>(63,92)</sup>

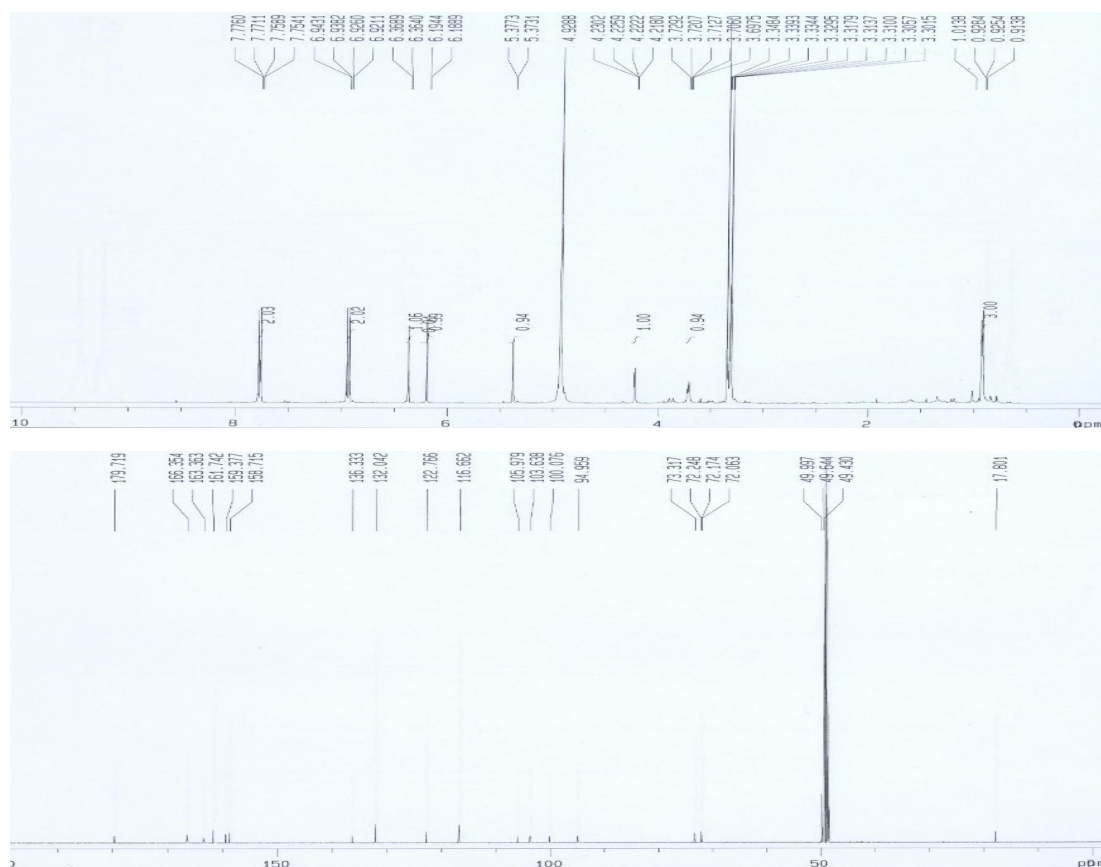


Figure 88. <sup>1</sup>H-NMR and <sup>13</sup>C-NMR spectra of kaempferol-3-*O*- $\alpha$ -L-rhamnoside (6) in CD<sub>3</sub>OD

## 3-2. Biological activities

### 3-2-1. Antioxidant activity

#### 3-2-1-1. Free radical scavenging activity of the crude 70% *aq.* EtOH extract

Antioxidative activity was determined using crude 70% *aq.* EtOH extract and isolated compounds by DPPH radical scavenging activity assay. The DPPH radical scavenging activity of the 70% *aq.* EtOH extract by comparison with positive control was showed in Table 16. It showed that 70% *aq.* EtOH extract of *C. macrophylla* gradually increased with increasing concentration and scavenging (Data did not shown). The 70% *aq.* EtOH extract exhibited higher free radical scavenging activity and its also showed remarkably similar good activity than positive control (Vitamin C,  $RC_{50} = 4.4 \mu\text{g/mL}$ ) except the lower concentration at  $RC_{50} = 9.8 \mu\text{g/mL}$ .

Table 16. DPPH radical scavenging effect of the crude 70% *aq.* EtOH extract

Samples	$RC_{50}$ ( $\mu\text{g/mL}$ )		
	DPPH radical scavenging activity		
70% <i>aq.</i> EtOH ext.	9.8	±	1.02
Positive control (Vitamin C)	4.4	±	0.32

Primarily radical scavenging activity was determined at 0 to 200  $\mu\text{g/mL}$  concentration of samples. Scavenging concentration for 50% of free radical ( $RC_{50}$ ) was calculated from logarithmic regression equation obtained from the values of at least five dilutions of the primary concentration. Values represent mean  $\pm$  SDs ( $n = 3$ ); in parentheses is  $RC_{50}$  value of respective sample

N/A. not assay; >. out of range



### 3-2-1-2. Free radical scavenging activity of the isolated compounds

The DPPH radical scavenging activity of the isolated compounds from the EtOAc fraction showed to the Table 17, Among the isolated compounds, ethyl gallate (2) and catechin (3) had more potent free radical scavenging activity which is stronger than positive control (BHA,  $RC_{50} = 14.9 \mu\text{g/mL}$ ) and according to reference of antioxidant that two compounds which type of flavonoid that have aromatic rings also exhibited stronger activities. This result was showed that ethyl gallate (2) and (+)-catechin (3) might be the major active compounds responsible for the DPPH radical scavenging activity of leaves of *C. macrophylla*.

Table 17. DPPH radical scavenging effect of the isolated compounds

Samples	$RC_{50}$ ( $\mu\text{g/mL}$ )	
	DPPH radical scavenging activity	
Compound 1 renyolone	>	100
Compound 2 ethyl gallate	3.8	$\pm$ 0.4
Compound 3 (+)-catechin	8.6	$\pm$ 0.5
Compound 4 ursolic acid	>	100
Compound 5 quercitrin	20.1	$\pm$ 0.8
Compound 6 afzelin	25.4	$\pm$ 0.3
Positive control (BHA) <sup>1)</sup>	14.9	$\pm$ 0.4

Primarily radical scavenging activity was determined at 0 to 200  $\mu\text{g/mL}$  concentration of samples. Scavenging concentration for 50% of free radical ( $RC_{50}$ ) was calculated from logarithmic regression equation obtained from the values of at least five dilutions of the primary concentration. Values represent mean  $\pm$  SDs (n = 3); in parentheses is  $RC_{50}$  value of respective sample

N/A. not assay; BHA. butylated hydroxyanisole<sup>1)</sup>; >. out of range

#### 4. Discussion

In this study, *C. macrophylla* were evaluated for the activities on antioxidant activity. The active constituents were identified following activity-guided isolation with chromatography.

1. The dried leaves of *C. macrophylla* were extracted with 70% *aq.* EtOH at room temperature. This extract was tested for their inhibitory effects;

- DPPH radical scavenging activity test for the antioxidant activity

As the 70% *aq.* EtOH extract of *C. macrophylla* exhibited considerable good activities. This extract was investigated extensively to find active compounds.

2. The EtOAc fraction of *C. macrophylla* was subjected to a series of chromatographic separations and led to the isolation of six compounds. The structures of six known compounds were determined by the spectroscopic methods (UV/VIS, and 1D - 2D NMR).

- Rengyolone (1), ethyl gallate (2), (+)-catechin (3), ursolic acid (4), quercitrin (5), afzelin (6)

3. In DPPH radical scavenging activity studies ethyl gallate ( $RC_{50} = 3.8 \mu\text{g/mL}$ ) and catechin ( $RC_{50} = 8.6 \mu\text{g/mL}$ ) had more potent radical scavenging activity higher than activity value of positive control (BHA,  $RC_{50} = 14.9 \mu\text{g/mL}$ )

In conclusion, the extracts and isolated compounds from *C. macrophylla* provided antioxidation. Due to these biological activities, this plant could be a potential source applicable as for the anti-aging cosmetics material.

### III. RESEARCH 3 : *Aster subulatus* Michx

#### 1. General Plants Information

- **Scientific name** *Aster subulatus* Michx
- **Korean name** 비짜루국화
- **Nickname** 황무지쭉부쟁
- **Family name** Compositae
- **Habitat** Annual grass native to America<sup>93)</sup>
- **Flowering** Aug - Oct
- **Fruiting** Aug - Oct
- **Usage** Timber for furniture, gardening tree
- **Folk medicinal use**

No data available

- **Identified constituents in the literature**

flavonoids, flavonoid glycosides, chlorogenic acid<sup>94)</sup>

- **Biological activities in the literature**

No information

- **Research objective**

Standard material : 70% aq. EtOH extract of *A. subulatus*

For ingredient of cosmeceutical (whitening and anti-aging)

1. Antioxidant : Superoxide radical scavenging test ( $RC_{50} = 14.2 \mu\text{g/mL}$ )

2. Melanogenesis inhibition activity

: In 100  $\mu\text{g/mL}$ , the 47.7% melanin contents inhibitory activity on B16F10 cell  
(the cytotoxin none)



Photo 10. The specimen of *A. subulatus*



Photo 11. Photograph of the whole plant of *A. subulatus*



Photo 12. Photograph of the flower of *A. subulatus*



Photo 13. Photograph of the spore of *A. subulatus*

## 2. Experimental Methods

### 2-1. Plant material

The plant of *A. subulatus* Michx was collected from Shinpyung, Jeju Island in August 2004. A voucher specimen (04-347) is deposited at Extraction Bank of Bio-Conversion Center, Jutechnopark (JTP), Jeju, Korea.

### 2-2. Extraction and solvent fractionation

#### 2-2-1. Extraction from the whole plant

The fresh whole plant of *A. subulatus* was washed and dried by hot blast at 40 °C for three days. The shade dried whole plant of *A. subulatus* (364.7 g) was extracted with 70% *aq.* ethanol under stirring for two days at room temperature. The extract was filtered to remove the insoluble residue and filtrate was concentrated to afford a gummy residue (36.5 g). A portion of H<sub>2</sub>O (30.2 g) was suspended in water (1.0 L) and, partitioned with *n*-hexane, methylene chloride, ethyl acetate and *n*-butanol successively to give *n*-hexane (1.0 g), methylene chloride (1.1 g), ethyl acetate (1.9 g), *n*-butanol (5.1 g) and water (12.2 g) fractions (Scheme 5).

### 2-3. Isolation and purification

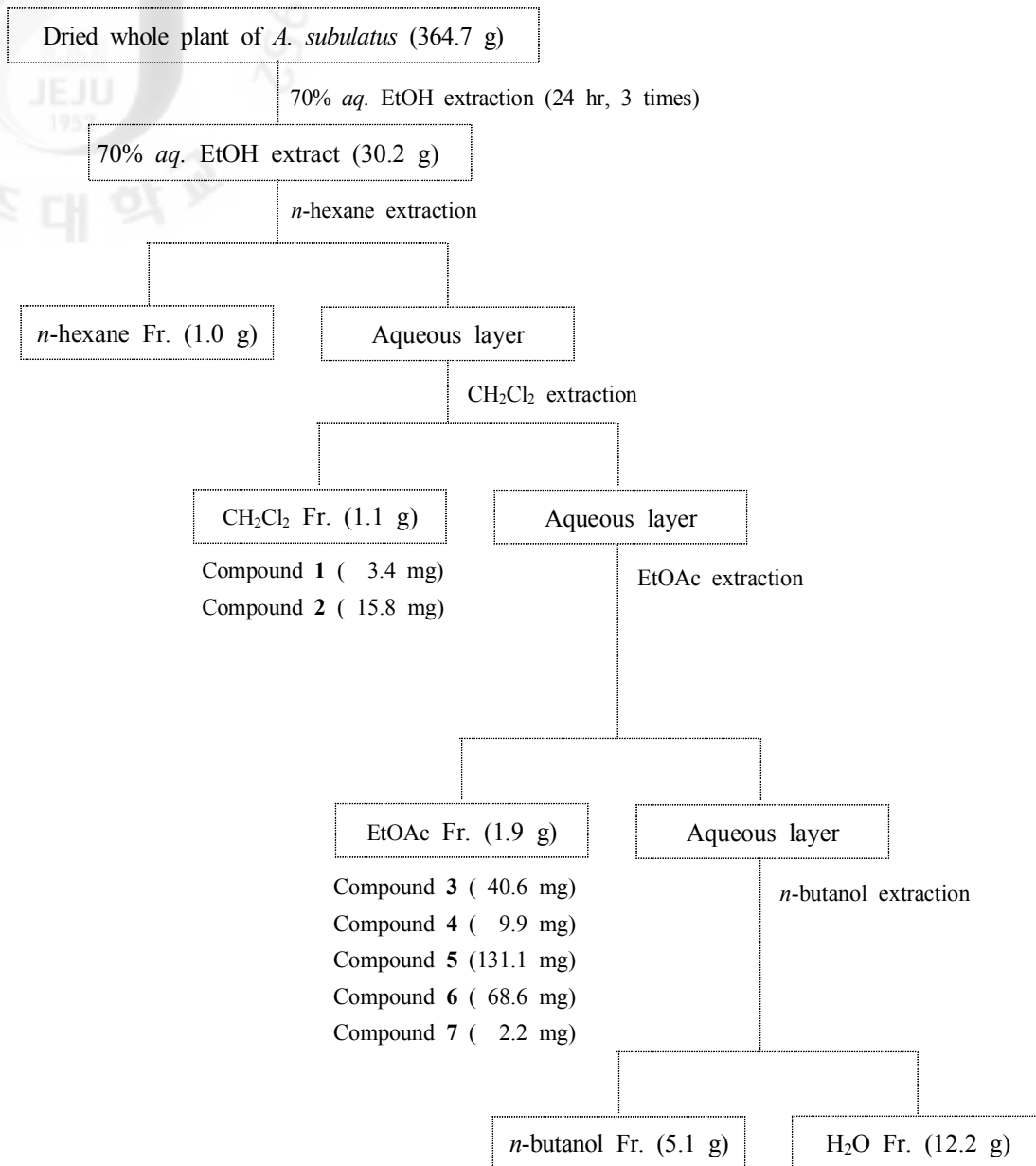
#### 2-3-1. Isolation produce of methylene chloride fraction (AM)

The methylene chloride fraction (1.1 g) was fractionated by VLC over silica gel eluting with stepwise gradient solvents of *n*-Hex/EtOAc (0 ~ 100%) and then a total of

10 fractions were collected (AM-I ~ X). The AM-III was applied to recrystallization and provided the compound **1** (3.4 mg). Subjection of AM-IV was chromatographed over silica gel CC with CHCl<sub>3</sub>/MeOH (10/1) to provide 3 fractions and than AM-IV-3 provided the compound **2** (15.8 mg) (Scheme 5).

#### 2-3-2. Isolation produce of ethyl acetate fraction (AE)

The EtOAc fraction (1.9 g) was subjected to reversed-phase silica gel CC using step wise elution with water and methanol to give 10 fractions (AE- I ~ X). The AE-III was purified by a short column and then provided the compound **3** (40.6 mg). AE-V fraction was further purified with silica gel column chromatography eluting with CHCl<sub>3</sub>/MeOH (3/1) system to afford 3 subfractions (AE-V-1 ~ 3). The AE-V-1 and AE-V-3 fractions were identified as the compound **4** (9.9 mg) and the compound **5** (131 mg), respectively. The AE-VI fraction was purified by short silica gel column with CHCl<sub>3</sub>/MeOH (3/1) to give the compound **6** (68.6 mg) and AE-IX was provided the compound **7** (2.2 mg) (Scheme 5).



Scheme 5. Extraction and fractionation of the whole plant of *A. subulatus*





### 3-1-2. Compound 2

- Compound Name ethyl (*E*)-3-(3,4-dihydroxyphenyl)prop-2-enoate; ethyl caffeate
- Synonym(s) caffeic acid ethyl ester, caffeoyl ethyl ester
- CAS Registry Number 102-37-4
- Appearance colorless powder
- Chemical Formula  $C_{11}H_{12}O_4$
- Molecular Weight (g/mol) 208.21
- Melting Point ( $^{\circ}C$ ) 148 - 152
- $^1H$ -NMR (500 MHz,  $CD_3OD$ )  
 $\delta$ : 7.03 (1H, *d*,  $J = 2.0$ , H-1), 6.78 (1H, *d*,  $J = 8.0$ , H-5), 6.93 (1H, *dd*,  $J = 8.0, 2.0$ , H-6), 6.25 (1H, *d*,  $J = 16.0$ , H-7), 7.54 (1H, *d*,  $J = 16.0$ , H-8), 4.21 (2H, *q*,  $J = 7.5$ , H-10), 1.30 (3H, *t*,  $J = 7.0$ , H-11)
- $^{13}C$ -NMR (125 MHz,  $CD_3OD$ )  
 $\delta$ : 169.4 (C-9), 149.6 (C-4), 146.9 (C-7), 146.8 (C-3), 127.9 (C-1), 123.0 (C-6), 116.6 (C-5), 115.4 (C-2), 115.2 (C-8), 61.5 (C-10), 14.7 (C-11)

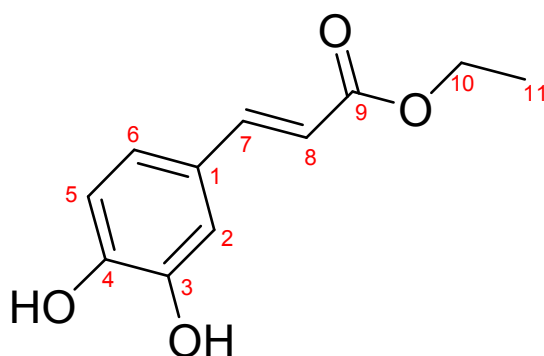


Figure 92. Structure of compound 2; Ethyl caffeate<sup>55,74,75</sup>

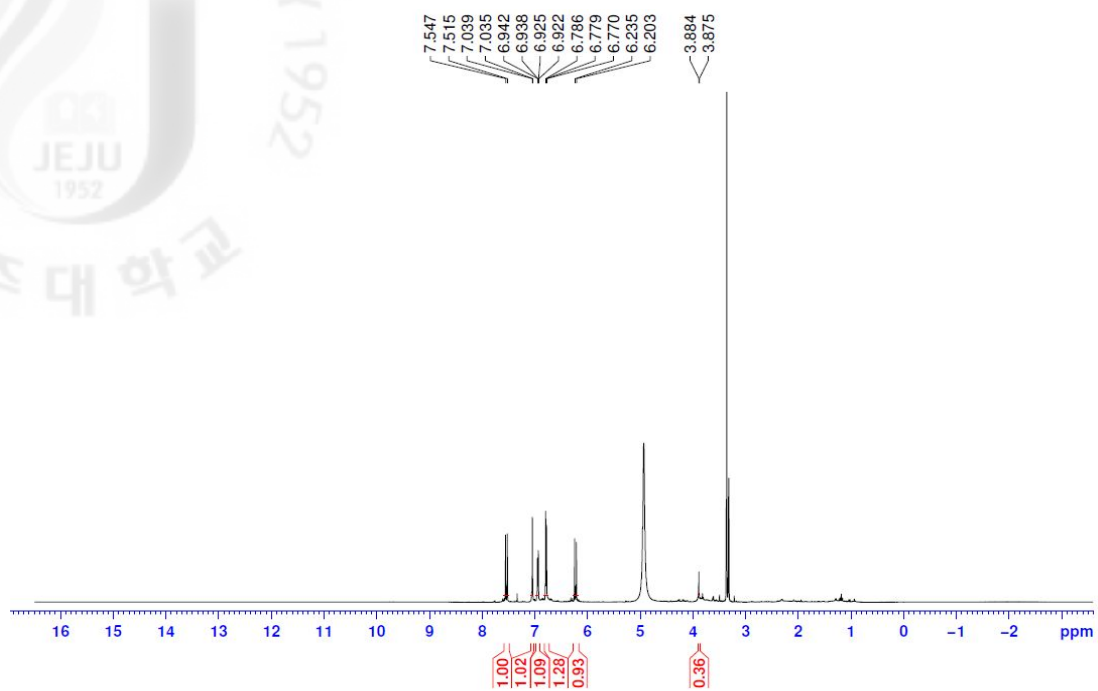


Figure 93.  $^1\text{H}$ -NMR spectrum of ethyl caffeate (2) in  $\text{CD}_3\text{OD}$

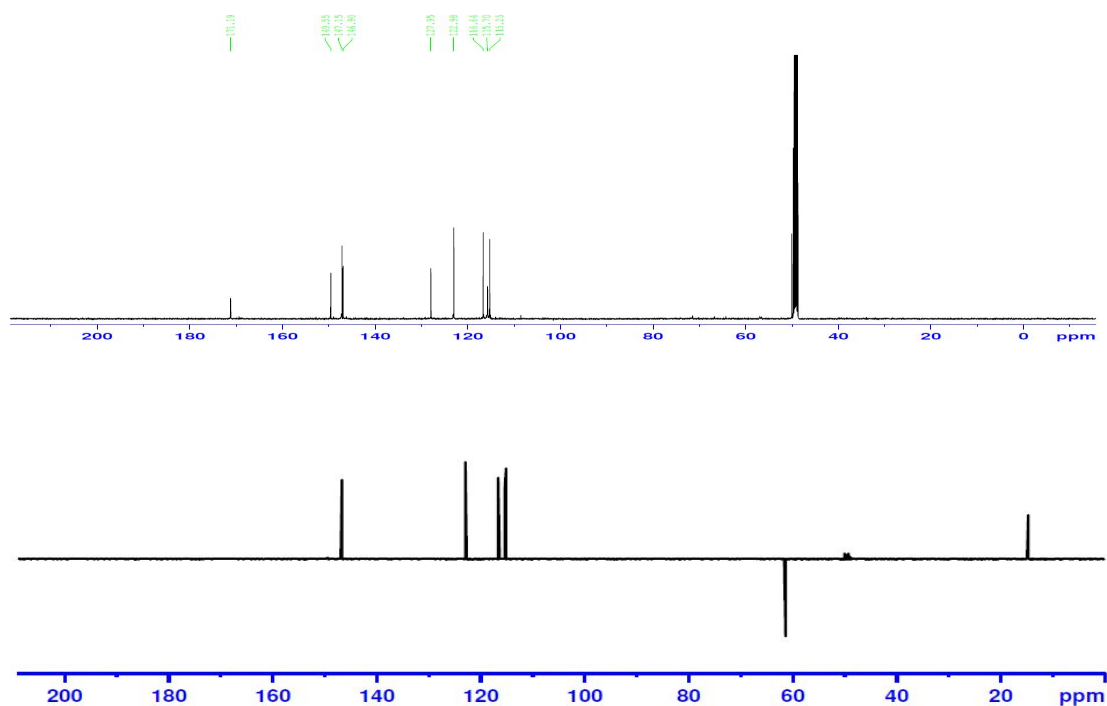


Figure 94.  $^{13}\text{C}$ -NMR and DEPT135 spectra of ethyl caffeate (2) in  $\text{CD}_3\text{OD}$

### 3-1-3. Compound 3

- Compound Name 3-(3,4-Dihydroxyphenyl)-2-propenoic acid
- Synonym(s) 3,4-Dihydroxycinnamic acid; caffeic acid
- CAS Registry Number 2316-26-9
- Appearance yellow needles
- Chemical Formula  $C_9H_8O_4$
- Molecular Weight (g/mol) 180.04
- Melting Point ( $^{\circ}C$ ) 223 - 225
- $^1H$ -NMR (500 MHz,  $CD_3OD$ )  
 $\delta$ : 7.53 (1H, *d*,  $J = 16.0$  Hz, H-7), 7.03 (1H, *d*,  $J = 2.0$  Hz, H-2), 6.93 (1H, *dd*,  $J = 8.5, 2.0$  Hz, H-6), 6.77 (1H, *d*,  $J = 8.5$  Hz, H-5), 6.21 (1H, *d*,  $J = 16.0$  Hz, H-8)
- $^{13}C$ -NMR (125 MHz,  $CD_3OD$ )  
 $\delta$ : 171.2 (C-9), 149.5 (C-4), 147.1 (C-3), 146.9 (C-7), 127.9 (C-1), 122.9 (C-6), 116.6 (C-5), 115.7 (C-2), 115.2 (C-8)
- Biological activities in the literature  
HIV-1 integrase inhibitor, anti-inflammation, antioxidant, anti-glycation, neuroprotective effect, anti-fungicide
- Other data in the literature
  1. UV (MeOH)  $\lambda_{maxnm}$ : 327 and 295
  2. Density: 1.478  $g/cm^2$

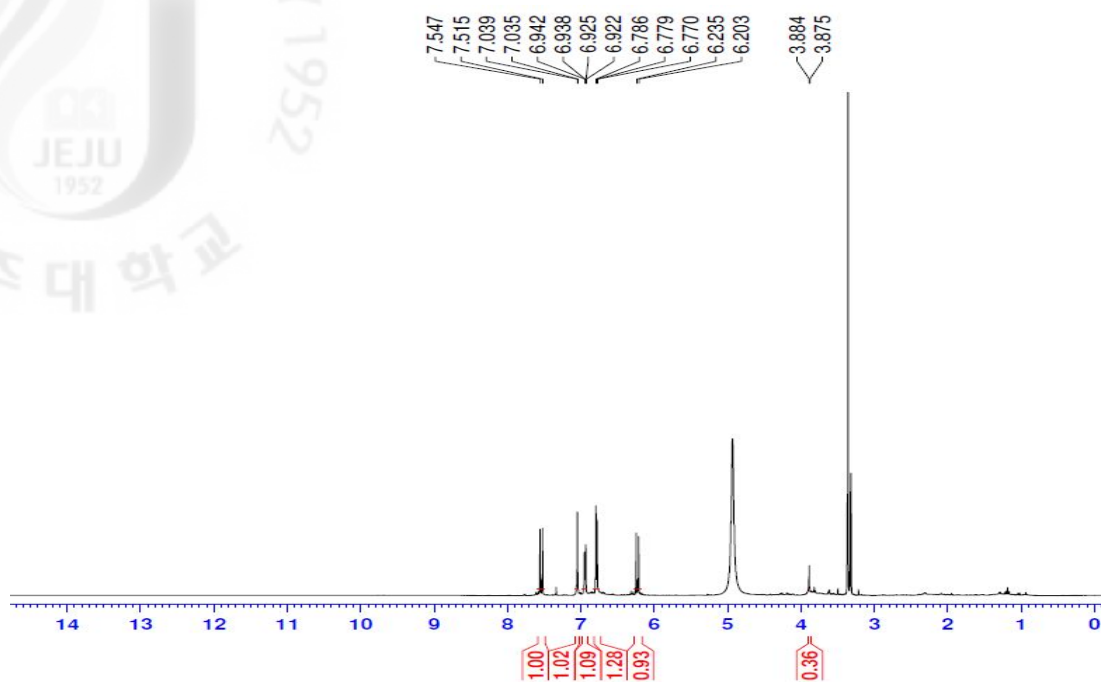


Figure 95.  $^1\text{H}$ -NMR spectrum of caffeic acid (**3**) in  $\text{CD}_3\text{OD}$

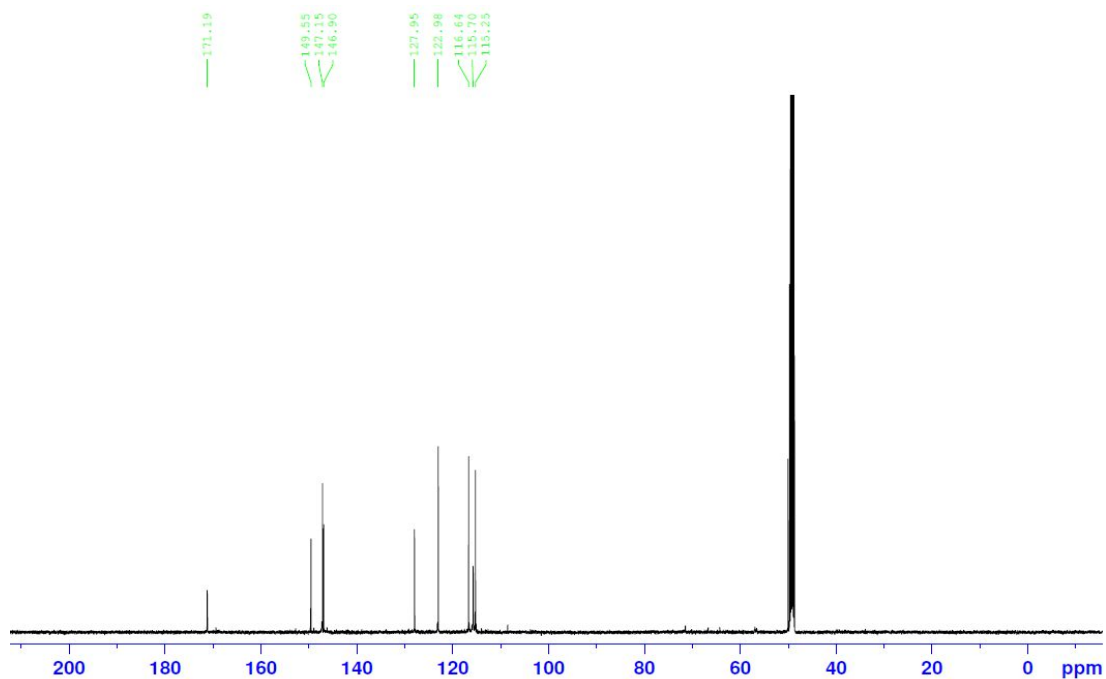


Figure 96.  $^{13}\text{C}$ -NMR spectrum of caffeic acid (**3**) in  $\text{CD}_3\text{OD}$

Compound **3** was isolated as yellow needles. The  $^1\text{H-NMR}$  spectrum of compound **3** was showed 3,4-dihydroxylation pattern for aromatic ring [ABX system signals at  $\delta_{\text{H}}$  7.03 (1H, *d*,  $J = 2.0$  Hz, H-2), 6.93 (1H, *dd*,  $J = 8.5, 2.0$  Hz, H-6), 6.77 (1H, *d*,  $J = 8.5$  Hz, H-5)], and two olefinic protons at  $\delta_{\text{H}}$  7.53 (1H, *d*,  $J = 16.0$  Hz, H-7), 6.21 (1H, *d*,  $J = 16.0$  Hz, H-8) with binding *trans*-form between them (Fig. 95). The  $^{13}\text{C-NMR}$  spectrum of compound **3** was showed nine carbon signals including one acid carbonyl group at  $\delta_{\text{C}}$  171.2 (C-9), two olefinic carbon peaks at  $\delta_{\text{C}}$  146.9 (C-7), 115.2 (C-8) (Fig. 96). All  $^1\text{H}$  and  $^{13}\text{C-NMR}$  spectra of compound **3** in  $\text{CD}_3\text{OD}$  was similar to caffeic acid ethyl ester except for moiety of ethyl group. Thus, the structure of compound **3** was determined as caffeic acid by comparison of its spectral data with those in the literature (Fig. 97).<sup>95,96)</sup>

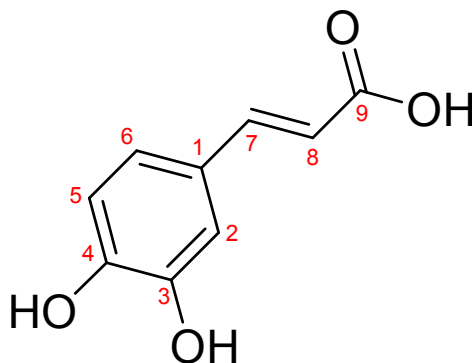


Figure 97. Structure of compound **3**; Caffeic acid

#### 3-1-4. Compound 4

- Compound Name 1-[(Butanoyl)phlorogluciny]- $\beta$ -D-glucopyranoside
- Synonym(s)
- CAS Registry Number - (new compound)
- Appearance amorphous powder
- Chemical Formula  $C_{16}H_{22}O_9$
- Molecular Weight (g/mol) 300.09
- Melting Point ( $^{\circ}C$ ) -
- $^1H$ -NMR (500 MHz,  $CD_3OD$ )

$\delta$ : 6.17 (1H, *d*,  $J = 2.0$  Hz, H-6), 5.94 (1H, *d*,  $J = 2.0$  Hz, H-4), 5.03 (1H, *d*,  $J = 7.5$  Hz, H-1"), 3.91 (1H, *dd*,  $J = 12.5, 2.5$  Hz, H-6"  $\alpha$ ), 3.72 (1H, *dd*,  $J = 12.5, 5.0$  Hz, H-6"  $\beta$ ), 3.53 (1H, *dd*,  $J = 9.0, 7.5$  Hz, H-2"), 3.46 (1H, *m*, H-3"), 3.46 (1H, *m*, H-5"), 3.41 (1H, *dd*,  $J = 9.0, 9.0$  Hz, H-4"), 3.16 (1H, *ddd*,  $J = 16.5, 7.5, 6.5$  Hz, H-2'  $\alpha$ ), 3.09 (1H, *ddd*,  $J = 16.5, 9.0, 7.0$  Hz, H-2'  $\beta$ ), 1.69 (2H, *m*, H-3'), 0.97 (3H, *t*,  $J = 7.5$  Hz, H-4')

- $^{13}C$ -NMR (125MHz,  $CD_3OD$ )

$\delta$ : 207.6 (C-1'), 167.8 (C-3), 165.9 (C-5), 162.4 (C-1), 106.9 (C-2), 101.9 (C-1"), 98.4 (C-4), 95.5 (C-6), 78.7 (C-3"), 78.5 (C-5"), 74.9 (C-2"), 71.3 (C-4"), 62.6 (C-6"), 47.3 (C-2'), 19.3 (C-3'), 14.4 (C-4')

- Other data

1. HR-FAB MS :  $m/z$  381.1160  $[M+Na]^+$  (calcd. for  $C_{16}H_{22}O_9Na$  381.1162,  $\Delta$ -0.2  $mamu$ )
2. UV (MeOH)  $\lambda_{max}nm$ : 228 and 286
3. Optical Rotation :  $[\alpha]_D^{20} = -46.2^{\circ}$  ( $c$  0.011, MeOH)

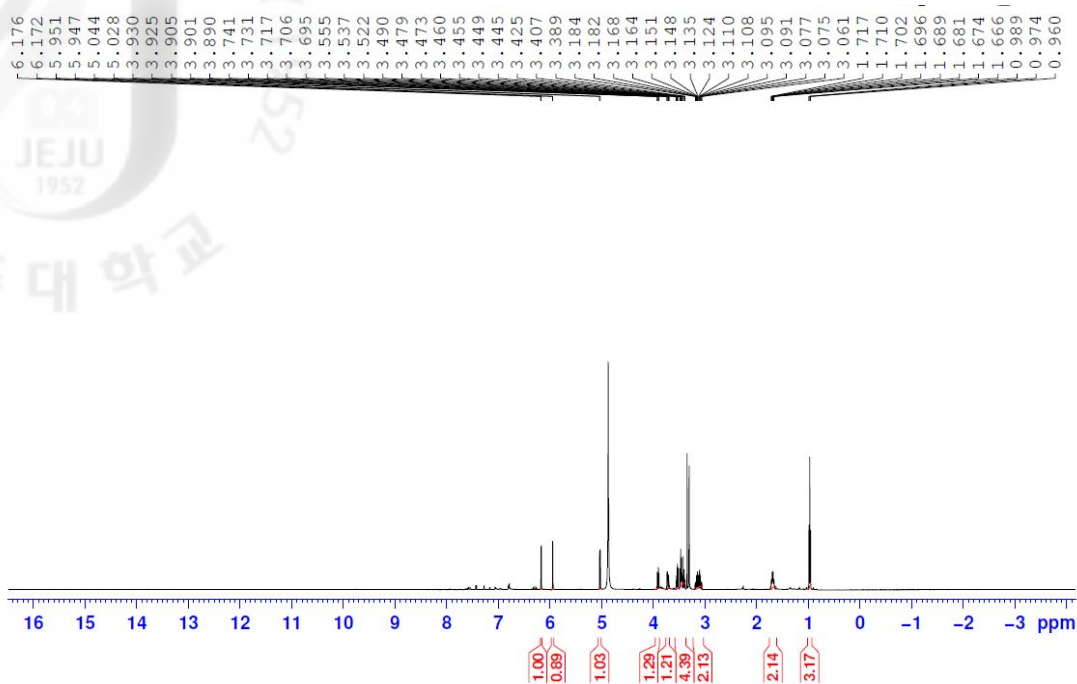


Figure 98.  $^1\text{H}$ -NMR spectrum of 1-[(Butanoyl)phlorogluciny]- $\beta$ -D-glucopyranoside (**4**) in  $\text{CD}_3\text{OD}$

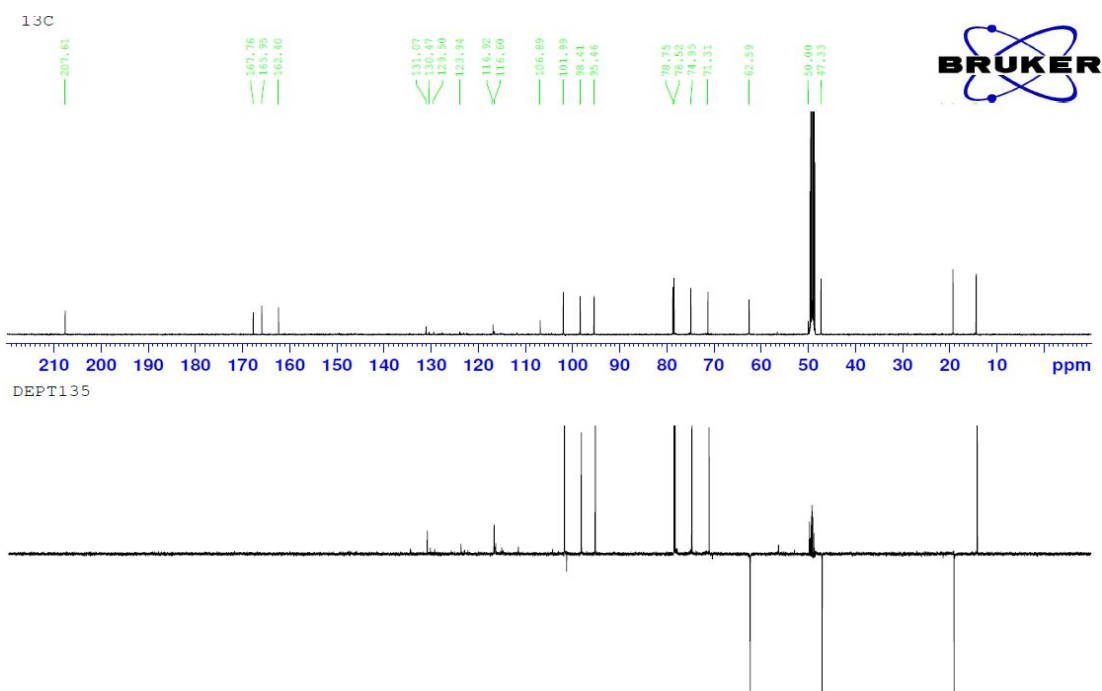


Figure 99.  $^{13}\text{C}$ -NMR and DEPT135 spectra of 1-[(Butanoyl)phlorogluciny]- $\beta$ -D-glucopyranoside (**4**) in  $\text{CD}_3\text{OD}$

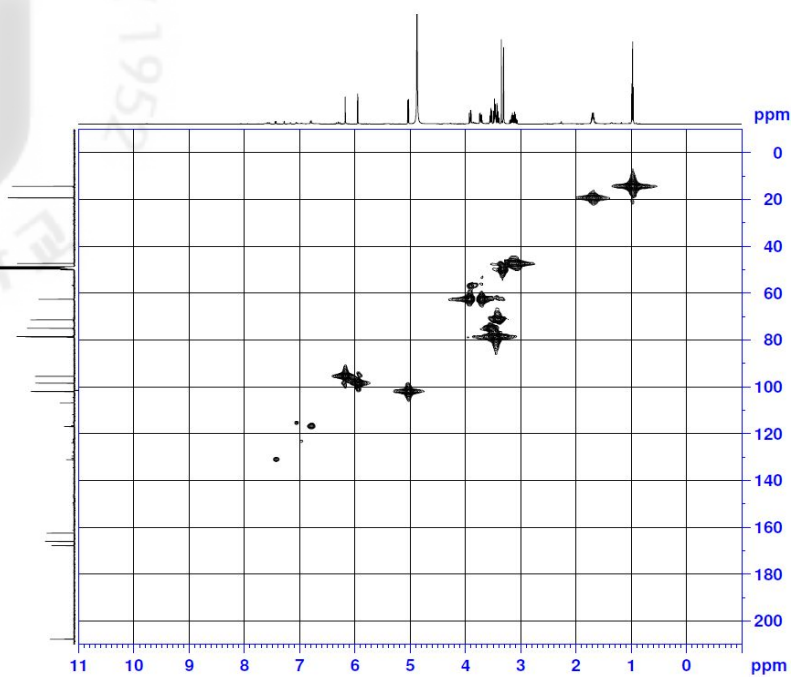


Figure 100. HMQC spectrum of 1-[(Butanoyl)phlorogluciny]- $\beta$ -D-glucopyranoside (**4**) in CD<sub>3</sub>OD

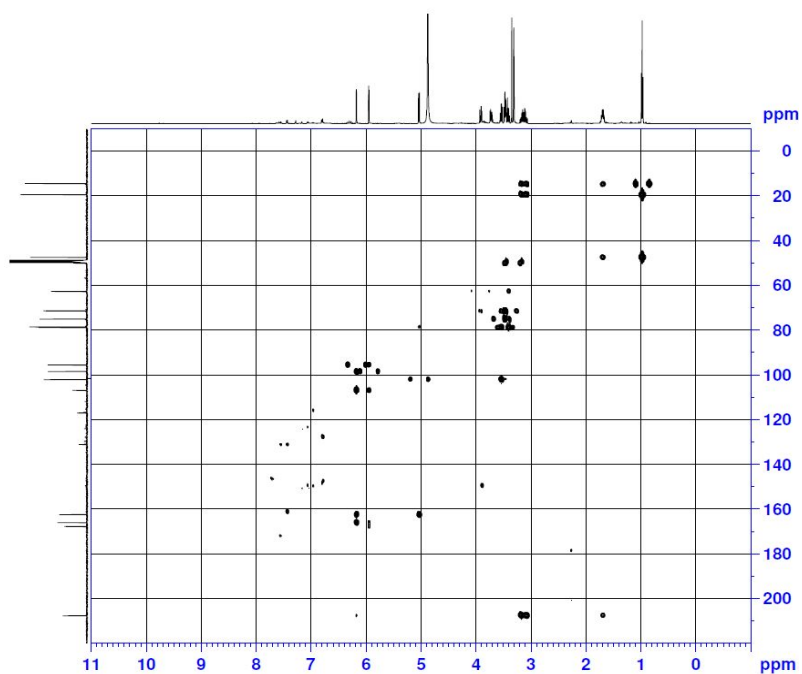


Figure 101. HMBC spectrum of 1-[(Butanoyl)phlorogluciny]- $\beta$ -D-glucopyranoside (**4**) in CD<sub>3</sub>OD



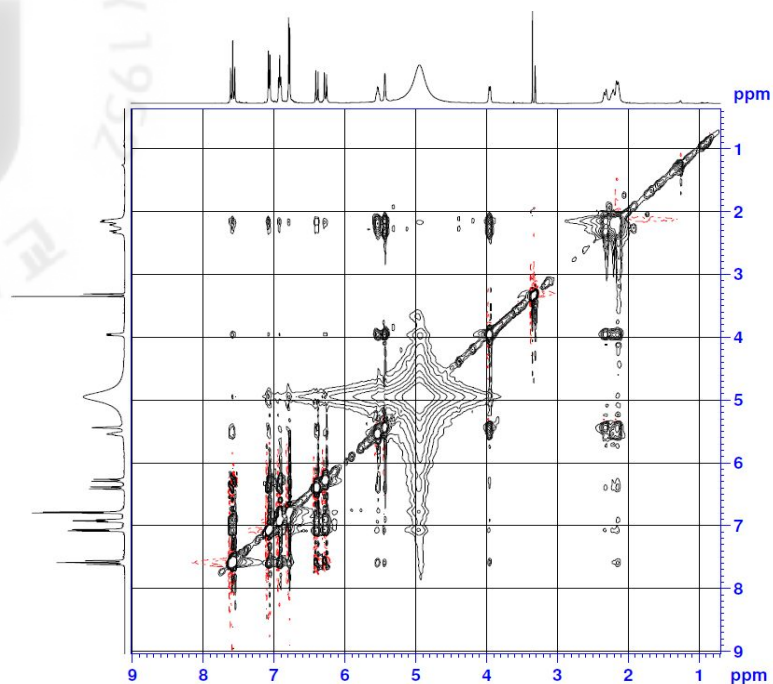


Figure 102. NOESY spectrum of 1-[(Butanoyl)phlorogluciny]- $\beta$ -D-glucopyranoside (4) in  $CD_3OD$

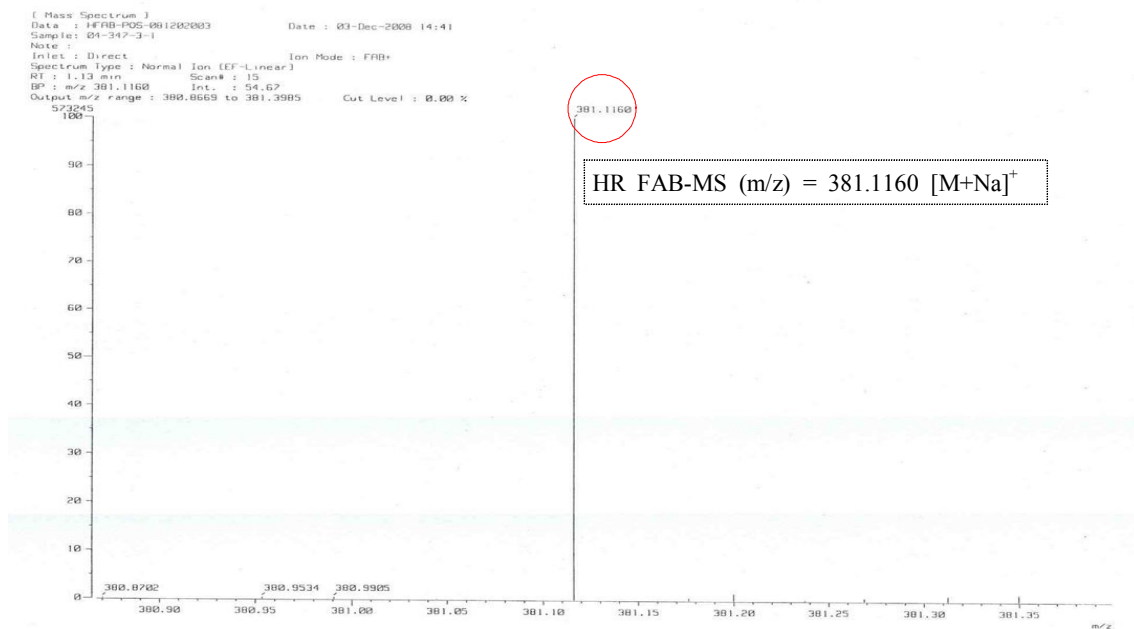


Figure 103. HR FAB MS spectrum of 1-[(Butanoyl)phlorogluciny]- $\beta$ -D-glucopyranoside (4) in  $CD_3OD$

Compound **4** was obtained as an amorphous powder, showed a  $[M+Na]^+$  peak at  $m/z$  381.1160 (calcd  $m/z$  381.1162) in the HR-FAB-MS, consistent with the molecular formula  $C_{16}H_{22}O_9$  (six unsaturations) (Fig. 103). This was supported by  $^{13}C$  and DEPT NMR spectra, which showed signals for 16 carbons, including six aromatic, one carbonyl, and nine aliphatic carbons (Fig. 99). The UV absorption maximum of in MeOH at 228 and 286 nm suggested the presence of an aromatic ring (Data did not shown). The aromatic ring is inferred to be phloroglucinol (1,3,5-trihydroxybenzene) moiety based on the observation of highly downfield shifts of three  $^{13}C$ -NMR signals ( $\delta$  162.4, 165.9, 167.8) and upfield shifts of other three  $^{13}C$ -NMR signals ( $\delta$  95.5, 98.4, 106.9), typical  $\delta_C$  pattern appeared in phloroglucinol analogue (Fig. 99). The aromatic protons at  $\delta_H$  6.17 (*d*,  $J = 2.0$  Hz) and 5.94 (*d*,  $J = 2.0$  Hz) were placed at H-6 and H-4 based on their HMQC correlation with carbons at  $\delta_C$  95.5 (C-6) and 98.4 (C-4), respectively (Fig. 100). The upfield chemical shift and small coupling constants of these protons showed that these meta coupled protons are between oxygenated quaternary carbons. Since only two aromatic protons were observed, there should be one substituent connected to aromatic carbon in this 1,3,5-trioxybenzene unit. The  $^1H$ -NMR spectrum showed signals at  $\delta_H$  0.97 (3H, *t*,  $J = 7.5$  Hz), 3.16 (1H, *ddd*,  $J = 16.5, 7.5, 6.5$  Hz) and 3.09 (1H, *ddd*,  $J = 16.5, 9.0, 7.0$  Hz), and 1.69 (2H, *m*) (Fig. 98). These signals were respectively assignable to one methyl and two methylene groups, revealing a propyl side chain in **4**, which was further confirmed by COSY experiment. The propyl group is connected to carbonyl to construct a butanoyl unit, which was verified by HMBC data (Fig. 101).

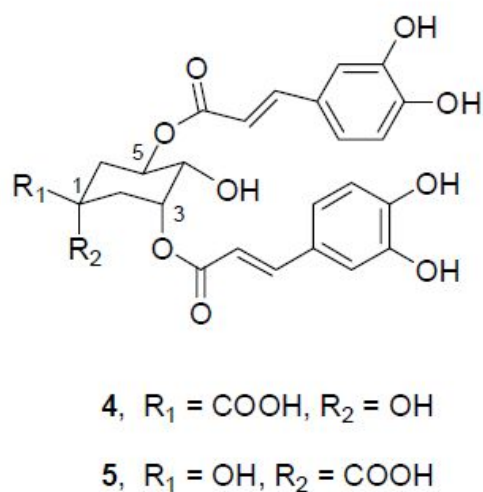
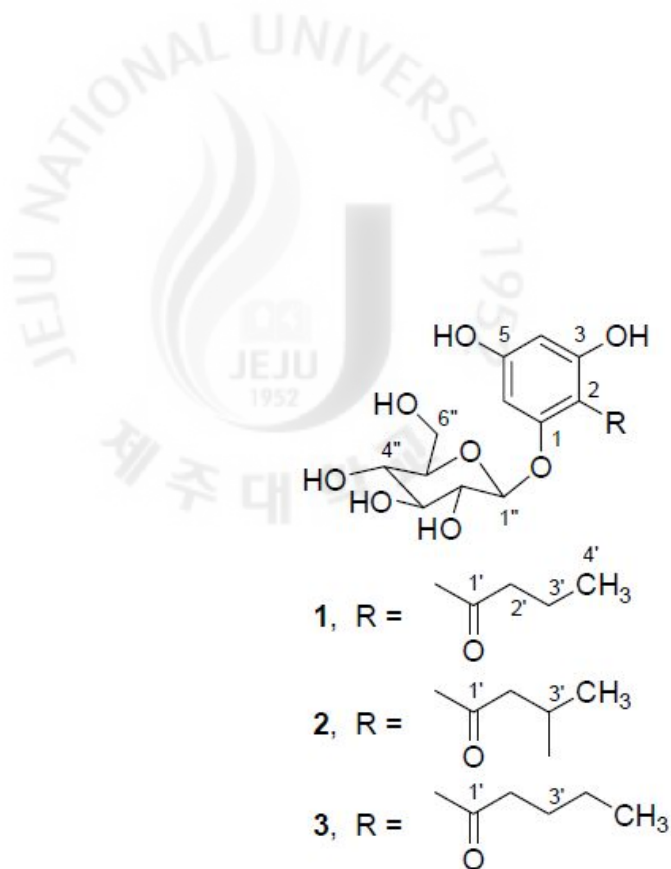


Figure 104. The structure of compound change according to the substitution

The carbonyl carbon (C-1') is attached to the aromatic carbon (C-2) of 1,3,5-trioxybenzene nucleus, based on long range (4J) HMBC correlation of H-6 with C-1', probably due to the conjugated  $\pi$ -system of the benzene ring. The presence of a sugar was suggested by the appearance of six oxygen-bearing  $sp^3$  carbons at  $\delta_C$  101-62 in combination with proton signals at  $\delta_H$  5.03 and 3.4-3.9. The large coupling constant ( $J = 7.5$  Hz) for the anomeric proton at  $\delta_H$  5.03 (H-1'') having HMQC cross peak with  $\delta_C$  101.9 indicated the sugar was in  $\beta$ -configuration. The sugar protons at  $\delta_H$  3.53 (*dd*,  $J = 9.0, 7.5$  Hz, H-2'') and  $\delta$  3.41 (*dd*,  $J = 9.0, 9.0$  Hz, H-4'') all showed axial-axial coupling constants, which suggested that all substituents in this hexose are in equatorial positions. Therefore, the sugar was identified as glucose. In butanoyl substituted phloroglucinols, the glucose unit can be attached to either 1-OH (3-OH) or 5-OH positions. If the substitution is made at 5-OH, it leads

to a symmetric benzene nucleus, which show only four aromatic  $^{13}\text{C}$ -NMR signals. Since it is not observed in 1, the glucose moiety should be attached to 1-OH. The HMBC correlation of H-1''/C-1 further confirms the placement of the glucose moiety to 1-OH. From the above spectral data, compound 4 was identified as 1-[(butanoyl)phlorogluciny]- $\beta$ -D-glucopyranoside (Fig. 105).<sup>98-100</sup> A 3-methylbutanoyl phloroglucinol analogue (2) has been reported previously from *Fragaria ananassa*<sup>97</sup> having cytochrome P450 enzyme inhibition activities.

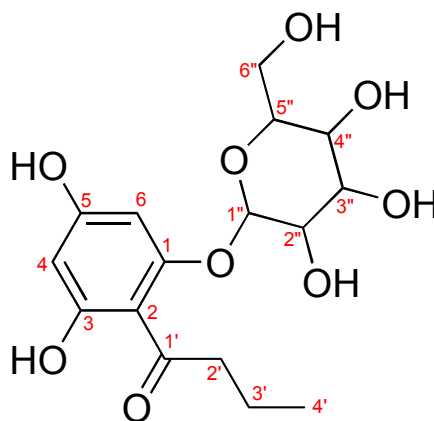


Figure 105. Structure of compound 4; 1-[(Butanoyl)phlorogluciny]- $\beta$ -D-glucopyranoside (new compound)

### 3-1-5. Compound 5

- Compound Name 3,5-di-*O*-caffeoylquinic acid
- Synonym(s) Isochlorogenic acid A. 3,5-Bis(3,4-dihydroxycinnamoyl)quinic acid; 3,5-DCQA
- CAS Registry Number 2450-53-5
- Appearance off-white powder
- Chemical Formula  $C_{25}H_{24}O_{12}$
- Molecular Weight (g/mol) 516.11
- Melting Point ( $^{\circ}C$ ) 170 - 172
- $^1H$ -NMR (500 MHz,  $CD_3OD$ )  
 $\delta$ : 7.61 (1H, *d*,  $J = 16.0$  Hz, H-7'), 7.58 (1H, *d*,  $J = 16.0$  Hz, H-7''), 7.06 (2H, *d*,  $J = 1.5$  Hz, H-2', 2''), 6.96 (2H, *dd*,  $J = 8.0, 1.5$  Hz, H-6', 6''), 6.78 (each 2H, *d*,  $J = 8.0$  Hz, H-5', 5''), 6.37 (1H, *d*,  $J = 16.0$  Hz, H-8'), 6.27 (1H, *d*,  $J = 16.0$  Hz, H-8''), 5.42 (2H, *m*, H-3, 5), 3.95 (1H, *dd*,  $J = 8.0, 3.0$  Hz, H-4), 2.32 - 2.12 (4H, *m*, H-4, 6)
- $^{13}C$ -NMR (125 MHz,  $CD_3OD$ )  
 $\delta$ : 178.9 (C-7), 169.1 (C-9'), 168.7 (C-9''), 149.7 (C-4'), 149.5 (C-4''), 147.2 (C-7'), 147.1 (C-7''), 146.9 (C-3', 3''), 128.1 (C-1'), 128.0 (C-1''), 123.1 (C-6', 6''), 116.6 (C-5'), 115.9 (C-5''), 115.4 (C-2'), 115.3 (C-2''), 115.3 (C-8', 8''), 73.3 (C-1), 72.3 (C-5), 71.6 (C-4), 49.8 (C-3), 38.8 (C-2), 36.7 (C-6)
- Biological activities in the literature  
active against HIV-1 integrase, anti-viral, anti-hepatotoxic, antioxidant, anti-proliferation
- Other data in the literature
  1. UV (MeOH)  $\lambda_{max}nm$ : 225, 247, 280 and 343
  2. Optical Rotation:  $[\alpha]_D^{22} = -198$  (MeOH)

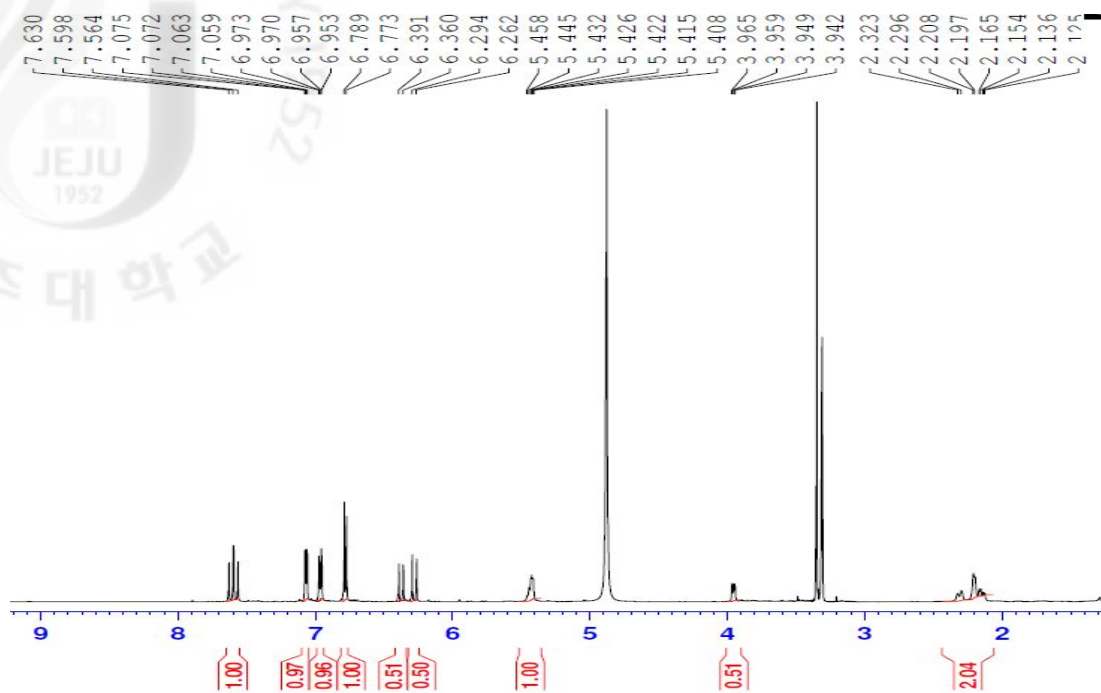


Figure 106.  $^1\text{H-NMR}$  spectrum of 3,5-di-*O*-caffeoylquinic acid (**5**) in  $\text{CD}_3\text{OD}$

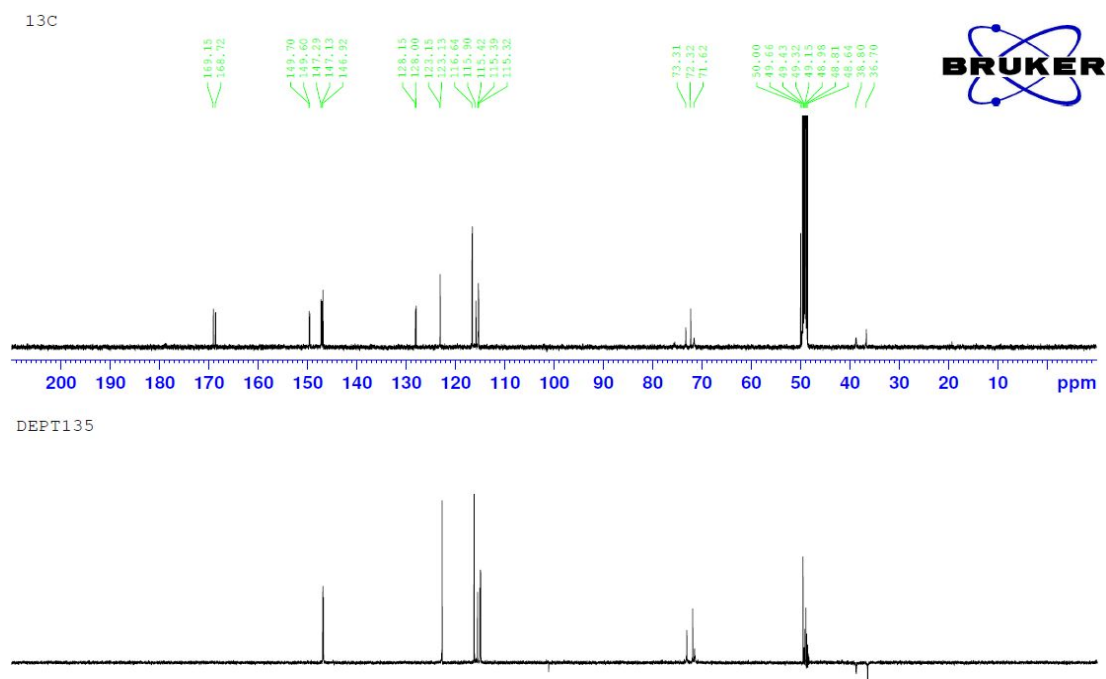


Figure 107.  $^{13}\text{C-NMR}$  and DEPT135 spectra of 3,5-di-*O*-caffeoylquinic acid (**5**) in  $\text{CD}_3\text{OD}$

Compound **5** was isolated as off-white powder and its molecular formula was determined to be  $C_{25}H_{24}O_{12}$  by NMR spectra data. The  $^1H$ -NMR spectrum of compound **5** indicated the presence of two *trans*-caffeoyl groups at  $\delta_H$  7.06 (2H, *d*,  $J = 1.5$  Hz, H-2', 2''), 6.96 (2H, *dd*,  $J = 8.0, 1.5$  Hz, H-6', 6''), 6.78 (2H, *d*,  $J = 8.0$  Hz, H-5', 5''), and three oxygenated protons at  $\delta_H$  5.42 (2H, *m*, H-3, 5) and 3.95 (1H, *dd*,  $J = 8.0, 3.0$  Hz, H-4) (Fig. 106).  $^{13}C$ -NMR spectrum was showed two methylene carbons at  $\delta_C$  38.8 (C-2) and 36.7 (C-6), four oxygenated carbons at  $\delta_C$  72.3 (C-5), 71.6 (C-4) and 49.8 (C-3), and a carbonyl carbon signal at  $\delta_C$  178.9 (C-7).  $^1H$  and  $^{13}C$ -NMR spectral data were typical of dicaffeoyl quinic acid derivatives (Fig. 107). The position of two caffeoyl groups was established by the downfield shift of 5.42 (2H, *m*, H-3, 5) in the  $^1H$ -NMR spectrum and of the  $\delta_C$  49.8 (C-3) and  $\delta_C$  72.3 (C-5) in the  $^{13}C$ -NMR spectrum. Thus, the structure of compound **5** was determined as 3,5-di-*O*-caffeoylquinic acid (3,5-DCQA) (Fig. 108).<sup>101-107</sup> The 3,5-di-*O*-caffeoylquinic acid was reported for the first time from this plant.

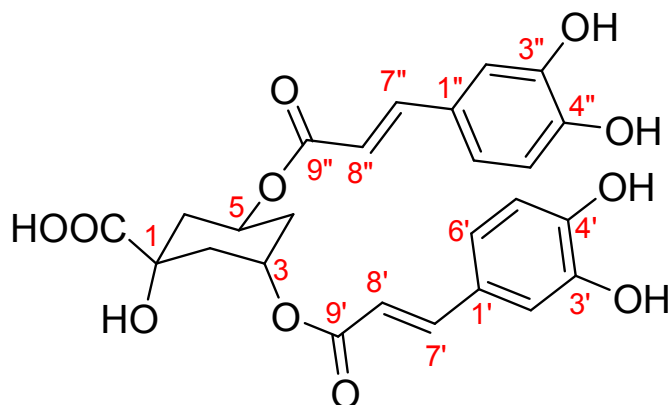


Figure 108. Structure of compound **5**; 3,5-di-*O*-caffeoylquinic acid (3,5-DCQA)

### 3-1-6. Compound 6

- Compound Name 3,5-di-*O*-caffeoyl *epi*-quinic acid
- Synonym(s) 3,5-*e*DCQA
- CAS Registry Number -

• Appearance Amorphous yellow powder

• Chemical Formula  $C_{25}H_{30}O_{12}$

• Molecular Weight (g/mol) 516.11

• Melting Point (°C) -

•  $^1\text{H-NMR}$  (500 MHz,  $\text{CD}_3\text{OD}$ )

$\delta$ : 7.61 (1H, *d*,  $J = 16.0$  Hz, H-7'), 7.57 (1H, *d*,  $J = 16.0$  Hz, H-7''), 7.06 (2H, *d*,  $J = 2.0$  Hz, H-2', 2''), 6.97 (1H, *dd*,  $J = 8.0, 2.0$  Hz, H-6'), 6.95 (1H, *dd*,  $J = 8.0, 2.0$  Hz, H-6''), 6.78 (2H, *d*,  $J = 8.0$  Hz, H-5', 5''), 6.35 (1H, *d*,  $J = 16.0$  Hz, H-8'), 6.26 (1H, *d*,  $J = 16.0$  Hz, H-8''), 5.41 (2H, *m*, H-3, 5), 3.98 (1H, *dd*,  $J = 7.0, 3.0$  Hz, H-4), 2.34 - 2.15 (4H, *m*, H-4, 6)

•  $^{13}\text{C-NMR}$  (125 MHz,  $\text{CD}_3\text{OD}$ )

$\delta$ : 177.4 (C-7), 169.0 (C-9'), 168.5 (C-9''), 149.6 (C-4'), 149.5 (C-4''), 147.4 (C-7'), 147.1 (C-7''), 146.8 (C-3', 3''), 128.0 (C-1'), 127.9 (C-1''), 123.2 (C-6'), 123.1 (C-6''), 116.6 (C-5'), 115.7 (C-5''), 115.4 (C-2'), 115.2 (C-2''), 115.2 (C-8', 8''), 74.8 (C-1), 72.6 (C-5), 72.1 (C-4), 50.2 (C-3), 37.7 (C-2), 36.1 (C-6)

• Biological activities in the literature

LDL oxidase inhibition, free radical scavenger, antiproliferative, interleukins inhibitors, anti-obesity, anti-diabetic (AGEs and aldose reductase inhibitor)



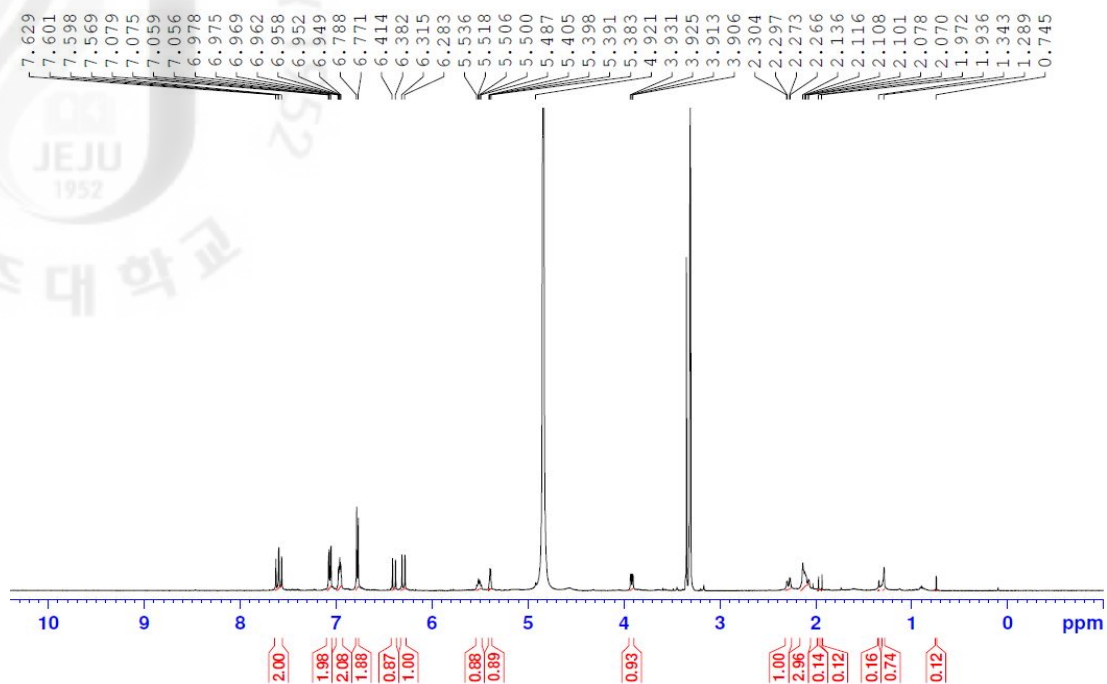


Figure 109.  $^1\text{H}$ -NMR spectrum of 3,5-di-*O*-caffeoyl *epi*-quinic acid (**6**) in  $\text{CD}_3\text{OD}$

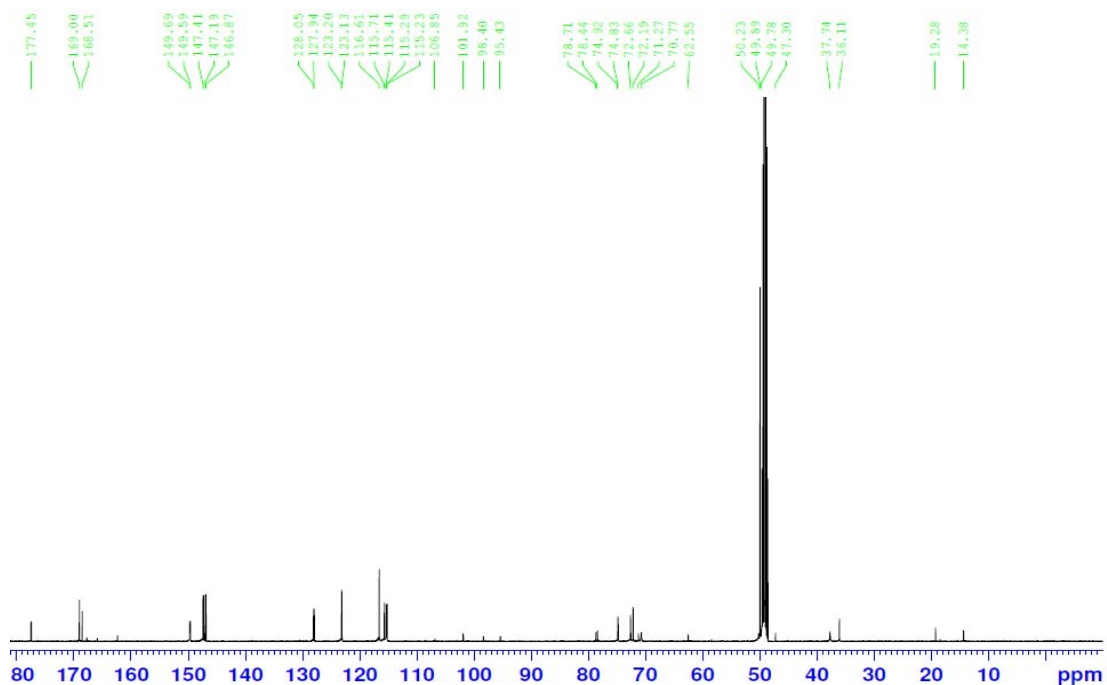


Figure 110.  $^{13}\text{C}$ -NMR spectrum of 3,5-di-*O*-caffeoyl *epi*-quinic acid (**6**) in  $\text{CD}_3\text{OD}$

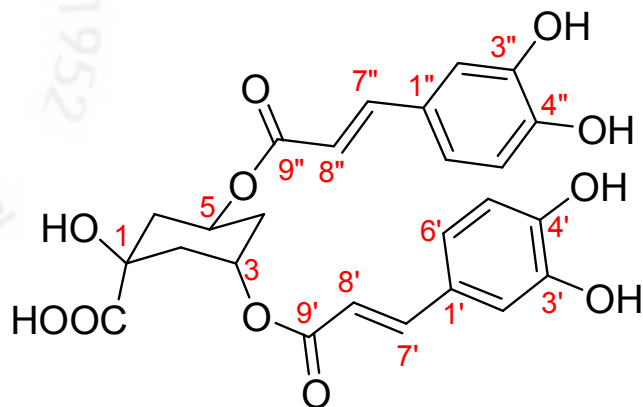


Figure 111. Structure of compound **6**; 3,5-di-*O*-caffeoyl *epi*-quinic acid (3,5-*e*DCQA)<sup>106,107</sup>

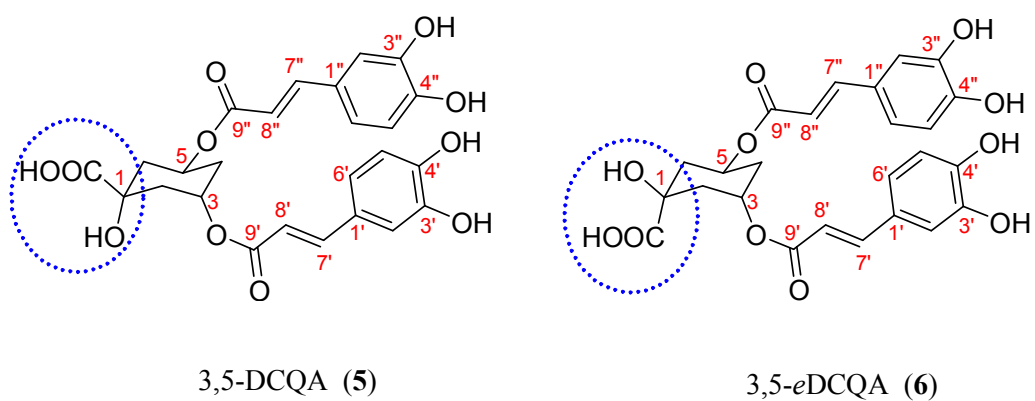


Figure 112. Comparison on each olefinic structure of carbonyl group of quinic acid at 1-position between 3,5-DCQA (**5**) and 3,5-*e*DCQA (**6**)

### 3-1-7. Compound 7

- Compound Name kaempferol-3-*O*- $\beta$ -D-glucoside; Astragalin
- Synonym(s) 3-*O*- $\beta$ -D-Glucopyranosyloxy-4',5,7-trihydroxyflavone.  
kaempferol 3-glucoside
- CAS Registry Number 480-10-4
- Appearance amorphous yellow powder
- Chemical Formula  $C_{21}H_{20}O_{11}$
- Molecular Weight (g/mol) 448.38
- Melting Point ( $^{\circ}C$ ) 178
- $^1H$ -NMR (500 MHz,  $CD_3OD$ )  
 $\delta$ : 8.06 (2H, *d*,  $J = 8.5$  Hz, H-2', 6'), 6.89 (2H, *d*,  $J = 8.5$  Hz, H-3', 5'), 6.84 (1H, *d*,  $J = 2.0$  Hz, H-6), 6.21 (1H, *d*,  $J = 2.0$  Hz, H-8), 5.26 (1H, *d*,  $J = 6.5$  Hz, H-1")
- $^{13}C$ -NMR (125 MHz,  $CD_3OD$ )  
 $\delta$ : 179.7 (C-4), 166.2 (C-7), 163.2 (C-5), 161.4 (C-4'), 159.2 (C-2), 158.7 (C-9), 135.6 (C-3), 132.4 (C-2'), 132.4 (C-5'), 122.9 (C-1'), 116.2 (C-3'), 116.2 (C-6'), 105.8 (C-10), 104.2 (C-1"), 100.0 (C-6), 94.9 (C-8), 78.2 (C-3"), 78.1 (C-5"), 75.9 (C-2"), 71.5 (C-4"), 62.5 (C-6")
- Biological activities in the literature  
Immunostimulant, anti-bacterial, anti-candidal, antioxidant, antileukemia
- Other data in the literature
  1. Optical Rotation:  $[\alpha]_D^{18} = + 16.9$  ( $c$  0.62 in MeOH)
  2. Biological Source: Isol. from *Astragalus* spp. and many other plant spp.

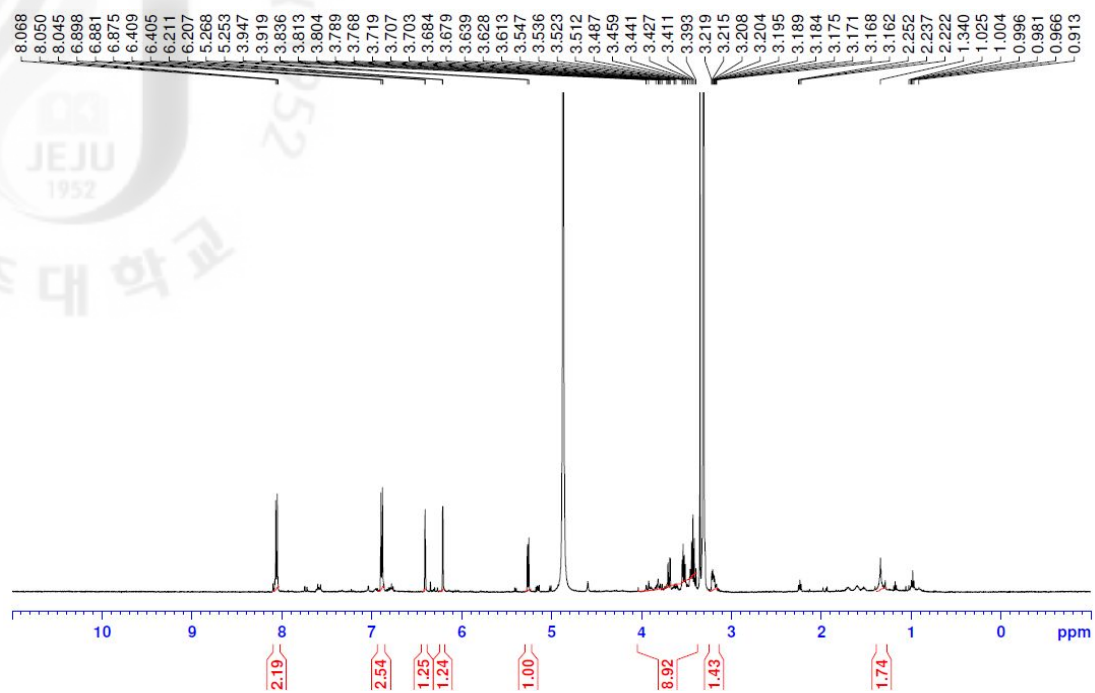


Figure 113.  $^1\text{H}$ -NMR spectrum of kaempferol-3-*O*- $\beta$ -D-glucoside (7) in  $\text{CD}_3\text{OD}$

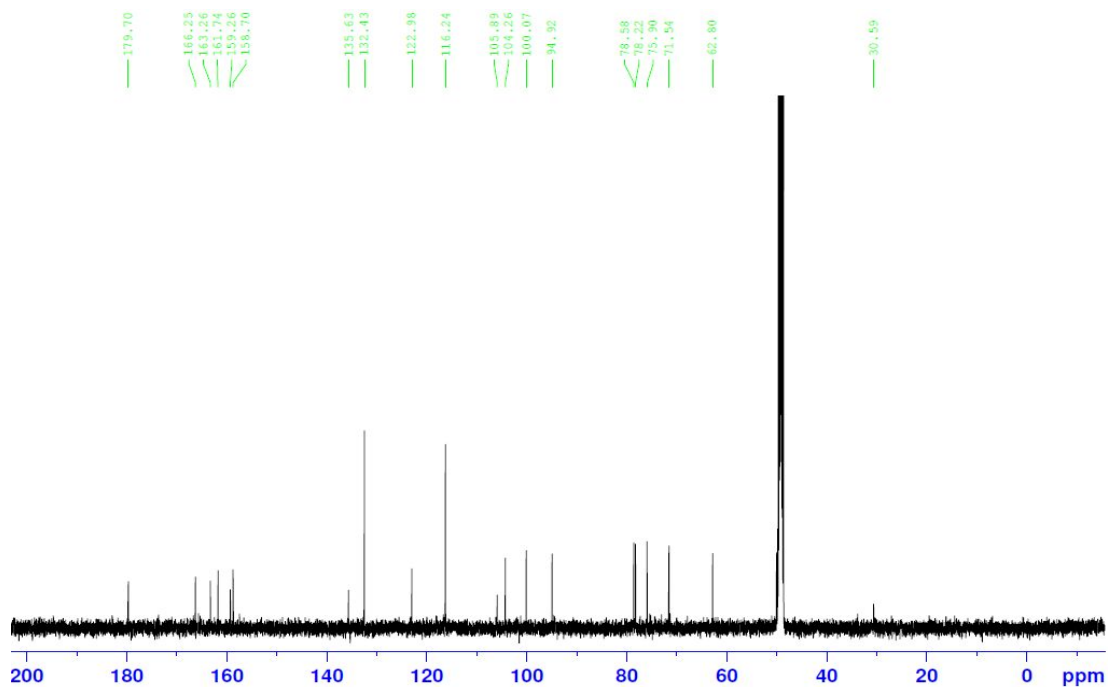


Figure 114.  $^{13}\text{C}$ -NMR spectrum of kaempferol-3-*O*- $\beta$ -D-glucoside (7) in  $\text{CD}_3\text{OD}$

Compound **7** was isolated as amorphous yellow powder and its molecular formula was determined to be  $C_{21}H_{20}O_{11}$  by NMR. The  $^1H$ -NMR spectrum showed the AB system at  $\delta_H$  8.06 (2H, *d*,  $J = 8.5$  Hz, H-2', 6'), 6.89 (1H, *d*,  $J = 8.5$  Hz, H-3', 5') and also showed two *meta*-coupled doublets at  $\delta_H$  6.84 (1H, *d*,  $J = 2.0$  Hz, H-6) and 6.21 (1H, *d*,  $J = 2.0$  Hz, H-8) (Fig. 113).  $^{13}C$ -NMR spectrum exhibited twelve-one carbon signals, consisting of fourteen olefinic signals at  $\delta_C$  94.9 to 166.2, and a carbonyl carbon signals at  $\delta_C$  179.7 (C-4) (Fig. 114). Analysis of the chemical shifts, signal multiplicities, absolute values of the coupling constants, and their magnitude in the  $^1H$  and  $^{13}C$ -NMR spectrum indicated the presence of one glucosyl residue with  $\beta$ -configuration at the anomeric proton at  $\delta_H$  5.26 (1H, *d*,  $J = 6.5$  Hz, H-1''). The HMBC spectrum showed a correlation between the anomeric glucoside proton and aglycon carbon at the 3-position, giving the attachment site of the glucose on aglycone and confirming mass hypotheses (Data did not shown). These spectral data suggested that compound **7** was a flavonol glycoside derivative. Based on the above mentioned data, the structure of compound **7** was determined to be kaempferol-3-*O*- $\beta$ -D-glucoside (Astragalin) (Fig. 115).<sup>108)</sup> Astragalin was reported for the first time from this plant.

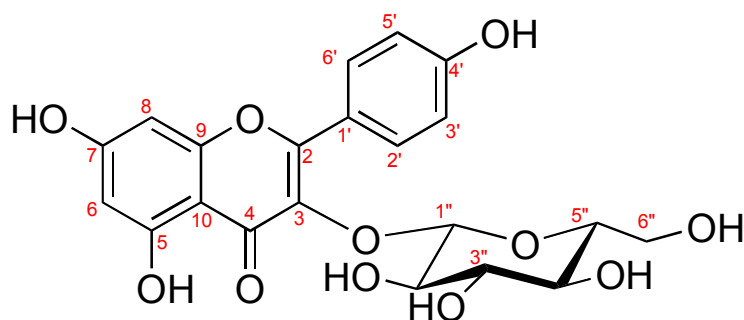


Figure 115. Structure of compound **7**; kaempferol-3-*O*- $\beta$ -D-glucoside (Astragalin)

## 3-2. Biological activities

### 3-2-1. Antioxidant activity

#### 3-2-1-1. Free radical scavenging activity of the solvent fractions

Antioxidative activity was determined by 3 types of free radical scavenging activity assays. DPPH radical scavenging activity of the 70% *aq.* EtOH extract and its solvent fractions of *A. subulatus* is shown in Table 18. It showed that the 70% *aq.* EtOH extract, *n*-Hex, CH<sub>2</sub>Cl<sub>2</sub>, EtOAc, *n*-BuOH and H<sub>2</sub>O solvent fractions exhibited DPPH radical scavenging activities dose-dependently. The activity increased in the following order : *n*-Hex fraction < H<sub>2</sub>O fraction < CH<sub>2</sub>Cl<sub>2</sub> fraction < *n*-BuOH fraction < EtOAc fraction. Among them, EtOAc solvent fraction exhibited higher scavenging activity comparing to other fractions with dose-dependent behavior. The xanthine oxidase inhibitory activity of the 70% *aq.* EtOH extract and its solvent fractions were shown in Table 18. When comparing Table 18 having the positive control (Allopurinol, IC<sub>50</sub> = 12.2 μg/mL), All solvent fractions did not show strongly enzyme inhibitory activity. On the other hand, EtOAc fraction has good radical scavenging activity on superoxide radical scavenging assay at RC<sub>50</sub> = 2.5 μg/mL, when compared to the positive control (Allopurinol, RC<sub>50</sub> = 2.1 μg/mL). This results showed that EtOAc solvent fractions should be the major fractions containing active constituents for the free radical scavenging activity of *A. subulatus*.

Table 18. Free radical scavenging effect of the solvent fractions

Samples	RC <sub>50</sub> (µg/mL)		
	DPPH radical scavenging activity	Xanthine oxidase inhibitory activity	Superoxide radical scavenging activity
70% <i>aq.</i> EtOH ext.	104.0 ± 11.77	657.7 ± 88.08	14.2 ± 1.29
<i>n</i> -Hex Fr.	907.2 ± 23.19	> 1000	526.1 ± 42.01
CH <sub>2</sub> Cl <sub>2</sub> Fr.	135.8 ± 3.47	> 1000	159.6 ± 8.34
EtOAc Fr.	17.6 ± 1.47	84.6 ± 1.23	2.5 ± 1.26
<i>n</i> -BuOH Fr.	61.0 ± 0.89	485.4 ± 5.91	29.9 ± 12.20
H <sub>2</sub> O Fr.	483.1 ± 82.19	> 1000	135.5 ± 2.84
Positive control (BHA) <sup>1)</sup>	5.9 ± 0.49	N/A	N/A
Positive control (Allopurinol)	N/A	12.2 ± 2.80	2.11 ± 0.91

Primarily radical scavenging activity was determined at 0 to 1000 µg/mL concentration of samples. Scavenging concentration for 50% of free radical (RC<sub>50</sub>) was calculated from logarithmic regression equation obtained from the values of at least five dilutions of the primary concentration. Values represent mean ± SDs (n = 3); in parentheses is RC<sub>50</sub> value of respective sample

N/A. not assay; BHA. butylated hydroxyanisole<sup>1)</sup>; >. out of range

### 3-2-1-2. Free radical scavenging activity of the isolated compounds

The DPPH radical scavenging activity of activity-guided isolation was carried out using the EtOAc solvent fractions and column chromatography finally led to isolations of compounds from *A. subulatus*. Among the isolated compounds, new compound (4), 3,5-di-*O*-caffeoylquinic acid (5), and 3,5-di-*O*-caffeoyl *epi* quinic acid (6) had more potent radical scavenging activity higher than positive control (BHA, RC<sub>50</sub> = 5.9 µg/mL) (Tab. 19).

Table 19. Free radical scavenging effect of the isolated compounds

Samples	RC <sub>50</sub> (µg/mL)		
	DPPH radical scavenging activity	Xanthine oxidase inhibitory activity	Superoxide radical scavenging activity
Compound 1 stigmasterol	N/A	N/A	N/A
Compound 2 ethyl cafferate	N/A	N/A	N/A
Compound 3 caffeic acid	N/A	N/A	N/A
Compound 4 new compound	4.2 ± 2.87	5.7 ± 0.20	4.5 ± 2.84
Compound 5 3,5-di- <i>O</i> -caffeoylquinic acid	1.3 ± 0.12	5.0 ± 3.31	1.6 ± 0.38
Compound 6 3,5-di- <i>O</i> -caffeoyl <i>epi</i> -quinic acid	1.4 ± 0.16	7.6 ± 1.61	1.8 ± 3.17
Compound 7 astragalin	N/A	N/A	N/A
Positive control (BHA) <sup>1)</sup>	5.9 ± 0.49	N/A	N/A
Positive control (Allopurinol)	N/A	12.2 ± 2.80	2.11 ± 0.91

Primarily radical scavenging activity was determined at 0 to 250 µg/mL concentration of samples. Scavenging concentration for 50% of free radical (RC<sub>50</sub>) was calculated from logarithmic regression equation obtained from the values of at least five dilutions of the primary concentration. Values represent mean ± SDs (n = 3); in parentheses is RC<sub>50</sub> value of respective sample

N/A. not assay; BHA. butylated hydroxyanisole<sup>1)</sup>; >. out of range

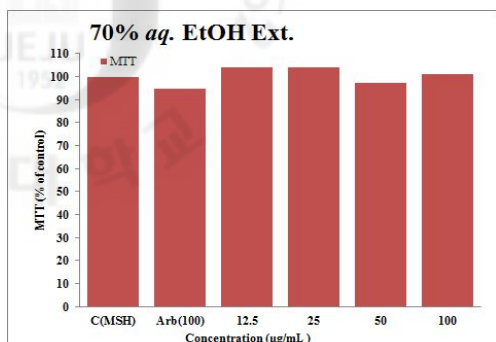


### 3-2-2. Melanogenesis inhibition activity

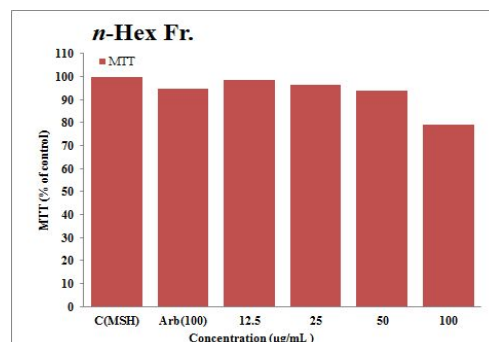
#### 3-2-2-1. Cell viability in B16F10 melanoma cell

This study on the melanogenesis inhibition effects of *A. subulatus* in murine melanoma B16F10 cells stimulated by  $\alpha$ -MSH. Five solvent fractions treated for the cell viability rates at the concentration of 12.5, 25, 50 and 100  $\mu\text{g}/\text{mL}$  by MTT assay (Fig. 116). All solvent fractions that was treated each process group did not affect of viability rate in comparison with the positive control group. Arbutin at the same concentrations had no damaged on cell viability rate (Data did not shown). Also, The isolated compounds cells were treated for cell viability rate by MTT assay. Ethyl caffeate (**2**), new compound (**4**), 3,6-DCQA (**5**), 3,5-*e*DCQA (**6**), and astragalin (**7**) that treated did not show the any cytotoxicity at the concentration of 20  $\mu\text{g}/\text{mL}$  on B16F10 cell. But, in 10  $\mu\text{g}/\text{mL}$ , caffeic acid (**3**) showed the light toxicity on B16F10 cell (Fig. 117).

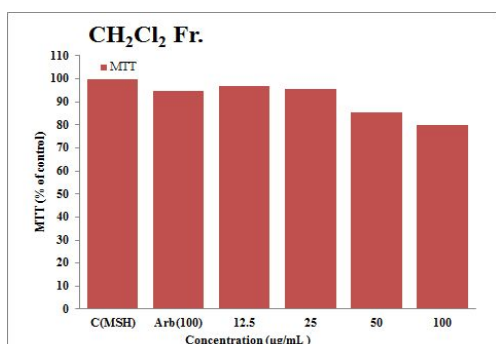
(A)



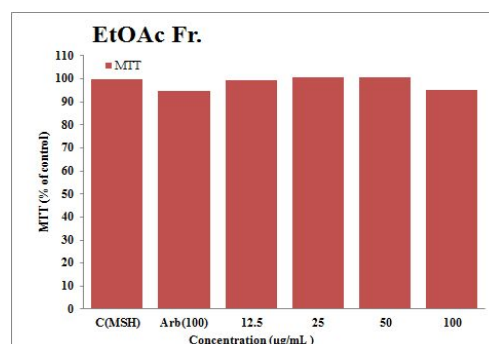
(B)



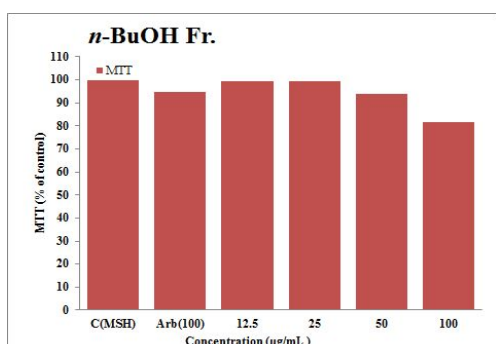
(C)



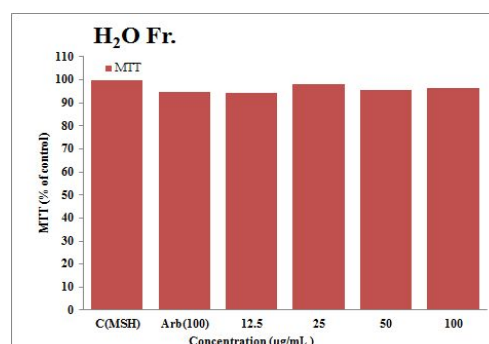
(D)



(E)



(F)

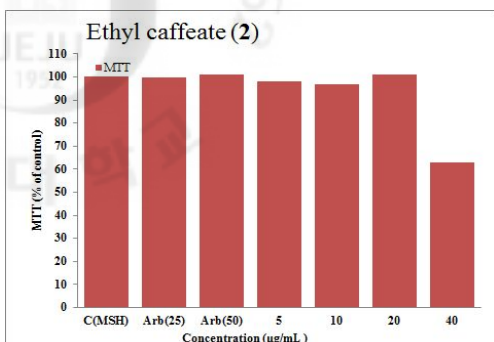


Values are mean  $\pm$  SD of 3 replicates

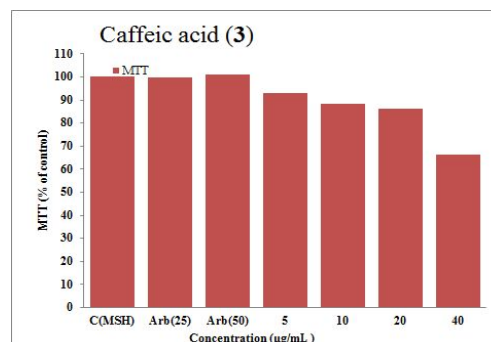
(A) 70% aq. EtOH Ext. (B) *n*-Hex Fr. (C) CH<sub>2</sub>Cl<sub>2</sub> Fr. (D) EtOAc Fr. (E) *n*-BuOH Fr. (F) H<sub>2</sub>O Fr.

Figure 116. Cell viability on B16F10 cells treated with the solvent fractions

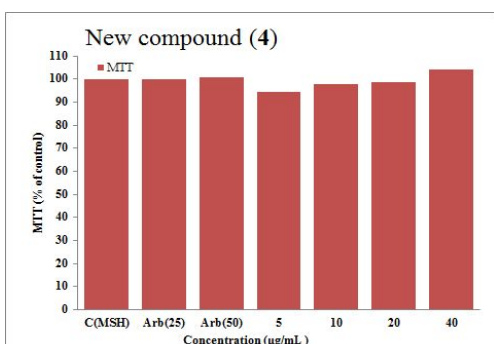
(A)



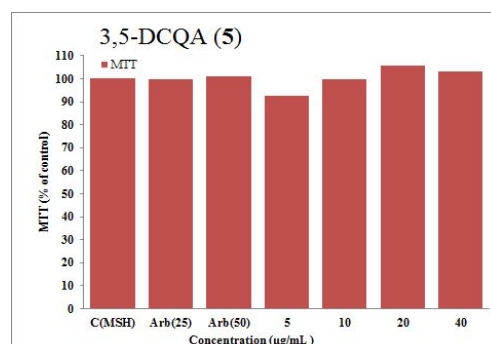
(B)



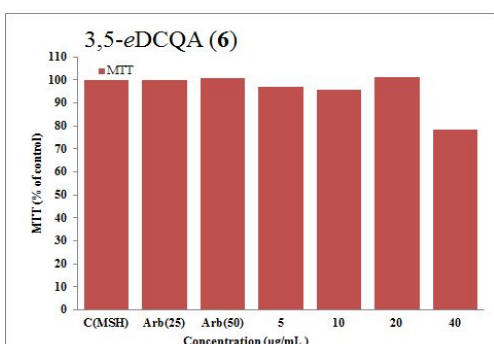
(C)



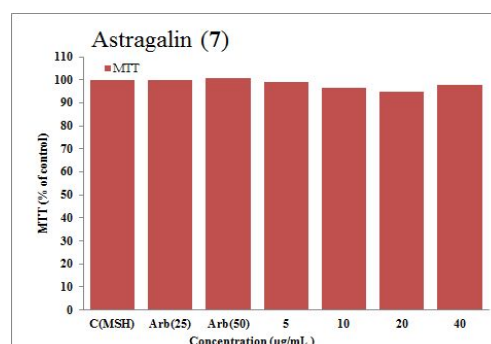
(D)



(E)



(F)



Values are mean  $\pm$  SD of 3 replicates

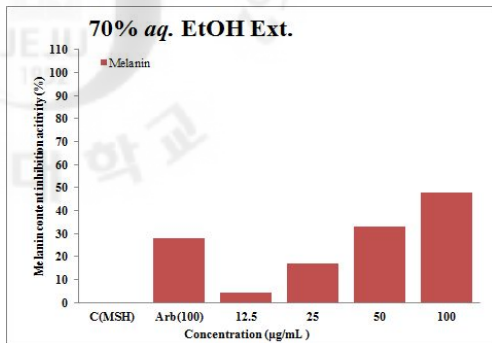
(A) Ethyl caffeate (B) Caffeic acid (C) New compound (D) 3,5-di-*O*-caffeoyl quinic acid (E) 3,5-di-*O*-caffeoyl *epi*-quinic acid (F) Astragalgin

Figure 117. Cell viability on B16F10 cells treated with the isolated compounds

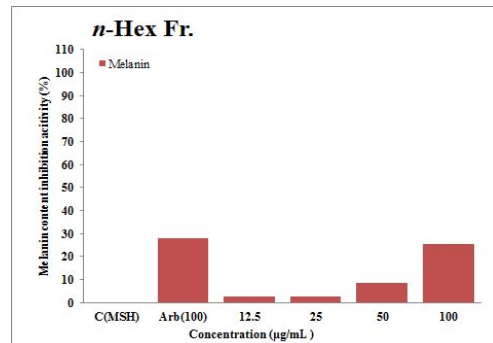
### 3-2-2-2. Effect on melanogenesis in B16F10 cells

We examined melanin contents inhibitory activity using B16F10 cells. As shown in Figure 118, the crude 70% *aq.* EtOH extract and its solvent fractions showed melanin contents inhibitory activity in a dose-dependent manner. In comparison with the positive control group, the melanin contents of the CH<sub>2</sub>Cl<sub>2</sub> fraction were significantly reduced at 25 µg/mL by 22.5%. Activity-guided isolation was carried out using the CH<sub>2</sub>Cl<sub>2</sub> solvent fraction and column chromatography finally led to isolated compounds that having activities, ethyl caffeate (**2**) and caffeic acid (**3**) that was isolated from *A. subulatus* reduced melanin contents inhibitory activity in a dose-dependent manner and shown in 10 µg/mL concentration, 12.1 and 17.2%. (Fig. 119). In the arbutin was 50 µg/mL. To treated group the contents of melanin were also significantly reduced by 30.8% (Fig. 119). Ethyl caffeate (**2**) and caffeic acid (**3**) had more good melanin contents inhibitory compared arbutin activity.

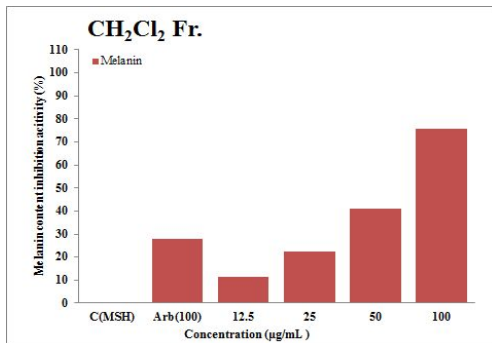
(A)



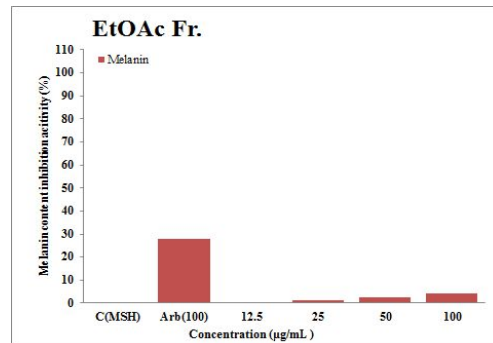
(B)



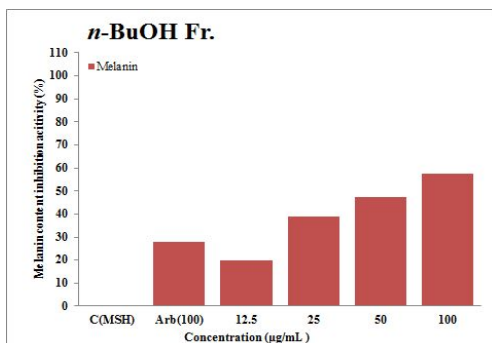
(C)



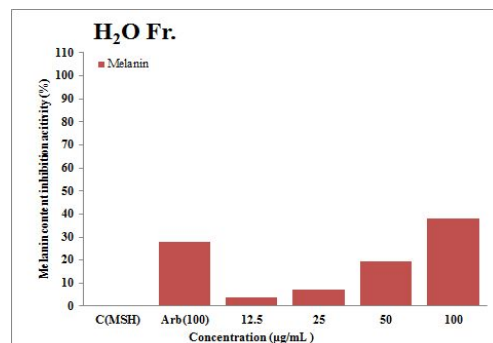
(D)



(E)



(F)

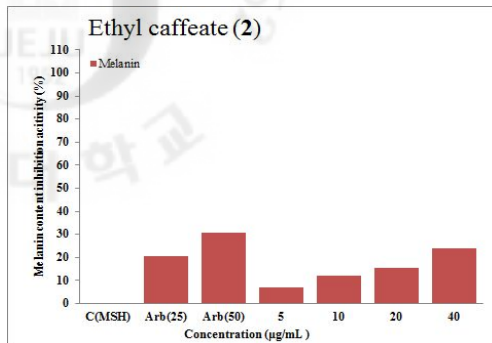


Values are mean  $\pm$  SD of 3 replicates

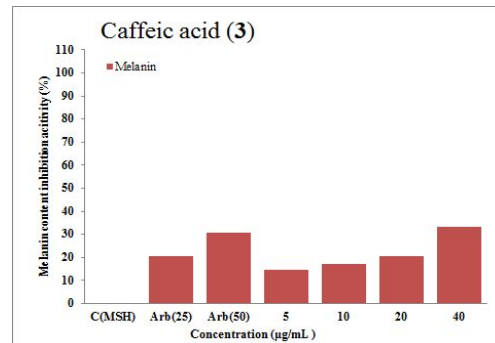
(A) 70% aq. EtOH Ext. (B) *n*-Hex Fr. (C) CH<sub>2</sub>Cl<sub>2</sub> Fr. (D) EtOAc Fr. (E) *n*-BuOH Fr. (F) H<sub>2</sub>O Fr.

Figure 118. Melanin contents inhibitory activity of the solvent fractions on B16F10 cells

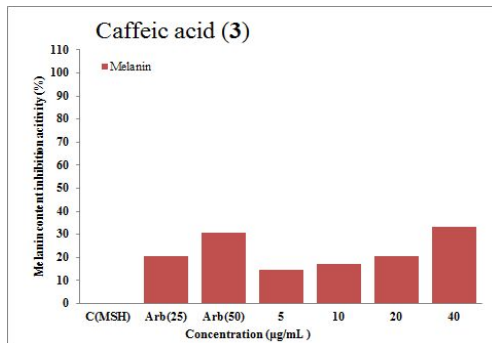
(A)



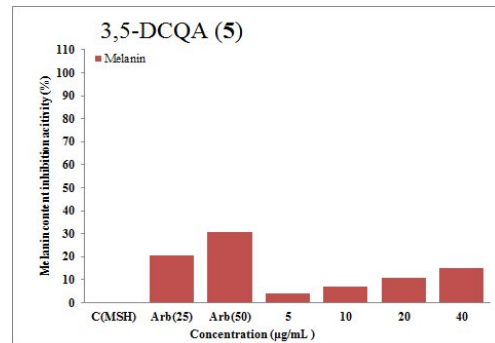
(B)



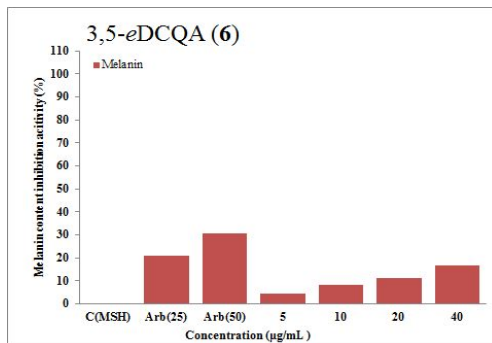
(C)



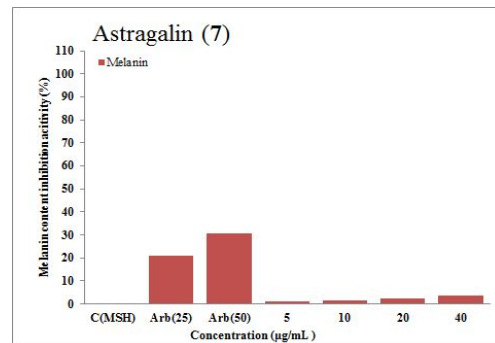
(D)



(E)



(F)



Values are mean ± SD of 3 replicates

(A) Ethyl caffeate (B) Caffeic acid (C) New compound (D) 3,5-di-O-caffeoyl quinic acid (E) 3,5-di-O-caffeoyl *epi*-quinic acid (F) Astragalin

Figure 119. Melanin contents inhibitory activity of the isolated compounds on B16F10 cells

### 3-2-3. Anti-obesity activity

#### 3-2-3-1. Inhibition effect on $\alpha$ -glucosidase

We examined the effect of yeast  $\alpha$ -glucosidase inhibition activity. The results were shown in Table 20, Various concentrations of the isolated compounds performed and showed  $\alpha$ -glucosidase inhibitory activity in a dose-dependent manner. According to Figure 120 shown, 3,5-di-*O*-caffeoylquinic acid (**5**) and 3,5-di-*O*-caffeoyl *epi*-quinic acid (**6**) has good activities on yeast  $\alpha$ -glucosidase inhibitory activity assay.  $IC_{50}$  values of 3,5-di-*O*-caffeoylquinic acid (**5**) and 3,5-di-*O*-caffeoyl *epi*-quinic acid (**6**) were each 337.4 and 414.1  $\mu\text{g/mL}$ . This active value was the good result. but, it was lower than the positive control (Acarbose,  $IC_{50} = 104.4 \mu\text{g/mL}$ ) on yeast  $\alpha$ -glucosidase inhibitory activity (Fig. 120).

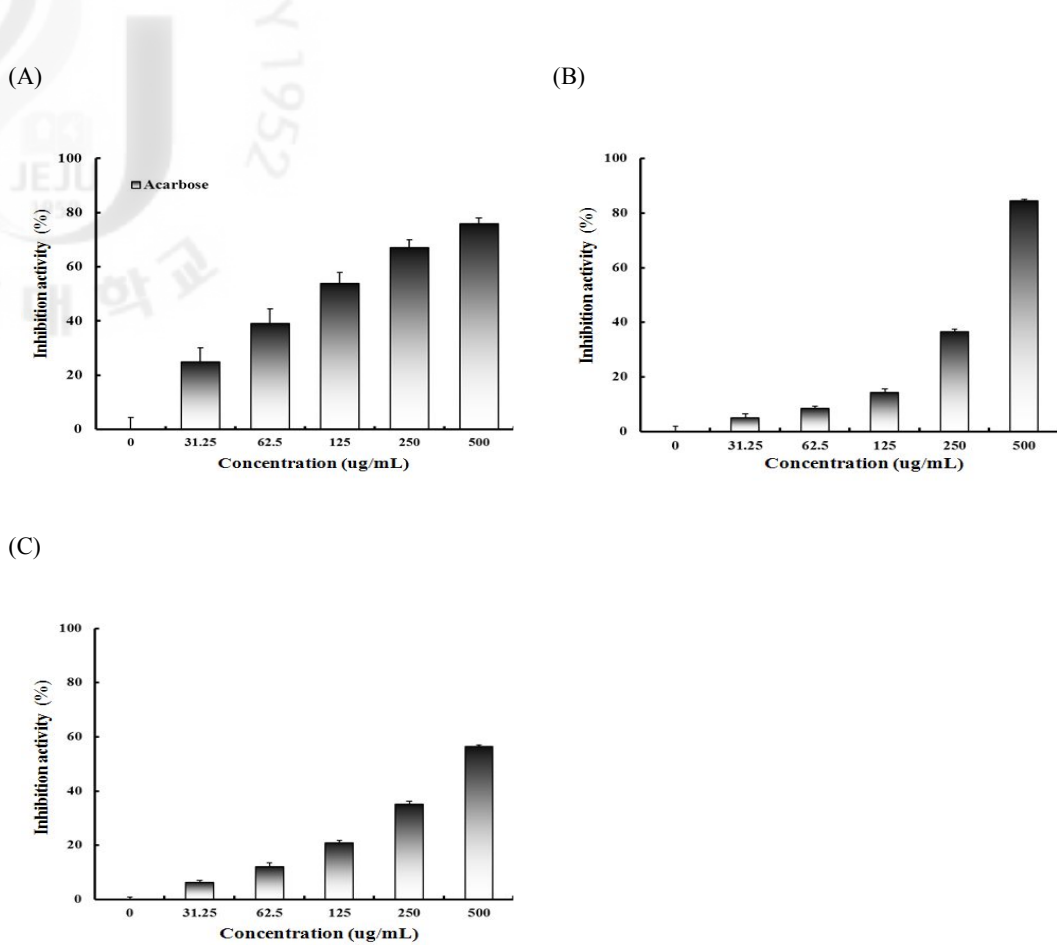
Table 20. Inhibition effect of the isolated compounds on yeast  $\alpha$ -glucosidase inhibitory assay

Samples	IC <sub>50</sub> (ug/mL)	
	yeast $\alpha$ -glucosidase inhibitory activity	
Compound 1 stigmasterol	N/A	
Compound 2 ethyl caffeate	>	100
Compound 3 caffeic acid	>	100
Compound 4 new compound	>	100
Compound 5 3,5-di- <i>O</i> -caffeoylquinic acid	337.4	± 4.38
Compound 6 3,5-di- <i>O</i> -caffeoyl <i>epi</i> -quinic acid	414.1	± 11.62
Compound 7 astragalin	>	100
Positive control (Acarbose)	104.4	± 27.08

Primarily enzyme inhibition activity was determined at 0 to 500 ug/mL concentration of samples. Inhibition concentration for 50% of enzyme inhibition (IC<sub>50</sub>) was calculated from logarithmic regression equation obtained from the values of at least five dilutions of the primary concentration. Values represent mean ± SDs (n = 3); in parentheses is IC<sub>50</sub> value of respective sample

N/A. not assay; >. out of range





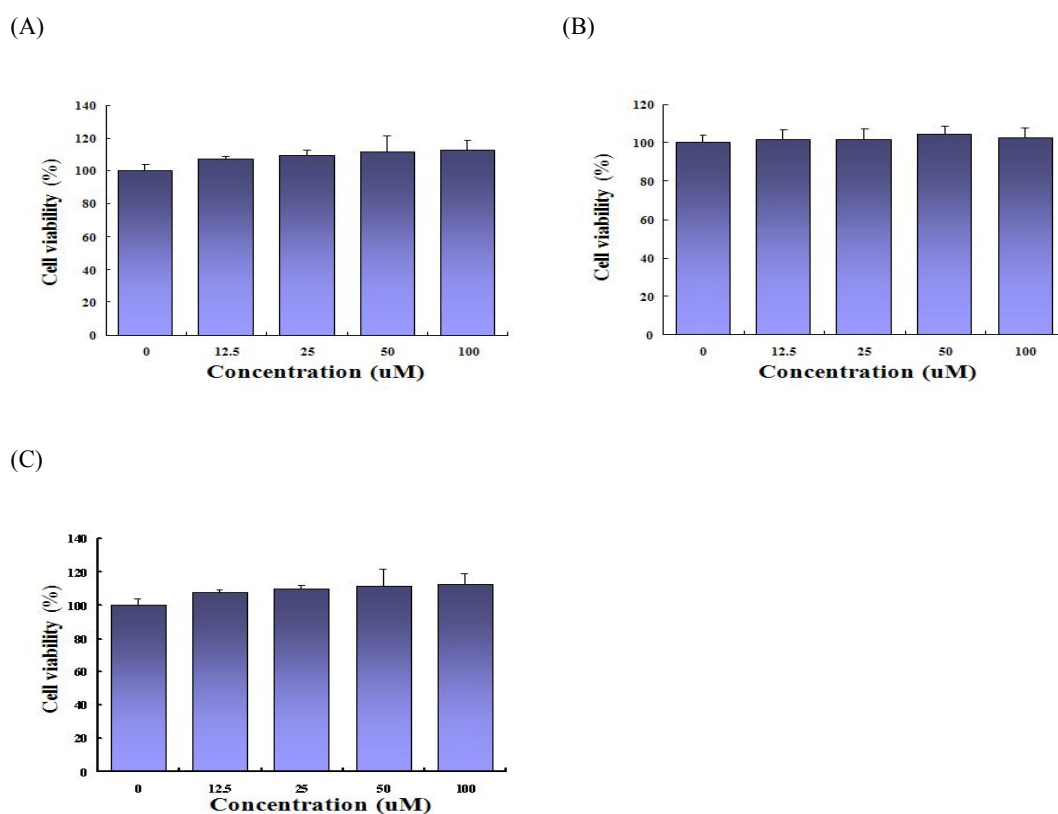
Values are mean ± SD of 3 replicates

(A) Acarbose (B) 3,5-di-O-caffeoyl quinic acid (C) 3,5-di-O-caffeoyl *epi*-quinic acid

Figure 120. Inhibition effect of the isolated compounds on yeast  $\alpha$ -glucosidase inhibitory assay

### 3-2-3-2. Cell viability in mouse 3T3-L1 preadipocytes

Pre-confluent 3T3-L1 preadipocytes were cultured in the presence and absence of various concentrations (12.5, 25, 50 and 100  $\mu\text{g}/\text{mL}$ ) of the 70% *aq.* EtOH extract and solvent fractions measured by MTT assay as like previously experimental method using *L. erythrocarpa*. As shown in Figure 121, all samples which treated 100  $\mu\text{M}$  concentration did not affect the cell viability at the concentration on MTT assay (Fig. 121).



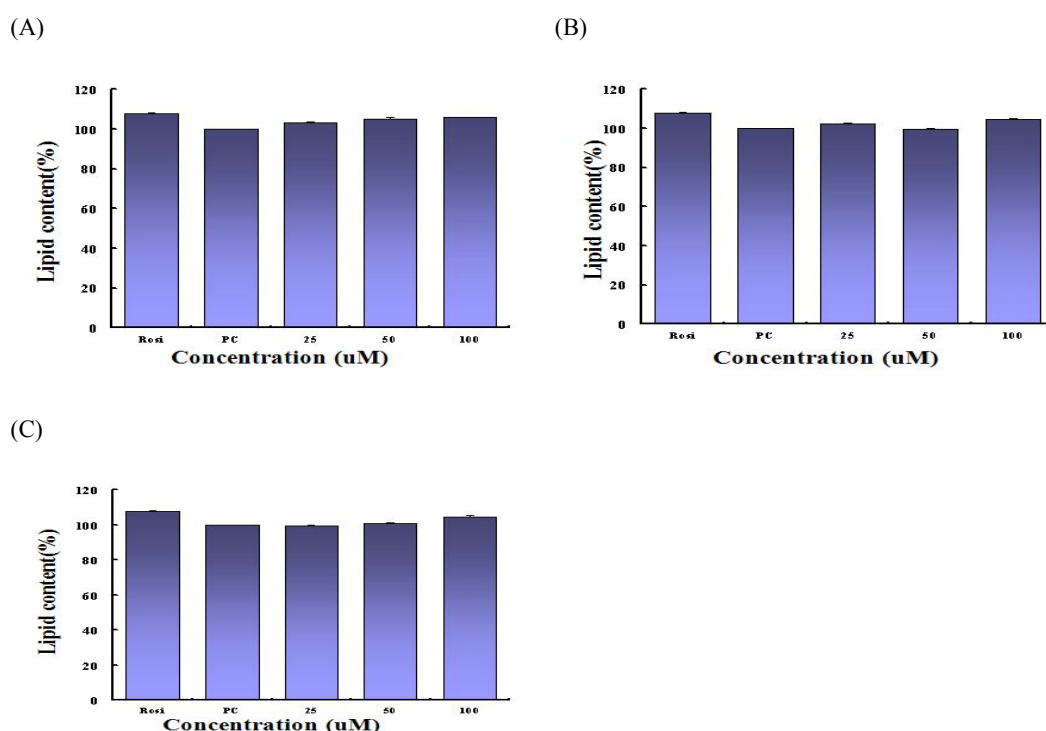
Values are mean  $\pm$  SD of 3 replicates

(A) 3,5-di-O-caffeoylquinic acid (B) 3,5-di-O-caffeoyl epi-quinic acid (C) New compound

Figure 121. Cell viability of the isolated compounds on mouse 3T3-L1 preadipocytes

3-2-3-3. Effects on reducing lipid accumulation in mouse 3T3-L1 preadipocytes differentiated adipocytes

All samples was treated to 3T3-L1 preadipocytes to investigate the effects of *A. subulatus* on obesity. During differentiation the cells were treated with various concentrations of isolated compounds (12.5, 25, 50 and 100  $\mu$ M) at 0 days with adipogenic hormone mixture and further exchanged culture medium every 3 days for 9 days. As shown in the Figure 122, the isolated compounds were not any effective to reduce lipid accumulation. From this results, The compounds that was treated did not reach any effect reducing lipid accumulation in 3T3-L1 preadipocyte.



Values are mean  $\pm$  SD of 3 replicates

(A) 3,5-di-O-caffeoylquinic acid (B) 3,5-di-O-caffeoyl epi-quinic acid (C) New compound

Figure 122. The reduction effects of the isolated compounds on lipid accumulation during differentiation of 3T3-L1 preadipocytes

#### 4. Discussion

In this study, *A. subulatus* was evaluated for the activities on antioxidant, melanogenesis inhibition activity and anti-obesity. The active constituents were identified following activity-guided isolation with chromatography.

1. The dried whole of the *A. subulatus* was extracted with 70% *aq.* EtOH at room temperature. This extract was partitioned successively into five solvent fractions. These fractions were tested for their inhibitory effects;
  - DPPH and superoxide radical scavenging activity test, xanthine oxidase inhibition activity test for the antioxidant activity
  - The effect of melanin contents inhibitory activity on B16F10 cells for the melanogenesis inhibition activity
  - yeast  $\alpha$ -glucosidase inhibitory activity test for the anti-obesity activity

As, the CH<sub>2</sub>Cl<sub>2</sub> and EtOAc solvent fractions indicated good activity, this fractions were investigated extensively to find activities compounds.

2. The CH<sub>2</sub>Cl<sub>2</sub> and EtOAc solvent fractions of *A. subulatus* were subjected to a series of chromatographic separations and led to the isolation of seven compounds. Among them, 1-[(butanoyl) phlorogluciny]- $\beta$ -D-glucopyranoside (**4**) was isolated for the first time in the nature. The structures of six known compounds and a new compound were determined by the spectroscopic methods (UV/VIS, HRFABMS, and 1D - 2D NMR).
  - $\beta$ -sitosterol (**1**), ethyl caffeate (**2**), caffeic acid (**3**), 1-[(butanoyl) phlorogluciny]- $\beta$ -D-glucopyranoside (new compound) (**4**), 3,5-di-*O*-caffeoyl quinic acid (**5**), 3,5-di-*O*-caffeoyl *epi*-quinic acid (**6**), astragalol (**7**)
3. In free radical scavenging activity studies new compound (**4**) (RC<sub>50</sub> = 4.2  $\mu$ g/mL), 3,5-di-*O*-caffeoylquinic acid (RC<sub>50</sub> = 1.3  $\mu$ g/mL) and 3,5-di-*O*-caffeoyl

*epi*-quinic acid ( $RC_{50} = 1.4 \mu\text{g/mL}$ ) had more potent DPPH radical scavenging activity higher than activity value of positive control (BHA,  $RC_{50} = 5.9 \mu\text{g/mL}$ ). And new compound ( $IC_{50} = 5.7 \mu\text{g/mL}$ ), 3,5-di-*O*-caffeoylquinic acid ( $IC_{50} = 5.0 \mu\text{g/mL}$ ) and 3,5-di-*O*-caffeoyl *epi*-quinic acid ( $IC_{50} = 7.6 \mu\text{g/mL}$ ) had more potent xanthine oxidase inhibitory activity higher than activity value of positive control (allopurinol,  $IC_{50} = 12.2 \mu\text{g/mL}$ ). New compound ( $RC_{50} = 4.5 \mu\text{g/mL}$ ), 3,5-di-*O*-caffeoylquinic acid ( $RC_{50} = 1.6 \mu\text{g/mL}$ ) and 3,5-di-*O*-caffeoyl *epi*-quinic acid ( $RC_{50} = 1.8 \mu\text{g/mL}$ ) had more potent superoxide radical scavenging activity similar than activity value of positive control (allopurinol,  $RC_{50} = 2.1 \mu\text{g/mL}$ )

4. In melanogenesis inhibition activity studies ethyl caffeate (**2**) and caffeic acid (**3**) exhibited good activity of considerable melanin contents inhibitory activity at 10  $\mu\text{g/mL}$  concentration, 12.1 and 17.2% when comparing with positive control group (In 50  $\mu\text{g/mL}$ , Arbutin has inhibition activity abilities in 30.8%)
5. In anti-obesity activity studies 3,5-di-*O*-caffeoylquinic acid ( $IC_{50} = 337.4 \mu\text{g/mL}$ ) and 3,5-di-*O*-caffeoyl *epi*-quinic acid ( $IC_{50} = 414.1 \mu\text{g/mL}$ ) had yeast  $\alpha$ -glucosidase inhibitory activity lower than activity value of positive control (acarbose,  $IC_{50} = 104.4 \mu\text{g/mL}$ )

In conclusion, the extract and isolated compounds from *A. subulatus* provided the antioxidation, melanogenesis inhibition activity, anti-obesity effect. Due to these biological activities, this plant could be a potential source applicable as the anti-aging, whitening and slimming cosmetics material.

### III. RESEARCH 4 : *Ishige sinicola* (Setchell et Gardner) Chihara

#### 1. General Plants Information

- **Scientific name** *Ishige sinicola* (Setchell et Gardner) Chihara
- **Korean name** 넓패
- **Nickname** -
- **Family name** Ishigeaceae (brown algae)
- **Distribution** The north pacific ocean, Jeju
- **Sporing** -
- **Usage** Food, animal feed, fertilizers, viscosifiers
- **Folk medicinal use**

medicine

- **Identified constituents in the literature**

di-2-ethylhexylphthalate<sup>109)</sup>

- **Biological activities in the literature**

angiotension- I converting enzyme inhibition, anti-bacterial (acne),<sup>110)</sup> antioxidation,<sup>111)</sup> melanogenesis inhibition,<sup>113)</sup> HIV-1 reverse transcriptase and integrase,<sup>114)</sup> anti-fouling<sup>109)</sup>

- **Research objective**

Standard material : 70% *aq.* EtOH extract of *I. sinicola*

For ingredient of cosmeceutical (whitening and slimming product)

1. Melanogenesis inhibition activity

: In 100  $\mu\text{g/mL}$ , the 66.9% melanin contents inhibitory activity on melanoma cell (the cytotoxin none)

2. Anti-obesity : yeast  $\alpha$ -glucosidase inhibition ( $\text{IC}_{50} = 385.1 \mu\text{g/mL}$ )

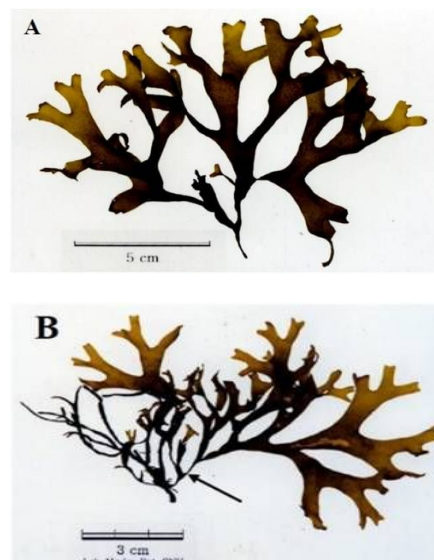


Photo 14. The specimen of *I. sinicola*

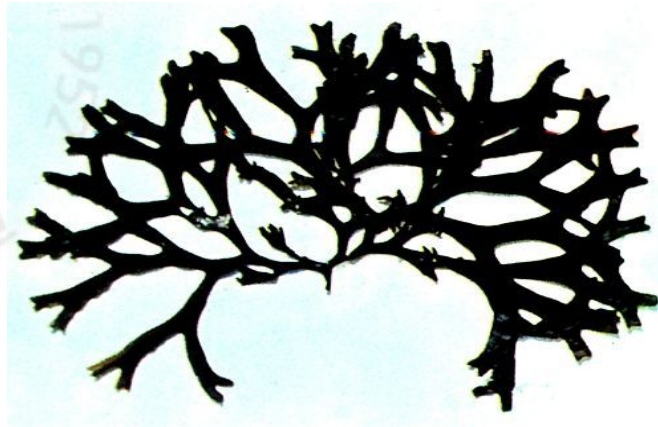


Photo 15. Photograph of *I. sinicola*



Photo 16. Photograph of the whole of *I. sinicola*



Photo 17. Photograph of the whole of *I. sinicola*

## 2. Experimental Methods

### 2-1. Plant material

The brown algae *I. sinicola* was collected from the coast of Kimnyung, Jeju Island, in July 2005. A voucher specimen (AP-055) was deposited at Extract bank of Bio-Conversion Center, Jejutechnopark (JTP), Jeju, Korea.

### 2-2. Solvent fraction from the whole sea plant

The samples were washed three times with water to remove salt, epiphytes, and sand attached to the surface, and then carefully rinsed with fresh water. The samples were dried at 60 °C for 24 hr in an oven and then ground in a grinder prior to extraction. The shade dried whole plant of *I. sinicola* (500 g) was extracted with 70% aqueous ethanol under stirring for 2 days at room temperature. The filtrate was concentrated under reduced pressure and freeze-dried to give a powder. The powdered extract (76.9 g) was then suspended in water (1.0 L) and successively partitioned into *n*-hexane (3.9 g), methylene chloride (12.6 g), ethyl acetate (15.3 g), *n*-butanol (15.5 g) and water (17.5 g) fractions (Scheme 6).

### 2-3. Isolation and purification

#### 2-3-1. Isolation produce of methylene chloride fraction (IM)

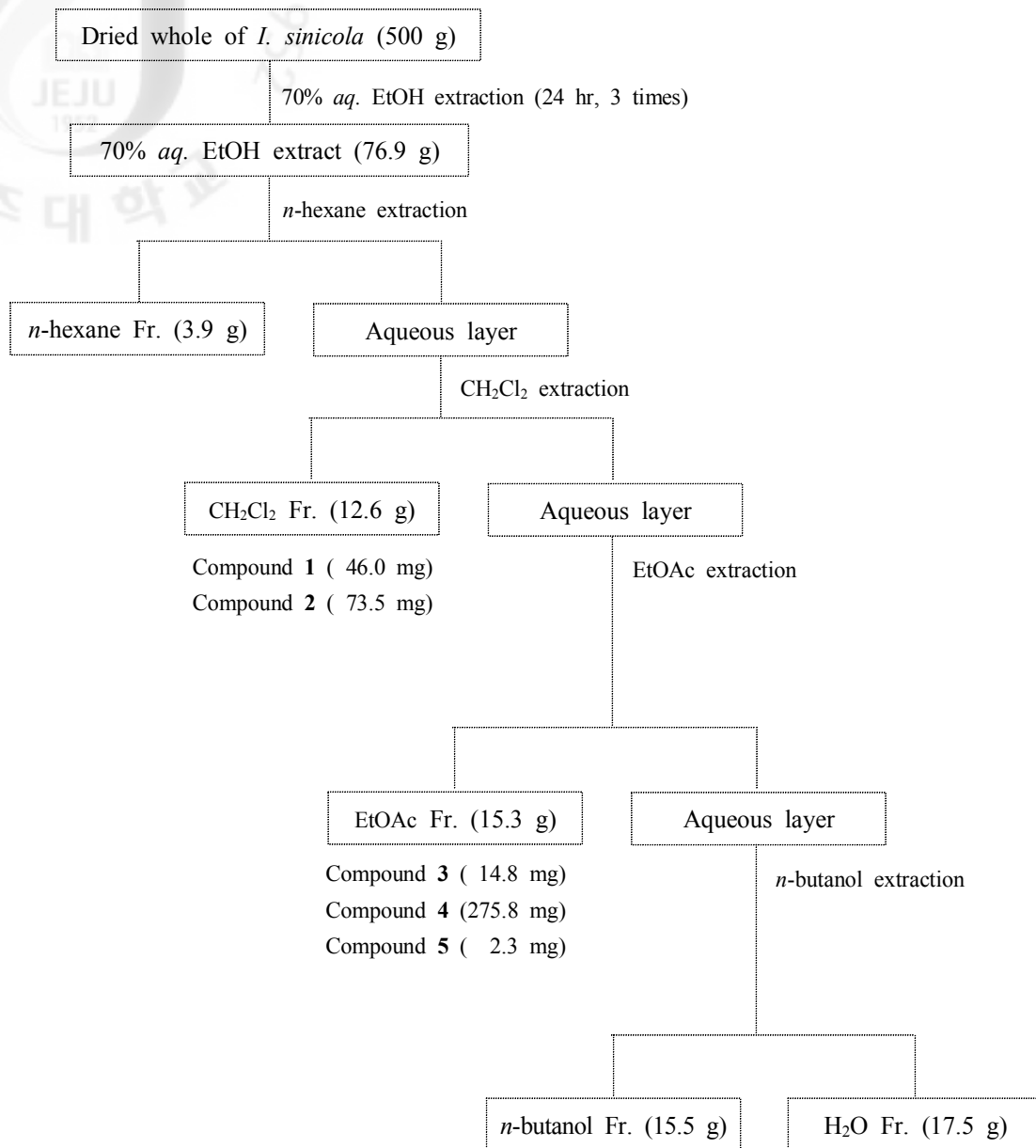
The methylene chloride fraction (12.6 g) was chromatographed over celite with *n*-hexane, CH<sub>2</sub>Cl<sub>2</sub> and Et<sub>2</sub>O successively. The obtained CH<sub>2</sub>Cl<sub>2</sub> fraction was re-fractionated by VLC over silica gel eluting with stepwise gradient solvents of *n*-Hex/EtOAc (0 ~ 100%) and then EtOAc/MeOH (0 ~ 100%). A total of 5 fractions



were collected (IM-I ~ V). The fraction of IM-II was provided compound **1** (46.0 mg). Subjection of IM-III to chromatography over silica gel using CHCl<sub>3</sub>/MeOH (13/2) provided 3 fractions. IM-III-3 provided compound **2** (73.5 mg) (Scheme 6).

#### 2-3-2. Isolation produce of ethyl acetate fraction (IE)

The EtOAc fraction (15.3 g) was chromatographed over celite with CH<sub>2</sub>Cl<sub>2</sub>, Et<sub>2</sub>O and EtOAc successively. The obtained Et<sub>2</sub>O fraction was chromatographed over reversed phase silica gel with gradient solvent (H<sub>2</sub>O/MeOH) system to provide 10 fractions (IE-I ~ X). The IE-I was applied recrystallization and provided the compound **3** (14.8 mg) and remaining solution was provided compound **4** (275.8 mg). Finally, The IE-X was chromatographed over silica gel CC with CHCl<sub>3</sub>/MeOH (4/1) to provide 4 fractions (IE-X-1 ~ 4), and than IE-X-1 provided compound **5** (2.3 mg) (Scheme 6).



Scheme 6. Extraction and fractionation of the whole of *I. sinicola*

### 3. Results

3-1. The structures of the compounds isolated from of *I. sinicola*

#### 3-1-1. Compound 1

- Compound Name 9Z,12Z-octadecadienoic acid; linoleic acid
- Synonym(s) leinolic acid, telfairic acid, linolic acid
- CAS Registry Number 60-33-3
- Appearance colorless oil
- Chemical Formula  $C_{18}H_{32}O_2$
- Molecular Weight (g/mol) 280.44
- Melting Point ( $^{\circ}C$ ) - 5
- $^1H$ -NMR (500 MHz,  $CDCl_3$ )  
 $\delta$ : 5.38 (4H, *m*, H-9, 10, 12, 13), 2.78 (2H, *m*, H-2), 2.31 (2H, *m*, H-11), 2.04 (4H, *m*, H-8, 14), 1.33 - 1.23 (16H, *m*, H-3~7, 15~17), 0.86 (3H, *m*, H-13)
- $^{13}C$ -NMR (125 MHz,  $CDCl_3$ )  
 $\delta$ : 180.2 (C-1), 130.6 (C-9), 130.2 (C-13), 128.2 (C-10), 128.1 (C-12), 34.2 (C-2), 32.1 (C-16), 29.8 (C-6), 29.8 (C-7), 29.6 (C-5), 29.5 (C-15), 29.4 (C-4), 29.2 (C-14), 27.4 (C-8), 25.8 (C-3), 24.9 (C-11), 22.9 (C-17), 14.3 (C-18)
- Biological activities in the literature  
anti-diabetic, anti-inflammation (prostaglandin precursor), anti-cancer, antioxidant

· Other data in the literature

1. Hazard and toxicity: Skin irritant. Gastrointestinal effects reported by ingestion. Fl. p. >66°

2. Density:  $d_4^{25} = 0.9$

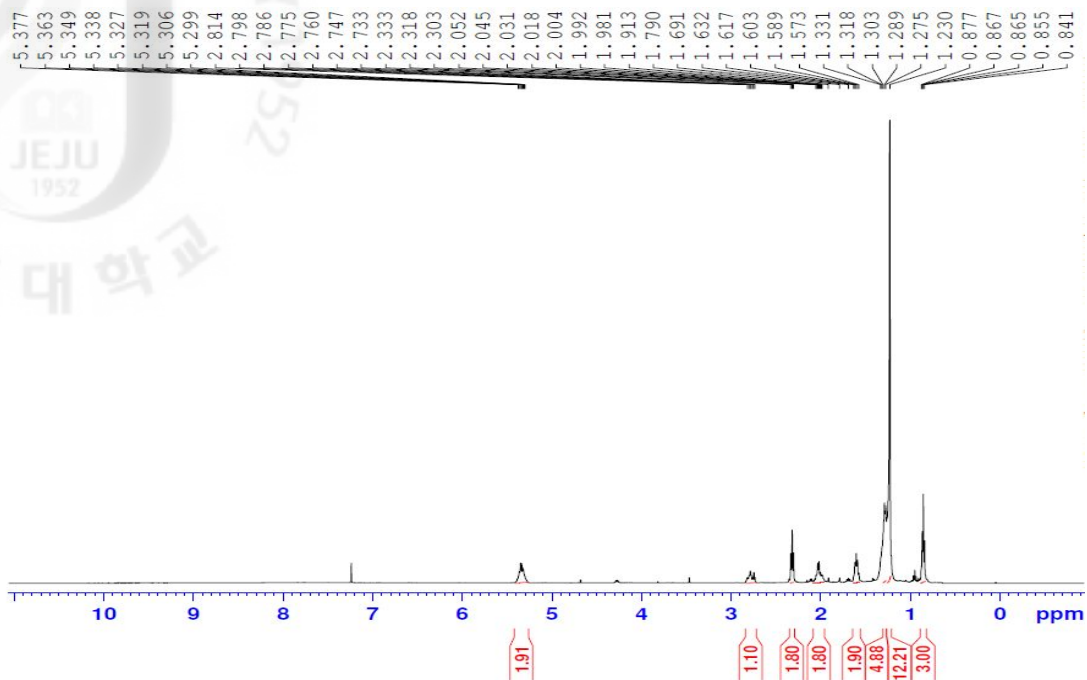


Figure 123.  $^1\text{H}$ -NMR spectrum of linoleic acid (**1**) in  $\text{CDCl}_3$

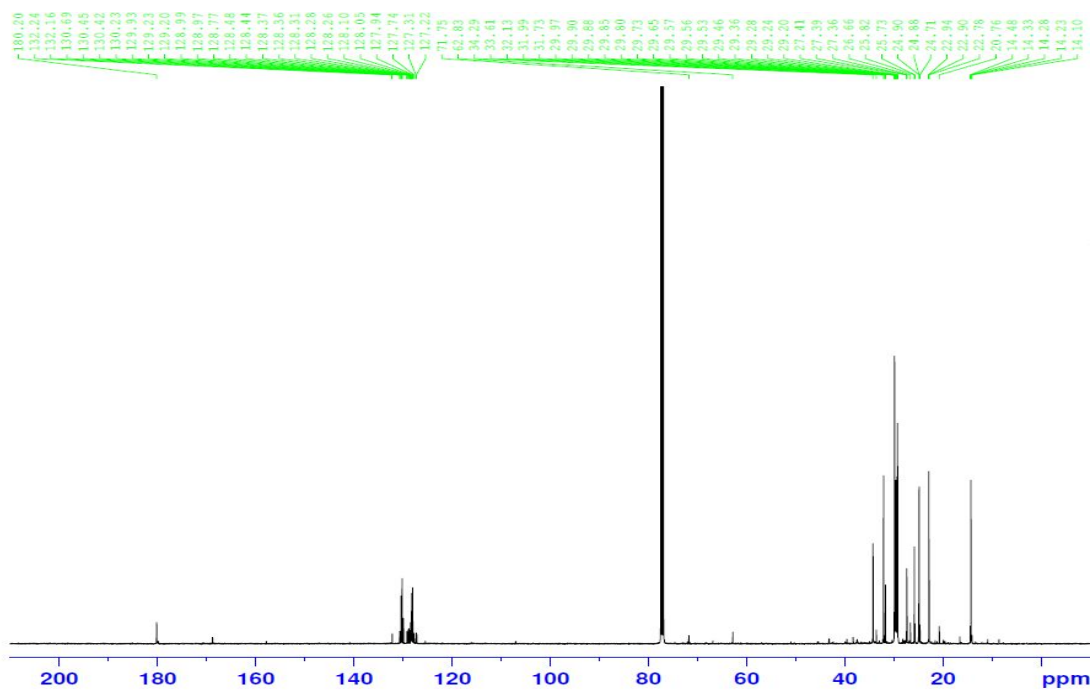


Figure 124.  $^{13}\text{C}$ -NMR spectrum of linoleic acid (**1**) in  $\text{CDCl}_3$

Compound **1** was a colorless oil. The molecular formula of compound **1** was determined to be  $C_{18}H_{32}O_2$  by NMR (18 carbon signals) datas.  $^1H$ -NMR spectrum data including correlations from the homo-COSY experiment illustrated signals attributable to a *tri*-unsaturated fatty acid, which were six olefinic methine protons of a multiplet resonance at  $\delta_H$  5.38 (4H, *m*, H-9, 10, 12, 13), allylic methylene protons at  $\delta_H$  2.78 (2H, *m*, H-2), 2.31 (2H, *m*, H-11) and 2.04 (4H, *m*, H-8, 14), numerous methylene protons at  $\delta_H$  1.33 - 1.23 (16H, *m*, H-3~7, 15~17), and terminal methyl proton at  $\delta_H$  0.86 (3H, *m*, H-13) (Fig. 123). The  $^{13}C$ -NMR and HSQC spectra of compound **1** allowed all proton signals to be assigned to their respective carbon signals (data did not shown). The olefinic protons correlated with carbons at  $\delta_C$  130.6 (C-9), 130.2 (C-13), 128.2 (C-10) and 128.1 (C-12), while the methylene protons correlated with 10 methylene carbons at  $\delta_C$  34.2 - 22.9, and the aliphatic methyl protons correlated with a carbon signal at  $\delta_C$  14.3 (C-18). The  $^{13}C$ -NMR spectrum of compound **1** also showed an additional signals attributed to a carboxylic carbon at  $\delta_C$  180.2 (C-1) (Fig. 124). By comparing all spectroscopic datas with literature values, compound **1** was identified as 9Z,12Z-octadecatrienoic acid, also called  *$\alpha$* -linolenic acid (Fig. 125).<sup>115-117)</sup>

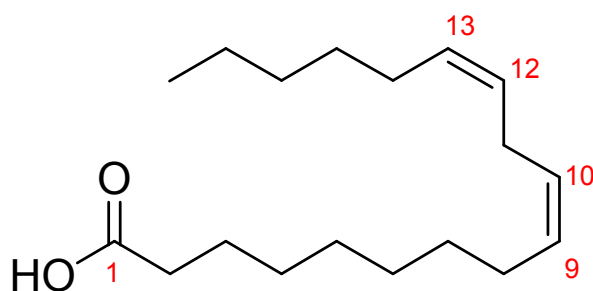


Figure 125. Structure of compound **1**; 9Z,12Z-octadecadienoic acid (linoleic acid; Telfairic acid)

### 3-1-2. Compound 2

• Compound Name 9Z,12Z-octadecadienoic acid, 1-glyceryl ester

• Synonym(s) 1-linoleoyl glycerol, 1-LG

• CAS Registry Number 2277-28-3

• Appearance colorless oil

• Chemical Formula  $C_{21}H_{38}O_4$

• Molecular Weight (g/mol) 354.52

• Melting Point ( $^{\circ}C$ ) -

•  $^1H$ -NMR (500 MHz,  $CD_3OD$ )

$\delta$ : 5.34 (4H, *m*, H-9', 10', 12', 13'), 4.16 - 4.04 (2H, *m*, H-1), 3.82 (1H, *m*, H-2), 3.70 - 3.54 (2H, *m*, H-3), 2.81 (2H, *m*, H-2'), 2.35 (2H, *m*, H-11'), 2.07 (4H, *m*, H-8', 14'), 1.36 - 1.29 (16H, *m*, H-3' - 7', 15' - 17'), 0.90 (3H, *m*, H-13')

•  $^{13}C$ -NMR (125 MHz,  $CD_3OD$ )

$\delta$ : 175.5 (C-1'), 131.0 (C-9'), 130.9 (C-13'), 129.2 (C-10'), 129.1 (C-12'), 71.2 (C-2), 66.6 (C-1), 64.1 (C-3), 35.2 (C-2'), 33.2 (C-16'), 32.8 (C-6'), 30.9 (C-7'), 30.9 (C-5'), 30.3 (C-15'), 30.3 (C-4'), 28.3 (C-14'), 26.6 (C-8'), 26.0 (C-3'), 23.9 (C-11'), 23.8 (C-17'), 14.6 (C-18')

• Biological activities in the literature

anti-atherogenic, anti-fungal, anti-allergy

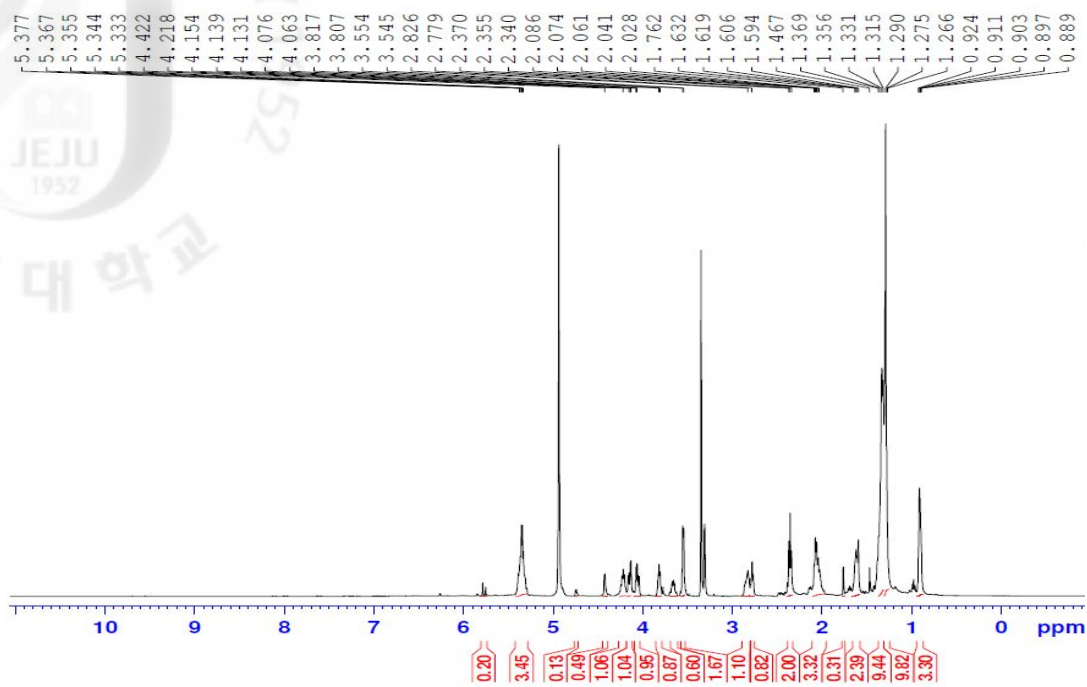


Figure 126.  $^1\text{H-NMR}$  spectrum of 1-linoleoyl glycerol (**2**) in  $\text{CD}_3\text{OD}$

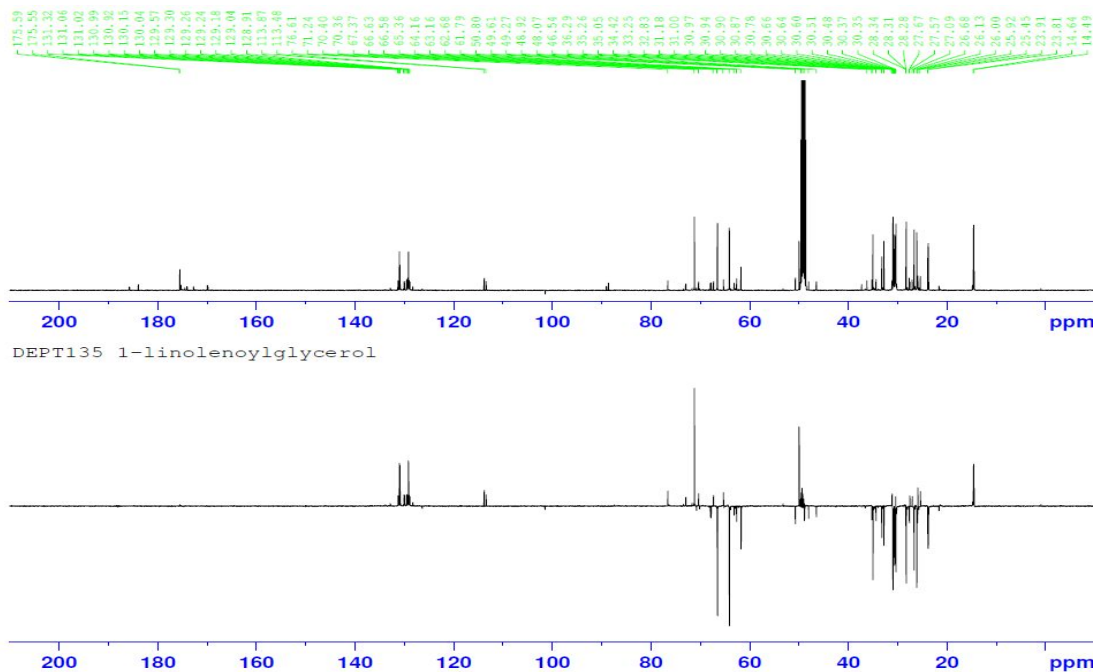


Figure 127.  $^{13}\text{C-NMR}$  and DEPT135 spectra of 1-linoleoyl glycerol (**2**) in  $\text{CD}_3\text{OD}$



Compound **2** was a colorless oil. The molecular formula of compound **2** was determined to be  $C_{21}H_{38}O_4$  by NMR (21 carbon signals) data (Fig. 127). The  $^1H$  and  $^{13}C$ -NMR spectra of compound **2** in  $CD_3OD$  was similar to those of compound **1** except for moiety of glycerol binding a fatty chain. By comparing all spectroscopic datas with literature values, compound **2** was identified as 9Z,12Z-octadecadienoic acid (1-linoleoyl glycerol) also called 1-LG (Fig. 128).<sup>115-117)</sup>

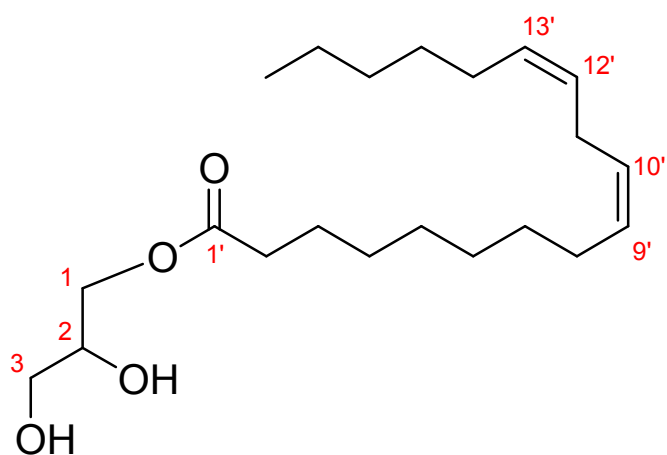


Figure 128. Structure of compound **2**; 1-linoleoyl glycerol (1-LG)

### 3-1-3. Compound 3

- Compound Name 3-hydroxy-4*H*-pyran-4-one
- Synonym(s) 3-hydroxy- $\gamma$ -pyrone, pyromeconic acid, pyrocomenic acid
- CAS Registry Number 496-63-9
- Appearance white crystalline powder
- Chemical Formula  $C_5H_4O_3$
- Molecular Weight (g/mol) 112.08
- Melting Point ( $^{\circ}C$ ) 117
- $^1H$ -NMR (500 MHz,  $CDCl_3$ )

$\delta$ : 7.85 (1H, *s*, H-2), 7.76 (1H, *d*,  $J = 5.5$  Hz, H-6), 6.46 (1H, *d*,  $J = 5.5$  Hz, H-5)

- $^{13}C$ -NMR (125 MHz,  $CDCl_3$ )

$\delta$ : 173.7 (C-4), 155.7 (C-6), 146.8 (C-3), 138.6 (C-2), 113.7 (C-4)

- Biological activities in the literature

siderophile activity, anti-chronic acid hepatitis

- Other data in the literature

1. Biological source: Constit. of *Erigeron annuus* and *Erigeron breviscapus*

2. UV (MeOH)  $\lambda_{max}nm$ : 210 and 271

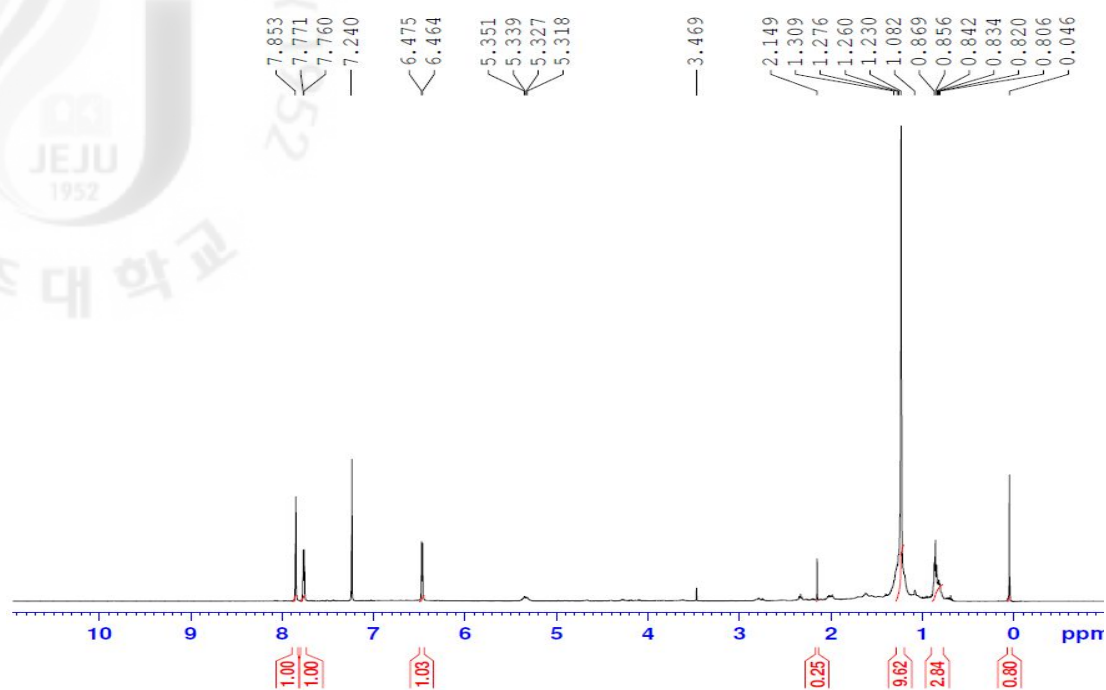


Figure 129.  $^1\text{H-NMR}$  spectrum of pyromeconic acid (**3**) in  $\text{CDCl}_3$

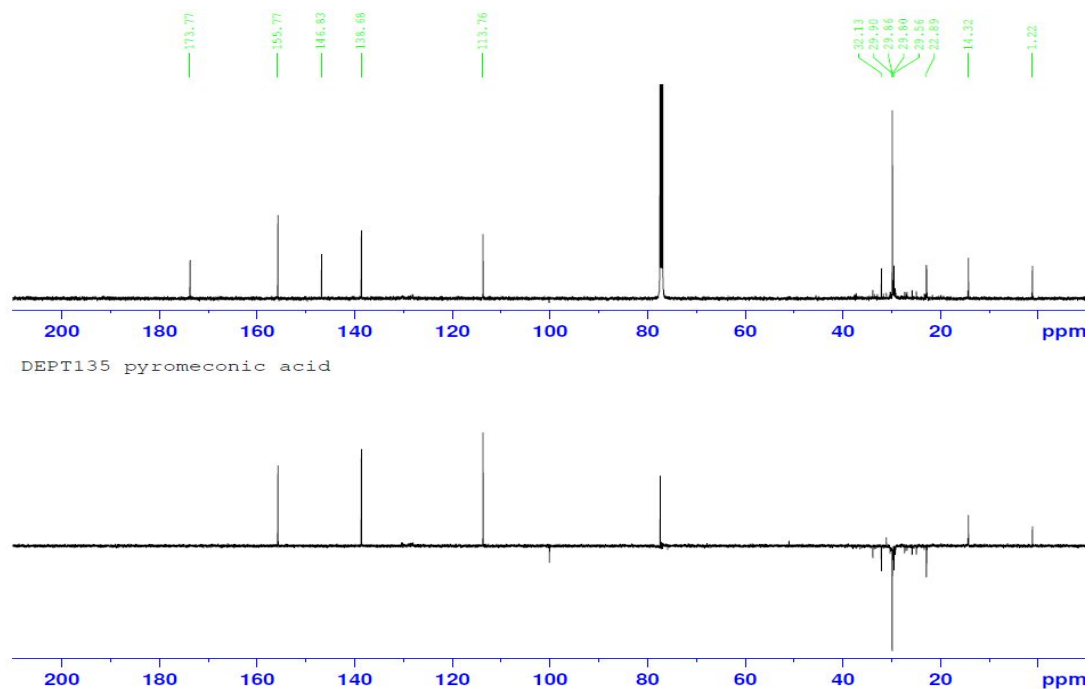


Figure 130.  $^{13}\text{C-NMR}$  and DEPT135 spectra of pyromeconic acid (**3**) in  $\text{CDCl}_3$

Compound **3** was a white crystalline powder. The molecular formula of compound **3** was determined to be  $C_5H_4O_3$  by NMR data.  $^1H$ -NMR spectrum showed a singlet signal at  $\delta_H$  7.85 (1H, *s*, H-2) and doublets at  $\delta_H$  7.76 (1H, *d*,  $J = 5.5$  Hz, H-6), 6.46 (1H, *d*,  $J = 5.5$  Hz, H-5) (Fig. 129). The  $^{13}C$ -NMR spectrum of compound **3** also showed an additional signal attributed to a  $\gamma$ -pyrone carbon signal at  $\delta_C$  173.7 (C-4) (Fig. 130). By comparing all spectroscopic data with literature values, compound **3** was identified as 3-hydroxy-4-pyrone (pyromeconic acid) (Fig. 131).<sup>118)</sup>

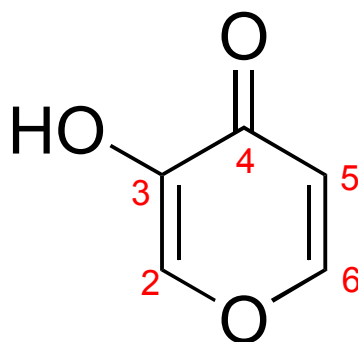


Figure 131. Structure of compound **3**; 3-hydroxy-4*H*-pyrone (pyromeconic acid)

### 3-1-4. Compound 4

- Compound Name *di*-phlorethohydroxycarmalol
- Synonym(s) DPHC
- CAS Registry Number -

• Appearance amorphous powder

• Chemical Formula  $C_{24}H_{16}O_{13}$

• Molecular Weight (g/mol) 512.37

• Melting Point (°C) -

•  $^1\text{H-NMR}$  (500 MHz,  $\text{CD}_3\text{OD}$ )

$\delta$ : 6.15 (1H, *s*, H-4), 5.98 (1H, *s*, H-9), 5.97 (2H, *s*, H-3', 5'), 5.92 (1H, *t*,  $J = 2.0$  Hz, H-2", 6"), 5.89 (2H, *d*,  $J = 2.0$  Hz, H-4")

•  $^{13}\text{C-NMR}$  (125 MHz,  $\text{CD}_3\text{OD}$ )

$\delta$ : 161.6 (C-1"), 159.9 (C-3", 5"), 156.2 (C-4'), 152.2 (C-2', 6'), 146.9 (C-5 $\alpha$ ), 144.0 (C-4 $\alpha$ ), 140.5 (C-6), 140.5 (C-7), 136.0 (C-1), 135.9 (C-3), 132.0 (C-10 $\alpha$ ), 128.1 (C-9 $\alpha$ ), 127.5 (C-2), 126.1 (C-8), 125.6 (C-1), 97.4 (C-4"), 96.4 (C-3', 5), 95.8 (C-9), 95.4 (C-4), 95.0 (C-2", 6")

• Biological activities in the literature

protective effect by radiation, anti-diabetic ( $\alpha$ -glucosidase inhibitor), antioxidant, HIV-1 inhibition

• Other data in the literature

1. Biological Source: Occurs in brown algae (*Ishige okamurae*)

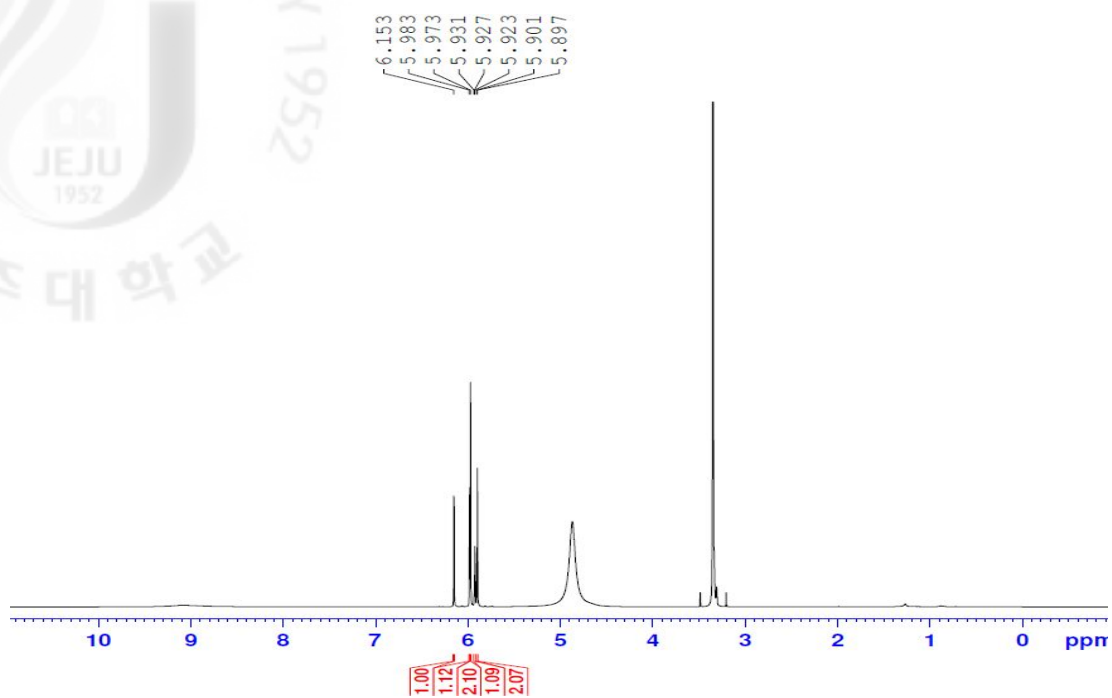


Figure 132.  $^1\text{H}$ -NMR spectrum of *di*-phlorethohydroxycarmalol (**4**) in  $\text{CD}_3\text{OD}$

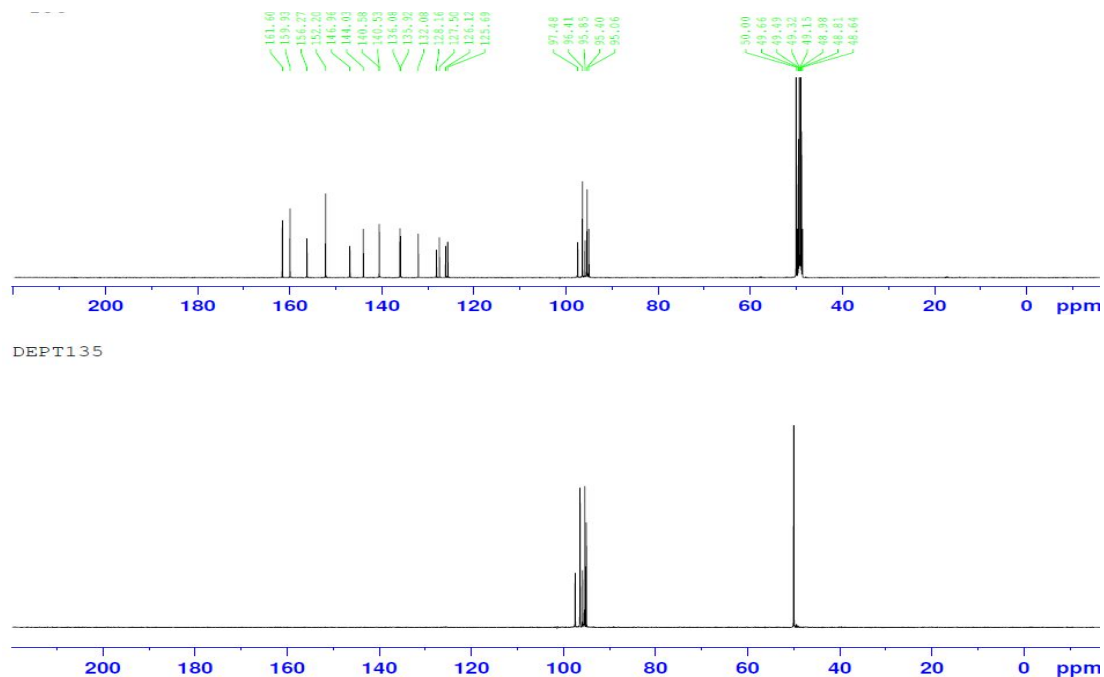


Figure 133.  $^{13}\text{C}$ -NMR and DEPT135 spectra of *di*-phlorethohydroxycarmalol (**4**) in  $\text{CD}_3\text{OD}$

Compound **4** was a amorphous powder. The molecular formula of compound **4** was determined to be  $C_{24}H_{16}O_{13}$  based on NMR data. By analysis of the  $^1H$  and  $^{13}C$ -NMR spectra in compound **4** only aromatic proton and carbon peaks were observed. Therefore, it was tentatively assumed that this compound **4** was a phloroglucinol oligomer, a class of common compounds detected in this alga. Further investigation of  $^{13}C$  and DEPT NMR data was suggested compound **4** has a structure of phloroglucinol tetramer. its characteristic peaks at  $\delta_H$  6.15 (1H, *s*, H-4), 5.98 (1H, *s*, H-9), 5.97 (2H, *s*, H-3', 5'), 5.92 (1H, *t*,  $J = 2.0$  Hz, H-2'', 6'') and 5.89 (2H, *d*,  $J = 2.0$  Hz, H-4'') attributable to seven methyl protons. and doublets at  $\delta_H$  7.76 (1H, *d*,  $J = 5.5$  Hz, H-6), 6.46 (1H, *d*,  $J = 5.5$  Hz, H-5) (Fig. 132), The  $^{13}C$ -NMR spectrum of compound **4** was showed only twenty carbon signals, which implies that two symmetric benzene units were involved in compound **4** was similar to that of *tri*-phlorethol-A. Identification of partial structure on compound **4** have tried to confirm the connection of each ring by HMBC long range correlation using NMR. But, we don't know how many hydroxyl group in this compound (Data did not shown). So, To prepare acetylated compound **4**. The compound **4** was prepared by the treatment of acetic anhydride and pyridine and further was tried analysis by NMR (Data did not shown). By comparing all spectroscopic datas with literature values, compound **4** was identified as *di*-phlorethohydroxycarmalol (DPHC) (Fig. 135).<sup>111,119)</sup>

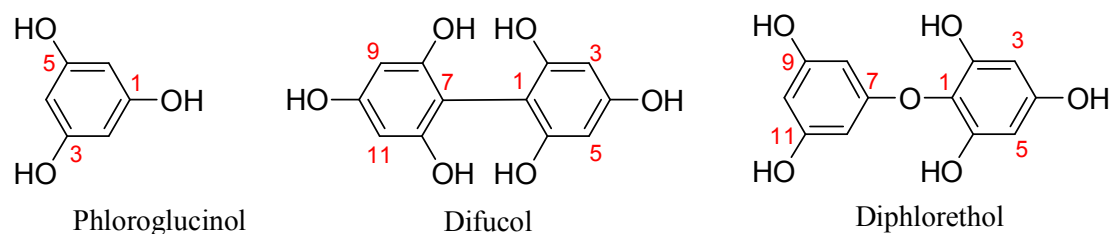


Figure 134. Basic units to structure of phlorotannin from brown alga

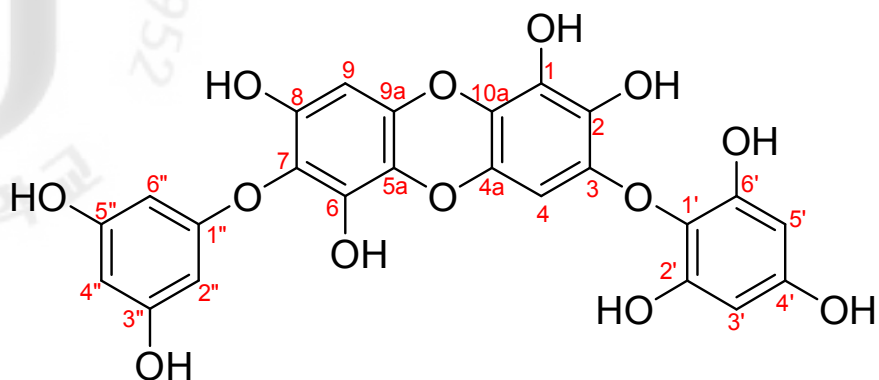


Figure 135. Structure of compound 4; *di*-phlorethohydroxycarmalol (DPHC)



### 3-1-5. Compound 5

- Compound Name 1,2-dilinoleoyl glycerol-3-*O*-D-glucoside
- Synonym(s) -
- CAS Registry Number -
- Appearance colorless oil
- Chemical Formula  $C_{45}H_{78}O_{10}$
- Molecular Weight (g/mol) 779.09
- Melting Point ( $^{\circ}C$ ) -
- $^{13}C$ -NMR (125 MHz,  $CD_3OD$ )

$\delta$ : 174.8 (C-1', 1"), 131.0 (C-9', 9"), 130.8 (C-13', 13"), 129.2 (C-10', 10"), 129.1 (C-12', 12"), 105.5 (C-1'''), 76.9 (C-3'''), 75.0 (C-2'''), 72.5 (C-2), 71.9 (C-4'''), 70.3 (C-1), 68.8 (C-6'''), 64.1 (C-1), 62.6 (C-6), 35.2 (C-2', 2"), 34.4 (C-16', 16"), 32.8 (C-6', 6"), 30.9 (C-5', 5"), 30.6 (C-15', 15"), 30.4 (C-4', 4"), 28.3 (C-14', 14"), 26.7 (C-8', 8"), 26.7 (C-3', 3"), 23.9 (C-11', 11"), 23.8 (C-17', 17"), 14.8 (C-18'), 14.8 (C-18")

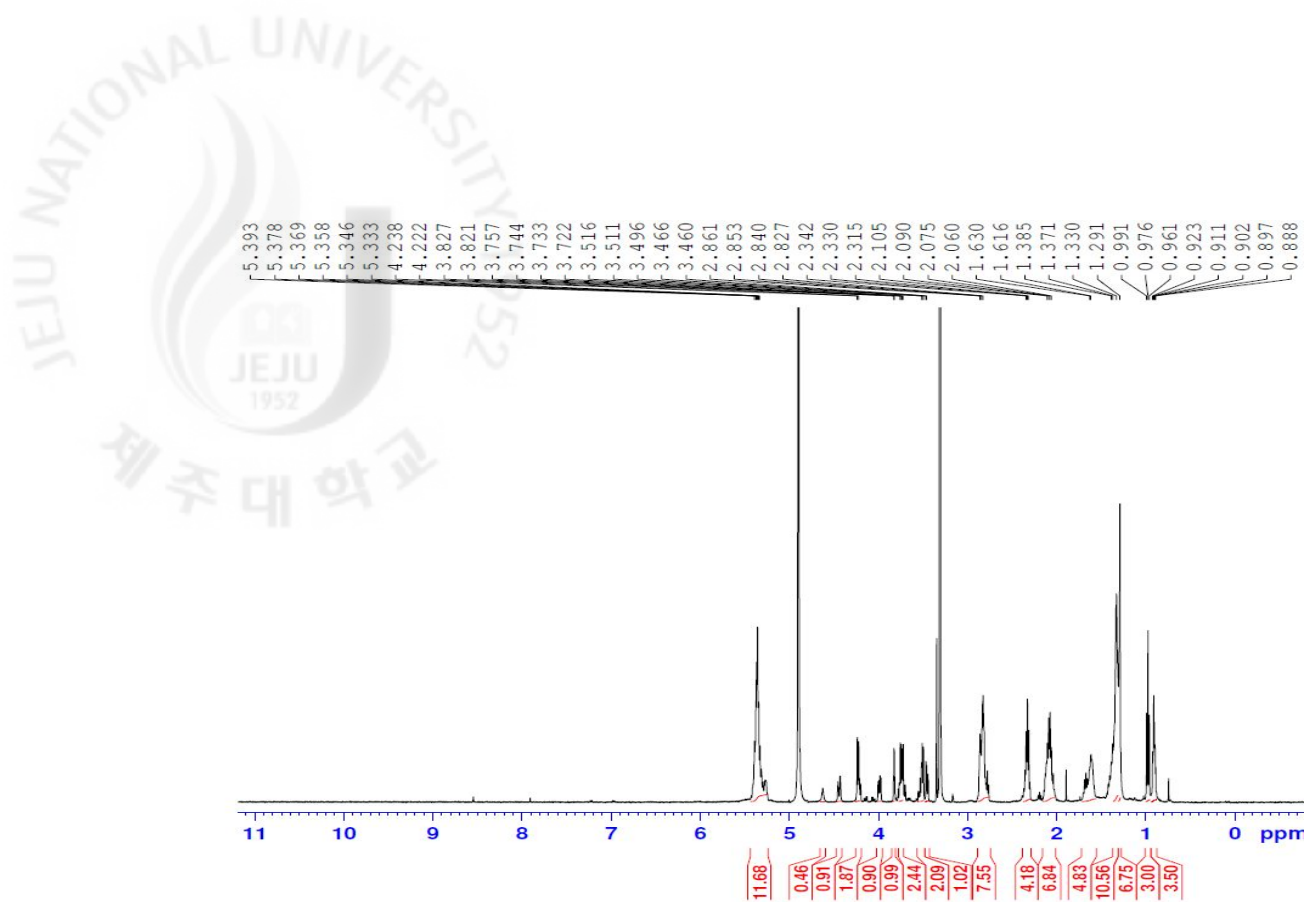


Figure 136. <sup>1</sup>H-NMR spectrum of 1,2-dilinoleoyl glycerol-3-*O*-D-glucoside (**5**) in CD<sub>3</sub>OD

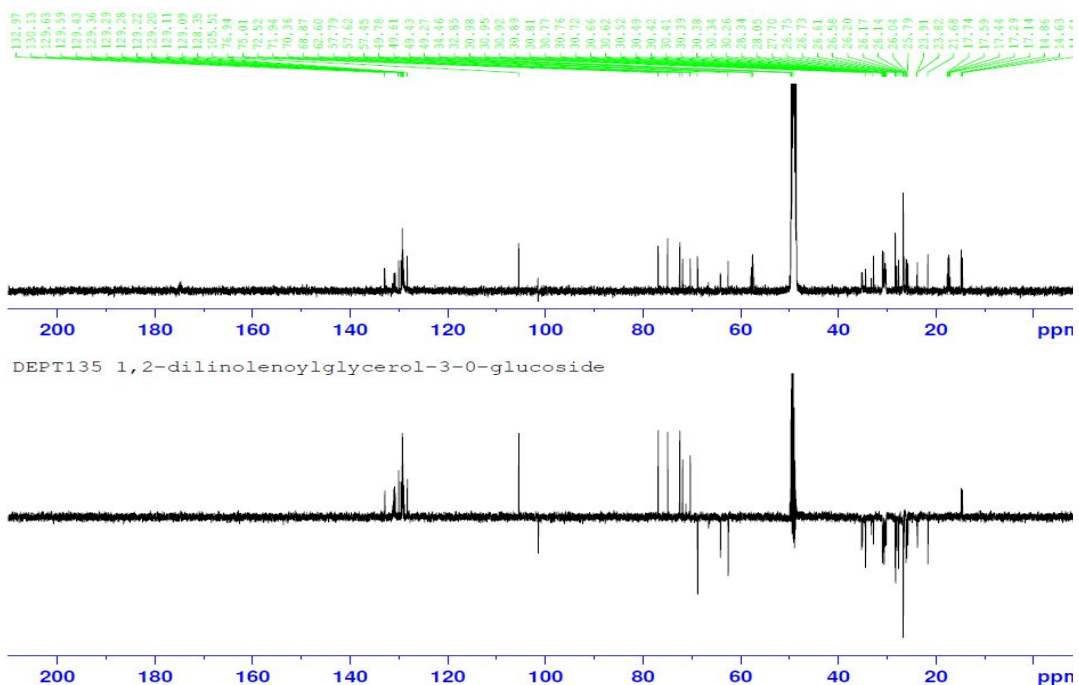


Figure 137. <sup>13</sup>C-NMR and DEPT135 spectra of 1,2-dilinoleoyl glycerol-3-*O*-D-glucoside (**5**) in CD<sub>3</sub>OD

Compound **5** was a colorless oil. The  $^1\text{H}$  and  $^{13}\text{C}$ -NMR spectra of compound **5** in  $\text{CD}_3\text{OD}$  was similar to those of compound **1** and **2** except for a moiety of sugar and 2 mole fatty chain as compound **2** binding a glycerol (Fig. 123-128). By comparing all spectroscopic data with literature values, compound **5** was identified as 1,2-dilinoleoyl glycerol-3-*O*-Dglucoside (Fig. 138).<sup>115-116)</sup>

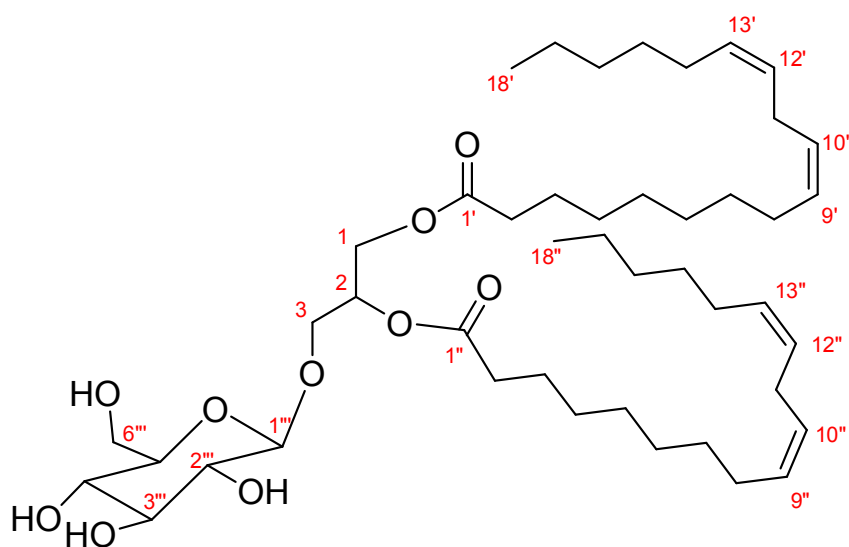


Figure 138. Structure of compound **5**; 1,2-dilinoleoyl glycerol-3-*O*-D-glucoside

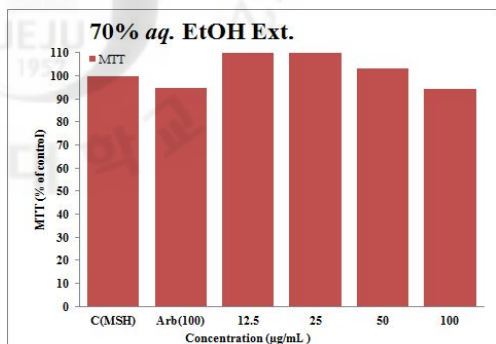
## 3-2. Biological activities

### 3-2-1. Melanogenesis inhibition activity

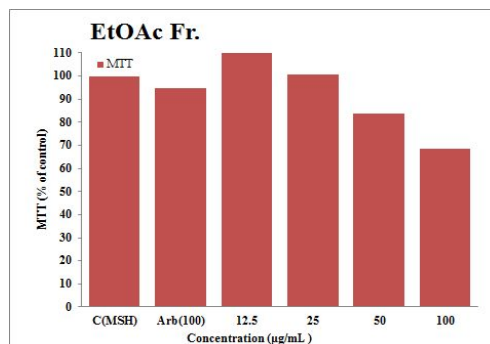
#### 3-2-2-1. Cell viability in B16F10 melanoma cell

The study examined the melanogenesis inhibition activity of the solvent fractions and the isolated compounds from *I. sinicola* on murine melanoma B16F10 cells stimulated by  $\alpha$ -MSH. Cell viability measured by MTT assay. The EtOAc fraction affect light cytotoxicity to the B16F10 cells at 50  $\mu$ g/mL concentrations. In 25  $\mu$ g/mL concentration, it did not show any toxicity of the B16F10 cell (Fig. 139). And also, B16F10 melanoma cells were treated with isolated compounds for cell viability rate. Pyromeconic acid (**3**) and *di*-phlorethohydroxycarmalol (**4**) did not affect cell viability at the concentration of 40  $\mu$ g/mL. However, linoleic acid (**1**), 1-linoleoyl glycerol (**2**) and 1,2-dilinoleoyl glycerol-3-*O*-glucoside (**3**) showed the strongly cytotoxicity over 20  $\mu$ g/mL to MTT assay (Fig. 139).

(A)



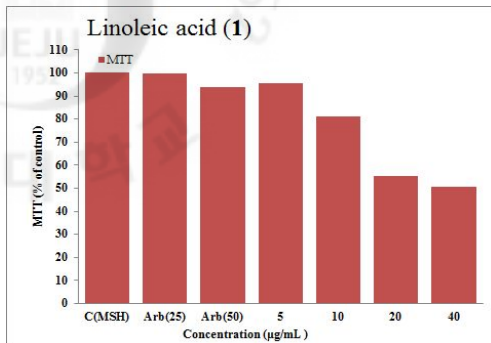
(B)



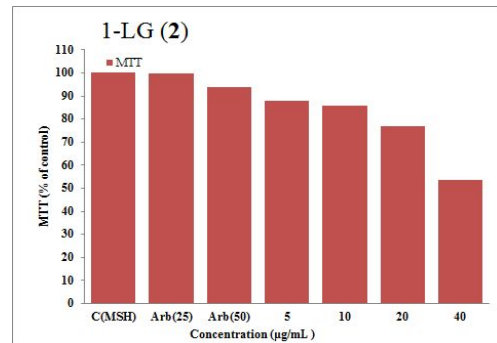
Values are mean  $\pm$  SD of 3 replicates  
 (A) 70% aq. EtOH Ext. (B) EtOAc Fr.

Figure 139. Cell viability on B16F10 cells treated with the solvent fractions

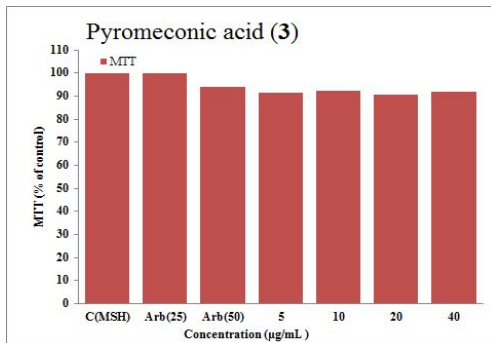
(A)



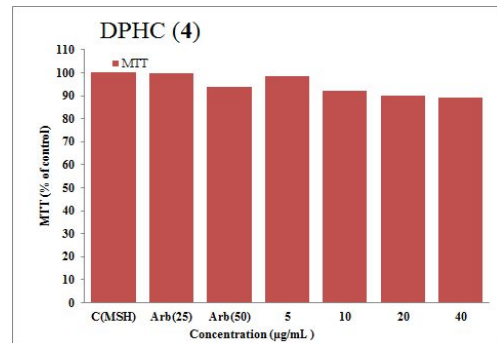
(B)



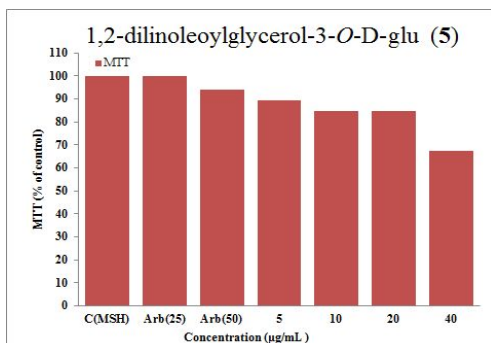
(C)



(D)



(E)



Values are mean  $\pm$  SD of 3 replicates

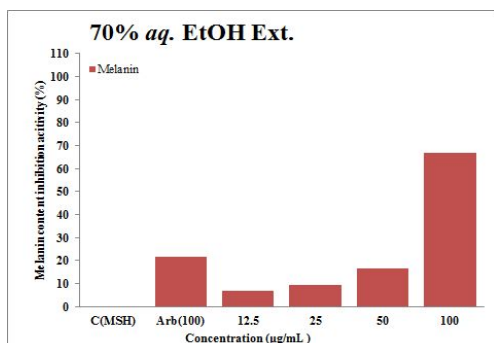
(A) linoleic acid (B) 1-linoleoyl glycerol (C) pyromeconic acid (D) *di*-phlorethohydroxycarmalol (E) 1,2-dilinoleoyl glycerol-3-*O*-glucoside

Figure 140. Cell viability on B16F10 cells treated with the isolated compounds

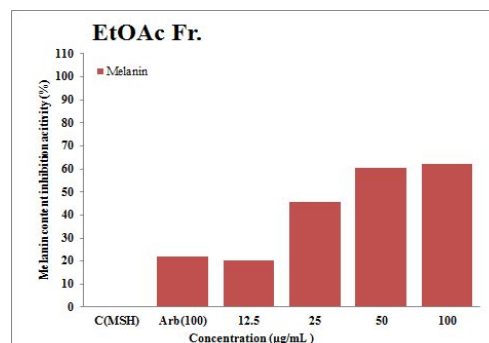
### 3-2-3-2. Effect on melanogenesis in B16F10 cells

We examined the melanin contents inhibitory activity using B16F10 melanoma cells. As shown in Figure 141, the EtOAc fraction showed melanin contents inhibitory activity in a dose-dependent manner. In comparison with the positive control group, the melanin contents of EtOAc fraction was respectively reduced at 25  $\mu\text{g/mL}$  by 45.4%. As shown in Figure 142, linoleic acid (1), 1-linoleoyl glycerol (2) and 1,2-dilinoleoyl glycerol-3-*O*-glucoside (3) reduced melanin contents inhibitory activity in a dose-dependent manner and shown in 10  $\mu\text{g/mL}$  concentration. Especially, linoleic acid (1) inhibited reducing melanin contents inhibitory activity at 10  $\mu\text{g/mL}$  by 43.5%. To treated arbutin group the content of melanin was also significantly reduced at 50  $\mu\text{g/mL}$  by 21.2% (Fig. 142).

(A)



(B)

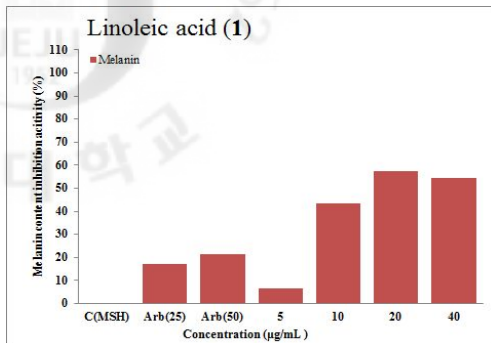


Values are mean  $\pm$  SD of 3 replicates

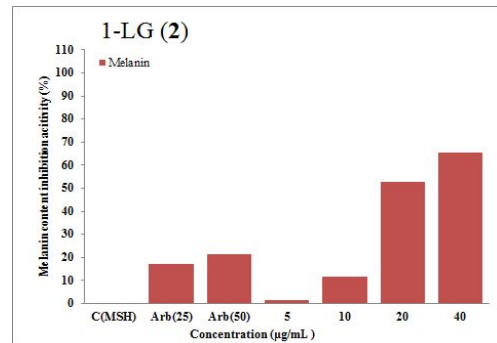
(A) 70% aq. EtOH Ext. (B) EtOAc Fr.

Figure 141. Melanin contents inhibitory activity of the solvent fractions on B16F10 cells

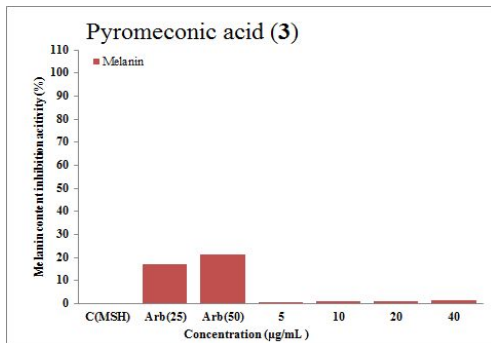
(A)



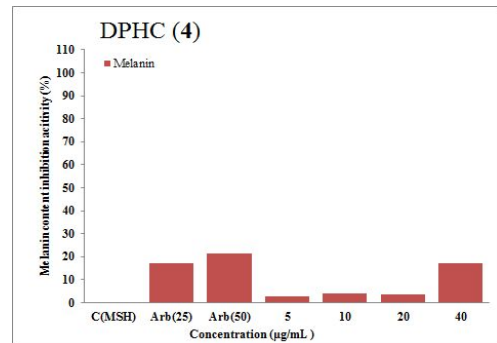
(B)



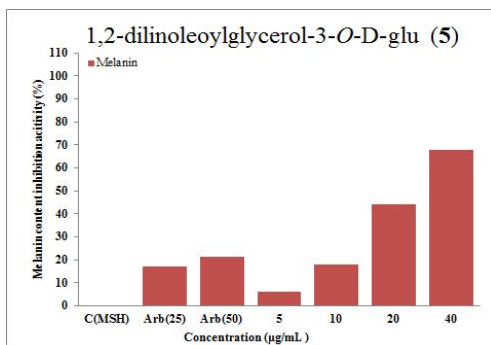
(C)



(D)



(E)



Values are mean  $\pm$  SD of 3 replicates

(A) linoleic acid (B) 1-linoleoyl glycerol (C) pyromeconic acid (D) *di*-phlorethohydroxycarmalol (E) 1,2-dilinoleoyl glycerol-3-*O*-glucoside

Figure 142. Melanin contents inhibitory activity of the isolated compounds on B16F10 cells



### 3-2-3. Anti-obesity activity

#### 3-2-3-1. Inhibition effect on $\alpha$ -glucosidase

We examined the inhibitory effect of *I. sinicola* for yeast  $\alpha$ -glucosidase activity and as shown in Table 21, Various concentrations of solvent fractions and isolated compounds were performed and showed  $\alpha$ -glucosidase inhibitory activity in a dose-dependent manner. According to Figure 143, the five solvent fractions showed gradually increased with increasing concentration and their activity increased in the following order : CH<sub>2</sub>Cl<sub>2</sub> fraction < H<sub>2</sub>O fraction < EtOAc fraction < *n*-BuOH fraction < *n*-Hex fraction (Fig. 143). Among them, EtOAc and *n*-BuOH solvent fractions exhibited strongly inhibition activity compared to other solvent fractions showing dose-dependent manner and also showed higher than positive control (Acarbose, IC<sub>50</sub> = 104.4  $\mu$ g/mL) except the lower concentration at IC<sub>50</sub> = 28.2 and 18.9  $\mu$ g/mL (Fig. 143). The isolated compounds among them, IC<sub>50</sub> values of *di*-phlorethohydroxycarmalol (**4**) was 65.2  $\mu$ M. This value was less than the positive control (Genistein, IC<sub>50</sub> = 11.5  $\mu$ M) on yeast  $\alpha$ -glucosidase inhibitory activity. However, This value was not bad activities compared to literatures (Tab. 22).

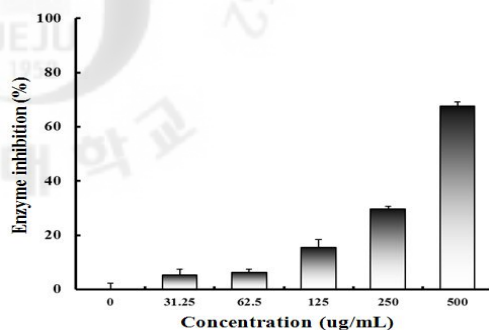
Table 21. Inhibition effect of the solvent fractions on yeast  $\alpha$ -glucosidase inhibitory assay

Samples	IC <sub>50</sub> ( $\mu$ g/mL)		
	yeast $\alpha$ -glucosidase inhibitory activity		
70% <i>aq.</i> EtOH ext.	385.1	±	6.88
<i>n</i> -Hex Fr.	10.4	±	0.11
CH <sub>2</sub> Cl <sub>2</sub> Fr.	N/A		
EtOAc Fr.	28.2	±	0.74
<i>n</i> -BuOH Fr.	18.9	±	0.50
H <sub>2</sub> O Fr.	84.2	±	1.31
Positive control (Acarbose)	104.4	±	27.0

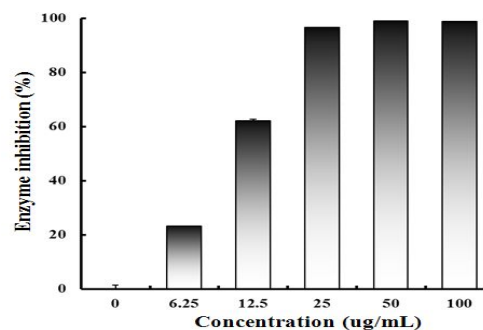
Primarily enzyme inhibition activity was determined at 0 to 100  $\mu$ g/mL concentration of samples. Inhibition concentration for 50% of enzyme inhibition (IC<sub>50</sub>) was calculated from logarithmic regression equation obtained from the values of at least five dilutions of the primary concentration. Values represent mean  $\pm$  SDs (n = 3); in parentheses is IC<sub>50</sub> value of respective sample

N/A. not assay; >. out of range

(A)



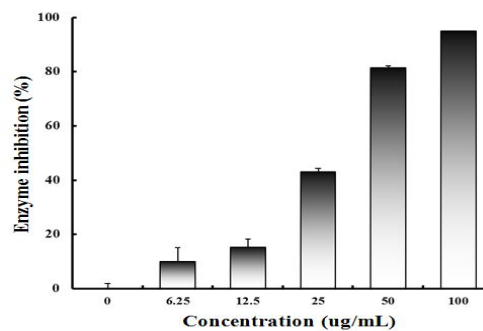
(B)



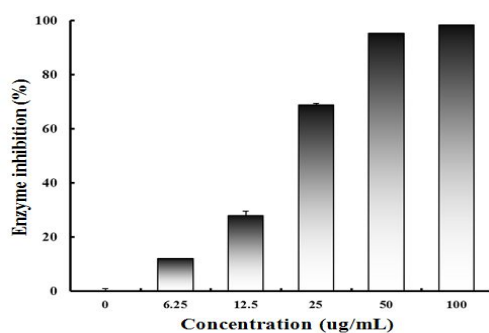
(C)

N/A

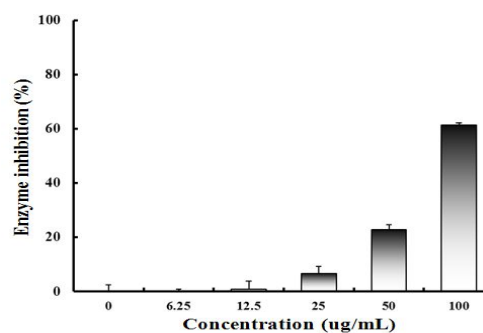
(D)



(E)



(F)



Values are mean  $\pm$  SD of 3 replicates

(A) 70% aq. EtOH Ext. (B) *n*-Hex Fr. (C) CH<sub>2</sub>Cl<sub>2</sub> Fr. (D) EtOAc Fr. (E) *n*-BuOH Fr. (F) H<sub>2</sub>O Fr.

Figure 143. Inhibition effect of the solvent fractions on yeast  $\alpha$ -glucosidase inhibitory assay

Table 22. Inhibition effect of the isolated compounds on yeast  $\alpha$ -glucosidase inhibitory assay

Samples	IC <sub>50</sub> (uM)	
	yeast $\alpha$ -glucosidase inhibitory activity	
Compound <b>1</b> linoleic acid	>	100
Compound <b>2</b> 1-linoleoyl glycerol	>	100
Compound <b>3</b> pyromeconic acid	N/A	
Compound <b>4</b> <i>di</i> -phlorethohydroxycarmalol	65.2	± 1.24
Compound <b>5</b> 1,2-dilinoleoyl glycerol-3- <i>O</i> -glucoside	>	100
Positive control (Genistein)	11.5	± 1.11

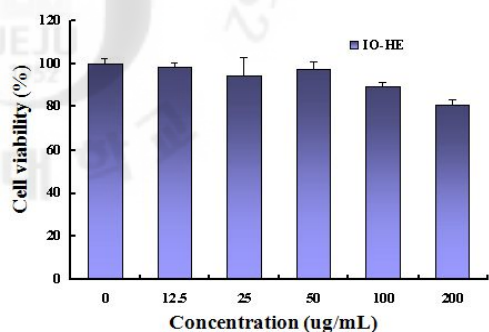
Primarily enzyme inhibition activity was determined at 0 to 100 uM concentration of samples. Inhibition concentration for 50% of enzyme inhibition (IC<sub>50</sub>) was calculated from logarithmic regression equation obtained from the values of at least five dilutions of the primary concentration. Values represent mean ± SDs (n = 3); in parentheses is IC<sub>50</sub> value of respective sample

N/A. not assay; >. out of range

### 3-2-3-2. Cell viability effect in mouse 3T3-L1 preadipocytes

Pre-confluent 3T3-L1 preadipocytes were cultured in the presence and absence of various concentrations (0 to 200  $\mu\text{g}/\text{mL}$ ) of the 70% *aq.* EtOH extract and solvent fractions were measured by MTT assay as like previously experimental method. As shown in Figure 144, EtOAc, *n*-BuOH and H<sub>2</sub>O fractions at 50  $\mu\text{g}/\text{mL}$  concentration did not affect cell viability at the concentration according to MTT assay. And also, 3T3-L1 preadipocytes treated with the isolated three compounds for cell viability rate. The isolated compounds also did not show any toxicity about cell viability rate at the concentration of 100  $\mu\text{M}$  (Fig. 145).

(A)



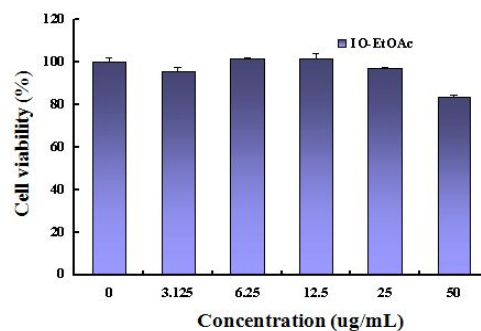
(B)

N/A

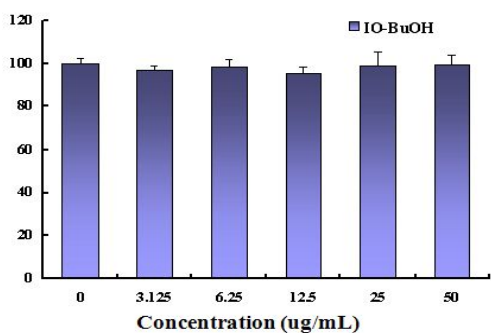
(C)

N/A

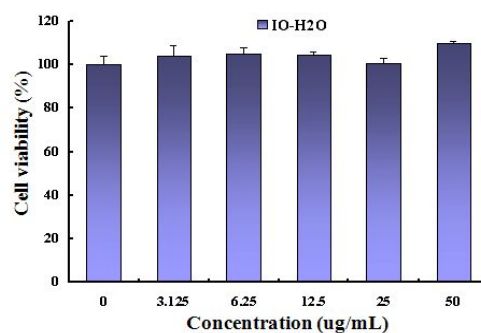
(D)



(E)



(F)

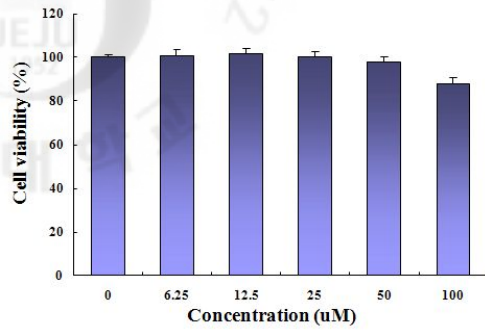


Values are mean  $\pm$  SD of 3 replicates

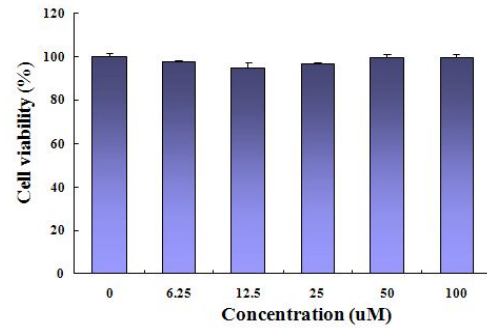
(A) 70% *aq.* EtOH Ext. (B) *n*-Hex Fr. (C) CH<sub>2</sub>Cl<sub>2</sub> Fr. (D) EtOAc Fr. (E) *n*-BuOH Fr. (F) H<sub>2</sub>O Fr.

Figure 144. Cell viability of the solvent fractions on mouse 3T3-L1 preadipocytes

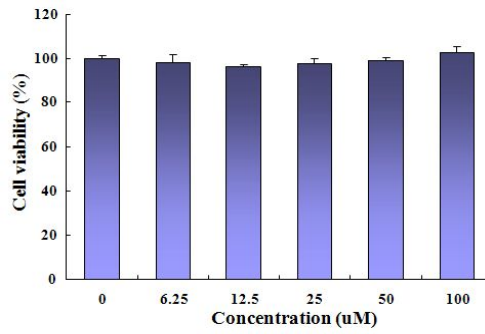
(A)



(B)



(C)



Values are mean  $\pm$  SD of 3 replicates

(A) *di-phlorethohydroxycarmalol* (B) *linoleic acid* (C) *1,2-dilinoleoyl glycerol-3-O-glucoside*

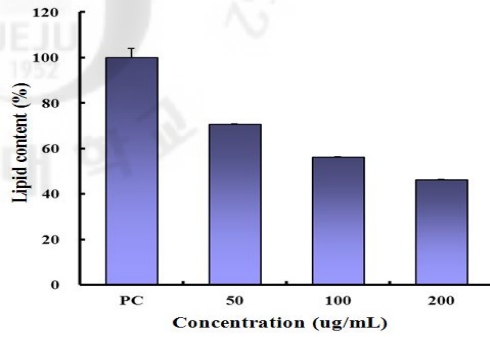
Figure 145. Cell viability of the isolated compounds on mouse 3T3-L1 preadipocytes

3-2-3-3. Effects on reducing lipid accumulation in mouse 3T3-L1 preadipocytes differentiated adipocytes

All samples were treated to 3T3-L1 preadipocytes to investigate the effects of *I. sinicola* on obesity. During differentiation the cells were treated with various concentrations of five solvent fractions (0 to 200 µg/mL) and the isolated three compounds (0, 25, 50 and 100 µM). As shown in the Figure 146, treatment of EtOAc fraction with 50 µg/mL significantly suppressed lipid accumulation to 55.4% compared to control cells. However, treated three compounds were not any effective to reduce lipid accumulation (Fig. 147). From these results suggested that all compounds did not reach any effect reducing lipid accumulation on 3T3-L1 preadipocyte. But, 70% *aq.* EtOH extract inhibited lipid accumulation possibly by decreasing lipogenesis in differentiated 3T3-L1 adipocytes.



(A)



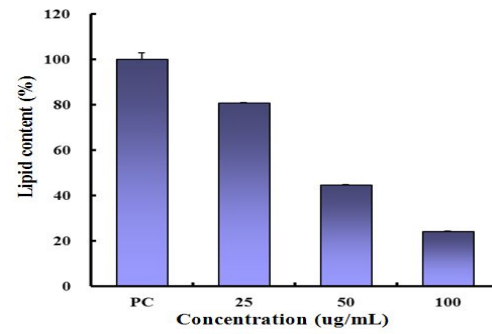
(B)

N/A

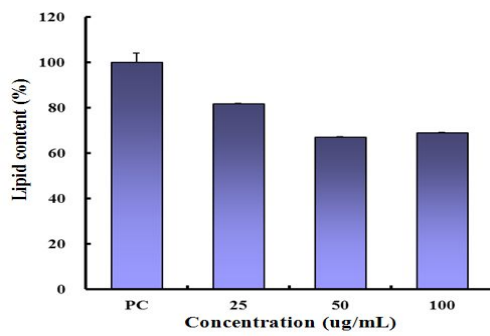
(C)

N/A

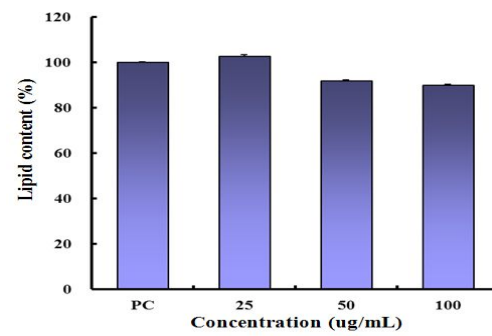
(D)



(E)



(F)

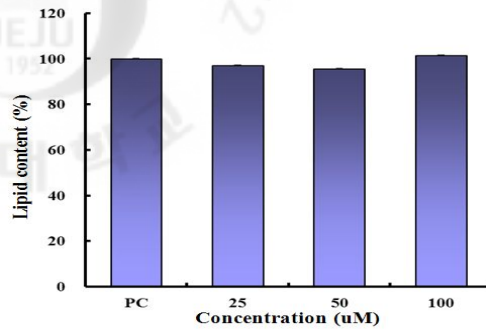


Values are mean  $\pm$  SD of 3 replicates

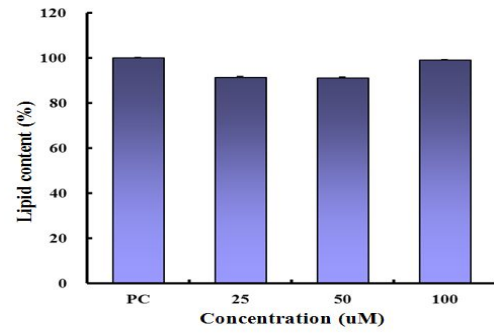
(A) 70% *aq.* EtOH Ext. (B) *n*-Hex Fr. (C) CH<sub>2</sub>Cl<sub>2</sub> Fr. (D) EtOAc Fr. (E) *n*-BuOH Fr. (F) H<sub>2</sub>O Fr.

Figure 146. The reduction effects of the solvent fractions on lipid accumulation during differentiation of 3T3-L1 preadipocytes

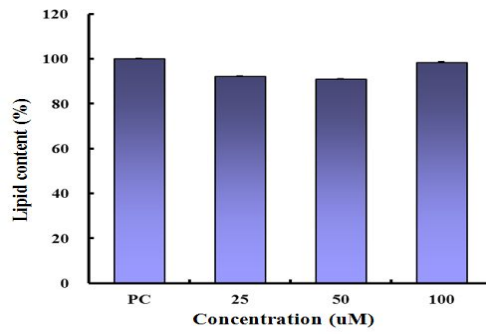
(A)



(B)



(C)



Values are mean  $\pm$  SD of 3 replicates

(A) *di-phlorethohydroxycarmalol* (B) *linoleic acid* (C) *1,2-dilinoleoyl glycerol-3-O-glucoside*

Figure 147. The reduction effects of the isolated compounds on lipid accumulation during differentiation of 3T3-L1 preadipocytes

#### 4. Discussion

In this study, *I. sinicola* was evaluated for the activities on melanogenesis inhibition activity, anti-obesity. The active constituents were identified following activity-guided isolation with chromatography.

1. The dried whole of *I. sinicola* was extracted with 70% *aq.* EtOH at room temperature. This extract was partitioned successively into five solvent fractions. These fractions were tested for their inhibitory effects;
  - The effect of melanin contents inhibitory activity on B16F10 cells for the melanogenesis inhibition activity
  - yeast  $\alpha$ -glucosidase inhibitory activity test for the anti-obesity activity
  - The effect of reducing lipid accumulation in 3T3-L1 preadipocytes for the anti-obesity activity

As the CH<sub>2</sub>Cl<sub>2</sub> and EtOAc solvent fractions indicated good activity, this fractions were investigated extensively to find activities compounds.

2. The CH<sub>2</sub>Cl<sub>2</sub> and EtOAc solvent fractions of *I. sinicola* were subjected to a series of chromatographic separations and led to the isolation of five compounds. The structures of five known compounds were determined by the spectroscopic methods (UV/VIS, 1D - 2D NMR).
  - linoleic acid (1), 1-linoleoyl glycerol (2), pyromeconic acid (3), *di*-phlorethohydroxycarmalol (4), 1,2-dilinoleoyl glycerol-3-*O*-D-glucoside (5)
3. In melanogenesis inhibition activity studies linoleic acid (1) exhibited good activities of considerable melanin contents inhibitory activity in 10  $\mu$ g/mL concentration, 43.5% compared to positive control group (Arbutin was at 50  $\mu$ g/mL by 21.2% inhibition activity)

4. In anti-obesity activity studies *di*-phlorethohydroxycarmalol ( $IC_{50} = 65.2 \mu M$ ) had good activities on yeast  $\alpha$ -glucosidase inhibitory activity at lower concentration compared to activity value of positive control (Genistein,  $IC_{50} = 11.5 \mu M$ )

In conclusion, the extract and isolated compounds from *I. sinicola* provided that the melanogenesis inhibition activity and effect. Due to these biological activities, this plant could be a potential source applicable as the whitening and slimming cosmetics material.

### III. RESEARCH 5 : *Dictyota coriacea* (Holmes) Hwang, Kim, et Lee

#### 1. General Plants Information

• **Scientific name** *Dictyota coriacea* (Holmes)  
Hwang, Kim, et Lee

• **Korean name** 참가죽그물바탕말

• **Nickname** -

• **Family name** Dictyotaceae

• **Distribution** Korea, Japan, Tailand

• **Sporing** -

• **Usage** Nature dyestuff

• **Folk medicinal use**

No information

• **Identified constituents in the literature**

acrylic acid, dolabellane, dictyol E, amijiol, isoamijiol, dictyodial<sup>121)</sup>

• **Biological activities in the literature**

anti-bacterial (gram positive),<sup>121)</sup> anti-inflammation,<sup>121)</sup> melanogenesis inhibition,<sup>122)</sup>  
anti-obesity,<sup>123)</sup> anti-cancer<sup>124)</sup>

• **Research objective**

Standard material : 70% aq. EtOH extract of *D. coriacea*

For ingredient of cosmeceutical (whitening product)

1. Melanogenesis inhibition

: In 100 µg/mL, the 47.8% melanin contents inhibitory activity on B16F10 cell  
(the cytotoxin none)



Photo 18. The specimen of *D. coriacea*



Photo 19. Photograph of the whole of *D. coriacea*



Photo 20. Photograph of the whole of *D. coriacea*



Photo 21. Photograph of the whole of *D. coriacea*

## 2. Experimental Methods

### 2-1. Plant material

The *D. coriacea* was collected from the coast of Sasudong, Jeju Island, in January 2005. A voucher specimen (AP-043) was deposited at Extract bank of Bio-Conversion Center, Jutechnopark (JTP), Jeju, Korea.

### 2-2. Solvent fraction from the whole sea plant

The samples were washed three times with water to remove salt, epiphytes, and sand attached to the surface, and then carefully rinsed with fresh water. The samples were dried at 60 °C for 24 hr in an oven and then ground in a grinder prior to extraction. The shade dried whole of *D. coriacea* (400 g) was extracted with 70% aqueous ethanol under stirring for 2 days at room temperature. The filtrate was concentrated under reduced pressure and freeze-dried to give a powder. The powdered extract (65.4 g) was then suspended in water (1.0 L) and successively partitioned into *n*-hexane (14.1 g), methylene chloride (0.9 g), ethyl acetate (0.1 g) and *n*-butanol (2.2 g) and water (43.5 g) fractions (Scheme 7).

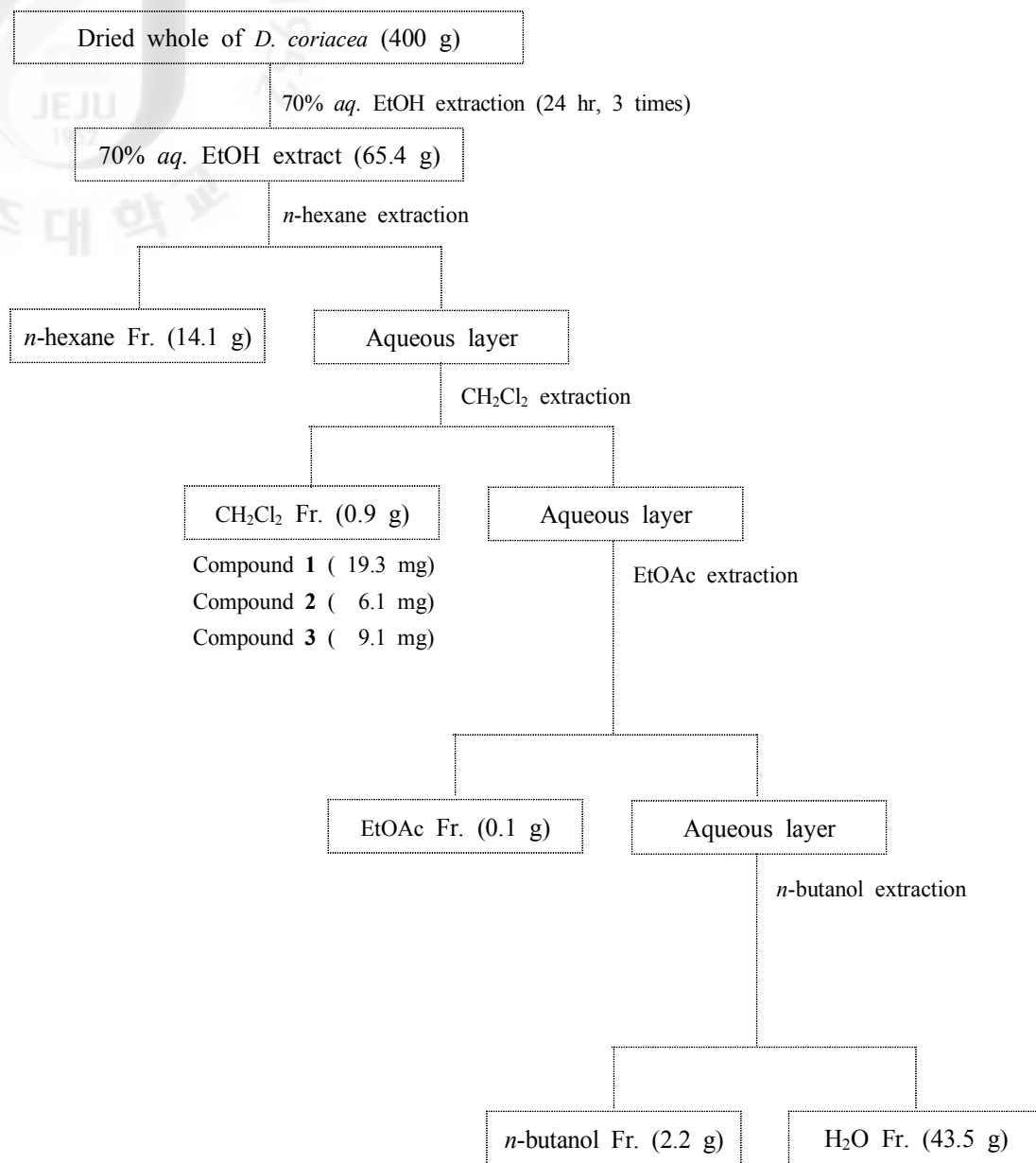
### 2-3. Isolation and purification

#### 2-3-1. Isolation produce of methylene chloride fraction (DM)

The methylene chloride fraction (870 mg) was chromatographed by VLC over silica gel eluting with stepwise gradient solvents of *n*-Hex/EtOAc (0 ~ 100%) and then EtOAc/MeOH (0 ~ 100%). A total of 7 fractions were collected (DM-I ~ VII). The fraction of DM-I was recrystallized to provide compound **1** (19.3 mg). The

fraction of DM-II to chromatography over silica gel using *n*-Hex/EtOAc (2/1) to provide 23 fractions, and DM-II-2 provided compound **2** (6.1 mg). The DM-V was chromatographed over silica gel CC with CH<sub>2</sub>Cl<sub>2</sub>/Me<sub>2</sub>CO (9/2) to provided 3 fractions (DM-V-1 ~ 3), and DM-V-2 provided compound **3** (9.1 mg) (Scheme 7).





Scheme 7. Extraction and fractionation of the whole of *D. coriacea*

### 3. Results

3-1. The structures of the compounds isolated from of *D. coriacea*

#### 3-1-1. Compound 1

- Compound Name D-mannitol
- Synonym(s) mannite, manno-hexitol, kurrine (obsol.), bronchitol
- CAS Registry Number 69-65-8
- Appearance white crystalline solid
- Chemical Formula  $C_6H_{14}O_6$
- Molecular Weight (g/mol) 182.2
- Melting Point ( $^{\circ}C$ ) 165 - 169
- $^{13}C$ -NMR (125 MHz,  $D_2O$  with  $CD_3OD$ )

$\delta$ : 72.0 (C-3, 4), 70.4 (C-2, 5), 64.4 (C-1, 6)

- Other data in the literature

Development Status: Granted orphan drug status by the FDA (2006) for the treatment of cystic fibrosi

Compound 1 was a white crystalline solid. The  $^1H$  and  $^{13}C$ -NMR spectra of compound 1 in  $D_2O$  with  $CD_3OD$  was showed general pattern of mono sugar (Fig. 148-149). By comparing all spectroscopic data with literature values, compound 1 was identified as D-mannitol (Fig. 150).<sup>125)</sup>

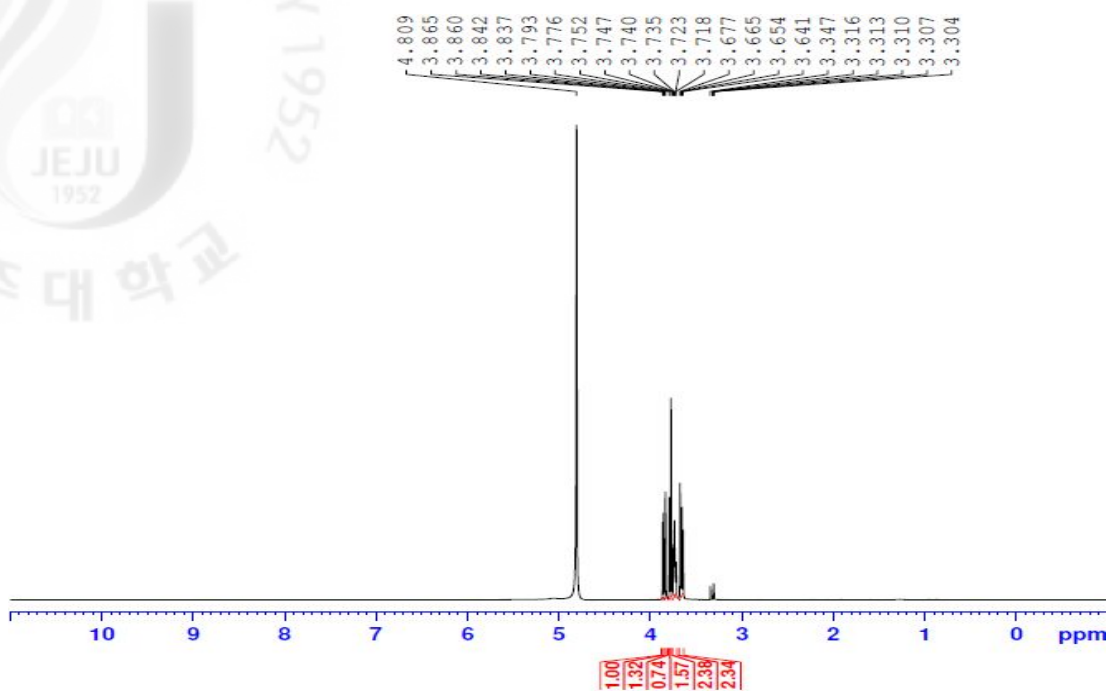


Figure 148.  $^1\text{H}$ -NMR spectrum of D-mannitol (**1**) in  $\text{D}_2\text{O}$  with  $\text{CD}_3\text{OD}$

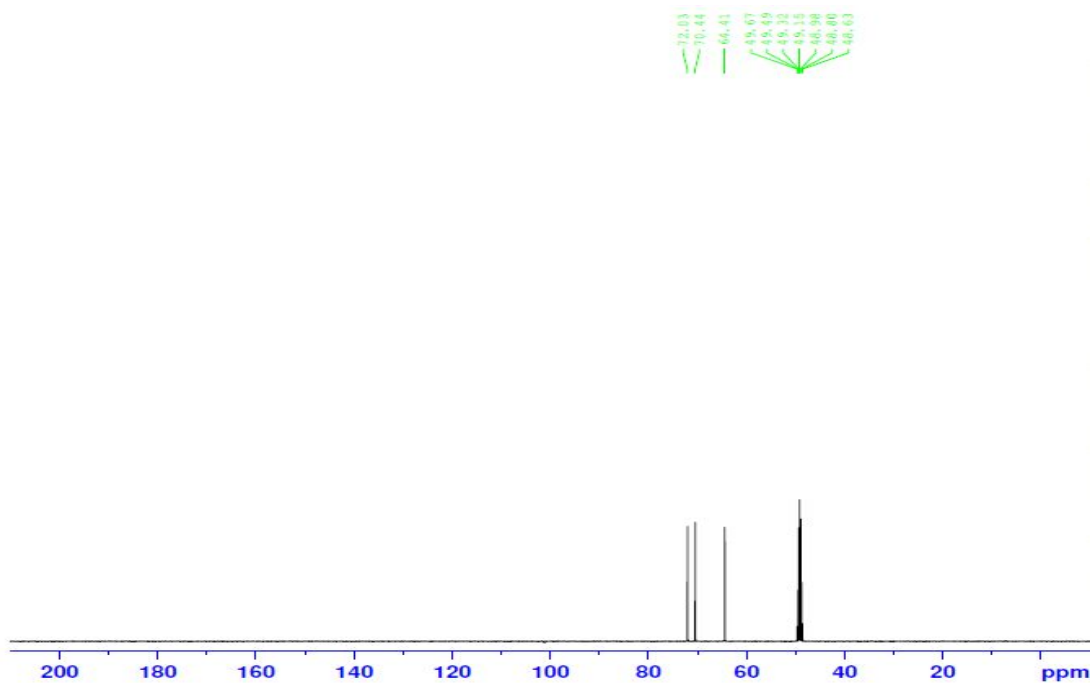


Figure 149.  $^{13}\text{C}$ -NMR spectrum of D-mannitol (**1**) in  $\text{D}_2\text{O}$  with  $\text{CD}_3\text{OD}$

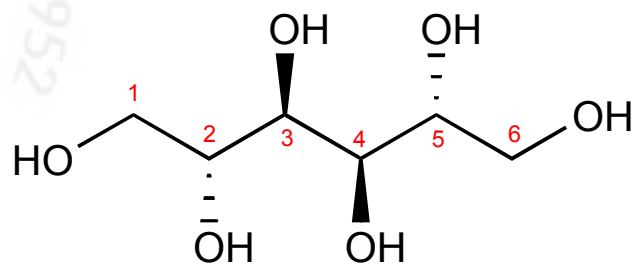


Figure 150. Structure of compound 1; D(-)mannitol

### 3-1-2. Compound 2

- Compound Name 1,9-dihydroxycrenulide
- Synonym(s) -
- CAS Registry Number -
- Appearance colorless oil
- Chemical Formula  $C_{20}H_{30}O_4$
- Molecular Weight (g/mol) 334.44
- Melting Point ( $^{\circ}C$ ) 114 - 115
- $^1H$ -NMR (500 MHz,  $CD_3OD$ )  
 $\delta$ : 5.95 (1H, *m*, H-18), 5.12 (1H, *m*, H-13), 4.32 (1H, *m*, H-4), 3.19 (1H, *d*,  $J = 9.5$  Hz, H-3), 2.03 (1H, *m*, H-10), 2.02 (2H, *m*, H-12a, 12b), 1.93 (1H, *m*, H-5b), 1.81 (1H, *m*, H-5a), 1.69 (3H, *s*, H-15), 1.61 (3H, *m*, H-16), 1.45 (1H, *m*, H-9), 1.28 (2H, *m*, H-11b, 6), 1.07 (1H, *m*, H-8b), 1.07 (3H, *d*,  $J = 6.5$  Hz, H-17), 1.01 (3H, *d*,  $J = 6.5$  Hz, H-20), 0.92 (1H, *m*, H-7), 0.28 (1H, *m*, H-8a)
- $^{13}C$ -NMR (125 MHz,  $CD_3OD$ )  
 $\delta$ : 173.6 (C-19), 167.4 (C-2), 134.3 (C-1), 133.2 (C-14), 125.1 (C-13), 98.3 (C-18), 70.9 (C-4), 50.8 (C-3), 49.7 (C-5), 37.4 (C-11), 33.6 (C-10), 29.7 (C-9), 27.3 (C-6), 26.5 (C-16), 26.0 (C-12), 24.1 (C-20), 17.8 (C-15), 17.5 (C-17), 11.2 (C-7), 9.34 (C-8)
- Biological activities in the literature  
anti-microbial
- Other data in the literature
  1. Biological Source: Occurs in brown algae (*Dilophus ligulatus*)

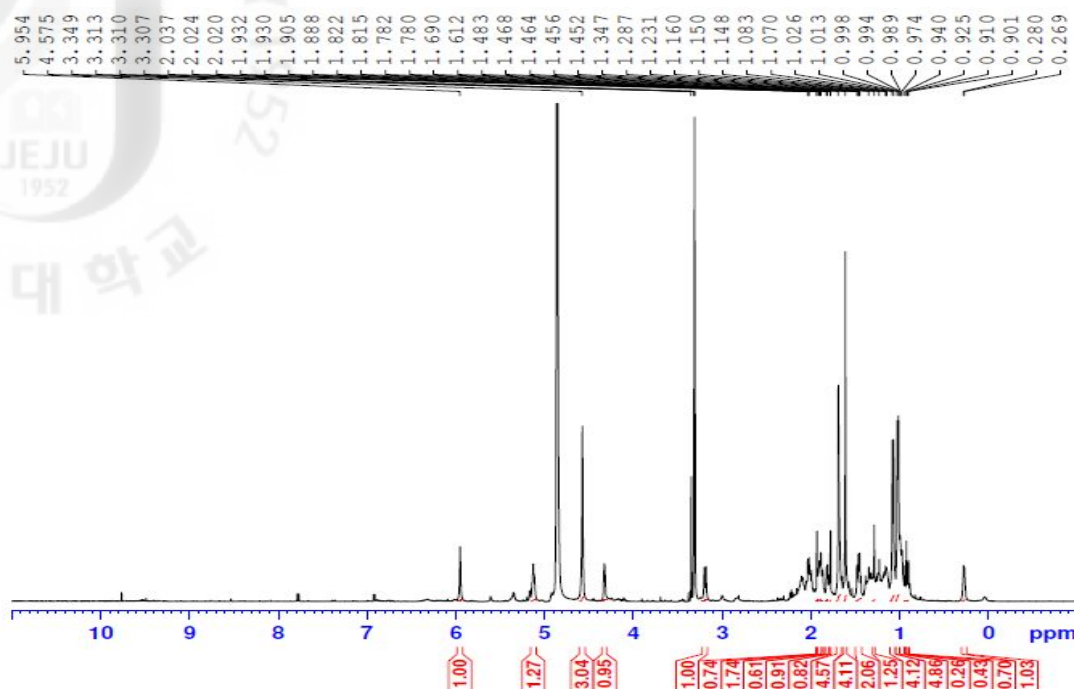


Figure 151.  $^1\text{H}$ -NMR spectrum of 1,9-dihydroxycrenulide (**2**) in  $\text{CD}_3\text{OD}$

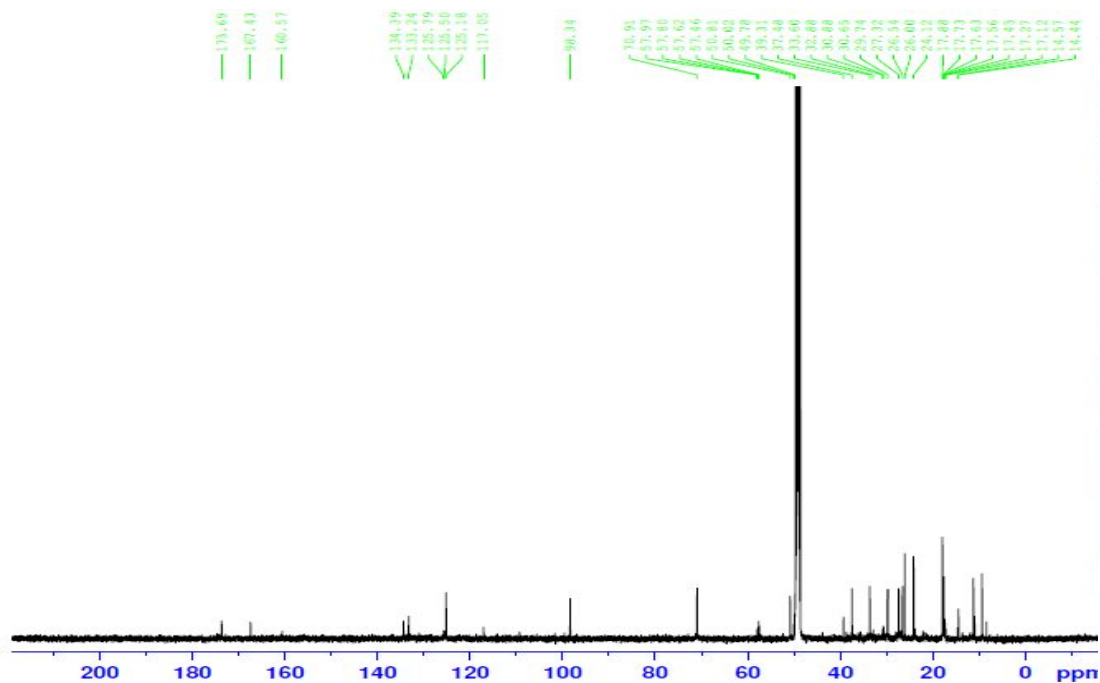


Figure 152.  $^{13}\text{C}$ -NMR spectrum of 1,9-dihydroxycrenulide (**2**) in  $\text{CD}_3\text{OD}$

Compound **2** was a colorless oil. The molecular formula of compound **2** was determined to be  $C_{20}H_{30}O_4$  based on NMR data. By analysis of the  $^1H$ -NMR spectrum in  $CD_3OD$  was showed at  $\delta_H$  5.95 (1H, *m*, H-18), suggested a  $\gamma$ -hydroxy- $\alpha,\beta$ -unsaturated  $\gamma$ -lactone. Base stabilizes the anion of the ring-opened hydroxy lactone. It was showed a cyclopropyl multiplet at  $\delta_H$  0.28 (1H, *m*, H-8a), two overlapping methyl doublets at  $\delta_H$  1.07 (3H, *d*,  $J = 6.5$  Hz, H-17), 1.01 (3H, *d*,  $J = 6.5$  Hz, H-20), two vinyl methyls at  $\delta_H$  1.69 (3H, *s*, H-15), 1.61 (3H, *m*, H-16), an olefinic triplet at  $\delta_H$  5.12 (1H, *m*, H-13), and two broad  $D_2O$ -exchangeable peaks as well as peaks at  $\delta_H$  5.95 (1H, *m*, H-18), 4.32 (1H, *m*, H-4) and 3.19 (1H, *d*,  $J = 9.5$  Hz, H-3) (Fig. 151). The  $^{13}C$ -NMR spectrum of compound **2** showed only twenty carbon signals, one ester carbonyl group at  $\delta_C$  173.6 (C-19) and five methyl group at  $\delta_C$  26.5 (C-16), 24.1 (C-20), 17.8 (C-15), 17.5 (C-17) with two olefinic group at  $\delta_C$  167.4 (C-2), 134.3 (C-1), 133.2 (C-14), 125.1 (C-13) (Fig. 152). Thus, the structure of compound **3** was determined as 1,9-dihydroxycrenulide by comparison of its spectral data with those in the literature (Fig. 153).<sup>126,127</sup> 1,9-dihydroxycrenulide was reported for the first time from this plant.

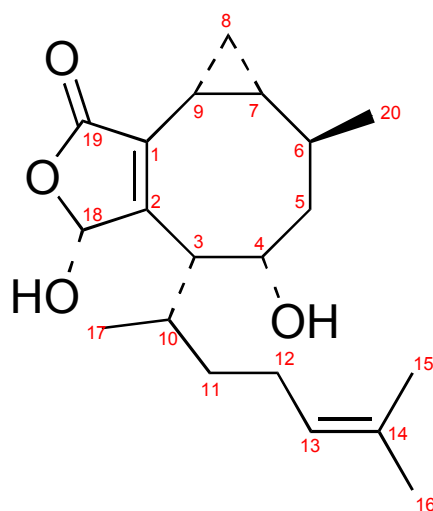


Figure 153. Structure of compound **2**; 1,9-dihydroxycrenulide

### 3-1-3. Compound 3

- Compound Name loliolide
- Synonym(s) 5,6,7,7*a*-tetrahydro-6-hydroxy-4,4,7*a*-trimethyl-2(4*H*)-benzofuranone, digiprolactone, calendin
- CAS Registry Number 5989-02-6
- Appearance Needles
- Chemical Formula  $C_{11}H_{16}O_3$
- Molecular Weight (g/mol) 196.24
- Melting Point ( $^{\circ}C$ ) 152.5 - 153
- $^1H$ -NMR (500 MHz,  $CD_3OD$ )  
 $\delta$ : 5.78 (1H, *s*, H-3), 4.10 (1H, *q*,  $J = 8.5, 4.0$  Hz, H-6), 2.47 (1H, *dt*,  $J = 11.5, 3.5, 2.0$  Hz, H-7*a*), 2.00 (1H, *dt*,  $J = 12.5, 3.2, 2.0$  Hz, H-5*a*), 1.59 (3H, *s*, 7*a*-Me), 1.42 (1H, *t*,  $J = 11.5$  Hz, H-5 $\beta$ ), 1.31, 1.28 (each 3H, *s*, 4-Me), 1.26 (1H, *m*, H-7 $\beta$ )
- $^{13}C$ -NMR (125 MHz,  $CD_3OD$ )  
 $\delta$ : 184.1 (C-3*a*), 174.2 (C-2), 113.9 (C-3), 88.7 (C-7*a*), 65.4 (C-6), 50.8 (C-5), 48.6 (C-7), 36.3 (C-4), 30.5, 25.4 (4-Me), 25.9 (7*a*-Me)
- Biological activities in the literature  
germination inhibitor, cytostatic against carcinoma, leukaemia cells, ants repellent
- Other datas in the literature
  1. UV (EtOH)  $\lambda_{max}nm$ : 214 and 217
  2. Optical Isomer : (6*S*,7*aR*) - form
  3. Optical Rotation :  $[\alpha]_D^{20} = -107.2$  ( $c$  1 in  $CHCl_3$ )



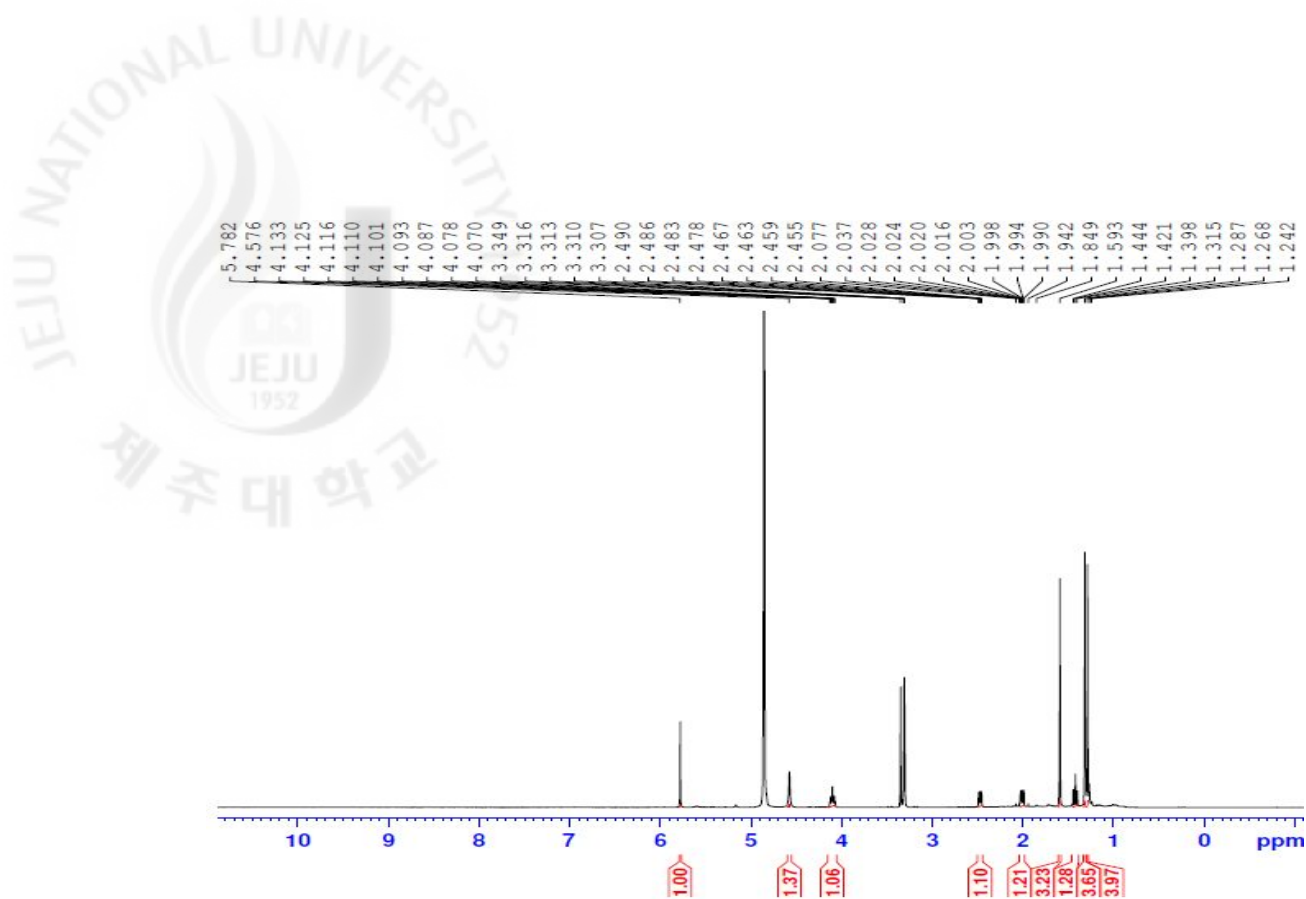


Figure 154.  $^1\text{H-NMR}$  spectrum of loliolide (3) in  $\text{CD}_3\text{OD}$

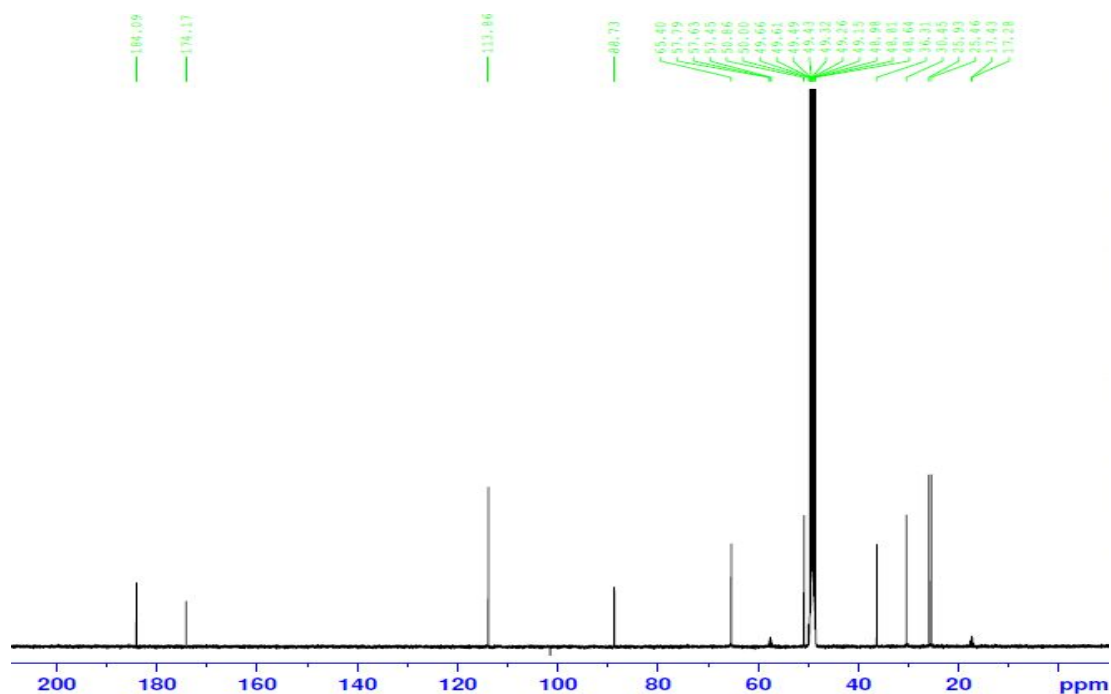


Figure 155.  $^{13}\text{C-NMR}$  spectrum of loliolide (3) in  $\text{CD}_3\text{OD}$

Compound **3** was a shape of needles. The molecular formula of compound **3** was determined to be  $C_{11}H_{16}O_3$  based on NMR data. Analysis of the  $^1H$ -NMR spectrum of compound **3** in  $CD_3OD$  exhibited signals for three methyl groups at  $\delta_H$  1.31, 1.28 (each 3H, *s*, 4-Me), 1.59 (1H, *s*, H-7aMe) attached to quaternary carbons, a vinylic proton  $\delta_H$  5.78 (1H, *s*, H-3) in a *tri*-substituted double bond, a carbinol proton  $\delta_H$  4.10 (1H, *q*,  $J = 8.5, 4.0$  Hz, H-6) (Fig. 154). Similarly, the  $^{13}C$ -NMR spectrum of compound **3** revealed the presence of three oxygen-bearing carbons at  $\delta_C$  184.1 (C-3 *a*) 88.7 (C-7 *a*) and 65.4 (C-6) this indicated the presence of an ester, or lactone, and a secondary alcohol in the structure of compound **3** (Fig. 155). On the basis of this data, the four unsaturation sites implied by the molecular formula could be explained by a bicyclic structure having an  $\alpha, \beta$ -unsaturated- $\gamma$ -lactone ring. Thus, the structure of compound **3** was determined as loliolide by comparison of its spectral data with those in the literature (Fig. 156).<sup>128,129</sup> Loliolide was reported for the first time from this plant.

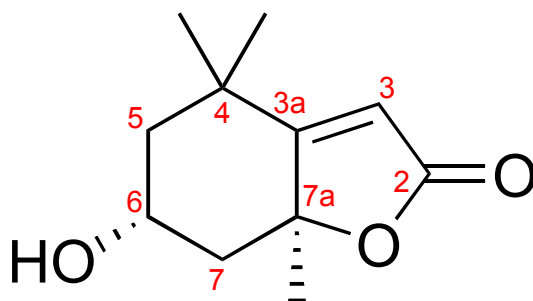


Figure 156. Structure of compound **3**; Loliolide (calendin)

## 3-2. Biological activities

### 3-2-1. Antioxidant activity

#### 3-2-1-1. Free radical scavenging activity of the solvent fractions

Antioxidative activity was determined by 3 types of free radical scavenging activity assay. The DPPH radical scavenging activity of the crude 70% *aq.* EtOH extract and its solvent fractions of *D. coriaceas* is shown in Table 23. It showed that the 70% *aq.* EtOH extract and its solvent fractions did not any good scavenging in 1000  $\mu\text{g/mL}$  concentration. Among them, *n*-Hex and EtOAc solvent fractions exhibited higher superoxide radical scavenging activity compared to other solvent extracts showing dose-dependent manner. However, its also did not show remarkably good activity than the Allopurinol ( $\text{RC}_{50} = 2.1 \mu\text{g/mL}$ ) excepted the lower concentration at  $\text{RC}_{50} = 737.4$  and  $352.1 \mu\text{g/mL}$ . As same results, the xanthine oxidase inhibitory activity of the 70% *aq.* EtOH extract and its solvent fractions showed in Table 23. All solvent fractions did not show strongly enzyme inhibitory activity in concentration of 0 to 1000  $\mu\text{g/mL}$  compared to positive control (Allopurinol,  $\text{IC}_{50} = 12.2 \mu\text{g/mL}$ ) (Tab. 23). These results showed that as to the 70% *aq.* EtOH extract and its solvent fractions of *D. coriacea*, the activity confirmed the none for antioxidant activity.

Table 23. Free radical scavenging effect of the solvent fractions

Samples	RC <sub>50</sub> (µg/mL)		
	DPPH radical scavenging activity	Xanthine oxidase inhibitory activity	Superoxide radical scavenging activity
70% <i>aq.</i> EtOH ext.	> 1000	> 1000	632.7
<i>n</i> -Hex Fr.	> 1000	> 1000	737.4
EtOAc Fr.	> 1000	> 1000	352.1
<i>n</i> -BuOH Fr.	> 1000	> 1000	> 1000
H <sub>2</sub> O Fr.	> 1000	> 1000	> 1000
Positive control (BHA) <sup>1)</sup>	5.9 ± 0.49	N/A	N/A
Positive control (Allopurinol)	N/A	12.2 ± 2.80	2.11 ± 0.91

Primarily radical scavenging activity was determined at 0 to 1000 µg/mL concentration of samples. Scavenging concentration for 50% of free radical (RC<sub>50</sub>) was calculated from logarithmic regression equation obtained from the values of at least five dilutions of the primary concentration. Values represent mean ± SDs (n = 3); in parentheses is RC<sub>50</sub> value of respective sample

N/A. not assay; BHA. butylated hydroxyanisole<sup>1)</sup>; >. out of range

### 3-2-2. Anti-inflammation activity

#### 3-2-2-1. Effect on cell viability and LPS-induced NO production

This study examined the suppressive effects of the 70% *aq.* EtOH extract with solvent fractions and isolated compounds from *D. coriacea* on LPS-induced NO production at 0 to 100  $\mu\text{g/mL}$  concentrations. The RAW264.7 cells were cultured in the presence at the concentrations of 12.5, 25, 50 and 100  $\mu\text{g/mL}$ . After treatment, cell viability was measured by MTT assay and expressed as % cell viability compared with the control group. Among them, *n*-Hex fraction significantly reduced the cell viability of RAW264.7 cells. All samples at 12.5  $\mu\text{g/mL}$  for 18 hr inhibited the cell viability by 63.7% (Data did not shown). These results should be confirmed that *n*-Hex fraction showed strong toxicity on RAW264.7 cells at lower concentration.

We tried to effects on LPS-induced NO production of solvent fractions. As results of Table. 24, *n*-Hex and EtOAc fractions significantly inhibited NO production activity compared to other solvent fractions showing by  $\text{IC}_{50} = 41.4$  and  $39.5 \mu\text{g/mL}$ . However, *n*-Hex fraction showed strong toxicity in RAW264.7 cells at 12.5  $\mu\text{g/mL}$  concentration (Data did not shown). Therefore, the effect on LPS-induced NO production of *n*-Hex fraction considered as the suppression by the cytotoxicity of RAW264.7 cells.

Table 24. Cell viability and effects of the solvent fractions on the production of nitric oxide in LPS-stimulated RAW264.7 cells

Samples	Anti-inflammatory activity		
	TC <sub>50</sub> <sup>1)</sup> (μg/mL)	IC <sub>50</sub> <sup>2)</sup> (μg/mL)	Selectivity index <sup>3)</sup>
70% <i>aq.</i> EtOH ext.	> 100	49.0	> 2.04
<i>n</i> -Hex Fr.	> 100	41.4	> 2.41
EtOAc Fr.	> 100	39.5	> 2.53
<i>n</i> -BuOH Fr.	> 100	> 100	> 1.00
H <sub>2</sub> O Fr.	> 100	> 100	> 1.00

Primarily, It was determined at 0 to 100 μg/mL concentration of samples. Inhibition concentration for 50% of NO production (IC<sub>50</sub>) was calculated from logarithmic regression equation obtained from the values of at least five dilutions of the primary concentration. Values represent mean ± SDs (n = 3); in parentheses is IC<sub>50</sub> value of respective sample

N/A. not assay; >. out of range

<sup>1)</sup> TC<sub>50</sub> is the concentration producing 50% toxicity in RAW264.7 cells.

<sup>2)</sup> IC<sub>50</sub> is the concentration producing 50% inhibition of NO production in RAW264.7 cells.

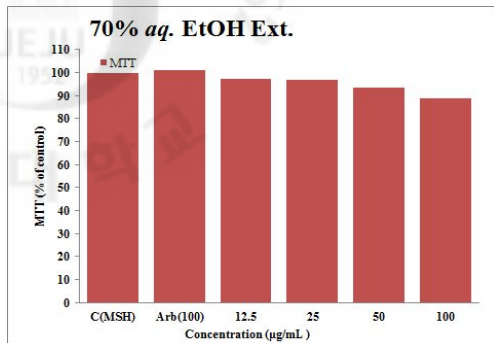
<sup>3)</sup> Selectivity Index = TC<sub>50</sub> / IC<sub>50</sub>

### 3-2-3. Melanogenesis inhibition activity

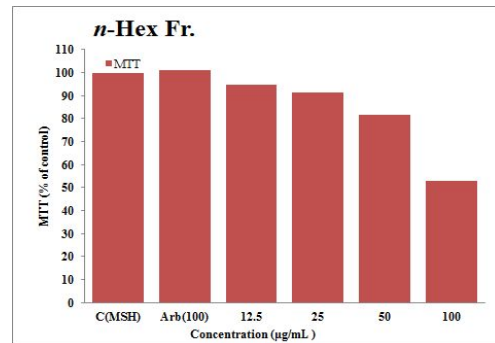
#### 3-2-3-1. Cell viability in B16F10 melanoma cell

The cell viability rates of *D. coriacea* examined in B16F10 melanoma cells respectively treated with 0, 12.5, 25, 50 and 100  $\mu\text{g/mL}$  concentration of the 70% *aq.* EtOH extract and its five solvent fractions. In the concentration less than 50  $\mu\text{g/mL}$ , all samples did not exhibit any kind of toxicity on the B16F10 cells (Fig. 157). Also, B16F10 melanoma cells were treated by 1,9-dihydroxycrenulide (**2**) and loliolide (**3**) for cell viability rate. They also did not affect the cell viability at the concentration of 30  $\mu\text{g/mL}$  on MTT assay (Fig. 158).

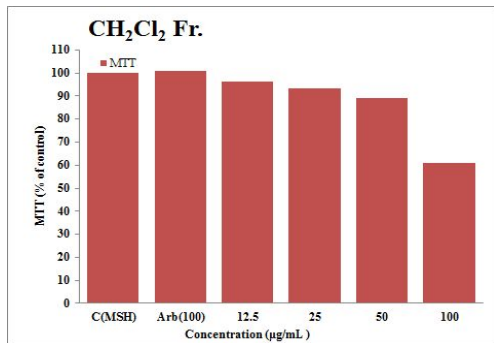
(A)



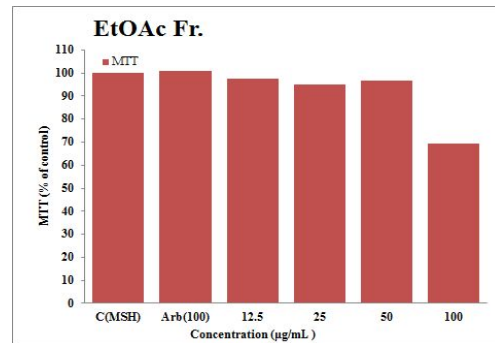
(B)



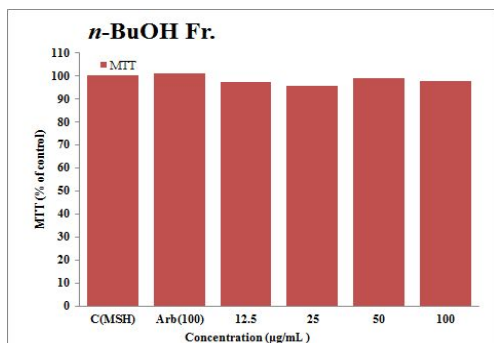
(C)



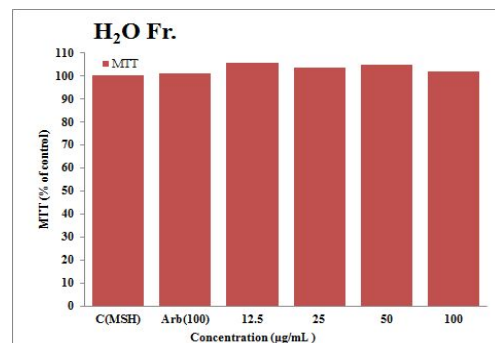
(D)



(E)



(F)



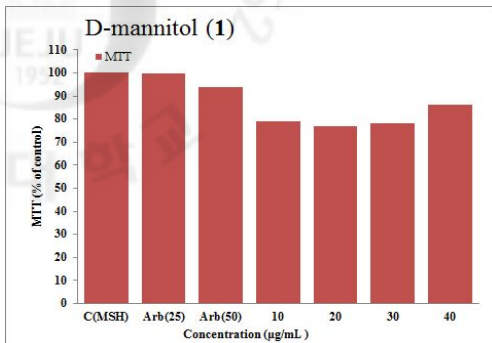
Values are mean ± SD of 3 replicates

(A) 70% aq. EtOH Ext. (B) *n*-Hex Fr. (C) CH<sub>2</sub>Cl<sub>2</sub> Fr. (D) EtOAc Fr. (E) *n*-BuOH Fr. (F) H<sub>2</sub>O Fr.

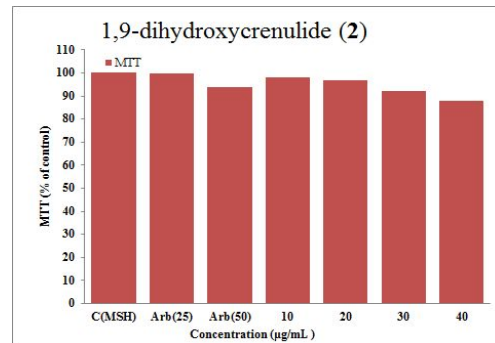
Figure 157. Cell viability on B16F10 cells treated with the solvent fractions



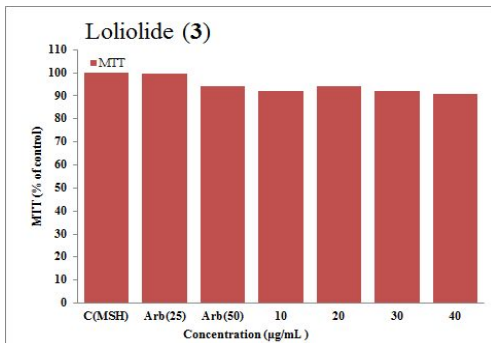
(A)



(B)



(C)



Values are mean  $\pm$  SD of 3 replicates

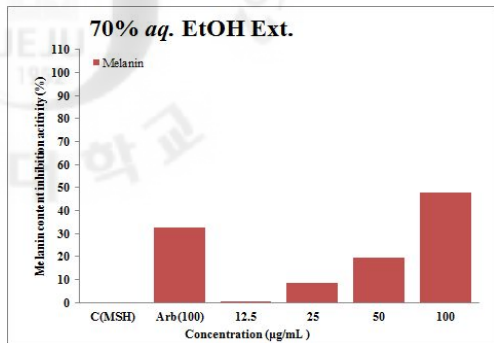
(A) D-mannitol (B) 1,9-dihydroxycrenulide (C) Loliolide

Figure 158. Cell viability on B16F10 cells treated with the isolated compounds

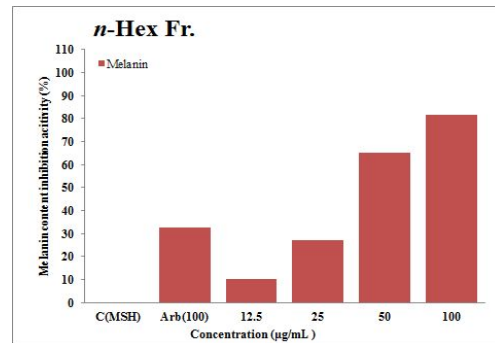
### 3-2-3-2. Effect on melanogenesis in B16F10 cells

We examined the effect of melanin contents inhibitory activity using B16F10 melanoma cells. As shown in Figure 159, the crude 70% *aq.* EtOH extract and fractions showed melanin contents inhibitory activity in a dose-dependent manner. In comparison with the positive control group, the melanin contents of EtOAc fraction were significantly reduced by 34.6% at 50  $\mu\text{g/mL}$  (Fig. 159). And 1,9-dihydroxycrenulide (**2**) and loliolide (**3**) showed melanin contents inhibitory activity in a dose-dependent manner at 30  $\mu\text{g/mL}$  concentration by 27.8 and 22.6% (Fig. 160). Respectively, while the melanin contents value of reference compound, in the arbutin was 50  $\mu\text{g/mL}$ . To treated group the contents of melanin was also significantly reduced by 21.3% (Fig. 160). 1,9-dihydroxycrenulide (**2**) and loliolide (**3**) had more potent melanin contents inhibitory activity compared to arbutin.

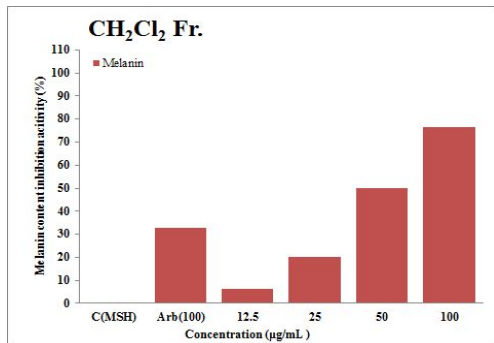
(A)



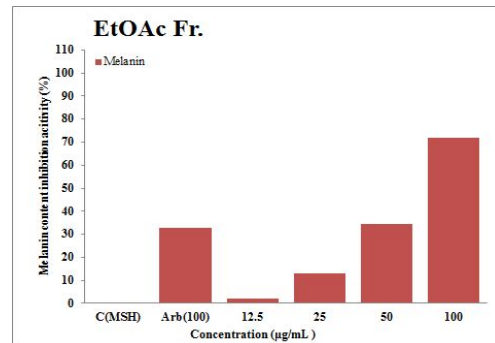
(B)



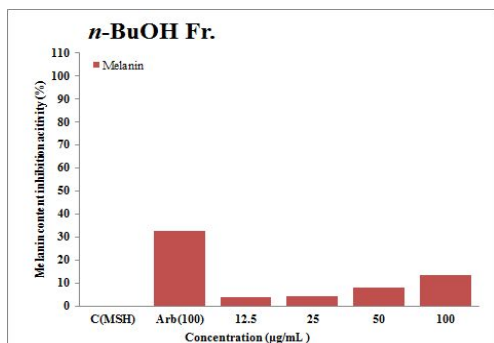
(C)



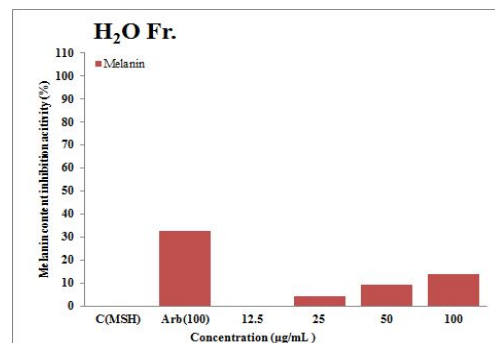
(D)



(E)



(F)

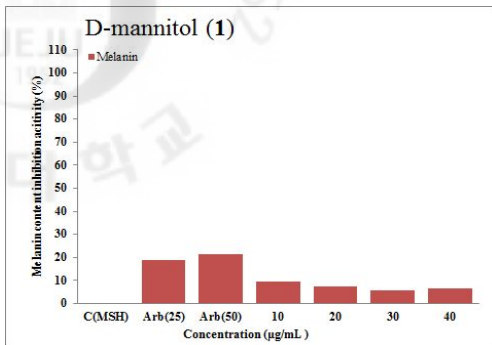


Values are mean  $\pm$  SD of 3 replicates

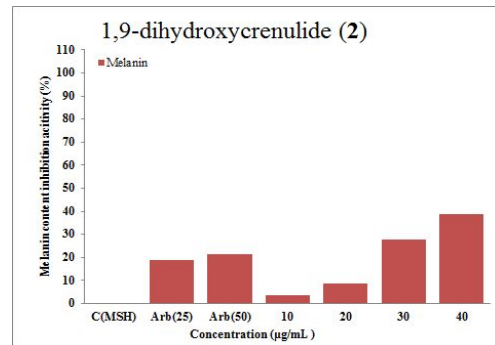
(A) 70% aq. EtOH Ext. (B) *n*-Hex Fr. (C) CH<sub>2</sub>Cl<sub>2</sub> Fr. (D) EtOAc Fr. (E) *n*-BuOH Fr. (F) H<sub>2</sub>O Fr.

Figure 159. Melanin contents inhibitory activity of the solvent fractions on B16F10 cells

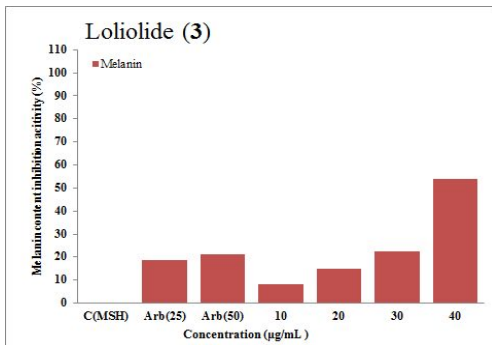
(A)



(B)



(C)



Values are mean  $\pm$  SD of 3 replicates

(A) D-mannitol (B) 1,9-dihydroxycrenulide (C) Loliolide

Figure 160. Melanin contents inhibitory activity of the isolated compounds on B16F10 cells

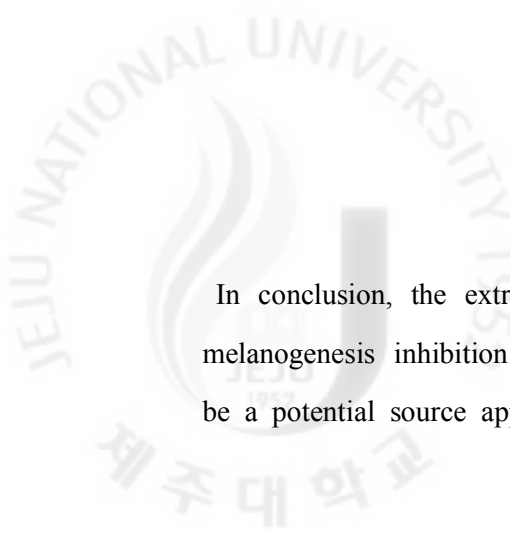
#### 4. Discussion

In this study, *D. coriacea* was evaluated for the activities on melanogenesis inhibition activity. The active constituents were identified following activity-guided isolation with chromatography.

1. The dried whole of *D. coriacea* was extracted with 70% *aq.* EtOH at room temperature. This extract was partitioned successively into five solvent fractions. These fractions were tested for their inhibitory effects;
  - DPPH and superoxide radical scavenging activity test, xanthine oxidase inhibition activity test for the antioxidant activity
  - The effect of LPS-induced NO production on RAW264.7 cell for the anti-inflammatory activity
  - The effect of melanin contents inhibitory activity on B16F10 cells for the melanogenesis inhibition activity

As the CH<sub>2</sub>Cl<sub>2</sub> solvent fraction indicated good activity, this fraction was investigated extensively to find activities compounds.

2. The CH<sub>2</sub>Cl<sub>2</sub> solvent fraction of *D. coriacea* was subjected to a series of chromatographic separations and led to the isolation of three compounds. The structures of three known compounds were determined by the spectroscopic methods (UV/VIS, 1D - 2D NMR).
  - D(-)mannitol (1), 1,9-dihydroxycrenulide (2), Loliolide (3)
3. In melanogenesis inhibition activity studies 1,9-dihydroxycrenulide (2) and loliolide (3) exhibited good activity of considerable melanin contents inhibitory activity at 30 µg/mL concentration, 27.8 and 22.6% compared to positive control (Arbutin was at 50 µg/mL by 21.3% inhibition activity).



In conclusion, the extracts and isolated compounds from *D. coriacea* provided the melanogenesis inhibition activity. Due to these biological activities, this plant could be a potential source applicable as the whitening cosmetics material.

### III. RESEARCH 6 : *Styrax obassia* Siebold & Zucc

#### 1. General Plants Information

- **Scientific name** *Styrax obassia* Siebold & Zucc
- **Korean name** 쪽동백나무
- **Nickname** 물박달나무, 산아주까리나무, 녹축낭 (Jeju)
- **Family name** Styracaceae
- **Distribution** Korea, Japan, China
- **Flowering** May - June
- **Fruiting** September
- **Usage** furniture, landscape, spice, reserved timber<sup>130,135)</sup>
- **Folk medicinal use**

Remove boil, expectorant, throats, toothache

- **Identified constituents in the literature**

Benzofuran, demethoxy-egonol<sup>131-133)</sup>

- **Biological activities in the literature**

-

- **Research objective**

Standard material : 70% aq. EtOH extract of *S. obassia*

For ingredient of cosmeceutical (sliming product)

1. Anti-obesity activity

- yeast  $\alpha$ -glucosidase inhibition activity ( $IC_{50} = 59.4 \mu\text{g/mL}$ )
- In 100  $\mu\text{g/mL}$ , the 80.5% lipid accumulation reduction on 3T3-L1 preadipocytes (the cytotoxin none)



Photo 22. The specimen of *S. obassia*



Photo 23. Photograph of the whole plant of *S. obassia*



Photo 24. Photograph of the leave of *S. obassia*



Photo 25. Photograph of the flower of *S. obassia*



## 2. Experimental Methods

### 2-1. Plant material

The *S. obassia* was collected from the Jeju Island, in October 2005. A voucher specimen (04-73) was deposited at Extract bank of Bio-Conversion Center, Jejutechnopark (JTP), Jeju, Korea.

### 2-2. Solvent fraction of the leaves

The fresh leaves of *S. obassia* was washed and dried by hot blast at 40 °C for three days. The powder of leave (100 g) was extracted with 70% *aq.* ethanol in glass jar at room temperature under stirring for three days. The extract was filtered to remove the insoluble residue and filtrated was concentrated to afford a gummy residue (24.2 g). A part of the residue (20 g) was suspended in water, and successively partitioned to give *n*-hexane (0.7 g), methylene chloride (1.7 g), ethyl acetate (0.9 g), *n*-butanol (3.4 g) and water (6.2 g) fractions (Scheme 8).

### 2-3. Isolation and purification

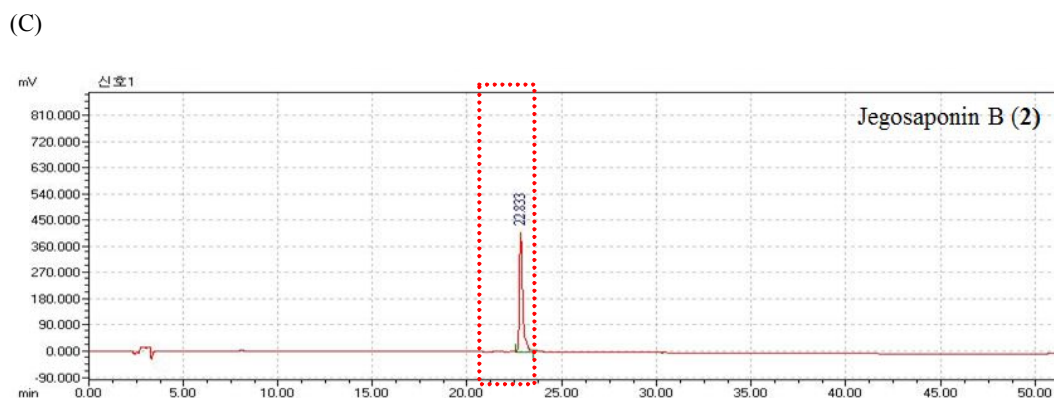
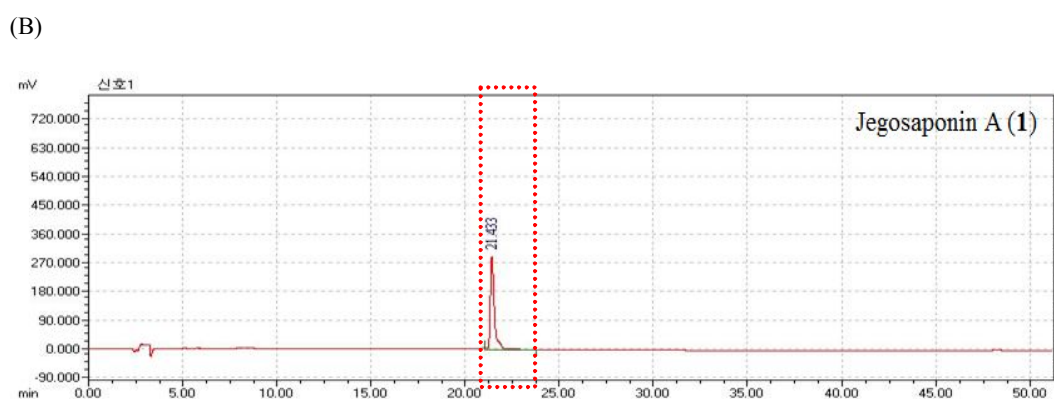
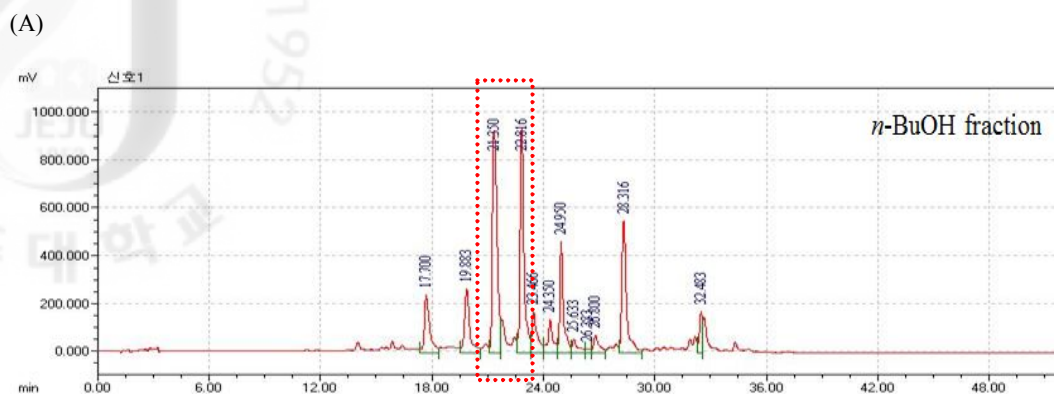
#### 2-3-1. Isolation produce of *n*-butanol fraction from *S. obassia* (SB)

The *n*-BuOH fraction (3.4 g) was chromatographed over reverse phase silica gel eluting with stepwise gradient solvents of H<sub>2</sub>O/MeOH (0 ~ 100%). A total of five fractions were collected (SB-I ~ V) from *n*-BuOH fraction of *S. obassia*. The fraction of SB-V was further purified using prep-LC system equipped with ODS column using solvent system as described in Table 25 (Scheme 8).

Table 25. Gradient elution condition for prep-HPLC separation

Time (min)	Flow (mL/min)	(%) A <sup>(1)</sup>	(%) B <sup>(1)</sup>	Curve
	1.0	100	0	6
3.0	1.0	100	0	6
7.7	1.0	75	25	6
10.0	1.0	75	25	6
15.4	1.0	50	50	6
19.0	1.0	50	50	6
23.1	1.0	25	75	6
27.0	1.0	25	75	6
30.8	1.0	0	100	6

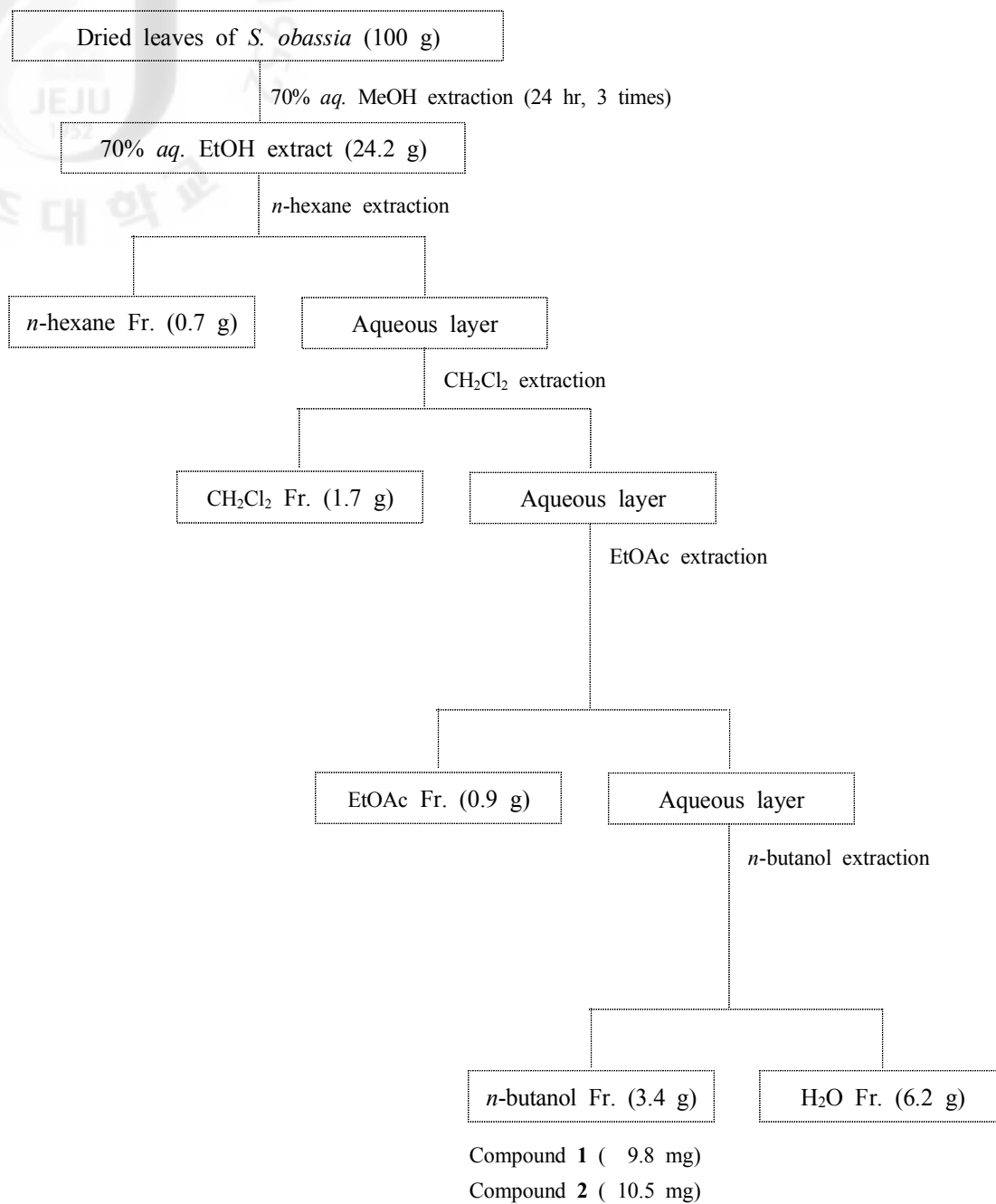
As in the Figure 161-(a), preparative HPLC chromatogram of SB-V. The compounds at retention time of 21.4 min. (SB-V-1) and 22.8 min. (SB-V-2) were isolate the saponins of *S. obassia* provide compound **1** (9.8 mg) (Fig. 161-(b)) and compound **2** (10.5 mg) (Fig. 161-(c)) and the structures were elucidated using spectral analysis including UV, 1D and 2D NMR. Similarly, SB-V containing mixtures of saponins was separated by HPLC using ODS column shows the analytical HPLC separation of the saponins SB-V-1 and SB-V-2 which after preparative scale up was used to isolate the major saponin fractions. The two major peaks at retention time of 21.4 (compound **1**) and 22.8 (compound **2**) min were isolated (Fig. 161).



Column : Sun-fire prep C<sub>18</sub> column 250 × 100 mm, I.D. 5 μm (Waters Co. Ltd. USA); mobile phase 30% ACN in 50 mM KH<sub>2</sub>PO<sub>4</sub> (A), 65% ACN in 50 mM KH<sub>2</sub>PO<sub>4</sub> (B); flow rate : 1.0 mL/min; Detection: UV at 210 nm; Injection vol.: 250 μL

(A) HPLC chromatogram of *n*-BuOH fraction; (B) Isolated Jegosaponin A (1); (C) Isolated Jegosaponin B (2)

Figure 161. Prep-HPLC isolation of compound 1 and 2 of SB-V isolated from *n*-BuOH fraction



Scheme 8. Extraction and fractionation of the leaves of *S. obassia*

### 3. Results

3-1. The structures of the compounds isolated from of *S. obassia*

#### 3-1-1. Compound 1

- Compound Name 12-Oleanene-3,16,21,22,28-pentol; (3 $\beta$ ,16 $\alpha$ ,21 $\beta$ ,22 $\alpha$ )-form, 21-tigloyl, 22-Ac, 3-*O*-[ $\alpha$ -L-rhamnopyranosyl-(1 $\rightarrow$ 2)- $\beta$ -D-galactopyranosyl-(1 $\rightarrow$ 3)-[ $\beta$ -D-glucopyranosyl-(1 $\rightarrow$ 2)]- $\beta$ -D-glucuronopyranoside]
- Synonym(s) Jegosaponin A
- CAS Registry Number -
- Appearance needles
- Chemical Formula C<sub>61</sub>H<sub>96</sub>O<sub>27</sub>
- Molecular Weight (g/mol) 1260
- Melting Point (°C) 246 - 248
- <sup>1</sup>H-NMR (500 MHz, CD<sub>3</sub>OD)

$\delta$ : 7.11 (1H, *q*, *J* = 7.2 Hz, H-3'), 6.43 (1H, *d*, *J* = 10.2 Hz, H-21), 6.10 (1H, *d*, *J* = 10.2 Hz, H-22), 6.03 (1H, *brs*, Rha-1), 5.97 (1H, *d*, *J* = 7.7 Hz, Gal-1), 5.63 (1H, *d*, *J* = 7.1 Hz, Glc-1), 5.50 (1H, *m*, H-12), 4.78 (1H, *d*, *J* = 8.0 Hz, GlcA-1), 4.63 (1H, *dd*, *J* = 9.1, 8.8 Hz, GlcA-3), 4.56 (1H, *dd*, *J* = 8.8, 8.0 Hz, GlcA-2), 4.52 (1H, *dd*, *J* = 8.5, 7.7 Hz, Gal-2), 4.44 (1H, *m*, H-16), 3.37, 3.61 (2H, *d*, *J* = 10.9, H-28), 3.29 (1H, *dd*, *J* = 11.5, 4.0 Hz, H-3), 3.01 (1H, *dd*, *J* = 13.5, 4.0 Hz, H-18), 2.03 (H, *s*, Ac-1), 2.02 (3H, *s*, H-5'), 1.83 (3H, *d*, *J* = 7.2 Hz, H-4'), 1.82 (3H, *s*, H-27), 1.44 (3H, *d*, *J* = 6.0 Hz, Rha-6), 1.34 (3H, *s*, H-30), 1.20 (3H, *s*, H-23), 1.10 (3H, *s*, H-29), 1.09 (3H, *s*, H-24), 0.99 (3H, *s*, H-26), 0.96 (3H, *s*, H-25)

• <sup>13</sup>C-NMR (125 MHz, CD<sub>3</sub>OD)

δ: 172.2 (GlcA-6), 171.1 (Ac-1), 168.1 (C-1'), 142.9 (C-13), 137.1 (C-3'), 129.6 (C-2'), 124.7 (C-12), 105.8 (GlcA-1), 102.8 (Glc-1), 102.3 (Rha-1), 101.2 (Gal-1), 90.3 (C-3), 81.7 (GlcA-3), 79.7 (C-21), 79.1 (GlcA-2), 78.3 (Glc-3), 77.2 (Gal-5), 77.0 (GlcA-5), 76.4 (Glc-2), 76.2 (Gal-2), 76.2 (Gal-3), 74.6 (C-22), 73.9 (Rha-4), 72.8 (Rha-2), 72.8 (Glc-4), 72.6 (Rha-3), 71.9 (GlcA-4), 71.6 (Gal-4), 70.1 (Rha-5), 68.4 (C-16), 63.9 (C-28), 63.8 (Glc-6), 62.6 (Gal-6), 56.0 (C-5), 48.3 (C-17), 47.5 (C-19), 47.2 (C-9), 42.0 (C-14), 40.4 (C-8), 40.4 (C-18), 40.1 (C-4), 39.2 (C-1), 37.1 (C-10), 36.8 (C-20), 35.0 (C-15), 33.5 (C-7), 29.9 (C-29), 28.2 (C-23), 27.9 (C-27), 26.8 (C-2), 24.3 (C-11), 21.3 (C-2'), 20.6 (C-30), 18.9 (C-6), 18.4 (Rha-6), 17.3 (C-26), 17.1 (C-24), 16.1 (C-25), 14.7 (C-4'), 12.9 (C-5')

• Biological activities in the literature

antisweet

• Other data in the literature

1. HR-FAB MS:  $m/z$  1259.3908 [M-H]<sup>-</sup> (calcd. for C<sub>61</sub>H<sub>96</sub>O<sub>27</sub> 1259.6061, Δ - 0.2 mamu)
2. IR (film) cm<sup>-1</sup>: 3400 (*br*), 1730 (*br*), 1660, 1245, 1160
3. Optical Rotation:  $[\alpha]_D^{25} = -24.6^\circ$  (*c* 1.1, MeOH)

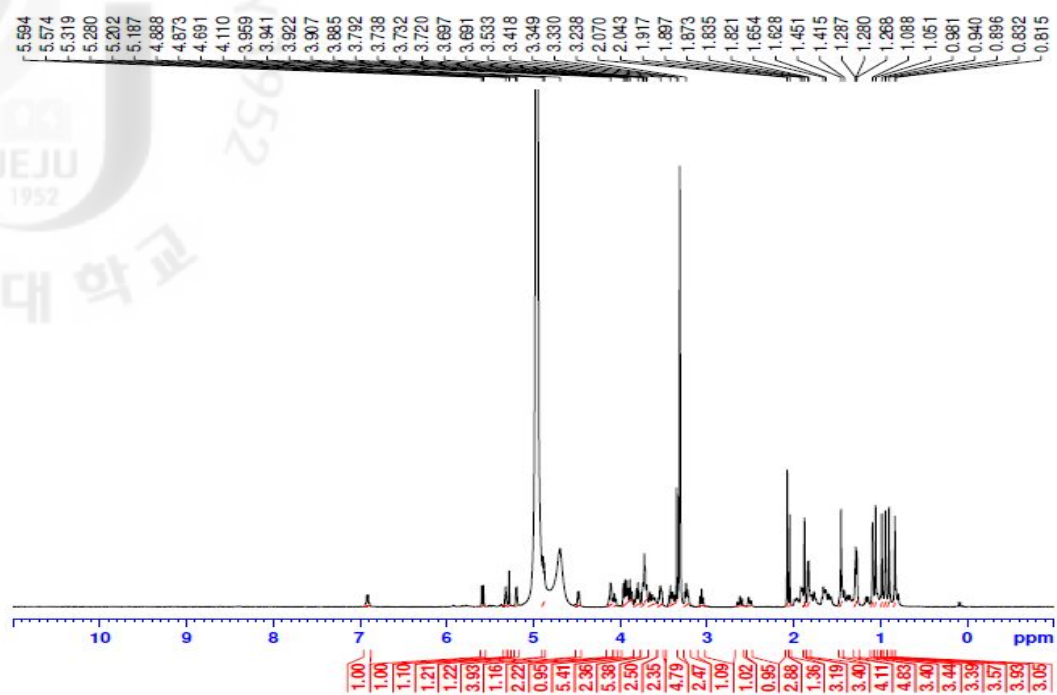


Figure 162.  $^1\text{H}$ -NMR spectrum of Jegosaponin A (**1**) in  $\text{CD}_3\text{OD}$

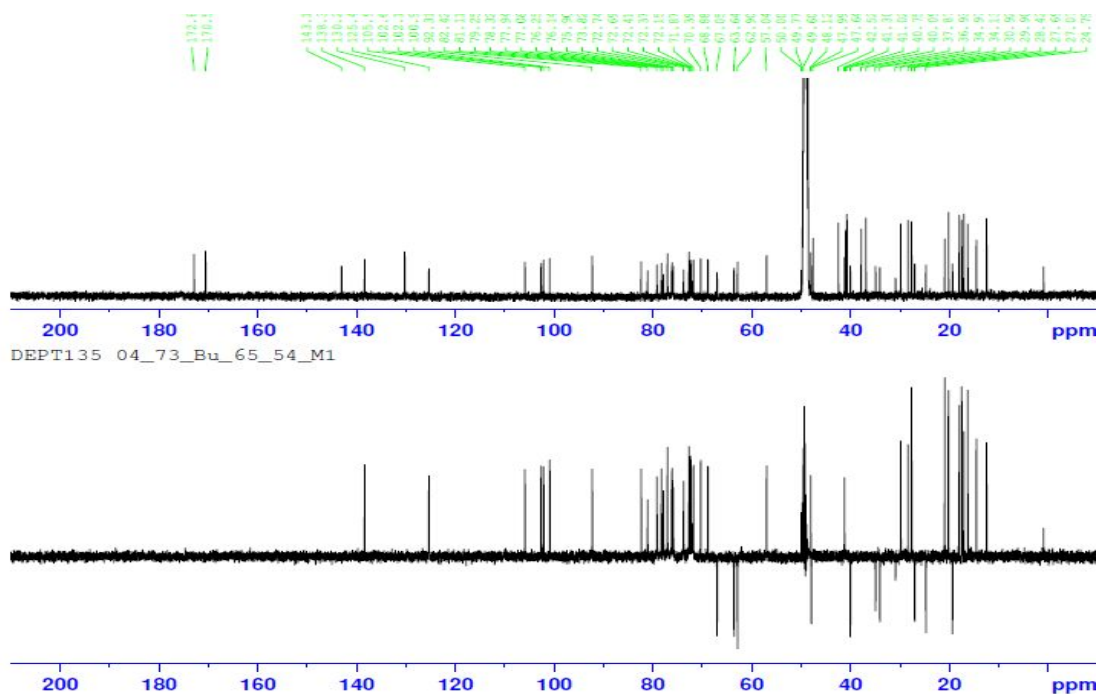


Figure 163.  $^{13}\text{C}$ -NMR and DEPT135 spectra of Jegosaponin A (**1**) in  $\text{CD}_3\text{OD}$

Compound **1** was needles. The molecular formula of compound **1** was determined to be C<sub>61</sub>H<sub>96</sub>O<sub>27</sub> based on NMR data. Compound **1** the main saponin, had the molecular (negative FAB-MS, *m/z* 1259 [M-H]<sup>-</sup>) (Data did not shown). Acid hydrolysis of compound **1** afforded barringtogenol C as the aglycone, besides D-galactose, D-glucose, L-rhamnose, which were confirmed by specific rotation using HPLC with chiral detection. However, homonuclear COSY spectroscopy, HMQC and HMBC experiments revealed the presence of glucuronic acid in the sugar units (Data did not shown). Therefore, in the <sup>1</sup>H-NMR spectrum, four anomeric protons were observed at δ<sub>H</sub> 6.03 (1H, *brs*, Rha-1), 5.97 (1H, *d*, *J* = 7.7 Hz, Gal-1), 5.63 (1H, *d*, *J* = 7.1 Hz, Glc-1) and 4.78 (1H, *d*, *J* = 8.0 Hz, GlcA-1) (Fig. 162). The configuration of all the sugars in the pyranose form in compound **1** was completely defined from the chemical shift and the coupling constant of each of the anomeric protons. Accordingly, each galactose, glucose and glucuronic acid moiety was established to have the β configuration, and one rhamnose had the α configuration. A marked downfield-shift in <sup>13</sup>C-NMR resonance among the aglycon was observed at δ<sub>C</sub> 90.3 (C-3) indicating that the likely point of glycosidic linkage in the oligosaccharide was at C-3 (Fig. 163). The sugar attached at C-3 was detected by the nuclear overhauser effect (NOE) between H-3 at δ<sub>H</sub> 3.29 (1H, *dd*, *J* = 11.5, 4.0 Hz, H-3) and H-1 at δ<sub>H</sub> 4.78 (1H, *d*, *J* = 8.0 Hz, GlcA-1). Further, the HMBC spectrum showed connectivities between the H-1 signal at δ<sub>H</sub> 5.63 (1H, *d*, *J* = 7.1 Hz, Glc-1) of Glc and the δ<sub>C</sub> 79.1 (GlcA-2) of GlcA, the H-1 signal at δ<sub>H</sub> 5.97 (1H, *d*, *J* = 7.7 Hz, Gal-1) of Gal and the δ<sub>C</sub> 81.7 (GlcA-3) of GlcA, the H-1 signal at δ<sub>H</sub> 6.03 (1H, *brs*, Rha-1) and the carbon signal at δ<sub>C</sub> 76.2 (Gal-2), which could be assigned to the C-2 of galactose by homo COSY and HMQC. Thus, the structure of compound **1** was determined as barringtogenol C 21-*O*-tigloyl-22-*O*-acetyl-3-*O*-L-*α*-rhamnonopyranosyl-(1→2)-β-D-galactopyranosyl-(1→3)-[β-D-glucopyranosyl-(1→2)]-β-D-glucuronopyranoside (Jegosaponin A) by comparison its spectral data with those of literature (Fig. 164).<sup>134)</sup> Jegosaponin A was reported for the first time from this plant.



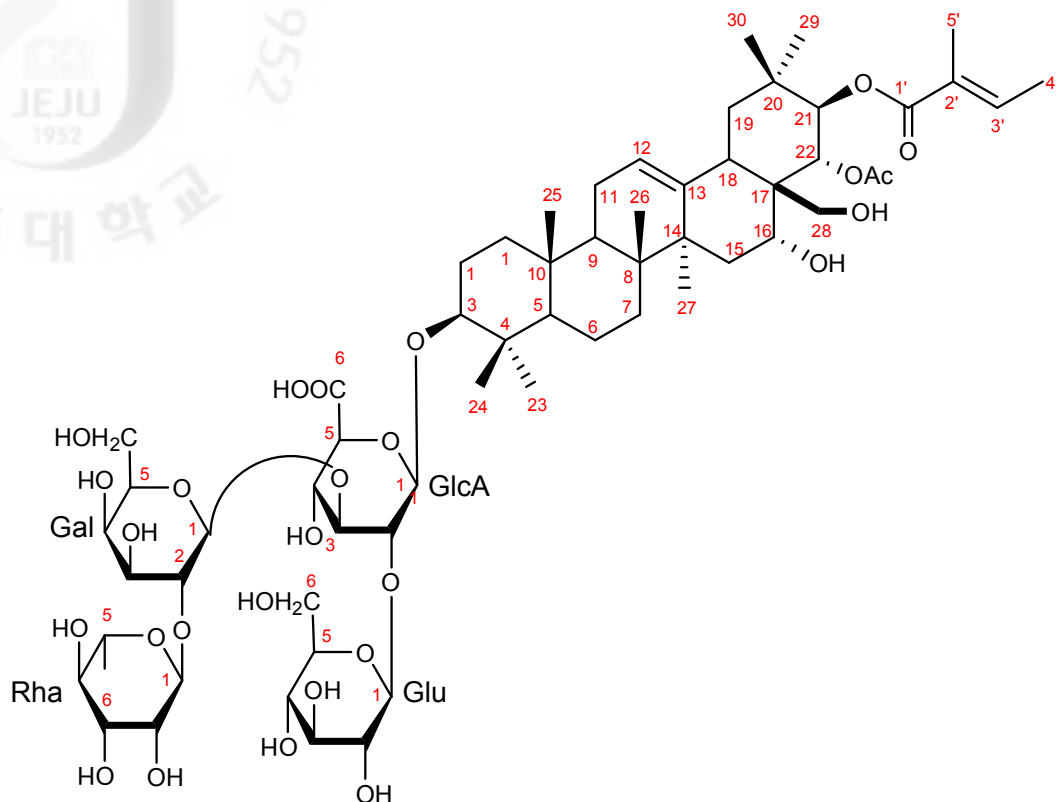


Figure 164. Structure of compound 1; Jegosaponin A

### 3-1-2. Compound 2

• Compound Name 12-Oleanene-3,16,21,22,28-pentol; (3 $\beta$ ,16 $\alpha$ ,21 $\beta$ ,22 $\alpha$ )-form, 21-tigloyl, 22-Ac, 3-*O*-[ $\alpha$ -L-rhamnopyranosyl-(1 $\rightarrow$ 2)- $\beta$ -D-galactopyranosyl-(1 $\rightarrow$ 3)-[ $\beta$ -D-glucopyranosyl-(1 $\rightarrow$ 2)]- $\beta$ -D-glucuronopyranoside]

• Synonym(s) Jegosaponin B

• CAS Registry Number -

• Appearance needles

• Chemical Formula C<sub>61</sub>H<sub>96</sub>O<sub>27</sub>

• Molecular Weight (g/mol) 1260

• Melting Point (°C) 218 - 220

• <sup>1</sup>H-NMR (500 MHz, CD<sub>3</sub>OD)

$\delta$ : 7.01 (1H, *q*, *J* = 6.0 Hz, H-3'), 6.43 (1H, *d*, *J* = 10.0 Hz, H-21), 6.22 (1H, *brs*, Rha-1), 6.21 (1H, *d*, *J* = 7.0 Hz, Gal-1), 5.09 (1H, *d*, *J* = 7.0 Hz, Glc-1), 5.46 (1H, *m*, H-12), 4.85 (1H, *d*, *J* = 7.1 Hz, GlcA-1), 4.76 (1H, *m*, H-16), 4.75 (1H, *dd*, *J* = 9.1, 8.8 Hz, GlcA-3), 4.75 (1H, *dd*, *J* = 8.8, 7.1 Hz, GlcA-2), 4.74 (1H, *dd*, *J* = 8.5, 7.0 Hz, Gal-2), 4.51 (1H, *d*, *J* = 10.0, H-22), 4.21, 4.32 (2H, *d*, *J* = 11.8 Hz, H-28), 3.22 (1H, *dd*, *J* = 11.5, 4.4 Hz, H-3), 2.86 (1H, *dd*, *J* = 13.0, 4.5 Hz, H-18), 2.03 (H, *s*, Ac-1), 1.86 (3H, *s*, H-5'), 1.82 (3H, *s*, H-27), 1.60 (3H, *d*, *J* = 6.0 Hz, H-4'), 1.40 (3H, *d*, *J* = 6.0 Hz, Rha-6), 1.31 (3H, *s*, H-30), 1.15 (3H, *s*, H-23), 1.10 (3H, *s*, H-29), 1.06 (3H, *s*, H-24), 0.97 (3H, *s*, H-26), 0.79 (3H, *s*, H-25)

• <sup>13</sup>C-NMR (125 MHz, CD<sub>3</sub>OD)

$\delta$ : 172.4 (GlcA-6), 170.9 (Ac-1), 168.7 (C-1'), 142.9 (C-13), 136.3 (C-3'), 129.9 (C-2'), 124.0 (C-12), 105.5 (GlcA-1), 102.8 (Glc-1), 102.4 (Rha-1), 101.4

(Gal-1), 90.1 (C-3), 82.6 (GlcA-3), 81.8 (C-21), 79.5 (GlcA-2), 78.5 (Glc-3), 78.2 (Gal-5), 77.5 (GlcA-5), 77.1 (Glc-2), 76.5 (Gal-2), 76.3 (Gal-2), 76.1 (Gal-3), 74.0 (Rha-4), 72.7 (Rha-2), 72.7 (Rha-3), 72.7 (Glc-4), 71.4 (GlcA), 71.4 (C-22), 71.3 (Gal-4), 69.9 (Rha-5), 67.9 (C-16), 66.7 (C-28), 63.7 (Glc-6), 62.2 (Gal-6), 55.9 (C-5), 47.5 (C-19), 47.2 (C-17), 47.1 (C-9), 41.9 (C-14), 40.7 (C-18), 40.2 (C-8), 39.8 (C-4), 39.0 (C-1), 36.9 (C-10), 36.4 (C-20), 34.8 (C-15), 33.3 (C-7), 29.9 (C-29), 28.1 (C-23), 27.6 (C-27), 26.6 (C-2), 24.1 (C-11), 20.9 (Ac-2), 20.3 (C-30), 18.5 (C-6), 18.3 (Rha-6), 17.2 (C-24), 16.9 (C-26), 15.8 (C-25), 14.3 (C-4'), 12.6 (C-5')

• Biological activities in the literature

anti-sweet

• Other data in the literature

1. HR-FAB MS:  $m/z$  1259.3908  $[M-H]^-$  (calcd. for  $C_{61}H_{96}O_{27}$  1259.6061,  $\Delta$  - 0.2 mamu)
2. IR (film)  $cm^{-1}$ : 3400 (*br*), 1730 (*br*), 1665, 1240, 1160
3. Optical Rotation:  $[\alpha]_D^{25} = -8.2^\circ$  (*c* 11.1, MeOH)

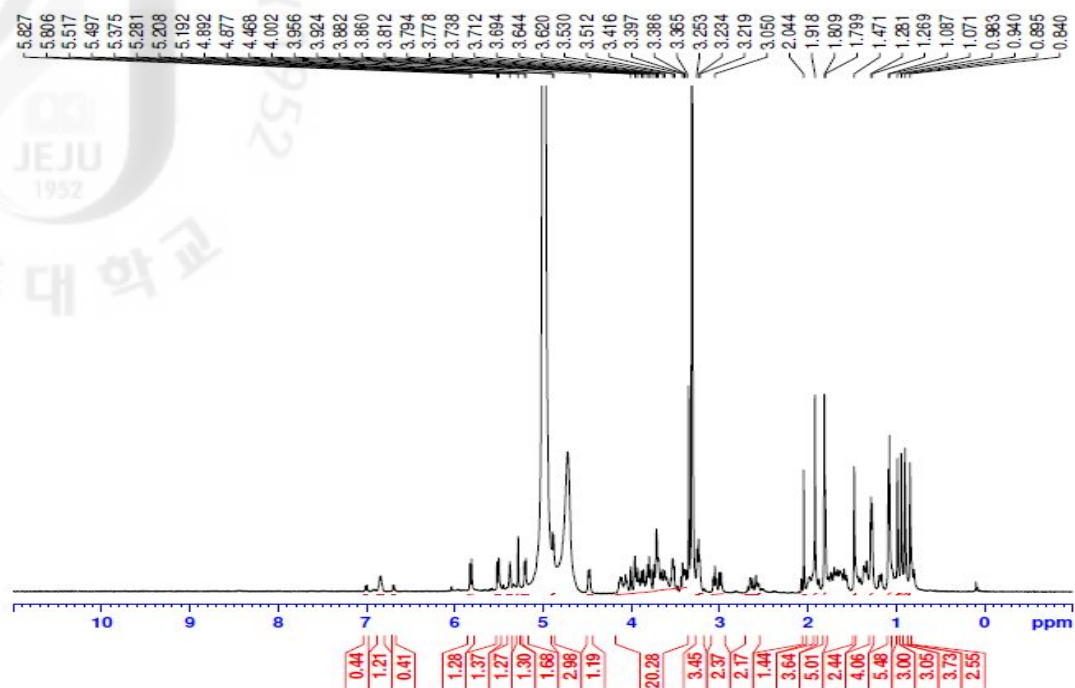


Figure 165.  $^1\text{H}$ -NMR spectrum of Jegosaponin B (**2**) in  $\text{CD}_3\text{OD}$

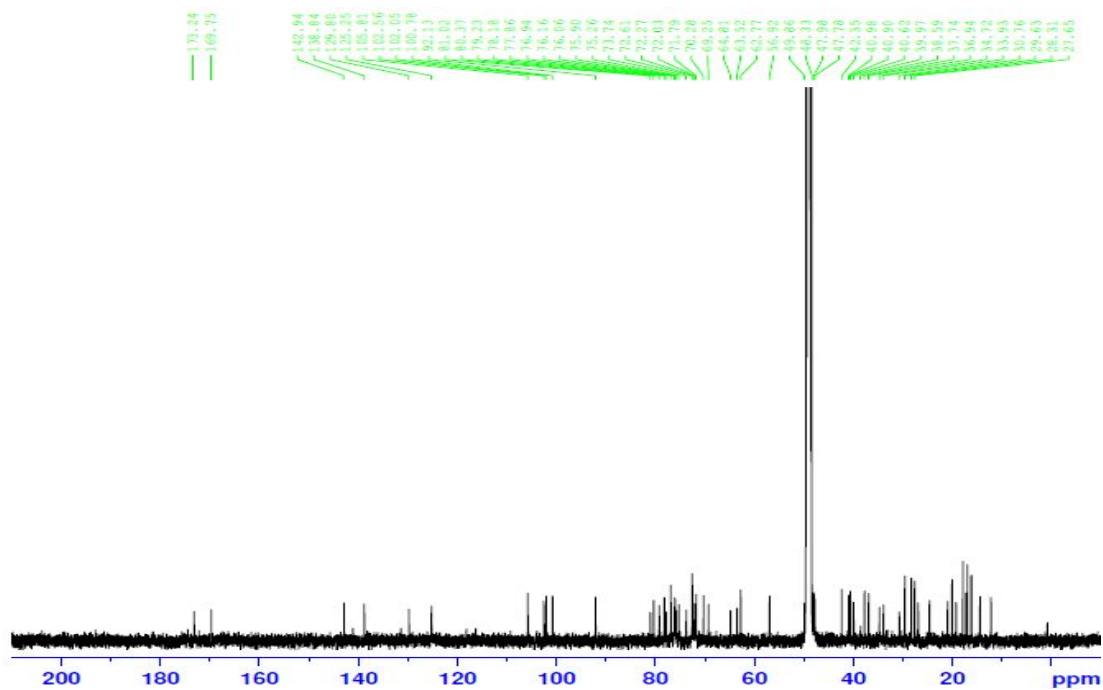


Figure 166.  $^{13}\text{C}$ -NMR spectrum of Jegosaponin B (**2**) in  $\text{CD}_3\text{OD}$

Compound **2** was needles. The molecular formula of compound **2** was determined to be  $C_{61}H_{96}O_{27}$  based on NMR data. Compound **2** the main saponin, had the molecular (negative FAB-MS,  $m/z$  1259 [M-H]) as compound **1** (Data did not shown). The carbon signals due to the sugar moieties in compound **2** were superimposable on those of compound **1**, indicating that both sugar moieties at C-3 are the same. Indeed, alkaline treatment of compound **2** gave deacyl Jegosaponin A, along with tiglic acid and acetic acid. The locations of the acyl groups were determined in the same way as for compound **1**; three proton signals shifted by acylation were observed at  $\delta_H$  6.43 (1H, *d*,  $J = 10.0$  Hz, H-21) which was assigned to H-21, and at  $\delta_H$  4.21, 4.32 (2H, *d*,  $J = 11.8$ , H-28) to H<sub>2</sub>-28 by a rotating-frame nuclear overhauser effect spectroscopy (ROESY) experiment (Data did not shown). In the HMBC spectrum, H-21 and H<sub>2</sub>-28 signals showed long-range correlations with C-1 ( $\delta_C$  168.7) in a tigloyl group and the  $\delta_C$  170.9 (Ac-1) of an acetyl, respectively. Thus, the structure of compound **2** was determined as barringtogenol C 21-*O*-tigloyl-28-*O*-acetyl-3-*O*- $\alpha$ -L-rhamonopyranosyl-(1 $\rightarrow$ 2)- $\beta$ -D-galactopyranosyl-(1 $\rightarrow$ 3)-[ $\beta$ -D-glucopyranosyl-(1 $\rightarrow$ 2)]- $\beta$ -D-glucuronopyranoside (Jegosaponin B) by comparison *D. coriacea* (Fig. 167).<sup>134)</sup> Jegosaponin B also was reported for the first time from this plant.

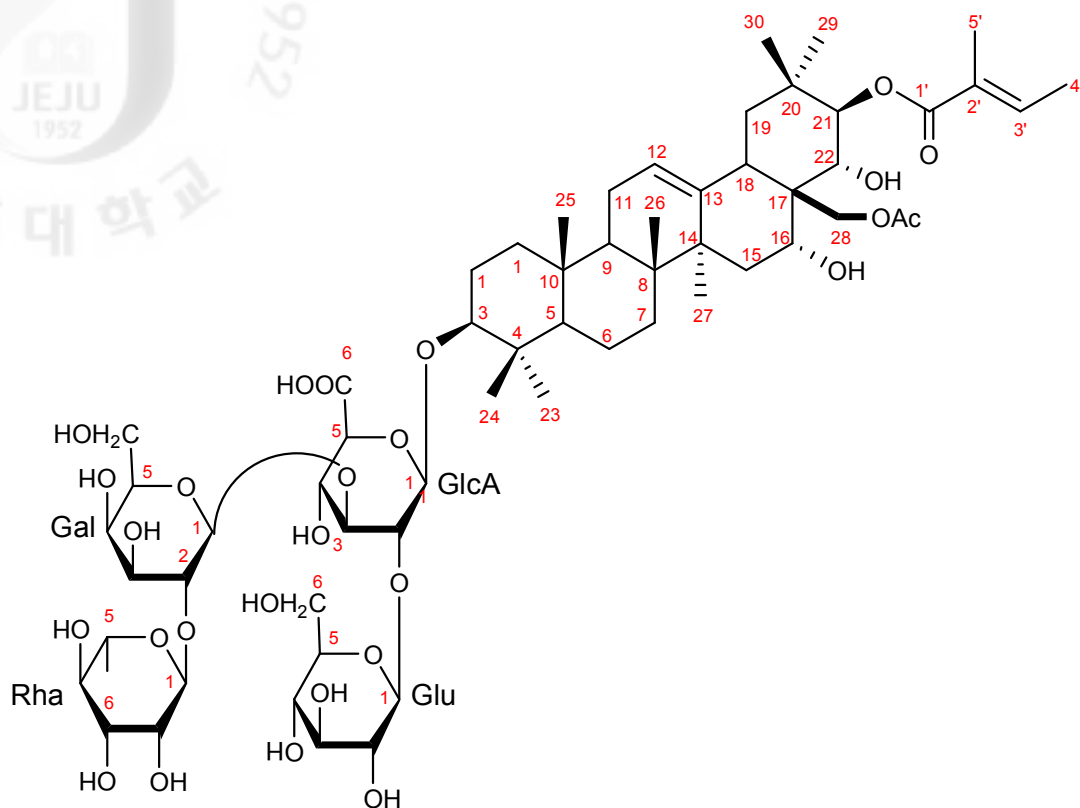


Figure 167. Structure of compound 2; Jegosaponin B

## 3-2. Biological activities

### 3-2-1. Antioxidant activity

#### 3-2-1-1. Free radical scavenging activity of the solvent fractions

Antioxidative activity was determined by 3 types of free radical scavenging activity assay. The DPPH radical scavenging activity of the crude 70% *aq.* EtOH extract and its solvent fractions of *S. obassia* showed in Table 26. EtOAc solvent fraction exhibited higher radical scavenging activity compared to other solvent fractions with dose-dependent manner. As same results, the xanthine oxidase inhibitory activity of the 70% *aq.* EtOH extract and fractions showed in Table 26. All solvent fractions did not show highly enzyme inhibitory activity in 1000  $\mu\text{g/mL}$  compared to positive control (Allopurinol,  $\text{IC}_{50} = 4.8 \mu\text{g/mL}$ ) (Tab. 26). These results showed that as to the crude 70% *aq.* EtOH extract and its solvent fractions of *S. obassia*, the activity confirmed the none for antioxidant activity.

Table 26. Free radical scavenging effect of the solvent fractions

Samples	RC <sub>50</sub> (µg/mL)		
	DPPH radical scavenging activity	Xanthine oxidase inhibitory activity	Superoxide radical scavenging activity
70% <i>aq.</i> EtOH ext.	59.4 ± 2.88	N/A	86.9 ± 5.01
<i>n</i> -Hex Fr.	815.5 ± 1.25	N/A	205.6 ± 2.12
CH <sub>2</sub> Cl <sub>2</sub> Fr.	446.3 ± 7.93	N/A	97.6 ± 3.96
EtOAc Fr.	49.9 ± 0.56	217.6 ± 5.00	20.1 ± 1.35
<i>n</i> -BuOH Fr.	56.6 ± 1.99	N/A	76.5 ± 0.38
H <sub>2</sub> O Fr.	107.4 ± 2.69	N/A	66.7 ± 3.09
Positive control (BHA) <sup>1)</sup>	13.1 ± 2.29	N/A	N/A
Positive control (Allopurinol)	N/A	4.8 ± 0.38	5.4 ± 0.40

Primarily radical scavenging activity was determined at 0 to 1000 µg/mL concentration of samples. Scavenging concentration for 50% of free radical (RC<sub>50</sub>) was calculated from logarithmic regression equation obtained from the values of at least five dilutions of the primary concentration. Values represent mean ± SDs (n = 3); in parentheses is RC<sub>50</sub> value of respective sample

N/A. not assay; BHA. butylated hydroxyanisole<sup>1)</sup>; >. out of range

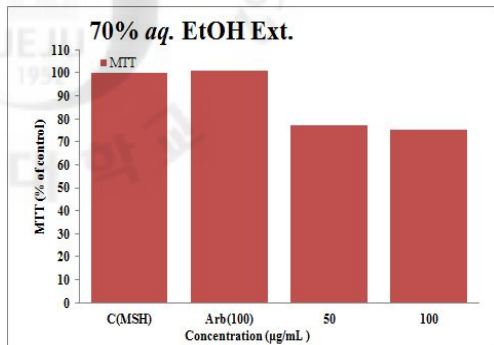


### 3-2-2. Melanogenesis inhibition activity

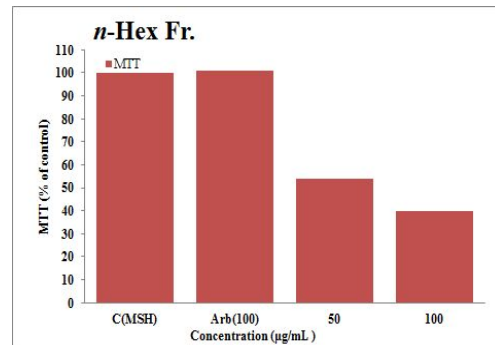
#### 3-2-2-1. Cell viability in B16F10 melanoma cell

We examined the suppressive effects of the crude 70% *aq.* EtOH extract with solvent fractions from *S. obassia* on B16F10 melanoma cells. B16F10 melanoma cells were cultured in the presence and absence of various concentrations of samples at 0 to 100  $\mu\text{g/mL}$ . After treatment, cell viability was measured by MTT assay and expressed as % cell viability compared with the control. As shown Figure 168, all fractions except the H<sub>2</sub>O fraction significantly reduced the cell viability rate on B16F10 melanoma cells in regardless of the concentration. Specially, in *n*-BuOH fraction showed strongly cytotoxicity over 50  $\mu\text{g/mL}$  on B16F10 melanoma cells (Fig. 168).

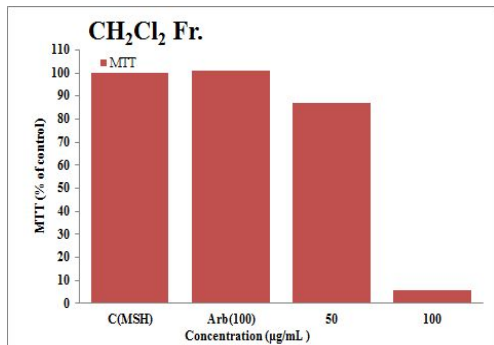
(A)



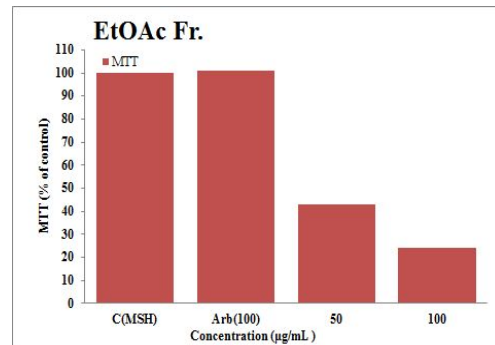
(B)



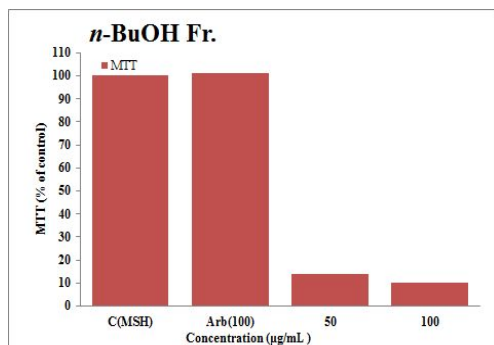
(C)



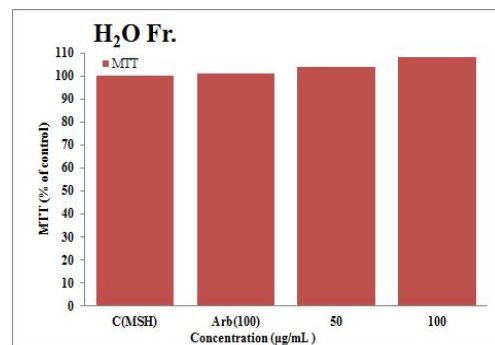
(D)



(E)



(F)



Values are mean  $\pm$  SD of 3 replicates

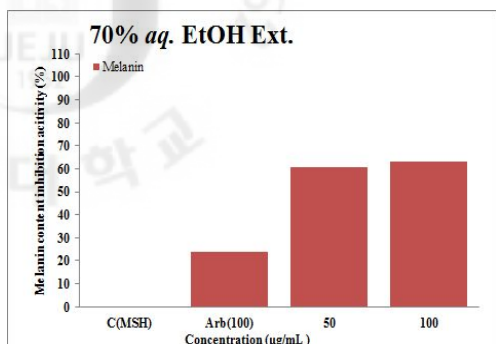
(A) 70% aq. EtOH Ext. (B) *n*-Hex Fr. (C) CH<sub>2</sub>Cl<sub>2</sub> Fr. (D) EtOAc Fr. (E) *n*-BuOH Fr. (F) H<sub>2</sub>O Fr.

Figure 168. Cell viability in B16F10 cells treated with the solvent fractions

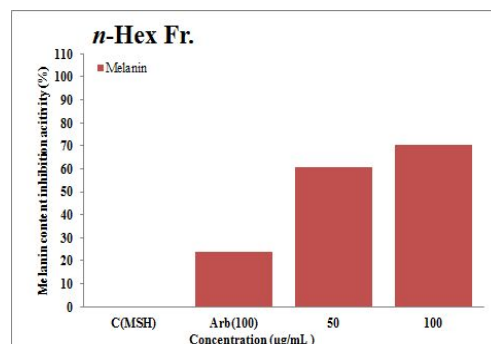
### 3-2-3-2. Effect on melanogenesis in B16F10 cells

We examined the effect of melanin contents inhibitory activity using B16F10 melanoma cells. As shown in Figure 169, the crude 70% *aq.* EtOH extract and solvent fractions showed melanin contents inhibitory activity in a dose-dependent manner. In comparison with the positive control group, the melanin contents of all fractions excepted the H<sub>2</sub>O fraction significantly reduced melanin contents at 50 ~ 100 µg/mL concentration (Fig. 169). Respectively, while the melanin contents of arbutin was at 100 µg/mL by 23.9%. However, as shown in previously MTT results using the 70% *aq.* EtOH extract and solvent fractions, this good results considered as the suppression by the cytotoxicity of B16F10 melanoma cells.

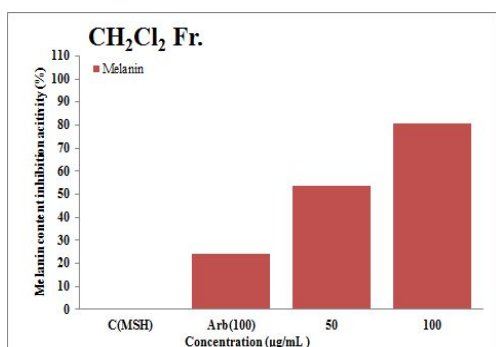
(A)



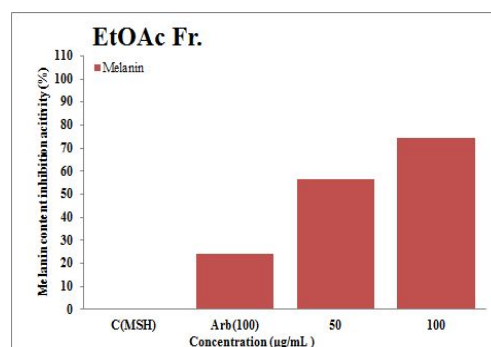
(B)



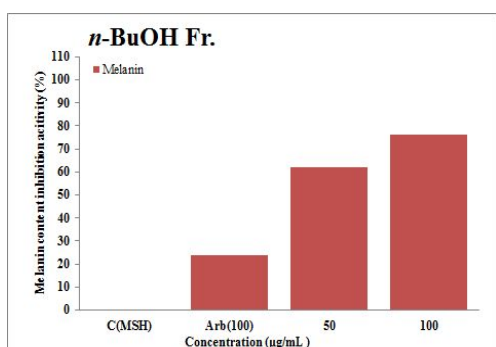
(C)



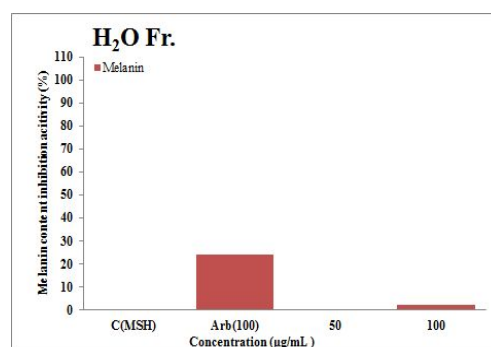
(D)



(E)



(F)



Values are mean  $\pm$  SD of 3 replicates

(A) 70% aq. EtOH Ext. (B) *n*-Hex Fr. (C) CH<sub>2</sub>Cl<sub>2</sub> Fr. (D) EtOAc Fr. (E) *n*-BuOH Fr. (F) H<sub>2</sub>O Fr.

Figure 169. Melanin contents inhibitory activity of the solvent fractions on B16F10 cells

### 3-2-3. Anti-obesity activity

#### 3-2-3-1. Inhibition effect on $\alpha$ -glucosidase

We examined the inhibitory effect of *S. obassia* for yeast  $\alpha$ -glucosidase activity and as shown in Table 27. Various concentrations of the solvent fractions were performed and showed  $\alpha$ -glucosidase inhibitory activity in a dose-dependent manner. According to Figure 170, the five solvent fractions showed gradually increased with increasing concentration and their activity increased in the following order : *n*-Hex and CH<sub>2</sub>Cl<sub>2</sub> fractions < H<sub>2</sub>O fraction < *n*-BuOH fraction < EtOAc fraction. Among them, EtOAc and *n*-BuOH solvent fractions exhibited higher inhibition activity compared to other solvent fractions with dose-dependent manner and also showed higher than positive control (Acarbose, IC<sub>50</sub> = 127.9  $\mu$ g/mL) except the lower concentration at IC<sub>50</sub> = 3.6 and 6.0  $\mu$ g/mL (Tab. 27).

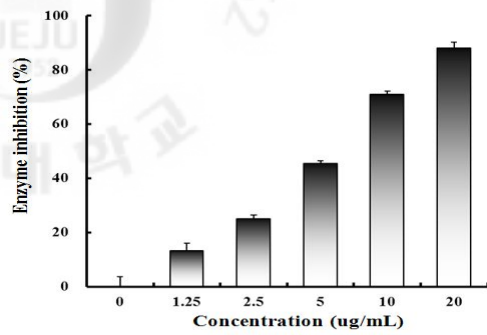
Table 27. Inhibition effect of the solvent fractions on yeast  $\alpha$ -glucosidase inhibitory assay

Samples	IC <sub>50</sub> ( $\mu$ g/mL)		
	yeast $\alpha$ -glucosidase inhibitory activity		
70% <i>aq.</i> EtOH ext.	6.0	±	0.03
<i>n</i> -Hex Fr.	>		100
CH <sub>2</sub> Cl <sub>2</sub> Fr.	>		100
EtOAc Fr.	3.6	±	0.03
<i>n</i> -BuOH Fr.	6.0	±	0.33
H <sub>2</sub> O Fr.	11.9	±	0.4
Positive control (Acarbose)	127.9	±	20.0

Primarily enzyme inhibition activity was determined at 0 to 100  $\mu$ g/mL concentration of samples. Inhibition concentration for 50% of enzyme inhibition (IC<sub>50</sub>) was calculated from logarithmic regression equation obtained from the values of at least five dilutions of the primary concentration. Values represent mean  $\pm$  SDs (n = 3); in parentheses is IC<sub>50</sub> value of respective sample

N/A. not assay; >. out of range

(A)



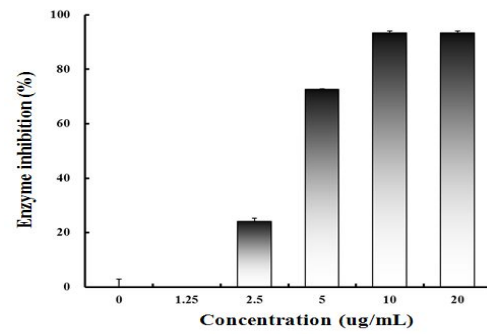
(B)

Out of range

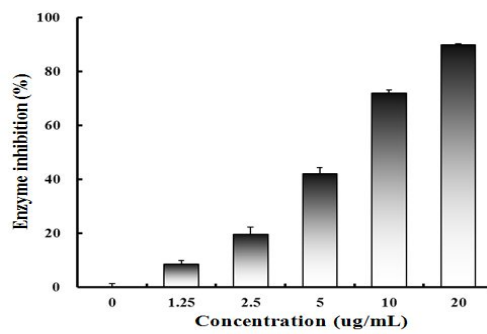
(C)

Out of range

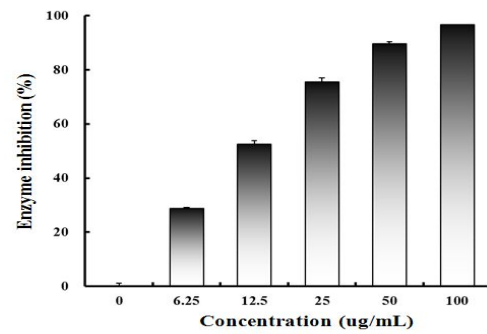
(D)



(E)



(F)



Values are mean  $\pm$  SD of 3 replicates

(A) 70% aq. EtOH Ext. (B) *n*-Hex Fr. (C) CH<sub>2</sub>Cl<sub>2</sub> Fr. (D) EtOAc Fr. (E) *n*-BuOH Fr. (F) H<sub>2</sub>O Fr.

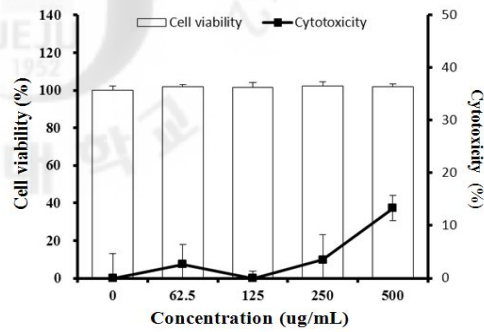
Figure 170. Inhibition effect of the solvent fractions on yeast  $\alpha$ -glucosidase inhibitory assay

### 3-2-3-2. Cell viability in mouse 3T3-L1 preadipocytes

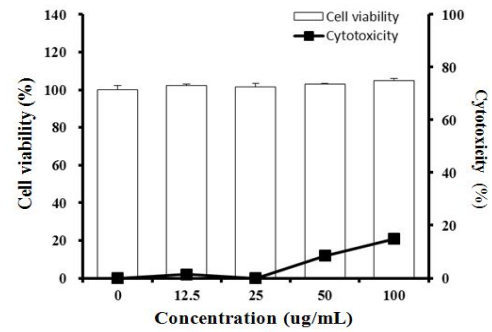
Pre-confluent 3T3-L1 preadipocytes were cultured in the presence and absence of various concentrations (0 to 500  $\mu\text{g/mL}$ ) of 70% *aq.* EtOH extract and their solvent fractions. MTT and LDH assay as like previously experimental method. As shown in Figure 171,  $\text{CH}_2\text{Cl}_2$ , EtOAc, *n*-BuOH and  $\text{H}_2\text{O}$  fractions at 100  $\mu\text{g/mL}$  concentration did not affect cell viability and any cytotoxicity at the concentration based on MTT and LDH assay. And then, 3T3-L1 preadipocytes were treated with isolated two compounds for cell viability rate and cytotoxicity effect on 3T3-L1 preadipocytes. Jegosaponin A (**1**) did not affect the cell viability and cytotoxicity at the 25  $\mu\text{M}$  concentration (Fig. 171). However, Jegosaponin B showed the toxicity over 12.5  $\mu\text{M}$  on MTT and LDH activities (Fig. 172).



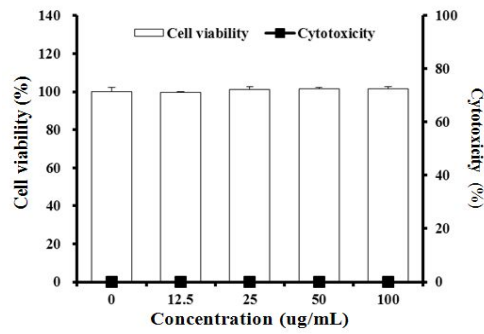
(A)



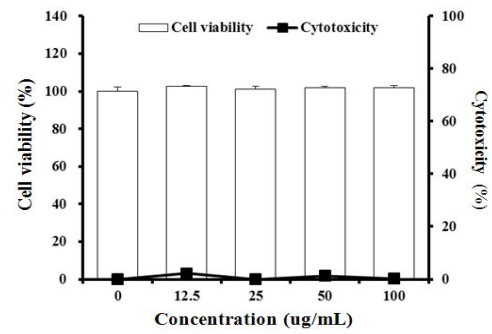
(B)



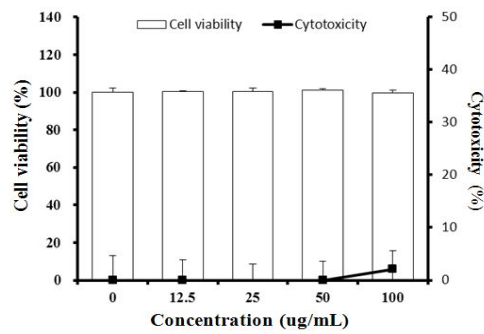
(C)



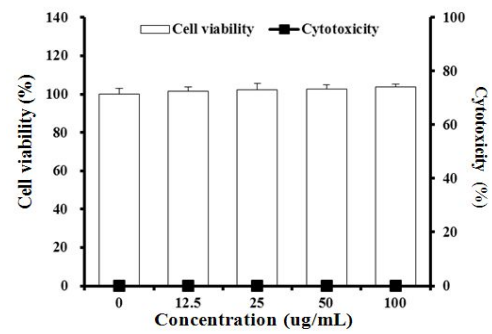
(D)



(E)



(F)

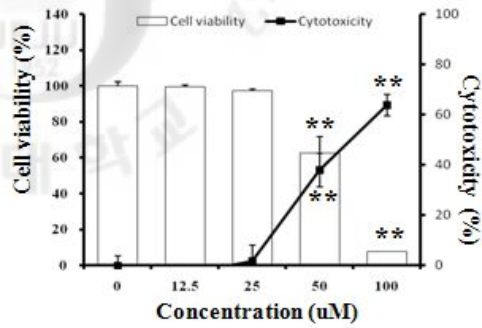


Values are mean ± SD of 3 replicates

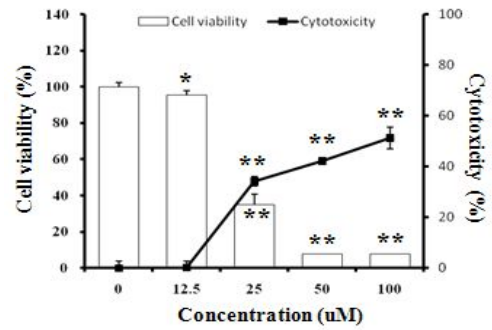
(A) 70% aq. EtOH Ext. (B) *n*-Hex Fr. (C) CH<sub>2</sub>Cl<sub>2</sub> Fr. (D) EtOAc Fr. (E) *n*-BuOH Fr. (F) H<sub>2</sub>O Fr.

Figure 171. Cell viability and cytotoxicity of the solvent fractions on mouse 3T3-L1 preadipocytes

(A)



(B)



Values are mean  $\pm$  SD of 3 replicates

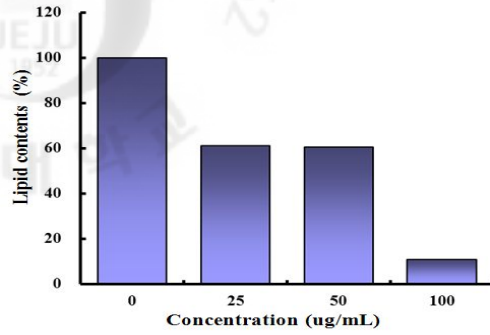
(A) Jegosaponin A (B) Jegosaponin B

Figure 172. Cell viability and cytotoxicity of the isolated compounds on mouse 3T3-L1 preadipocytes

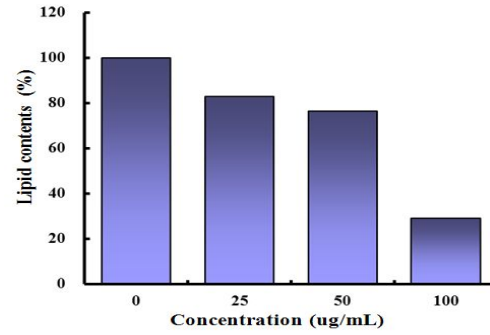
3-2-3-3. Effects on reducing lipid accumulation in mouse 3T3-L1 preadipocytes differentiated adipocytes

All samples were treated to 3T3-L1 preadipocytes to investigate the effects of *S. obassia* on obesity. During differentiation the cells were treated with various concentrations of five solvent fractions (0, 25, 50 and 100  $\mu\text{g}/\text{mL}$ ) and isolated two compounds from *S. obassia* (0. 0.625, 1.25, 2.5 and 5  $\mu\text{M}$ ). As shown in the Figure 173, treatment of *n*-BuOH fraction at 50  $\mu\text{g}/\text{mL}$  concentration significantly suppressed lipid accumulation around 89.0%, respectively, compared to control group. However, treated Jegosaponin A (**1**) and Jegosaponin B (**2**) were similar their structures with themselves. The isolated two compounds exhibited considerable inhibition on lipid accumulation (59.2 and 80.7% inhibition at 5  $\mu\text{M}$ ) compared to the non-treated control (Fig. 174). It was significantly good effective reducing lipid accumulation compared to positive control (Data did not shown). From these results suggested that Jegosaponin A (**1**) and Jegosaponin B (**2**) should be major active compounds responsible for the reducing lipid accumulation in mouse 3T3-L1 preadipocytes of *S. obassia*

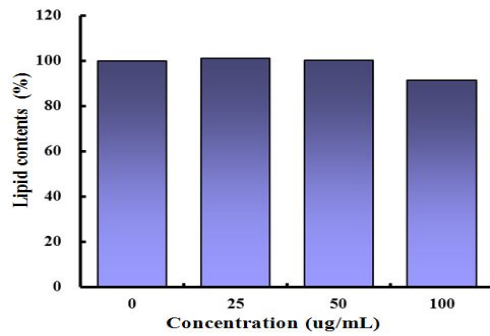
(A)



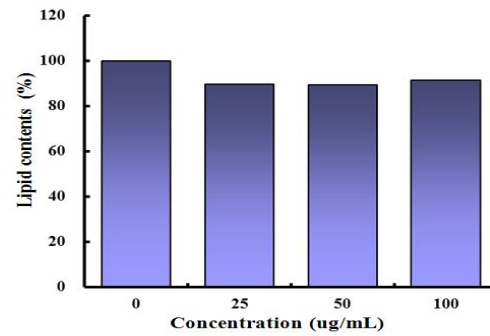
(B)



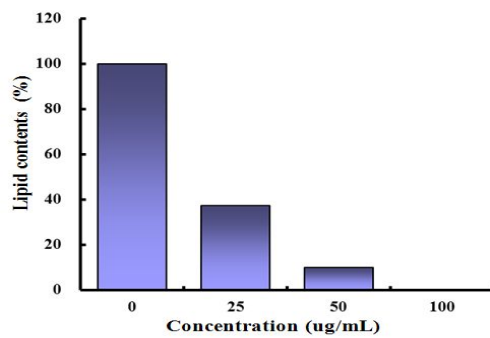
(C)



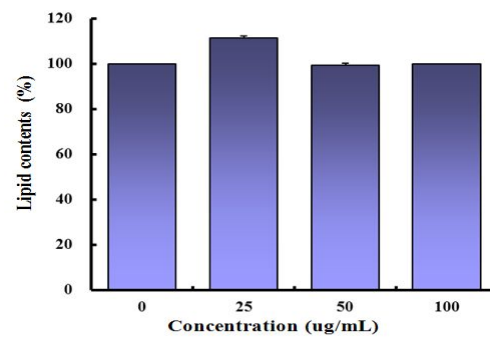
(D)



(E)



(F)

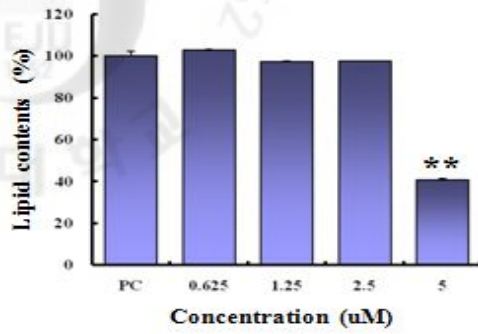


Values are mean  $\pm$  SD of 3 replicates

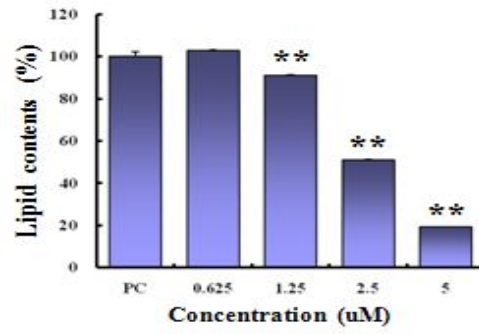
(A) 70% aq. EtOH Ext. (B) *n*-Hex Fr. (C) CH<sub>2</sub>Cl<sub>2</sub> Fr. (D) EtOAc Fr. (E) *n*-BuOH Fr. (F) H<sub>2</sub>O Fr.

Figure 173. The reduction effects of the solvent fractions on lipid accumulation during differentiation of 3T3-L1 preadipocyte

(A)



(B)



Values are mean  $\pm$  SD of 3 replicates

(A) Jegosaponin A (B) Jegosaponin B

Figure 174. The reduction effects of the isolated compounds on lipid accumulation during differentiation of 3T3-L1 preadipocytes

#### 4. Discussion

In this study, *S. obassia* was evaluated for the activities on anti-obesity. The active constituents were identified following activity-guided isolation with chromatography.

1. The dried leaves of *S. obassia* was extracted with 70% *aq.* EtOH at room temperature. This extract was partitioned successively into five solvent fractions. These fractions were tested for their inhibitory effects;
  - DPPH and superoxide radical scavenging activity test, xanthine oxidase inhibition activity test for the antioxidant activity
  - The effect of melanin contents inhibitory activity on B16F10 cells for the melanogenesis inhibition activity
  - The effect of reducing lipid accumulation in 3T3-L1 preadipocytes for the anti-obesity activity

As the *n*-BuOH solvent fraction indicated good activity, this fraction was investigated extensively to find activities compounds

2. The *n*-BuOH solvent fraction of *S. obassia* was subjected to a series of chromatographic separations and led to the isolation of two compounds. The structures of two known compounds were determined by the spectroscopic methods (UV/VIS, 1D and 2D NMR).
  - Jegosaponin A (**1**) and Jegosaponin B (**2**)
3. In anti-obesity activity studies Jegosaponin A (**1**) and Jegosaponin B (**2**) has good effects on reducing lipid accumulation in 5  $\mu$ M concentration, 59.2 and 80.7% as dose-dependent manner in differentiated 3T3-L1 preadipocytes

In conclusion, the extract and isolated compounds from *S. obassia* provided

anti-obesity effect. Due to these biological activities, this plant could be a potential source applicable as the slimming cosmetics material.

## IX. Overall Conclusion

With a view of proper utilization of plants (including sea plants) in Jeju island, we have studied on six plant species (*Lindera erythrocarpa* Makino, *Cornus macrophylla* Wall, *Aster subulatus* Michx, *Ishige sinicola* (Setchell et Gardner) Chihara, *Dictyota coriacea* (Holmes) Hwang, Kim, et Lee and *Styrax obassia* Siebold & Zucc) in order to develop functional ingredients applicable in cosmetic formulations.

Dried plant samples were extracted with 70% *aq.* ethanol, and the crude extracts were subjected to solvent fractionation according to polarity. The active components from the selected fraction were obtained by a series of chromatographic separations. The screenings of activities (antioxidant, anti-inflammatory, melanogenesis inhibition, and anti-obesity) were carried out for each fraction and isolates. Overall, 37 phytochemicals including 35 known compounds and two new compounds were isolated and identified. Chemical structures of the isolated substances were identified with analyzing data with spectrometers such as HR FAB MS, 1D and 2D NMR.

- 1. *Lindera erythrocarpa* Makino has good activities for antioxidation, anti-inflammatory, melanogenesis inhibition activity and anti-obesity effects.** *L. erythrocarpa* is a deciduous tree widely distributed in Asian countries including China, Japan and South Korea. This tree has been utilized as the timber for household furniture in the local communities. Its dried fruit have been used for the alleviation of neuralgia and stomachache as a folk medicine in Japan. In this study, we isolated 14 compounds including one new compound (**13**); Ethyl caffeate (**1**), methyl cinnamate (**2**), lucidone (**3**), methylinderone (**4**),  $\beta$ -sitosterol (**5**), quercetin (**6**) quercitrin (**7**), avicularin (**8**), afzerin (**9**), kanakugiol (**10**), methylucidone (**11**), stigmasterol (**12**), and linderone (**14**). We



investigated isolated compounds for be related biological activity assay by initial effect using extract from *L. erythrocarpa*. As the results, Separated lucidone (3), methyllinderone (4), methyllucidone (11), new compound (13), kanakugiol (10), and linderone (14) showed high melanogenesis inhibition activity compared with arbutin, the control group, in B16F10 cell. At the concentration where activity was appeared, the compounds showed no cytotoxicity. Furthermore, TRP-1 mRNA and tyrosinase expression were inhibited depending on concentration in the suppression experiment of mRNA expression in melanin synthesis. The extract and isolated compounds also provided anti-inflammatory and anti-obesity effect.

**2. *Cornus macrophylla* Wall has good activities for antioxidation activity effect.** *C.*

*macrophylla* belongs to a family Cornaceae and be called '웅수목(熊水木)' in South Korea. This plant wall is distributed in Korea, Japan, Taiwan and China. It is a small, often low-branched or multistemmed tree, usually no more than 8 ~ 10 m tall. Creamy white flowers are individually tiny, flowering is June to July. This tree has been utilized as the timber for household furniture or gardening tree in the local communities. In this study, we isolated six known compounds using crude 70% *aq.* EtOH extract; Rengyolone (1), ethyl gallate (2), (+)-catechin (3), ursolic acid (4), quercitrin (5), and afzelin (6). When ethyl gallate and (+)-catechin were compared with BHA, the positive control group, it had significant free radical scavenging effect.

**3. *Aster subulatus* Michx has good activities for antioxidation, anti-inflammatory,**

**melanogenesis inhibition activity and anti-obesity effects.** *A. subulatus* is Compositae and an annual grass native to America. In Korea, this species is widely distributed and now been accepted as a naturalized plant. Previous phytochemical study on this plant has resulted in the isolation of flavonoids and their glycosides as well as chlorogenic acid. In this study, we isolated seven

phytochemicals including one new compound;  $\beta$ -sitosterol (1), ethyl caffeate (2), caffeic acid (3), new compound (4), 3,5-di-*O*-caffeoylquinic acid (5), 3,5-di-*O*-caffeoyl *epi*-quinic acid (6), and astragalin (7). Among the isolates, ethyl caffeate (2) and caffeic acid (3) showed potent melanogenesis inhibition activity and few cytotoxic effect. They had also strong free radical scavenging effect.

**4. *Ishige sinicola* Chihara has good activities for melanogenesis inhibition activity and anti-obesity effects.** *I. sinicola* is a genus of brown algae (class Phaeophyceae) occurring in the warm temperate regions of the western Pacific Ocean. Especially, *I. sinicola* is distributed around Jeju Island of South Korea, although rare in other parts of the world. It is the only genus in the family Ishigeaceae and order Ishigeales and calling '늪괘' in South Korea. In this study, five phytochemicals were isolated from *I. sinicola* and their structures were identified in the same manner as above mentioned; linoleic acid (1), 1-linoleoyl glycerol (2), pyromeconic acid (3), *di*-phlorethohydroxycarmalol (4), and 1,2-dilinoleoyl glycerol-3-*O*-glucoside (5). The isolated linoleic acid (1) inhibited melanin synthesis more strongly compared with arbutin, the positive control group in the melanogenesis inhibition activity experiment. Furthermore, *di*-phlorethohydroxycarmalol (4) showed high  $\alpha$ -glucosidase inhibition activity compared with genistein, the positive control group. These results provided anti-obesity effect.

**5. *Dictyota coriacea* (Holmes) Hwang, Kim, et Lee has good activities for melanogenesis inhibition activity effects.** *D. coriacea* belongs to a family Dictyotaceae, which grows in the warm temperate regions of the western Pacific Ocean. We isolated three known compounds from crude 70% *aq.* EtOH extract; D(-)mannitol (1), 1,9-dihydroxycrenulide (2), and loliolide (3). The 1,9-dihydroxycrenulide (2) and loliolide (3) showed strong melanogenesis

inhibition activity compared with arbutin, the control group.

**6. *Styrax obassia* Siebold & Zucc has good activities for anti-obesity effects. *S.***

*obassia* belongs to a family Styrax distributing in Korea, Japan and China. This tree has been utilized as the gardening in the landscape. In the previous biological studies, its derivatives were reported to have activity of removing tumor, expectorant of throats and toothache activities. We identified two known compounds of saponins from crude 70% *aq.* EtOH extract; Jegosaponin A (**1**) and Jegosaponin B (**2**). They inhibited on reducing lipid accumulation in 3T3-L1 preadipocytes and formation of cellular triglyceride contents. The compounds did not exhibit toxic in cells at the concentration which showed activity by MTT and LDH assay. This results provided anti-obesity effect suggesting as a potential.

In this study, we have shown that the natural products isolated from Jeju terrestrial and marine plants possessed various biological activities. These results could be utilized to the industrial applications such as functional cosmetic additives in the future.

## X. Reference

### I. INTRODUCTION

- 1) 손은수, 천연물유래 화장품소재의 개발 동향, *KISTI 기술동향분석보고서* **2003**.
- 2) 고은지, 기능성 화장품 전성시대, *LG주간경제* **2003**.
- 3) 봉연근, 기능성과 한방화장품을 트렌드로 성장 지속, **2006**.
- 4) Upadhyay, B.; Dhaker, A. K.; Singh, K. P.; Kumar, A. Phytochemical Analysis and Influence of Edaphic Factors on Lawsone Content of Lawsonia inermis L. *J. Phytology* **2010**, 2(6), 47-54.
- 5) 김도훈; 이수진; 이현석; 오성근; 강학회; 김진웅 최근 화장품 산업의 신소재 개발 연구. *KIC News* **2010**, 13(4).
- 6) 이한영 변리사 최신특허 동향 천연물 화장품 *BT News*
- 7) 이상호; 배영일; 최진영; 강희찬; 이원희 중국 그린·바이오 산업의 저력과 한국의 대응 *CEO Information* **2011**, (제 781호).
- 8) Leem, H. *Chung-ang Univ. Master's thesis* **2004**.
- 9) Park, D. J. *Ajou Univ. Master's thesis* **2004**.
- 10) Elsner, P.; Maibach, H. I. Cosmeceuticals and Active Cosmetics, Drugs vs. Cosmetics, **2000**.
- 11) Hossain, M. A.; Asada, K. Monodehydroascorbate reductase from cucumber is a flavin adenine dinucleotide enzyme. *J. biological chem.*, **1985**, 260(24), 12920-12926.
- 12) Burlando, B.; Verotta, L.; Cornara, L.; Bottini-Massa, E. Herbal Principles in Cosmetics: Properties and Mechanisms of Action (Traditional Herbal Medicines for Modern Times).
- 13) Henle, F. Allgemeine anatomie. 1 edit. *Leopold Voss Verlag*, **1841**, 791-799.
- 14) Koelliker, A. Handbuch der Gewebelehre des Menschen für Aerzte und Studierende. *Verlag von wilhelm Engelmann*, **1852**, 51-89.
- 15) Duran-Reynals F. *CR Soc. Biol.* **1928**, 99, 6-7.
- 16) Duran-Reynals F. *CR Soc. Biol.* **1929**, 99, 1908-1911.
- 17) Duran-Reynals F. *J Exp Med.* **1933**, 58, 161-181.
- 18) Duran-Reynals, F. The effect of extracts of certain organs from normal and immunized animals on the infecting power of vaccine virus. *J. Exp. Med.* **1929**, 50, 327-340.
- 19) Duera-Reynals F. *Am. J Cancer.* **1933**, 15, 2790-2797.
- 20) Chain E; Duthie E. S. *Br J Expl Path* **1940**, 21, 324-338.
- 21) Hobby G. L.; Dawson M. H.; Meyer K.; Chaffee E. The relationship between spreading factor and hyaluronadase. *J Exp. Med.*, **1941**, 73, 109-123.
- 22) Casals J. *Viruses and cancer. Span. Bio-chemical Society Press*, **1971**, 416-424.
- 23) Buettner, G. R. Catalytic metals, Ascorbate and free radicals: Combinations to Avoid. *Radiation*

*Research*, **1996**, 145, 532-541.

### III. RESEARCH 1 : *Lindera erythrocarpa* Makino

- 24) Liu, S. Y.; Hisada, S.; Inagaki, I. Terpenes of *lindera erythrocarpa*. *Phytochem.* **1973**, *12*, 233.
- 25) Komae, H.; Hayashi, N. Terpenes from *Lindera erythrocarpa*. *Phytochem.* **1972**, *11*, 853.
- 26) Liu, S. Y.; Hisada, S.; Inaki, I. *Phytochem. Constituents of Lindera erythrocarpa*. *Phytochem.* **1973**, *12*, 472.
- 27) Kim, S. J.; Joh, Y. G. *Food Sci. Biotechnol.* **1973**, *12*, 472.
- 28) Lee, H. H.; Tan, C. H. *J. Chem. Soc.* **1965**, 2743.
- 29) Oh, H. M.; Choi, S. K.; Lee, J. M.; Lee, S. K.; Kim, H. Y.; Han, D. C.; Kim, K. M.; Son, K. H.; Kwon, B. M. Cyclopentenediones, inhibitors of farnesyl protein transferase and anti-tumor compounds, isolated from the fruit of *Lindera erythrocarpa* Makino. *Bioorg. Med. Chem.* **2005**, *13*, 6182-6187.
- 30) 최광수; 권광일; 이종구; 이륜경; 최종동; 유문균; 임무혁; 김기주; 홍영표; 안영순. 한국 전통간장 제조시 맥아첨가방법이 간장의 성분과 식미에 미치는 영향. *J. Korean Soc. Agric. Chem. Biotechnol.* **2003**, *46*, 150.
- 31) Wang, S. Y.; Lan, X. Y.; Xiao, J. H.; Yang, J. C.; Kao, Y. T.; Chang, S. T. Antiinflammatory activity of *Lindera erythrocarpa* fruits. *Phytotherapy Res.* **2008**, *22*, 213-216.
- 32) Lee, S. M.; Baek, S. H.; Lee, C. H.; Lee, H. B.; Kho, Y. H. Cytotoxicity of lignans from *lindera erythrocarpa* Makino. *Natural Product Sciences.* **2002**, *8*(3), 100-102.
- 33) Oh, H. M.; Choi, S. K.; Lee, J. M.; Lee, S. K.; Kim, H. Y.; Han, D. C.; Kim, H. M.; Son, K. H.; Kwon, B. M. Kwon, B. M. Cyclopentenediones, inhibitors of farnesyl protein transferase and anti-tumor compounds, isolated from the fruit of *Lindera erythrocarpa* Makino. *Bioorganic&Medicinal Chemistry* **2005**, *13*, 6182-6187.
- 34) Aoyama, Y.; Konoike, T.; Kanda, A.; Naya, N.; Nakajima, M. Total synthesis of human chymase inhibitor methyllinderone and structure-activity relationships of its derivatives. *Bioorganic&medicinal chemistry letters* **2001**, *11*, 1695-1697.
- 35) Blois, M. S. Antioxidant determinations by the use of a stable free radical. *Nature* **1958**, 181, 1199-1200.
- 36) Cheng, Z. J.; Kuo, S. C.; Chan, S. C.; Ko, F. N.; Teng, C. M. Antioxidant properties of butein isolated from *Dalbergia odorifera*. *Biochem. Biophys. Acta.* **1998**, *1392*, 291-299.
- 37) Choi, S. Y.; Kang, S. H.; Park, S. Y.; Jin, Y. J.; Moon, S. W.; Kim, S. J. Antioxidant and inducible nitric oxide synthase inhibitory activities of ethanol extract of *Pisidium guajava* leaf. *Cheju Journal of Life Science* **2004**, *7*(1), 71-82.
- 38) Kim, S. B.; Kang, S. H.; Park, S. Y.; Choi, S. Y.; Kim, S. J.; Kim, W. T. Antioxidant Activity of

- Dragonfly Extracts. *Cheju Journal of Life Science* **2004**, 7(1), 35-51.
- 39) Wang, L.-Y.; Unehara, T.; Kitanaka, S. Anti-inflammatory Activity of New Guaianene Type Sesquiterpene from *Wikstroemia indica*. **2005**, *Chem. Pharm. Bull.* 53(1), 137-139.
- 40) Lee, S. M.; Na, M. K.; An, R. B.; Min, B. S.; Lee, H. K.; Antioxidant Activity of Two Phloroglucinol Derivatives from *Dryopteris crassirhizoma*. *Biol. Pharm. Bull.* **2003**, 26(9) 1354-1356.
- 41) Cals-Grierson, M. M.; Ormerod A. D. Nitric oxide function in the skin. *Elsevier Inc* **2004**, 10, 179-193.
- 42) Halaban, R.; Langdon, R.; Birchall, N.; Cuono C.; Bird, A.; Scott, G.; Moellmann, G.; Meguire, J. Basic fibroblast growth factor from normal human keratinocyte is a natural mitogen for melanocytes. *J. Cell Biol.* **1988**, 107, 1611-1619.
- 43) Kim, E. C.; Ahn, S. Y.; Hong, E. S.; Li, G. H.; Kim, E. K.; Row, K. H. Extraction of whitening agents from natural plants and whitening effect. *J. Kor. Ind. Eng. Chem.* **2005**, 16, 348-353.
- 44) Sakuma, K.; Ogawa, M.; Sugibayashi, K.; Yamada, K.; Yamamoto, K. Relationship between tyrosinase inhibitory action and oxidation-reduction potential of cosmetic whitening ingredients and phenol derivatives. *Arch Pharm Res.* **1990**, 22(4), 335-339.
- 45) Eisinger, M.; Marko, O. Selective proliferation of normal human melanocytes in vitro in the presence of phorbol ester and cholera toxin. *Proc. Natl. Acad. Sci USA* **1982**, 79(6), 2018-2022.
- 46) Gordon, P. R.; Mansur, C. P.; Gilchrist, B. A. Regulation of human melanocyte growth, dendricity, and melanization by keratinocyte derived factors *J. Invest Dermatol.* **1989** 92, 565-572.
- 47) Peter, S.; Barbara, A.; Gilchrist, B. A. Ultraviolet radiation directly induces pigment production by cultured human melanocytes. *J. Cellular physiology* **1987** 133, 88.
- 48) Imokawa, G.; Yada, Y.; Miyagishi, N. Endothelins secreted from human keratinocytes are intrinsic mitogens for human melanocytes. *J. Biol. Chem.* **1992** 267(34), 24675-24680.
- 49) Yoon, W. J. *Jeju national Univ. Doctoral dissertation* **2011**.
- 50) Yoon, W.J.; Lee, N. H.; Hyun, C. G. Limonene suppresses lipopolysaccharide-induced production of nitric oxide, prostaglandin E2, and pro-inflammatory cytokines in RAW264.7 macrophages. *J. of Oleo Science*, **2010**, 59(8), 415-421.
- 51) Gregoire, F. M.; Smas, C. M.; Sul, H. S. Understanding adipocyte differentiation. *physiol Rev.* **1998**, 78(3), 783-809.
- 52) Harmon, A. W.; Harp, J. B. Differential effects of flavonoids on 3T3-L1 adipogenesis and lipolysis. *AM J Physiol Cell Physiol*, **2001**, 280(4), 807-813.
- 53) Farmer, S. R. Regulation of PPARgamma activity during adipogenesis. *Inter. J. Obesity*, **2005**, 29(1), 13-16.
- 54) Kim, S. K.; Kong, C. S. Anti-adipogenic effect of dioxinohydroeckol via AMPK activation in 3T3-L1 adipocytes. *Chemico-Biological Interactions* **2010**, 186, 24-29.

- 55) Cuong, T. D.; Hung, T. M.; Lee, M. K.; Thao, N. T. P.; Jang, H. S.; Min, B. S. Cytotoxic compounds from the roots of *Pulsatilla koreana*. *Natural product Sciences* **2009**, 15(4), 250-255.
- 56) Lee, J. H.; Kim, Y. C.; Kim, M. Y.; Chung, H. S.; Chung, S. K. Antioxidative activity and related compounds of Apple pomace. *J. Food Sci. Technol.* **2000**, 32(4), 908-913.
- 57) Lee, S. M.; Baek, S. H.; Lee, C. H.; Lee, H. B.; Kho, Y. H. Cytotoxicity of lignans from *lindera erythrocarpa* Makino. *Natural Product Sciences.* **2002**, 8(3), 100-102.
- 58) Aoyama, Y.; Konoike, T.; Kanda, A.; Naya, N.; Nakajima, M. Total synthesis of human chymase inhibitor methylinderone and structure-activity relationships of its derivatives. **2001**, *Bioorganic&medicinal chemistry letters* 11, 1695-1697.
- 59) Arigoni, D.; Sagner, S.; Latzel, C.; Eisenreich, W.; Bacher, A.; Zenk, M. H. Terpenoid biosynthesis from 1-deoxy-D-xylulose in higher plants by intramolecular skeletal rearrangement. *Proc. Natl. Acad. Sci. USA*, **1997**, 94, 10600-10605.
- 60) Kim, M.; Lee, S.; Hwang, Y.; Lee, H.; Baek, B. Isolation of xanthine oxidase inhibitors from *Ginkgo biloba* leaves-derived components. *J. Food Science and Nutrition.* **2002**, 7(1).
- 61) Leong, Y. W.; Harrison, L. J.; Bennett, G. J.; Kadir, A. A.; Connolly, J. D. A dihydrochalcone from *Lindera lucida* *Phytochemistry* **1998**, 47(5), 891-894.
- 62) Lee, S. M.; Baek, S. H.; Lee, C. H.; Lee, H. B.; Kho, Y. K. Cytotoxicity of Lignans from *Lindera erythrocarpa* Makino. *Natural Product Sciences* **2002**, 8, 100-102.
- 63) Kitajima, J.; Takamori, Y.; Tnaka, Y. Studies on the constituents of *Acanthopanax sciadophylloides* Fr. et SAV. Leaves. *Yakukaku Zasshi* **1989**, 109(3), 188-191.
- 64) Demirezer, L. O.; Kuruuzum-Uz, A.; Guvenalp, Z.; Suleyman, H. Bioguided fractionation of *polygonum alpinum* and isolation and structure elucidation of active compounds. *Pharmaceutical Biology*, **2006**, 44, 462-466.
- 65) Ahn, M. J.; Yang, W. J.; Kang, S. H.; Kang, M. C.; Ko, R. K.; Kim, G. O.; Shin, T. K. *Lindera erythrocarpa* Makino extract reduces obesity induced by high-fat diet in rats. *OPEM*, **2010**, 10(4), 288-293.
- 66) 최용화; 권순열; 김진호; 백남인; 최경자; 조광연; 이병무. 비목나무(*Lindera erythrocarpa*) 잎으로부터 항진균성 활성물질의 분리. *J. Korean Soc. Agric. Chem. Biotechnol.* **2003**, 46(2), 150-153.
- 67) Jo, H. *Kyounghee Univ. Master's thesis* **2004**.
- 68) Moon, E. J.; Lee, Y. M.; Lee, O. H.; Lee, M. J.; Lee, S. K.; Chung, M. H.; Park, Y. I.; Sung, C. K.; Choi, J. S & Kim, K. W. A novel angiogenic factor derived from Aloe vera gel:  $\beta$ -sitosterol, a plant sterol. *Angiogenesis* **1999**, 3, 117-123.
- 69) Bei-Bei, Z.; Yuan, D.; Zhi-Xin L. Chemical Constituents of *Saussurea eopygmaea*. *Chinese Journal of Natural Medicines* **2011**, 9(1).
- 70) Sultana, N.; Lee, N. H. Antielastase and free radical scavenging activities of compounds from the

- stems of *Cornus kousa*. *Phytother. Res.* **2007**, *21*, 1171.
- 71) Kim, Y. H.; Kim, K. H.; Han, C. S.; Park, S. H.; Yang, H. C.; Lee, B. Y.; Eom, S. Y.; Kim, Y. S.; Kim, J. H.; Lee, N. H. *J. Cosmet. Sci.* **2008**, *59*, 419.
- 72) Kumar, K. J.; Yang, J. C.; Chu, F. H.; Chang, S. T.; Wang, S. Y. Lucidone, a novel melanin inhibitor from the fruit of *Lindera erythrocarpa* Makino. *Phytother Res.* **2009**, *24*(6), 1089-1098.
- 73) Kim, J. M.; Ko, R. K.; Hyun, J. W.; Lee, N. H. Identification of new dibenzofurans from *Distylium racemosum*. *Bull. Korean Chem. Soc.* **2009**, *30*(1), 261.
- 74) Mariano, C.; Mariel M.; Viviana C. B.; Leonor P. R. Antitumor activity of some natural flavonoids and synthetic derivatives on various human and murine cancer cell lines. *Bioorganic & Medicinal Chemistry* **2006**, *14*(9), 2966-2971.
- 75) Kim, J. A.; Jung, Y. S.; Kim, M. Y.; Yang, S. Y. Lee, S.; Kim, Y. H. Protective Effect of Components Isolated from *Lindera erythrocarpa* against Oxidative Stress-induced Apoptosis of H9c2 Cardiomyocytes. *Phytother Res.* **2011**, *25*(11), 1612-1617.
- 76) Ichino, K.; Tanaka, H.; Ito, K.; Tanaka, T.; Mizuno M. Two New Dihydrochalcones from *Lindera erythrocarpa*. **1988**, *51*(5), 915-917.

### III. RESEARCH 2 : *Cornus macrophylla* Wall

- 77) Kim, H. Y.; Oh, J. H. Screening of Korean forest plants for rat lens aldose reductase inhibition. *Biosci Biotechnol Biochem.* **1999**, *63*(1), 184-188.
- 78) Jo, H. *Kyunghee Univ. Master's thesis* **2004**.
- 79) Jin, L.; Han, J. G.; Ha, J. H.; Jeong, H. S.; Kim, C. H.; Kwon, M. C.; Lee, H. J.; Kang, H. Y.; Choi, G. P.; Lee, H. Y. Anticancer and immune-modulatory activities of extracts from various parts of *Cornus macrophylla* Wall. *Korean J. Medicinal Crop Sci.* **2008**, *16*(5), 349-355.
- 80) Oh, S. J.; Koh, S. C. Screening of Antioxidative Activity and  $\alpha$ -Amylase Inhibitory Activity in Angiosperm Plants Native to Jeju Island. *Korean J. Plant Res.* **2009**, *22*(1), 71-77.
- 81) Oh, H. M.; Choi, S. K.; Lee, J. M.; Lee, S. K.; Kim, H. Y.; Han, D. C.; Kim, K. M.; Son, K. H.; Kwon, B. M. Biosynthesis of  $\beta$ -sitosterol and stigmasterol in croton sublyratus proceeds via a mixed origin of isoprene units. *Bioorg. Med. Chem.* **2005**, *13*, 6182-6187.
- 82) Kim, J. H.; Kim, D. H.; Baek, S. H.; Lee, H. J.; Kim, M. R.; Kwon, H. J.; Lee, C. H. Rengyolone inhibits inducible nitric oxide synthase expression and nitric oxide production by down-regulation of NF- $\kappa$ B and p38 MAP kinase activity in LPS-stimulated RAW264.7 cells. *Biochemical pharmacology* **2006**, *71*, 1198-1205.
- 83) Kim, J. H.; Lee, C. H. Rengyolone inhibits apoptosis via etoposide-induced caspase downregulation. *J. Microbiol. Biotechnol.* **2009**, *19*(3), 286-290.
- 84) Kim, J. H.; Kho, Y. H.; Kim, M. R.; Kim, H. A.; Lee, S. M.; Lee, C. H. K. A caspase inducing



inhibitor isolated from *Forsythiae fructus*. *Korean J. Food Sci. Technol.* **2002**, 34(1), 114-117.

- 85) Hase, T.; Kawamoto, Y.; Ohtani, K.; Kasai, R.; Yamasaki, K.; Picheansoonthon, C. Cyclohexylethanoids and related glucosides from *Millingtonia hortensis*. *Phytochem.* **1995**, 39(1), 235-241.
- 86) Yumiko, N.; Sumiko, T. Method for Analysis of Tannic Acid and Its Metabolites in Biological Samples ; Application to Tannic acid Metabolism in the Rat. *Agr. and food chem.* **2003**, 331-339.
- 87) Taghvan, G.; Madgavan, V.; Annie, S. ctivity Guided Isolation of Antioxidant Tannoid Principles from *Anogeissus latifolia*. *Natural Product Sciences* **2005**, 11(3), 174-178.
- 88) Choi, B. R. Antioxidant Constituents from *Portulaca oleracea*. *Natural Product Sciences* **2005**, 11, 4, 229-232.
- 89) Oh, G.; Kim, S.; Chun, B.; Park, C.; Son, K. Isolation of Antimicrobial Components from *Moutan Cortex*. *Kor. J. Pharmacogn.* **1999**, 30, 3, 340-344.
- 90) 방면호; 송정춘; 이상양; 박남규; 백남인. 작약뿌리로부터 항산화활성 물질의 분리. *한국농화학회지*, **1999**, 42, 2, 170.
- 91) Bilia, A. R.; Mendez, J.; Morelli, I. Phytochemical investigations of *Licania* genus. Flavonoids and triterpenoids from *Licania carii*. *Pharmaceutica Acta Helvetiae* **1996**, 71(3), 191-197.
- 92) Nasr, C.; Haag-Berrurier, M.; Lobstein-Guth, A.; Anton, R. Kaempferol coumaroyl glucorhamnoside from *Ginkgo biloba* A. *Phytochem.* **1986**, 25, 3, 770.

### III. RESEARCH 3 : *Aster subulatus* Michx

- 93) Kim, H. S.; Lim, D. O.; Park, M. S. The distribution and management methods of naturalized plants in Jeollanamdo, Korea. *Kor. J. Plant Res.* **2007**, 20, 353.
- 94) El-Sayed, N. H.; Lenherr, A.; Sundberg, S.; Mabry, T. Flavonoids of *Aster subulatus*. *J. Biochem. Syst. Ecol.* **1987**, 15, 549.
- 95) Kwon, Y. S.; In, K. K.; Kim, C. M. Chemical constituents from the roots of *Ostericum koreanum*. *Kor. J. Pharmacogn.* **2000**, 31(3), 284-287.
- 96) Zhang, Z.; Li, S.; Ownby, S.; Wang, P.; Yuan, W.; Zhang, W.; Scott Beasley, R. Phenolic compounds and rare polyhydroxylated triterpenoid saponins from *Eryngium yuccifolium*. *Phytochem.* **2008**, 69(10), 2070-2080.
- 97) Tsukamoto, S.; Tomise, K.; Aburatani, M.; Onuki, H.; Hirorta, H.; Ishiharajima, E.; Ohta, T. Isolation of cytochrome P450 inhibitors from strawberry fruit, *Fragaria ananassa*. *J. Nat. Prod.* **2004**, 67(11), 1839-1841.
- 98) Rehman, A.-U.; Malik, A.; Riaz, N.; Ahmad, H.; Nawaz, S. A.; Choudhary, M. I. Lipoxxygenase inhibiting constituents from *Indigofera hetrantha*. *Chem. Pharm. Bull.* **2005**, 53, 263.
- 99) Ham, Y. M.; Baik, J. S.; Hyun, J. W.; Lee, N. H. Isolation of a New Phlorotannin,

- Fucodiphloretol G, from a Brown Alga *Ecklonia cava*. *Bull. Korean Chem. Soc.* **2007**, 28, 1595.
- 100) Ko, R. K.; Lee, N. H. Isolation of a New secolignan compound from *Quercus glauca*. *Bull. Korean Chem. Soc.* **2008**, 29, 2531.
- 101) Scarpati, M. L.; Guiso, M. Quinic acids of coffee (isochlorogenic acid). *Tetrahedron Lett.* **1964**, 5, 2851.
- 102) Kodoma, M.; Wada, H.; Otani, H.; Kohmoto, K.; Kimura, Y. 3,5-Di-*O*-caffeoylquinic acid, an infection-inhibiting factor from *Pyrus pyrifolia* induced by infection with *Alternaria alternata*. *Phytochem.* **1998**, 47(3), 371-373.
- 103) Ishikawa, A.; Yamashita, H.; Hiemori, M.; Inagaki, E.; Kimoto, M.; Okamoto, M.; Tsuji, H.; Memon, A. N.; Mohammadi, A.; Natori, Y. Characterization of inhibitors of postprandial hyperglycemia from the leaves of *Nerium indicum*. *J. Nutr. Sci. Vitamino.* **2007**, 53, 166-173.
- 104) Lee, S. E.; Chung, T. Y. Identification of an antioxidative compound, 3,5-Dicaffeoylquinic acid from *Aster scaber* Thunb. *Agric. Chem. Biotechnol.* **2002**, 45(1), 18-22.
- 105) Gao, H.; Huang, Y. N.; Gao, B.; Xu, P. Y.; Inagaki, C.; Kawabata, J.  $\alpha$ -Glucosidase inhibitory effect by the flower buds of *Tussilago farfara* L. *Food chem.* **2008**, 106, 1195-1201.
- 106) Kim, H. J.; Lee, Y. S. Identification of new dicaffeoylquinic acids from *Chrysanthemum morifolium* and their antioxidant activities. *Planta Med.* **2005**, 71, 871.
- 107) Lee, J. Y.; Song, D. G.; Lee, E. H.; Jung, S. H.; Nho, C. W.; Cha, K. H.; Pan, C. H. Inhibitory Effects of 3,5-*O*-Dicaffeoyl-*epi*-quinic acid from *Gymnaster koraiensis* on AKR1B10. *J. Korean Soc. Appl. Biol. Chem.* **2009**, 52(6), 731-734.
- 108) Kim, D. K.; Shin, T. Y. Flavonoids from *Sorbaria sorbifolia* var. *stellipila*. *Kor. J. Pharmacogn.* **1998**, 29(3), 254-257.

### III. RESEARCH 4 : *Ishige sinicola* (Setchell et Gardner) Chihara

- 109) Jo, J. Y. *Pukyong Univ. Doctor's thesis* **2002**.
- 110) 차선희; 안긴내; 허수진; 김길남; 이기완; 송춘복; 김소미; 전유진, 제주 자생 해양 녹조류와 갈조류 추출물로부터의 항고혈압 활성. *한국식품영양과학회지* **2006**, 35(3), 307-314.
- 111) Heo, S. J.; Kim, J. P.; Jung, W. K.; Lee, N. H.; Kang, H. S.; Jun, E. M. Park, S. H.; Kang, S. M.; Lee, Y. J.; Park, P. J.; Jeon, Y. J. Identification of chemical structure and free radical scavenging activity of Diphloretohydroxycarmalol isolated from a brown alga, *Ishige okamurae*. *J. Microbiol. Biotechnol.* **2008**, 18(4), 676-681.
- 113) Huh, S. J. *Jeju National Univ. Doctor's thesis* **2008**.
- 114) Ahn, M. J.; Yoon, K. D.; Kim, C. Y.; Kim, J. H.; Shin, C. G.; Kim, J. Inhibitory activity on HIV-1 reverse transcriptase and integrase of a carmalol derivative from a Brown Alga, *Ishige okamurae*. *J. Phytother. Res.* **2006**, 20, 711-713.

- 115) Park, H. M.; Son, M. W.; Kim, D. H.; Kim, S. H.; Kim, S. H.; Kwon, H. C.; Kim, S. Y. Fatty acid components of hardy kiwifruit (*Actinidia arguta*) as IL-4 production inhibitor. *Biomol Ther.* **2011**, 19(1), 126-133.
- 116) Song, M. C.; Han, M. W.; Yang, H. J.; Lee, D. Y.; Rho, Y. D.; Baek, N. I. 생명자원과학연구 논문집 **2007**, 26, 42-46.
- 117) Jung, S.; Kang, S. T.; Choi, C. Y.; Oh, K. Y.; Cho, J. K.; Rengasamy, R.; Park, K. H. Linoleic Acid from Bamboo (*Phyllostachys Bambusoides*) Displaying Potent  $\alpha$ -Glucosidase Inhibition. *J. Life Sci.* **2009**, 19(5), 680-683.
- 118) Nalewajko-Sieliwoniuk, E.; Nazaruk, J.; Antypiuk, E.; Kojlo, A. Determination of phenolic compounds and their antioxidant activity in *Erigeron acris* L. extracts and pharmaceutical formulation by flow injection analysis with inhibited chemiluminescent detection. *J. Pharma. and Biomedical Anal.* **2008**, 48, 579-586.
- 119) Zou, Y.; Qian, Z. J.; Li, Y.; Kim, M. M.; Lee, S. H.; Kim, S. K. Antioxidant effect of phlorotannins isolated from *Ishige okamurae* in free radical mediated oxidative systems. *J. Agric. Food. Chem.* **2008**, 56, 7001-7009.

### III. RESEARCH 5 : *Dictyota coriacea*

- 120) 이용필, 제주의 바닷말, *아카데미서적* **2008**, 479.
- 121) 이종수, 해조의 화학과 이용, *효일* **2008**, 458.
- 122) 강민철; 이주엽; 고려경; 김행범; 홍승호; 김기욱, 제주도 근해에 자생하는 참가죽그물바탕말 (*Dictyota coriacea*) 추출물의 멜라닌 억제 효과 및 항염증 효과. *한국생물공학회* **2008**, 23(4), 311-316.
- 123) Kim, J. Y. *Hanbat national Univ. M. S. thesis* **2006**.
- 124) Lee, S. B.; Nho, C. W.; Lee, S. B.; Lee, J. Y.; Sonmg, D. G.; Pan, C. H.; Kim, M. C.; Lee, E. H.; Jung, S. H.; Kim, H. S.; Kim, Y. S.; Um, Y. H. Cancer chemopreventive effects of korean seaweed extracts. *Food Sci. Biotech.* **2008**, 17(3), 613-622.
- 125) Krahulec, S.; Armao, G. C.; Weber, H.; Klimacek, M.; Nidetzky, B. Characterization of recombinant *Aspergillus fumigatus* mannitol-1-phosphate 5-dehydrogenase and its application for the stereoselective synthesis of protio and deuterio forms of D-mannitol 1-phosphate. *Carbohydrate Res.* **2008**, 343, 1414-1423.
- 126) Tringali, C.; Oriente, G.; Piattelli, M.; Geraci, C.; Nicolosi, G.; Breitmaier, E. *Can. J. Chem.* **1988**, 66(11), 2799-2802.
- 127) Midland, S. L.; Wing, R. M.; Sims, J. J. New crenulides from the sea hare *Aplysia vaccaria*. *J. Org. Chem.* **1983**, 48(11), 1907.
- 128) Jones, L.; Bartholomew, B.; Latif, Z.; Sarker, S. D.; Nash, R. Constituents of *Cassia laevigata*. *J.*

*Fitoterapia* **2000**, 71, 580-583.

129) Erosa-Rejón, G.; Peña-Rodríguez, L. M.; Sterner, O. Secondary Metabolites from *Heliotropium angiospermum*. *J. Mex. Chem. Soc.* **2009**, 53(2), 44-47.

### III. RESEARCH 6 : *Styrax obassia* Siebold & Zucc

130) Kim, H.; Song, M. J.; Potter, D. Medicinal efficacy of plants utilized as temple food in traditional Korean Buddhism. *J. of Ethnopharmacology* **2006**, 104, 32-46.

131) Yang, E. J.; Yim, E. Y.; Song, G.; Kim, G. O.; Hyun, C. G. Inhibition of nitric oxide production in lipopolysaccharide-activated RAW264.7 macrophages by Jeju plant extracts. *Interdiscip Toxicol.* **2009**, 2(4), 245-249.

132) Akgul, Y. Y.; Anil, H. Benzofurans and another constituent from seeds of *Styrax officinalis*. *Phytochemistry* **2003**, 63(8), 939-943.

133) Choi, H. D.; Ha, M. C.; Seo, P. J.; Son, B. W.; Song, J. C. Total synthesis of a demethoxy-egonol from *Styrax obassia*. *Arch Pharm Res.* **2000**, 23(5), 438-440.

134) Yoshikawa, K.; Hirai, H.; Tanaka, M.; Arihara, S. Antisweet natural products. XV. structures of Jegosaponins A-D from *Styrax japonica* SIEB. et ZUCC. *Chem. Pharm. Bull.* 2000, 28(7), 1093-1096.

135) Park, S. Y. Structural identification and antioxidant activity of the extractive from *Styrax obassia* Sieb. et Zucc. *Korea Univ. M. S. thesis* **2006**.

136) Jang, S. H. Effects of *Curcuma longa* and *Magnolia obovata* on skin aging. *Seoul Nat. Univ. M. S. thesis* **2010**.

137) Kim, S. N. Simultaneous quantification of major ginsenosides in *Panax ginseng* C.A. Meyer and their effects on lipid accumulation in 3T3-L1 adipocytes. *Seoul Nat. Univ. M. S. thesis* **2008**.

138) Jang, J. Y. Partially purified oriental herbs inhibit melanogenesis in B16F10 cells. *Busan Univ. Doctor's thesis* **2010**.

139) Shin, J. Y. Analysis of anti-obesity of some foodstuffs using 3T3-L1 adipocytes. *Catholic of daegu Univ. M. S. thesis* **2006**.

140) Kim, J. M.; Ko, R. K.; Jung, D. S.; Kim, S. S.; Lee, N. H. Tyrosinase inhibitory constituents from the stems of *maackia fauriei*. *Phyto. Res.* **2010**, 24, 70-75.

141) Ko, R. K. Isolation and identification of cosmetically active compounds from *Quercus glauca*, *Distylium raemosu* and *Nymphaea tetragona*. *Jeju Nat. Univ. M. S. thesis* **2008**.

142) Yu, S. W. Chemical components of fruits and leaves of *Euodia daniellii*. *Seoul Nat. Univ. Doctor's thesis* **2003**.

143) Lee, Y. J. Chemical constituents from the flower buds of *Lonicera japonica* and their

5-lipoxygenase inhibitory activities. *Seoul Nat. Univ. Doctor's thesis* **2010**.

144) Lee, S. A. Regulatory mechanism of acteoside and ascorbic acid on melanogenesis in B16F10 melanoma cells. *Chonbuk Nat. Univ. Doctor's thesis* **2011**.

145) Kim, S. H. Anti-oxidant, Anti-wrinkle and whitening effects of cosmetics using black garlic extract on skin care. *Dongduk woman Univ. Doctor's thesis* **2011**.

146) Chon, J. W. Anti-obesity effect of methanol extract of gromwell (*Lithospermum erythrorhizon* Sieb. et Zucc) in 3T3-L1 cells and obese mice models. *Kyung-Hee Univ. Doctor's thesis* **2010**.

147) An, S. M. Anti-melanogenic effects of *p*-coumaric acid and its derivatives. *kyunpook Nat. Univ. Doctor's thesis* **2010**.

Appendix 1 (*Lindera erythrocarpa* Makino)

Journal Bulletin of the Korean Chemical Society (BKCS) Grade SCI Language English  
 Year 2010 Volume 32 Number 3 Page 739

Notes

Bull. Korean Chem. Soc. 2010, Vol. 31, No. 3 739  
 DOI 10.5012/bkcs.2010.31.03.739

A New Diarylpropane from the Stem Bark of *Lindera erythrocarpa* Makino<sup>†</sup>

Ryeo Kyeong Ko, Min-Chul Kang, Yeon-Jun Jin, Ho-Min Choi, Bong-Seok Kim, Jong-Heon Han, Gi-Ok Kim,<sup>\*</sup> and Nam Ho Lee<sup>†,\*</sup>

Jeju Bio-Industry Development Center, Hi-Tech Industry Development Institute, Jeju 690-121, Korea

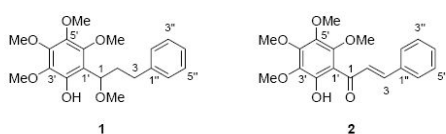
<sup>\*</sup>E-mail: kingk350@jejuhidi.or.kr

<sup>†</sup>Department of Chemistry, Cheju National University, Jeju 690-756, Korea. <sup>\*</sup>E-mail: namho@cheju.ac.kr

Received October 1, 2009, Accepted December 23, 2009

**Key Words:** *Lindera erythrocarpa*, Lauraceae, Diarylpropane, Kanakugiol

*Lindera erythrocarpa* Makino (Lauraceae) is a deciduous tree widely distributed in Asian countries including China, Japan and Korea. This tree has been utilized as the timber for household furniture in the local communities. Its dried fruits have been used for the alleviation of neuralgia and stomachache as a folk medicine in Japan.<sup>1</sup> In the previous chemical studies, different type of compounds such as terpenes,<sup>2</sup> cyclopentenoides<sup>3</sup> and unsaturated fatty acids,<sup>4</sup> have been identified from this plant. Recently, the isolated cyclopentenoides, linderone and its derivatives, were reported to have anti-tumor,<sup>5</sup> anti-fungus<sup>6</sup> and anti-inflammation<sup>7</sup> activities. In continuation of our efforts searching for bioactive compounds from plants in Jeju Island,<sup>8</sup> we became interested in the antioxidative ethanol extract prepared from the stem bark of *L. erythrocarpa*. As a result of phytochemical investigation for this extract, we herein report the isolation of a new compound, 1-(2-hydroxy-3,4,5,6-tetramethoxyphenyl)-1-methoxy-3-phenylpropane (**1**), named as erythrane. A known compound, kanakugiol (**2**) was also isolated in this study.



Compound **1** was obtained as a greenish viscous oil. It showed a [M+Na]<sup>+</sup> peak at *m/z* 385.1629 (calcd *m/z* 385.1627) in the HR-FABMS, consistent with the molecular formula C<sub>20</sub>H<sub>26</sub>O<sub>6</sub> (eight unsaturations). Examination of <sup>13</sup>C and DEPT NMR spectra showed 18 signals accounting for ten aromatic carbons, five methoxy carbons, two methylene carbons and one oxygen-bearing methine carbon (Table 1). The presence of aromatic ring(s) were also supported by the UV absorption maxima at 216 and 285 nm. One of the aromatic rings was inferred as phenyl group based on the observation of its typical <sup>13</sup>C NMR peaks ( $\delta$  126.6, 129.2, 129.4, 142.8) coupled with <sup>1</sup>H NMR signals at  $\delta$  7.16 (1H, t, *J* = 7.5 Hz), 7.22 (2H, d, *J* = 7.5 Hz) and 7.27 (2H, t, *J* = 7.5 Hz). The other aromatic ring was identified as a fully substituted benzene by <sup>13</sup>C and DEPT NMR experi-

ments. Besides the above mentioned two aromatic rings, a linear spin chain, -CH-CH<sub>2</sub>-CH<sub>2</sub>-, was also characterized by <sup>1</sup>H, <sup>13</sup>C and COSY NMR data.

The connection of these subunits was established using HMBC (heteronuclear multiple bond correlations) as well as NOESY NMR experiments (Figure 1). A methoxy group at  $\delta_{\text{H}}$  3.34 is attached to the methine carbon ( $\delta$  78.9, C-1) in the propyl chain, which was confirmed by their HMBC cross peak. The observation of <sup>2</sup>JHMBC correlation between H-1 ( $\delta$  4.71) and

Table 1. 1D and 2D NMR data for **1** in acetone-*d*<sub>6</sub>

No	$\delta_{\text{C}}$ (mult) <sup>a</sup>	$\delta_{\text{H}}$ (int, mult, <i>J</i> in Hz)	HMBC (H→C)
1	78.9 (d)	4.71 (1H, dd, 8.5, 4.5)	C-2, C-3, C-1'
2	37.8 (t)	1.98 (1H, m), 2.26 (1H, m)	C-1, C-3, C-1'
3	32.8 (t)	2.65 (1H, ddd, 15.0, 9.0, 7.5) 2.82 (1H, ddd, 15.0, 9.5, 4.0)	C-1, C-2
1-OCH <sub>3</sub>	57.5 (q)	3.34 (3H, s)	C-1
1'	115.3 (s)	-	
2'	146.5 (s)	-	
3'	138.6 (s)	-	
4'	140.3 (s)	-	
5'	148.0 (s)	-	
6'	148.4 (s)	-	
2''-OH	-	8.8 (1H, s)	C-1', C-2', C-3'
3''-OCH <sub>3</sub>	61.4 (q)	3.78 (3H, s)	C-3'
4''-OCH <sub>3</sub>	61.4 (q)	3.76 (3H, s)	C-4'
5''-OCH <sub>3</sub>	61.5 (q)	3.87 (3H, s)	C-5'
6''-OCH <sub>3</sub>	61.1 (q)	3.72 (3H, s)	C-6'
1''	142.8 (s)	-	
2'' & 6''	129.4 (d)	7.22 (2H, d, 7.5)	
3'' & 5''	129.2 (d)	7.27 (2H, t, 7.5)	C-3, C-1''
4''	126.6 (d)	7.16 (1H, t, 7.5)	

<sup>a</sup>Determined by DEPT experiments.

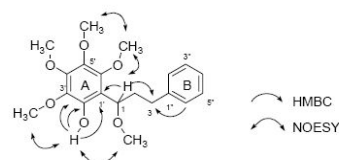


Figure 1. Key HMBC and NOESY correlations in compound **1**.

<sup>†</sup>This paper is dedicated to Professor Sunggak Kim on the occasion of his honorable retirement.

Appendix 2 (*Lindera erythrocarpa* Makino)

Journal	KSBB Journal	Grade	SCIE	Language	Korean
Year	2010	Volume	25	Number	Page
					330 - 336

KSBB Journal 2010, 25: 330-336

KSBB

## 비목나무 (*Lindera erythrocarpa* Makino) 껍질에서 분리한 신규화합물 (Jeju-Erythrane)의 멜라닌 생합성 억제 효과

강민철 · 고려경 · 김수경 · 최호민 · 진영준 · 한중헌 · 김봉석 · 이남호<sup>1</sup> · 김기옥\*

(재)제주테크노파크 생물산업진흥센터, <sup>1</sup>제주대학교 자연과학대학 화학과

## Melanin Biosynthesis Inhibitory Effect of New Compound (Jeju-Erythrane) Isolated from Bark of *Lindera erythrocarpa* Makino

Min-Chul Kang, Ryeo Kyeong Ko, Su-Gyeong Kim, Ho-Min Choi, Yeong-Jun Jin, Jong-Heon Han, Bong-Seok Kim, Nam Ho Lee<sup>1</sup>, and Gi-Ok Kim\*

Jeju Bio-Industry Development Center, Jeju Technopark, Jeju 690-121, Korea

<sup>1</sup>Department of Chemistry, College of Natural Sciences, Cheju National University, Jeju 690-756, Korea

**Abstract** In this study, a new compound, 1-(2-hydroxy-3,4,5,6-tetramethoxyphenyl)-1-methoxy-3-phenylpropane; (Jeju-Erythrane) was isolated and identified from the bark of *Lindera erythrocarpa* Makino. Also, we investigated the effects of Jeju-Erythrane on alpha melanocyte-stimulating hormone (MSH)-induced melanogenesis in mouse B16F10 melanoma cells. The new compound dose dependently inhibited the tyrosinase activity and melanin synthesis in B16F10 cells. The new compound showed inhibitory effect on the Tyrosinase and TRP-1 gene transcription but not on the TRP-2 gene. These results suggest that the new compound of *L. erythrocarpa* could be used as a functional biomaterial in developing skin whitening agent.

**Keywords:** *Lindera erythrocarpa* Makino, Jeju-Erythrane, tyrosinase activity, melanin content

### 서 론

인간의 피부색깔은 환경, 인종, 성별 등의 요인과 멜라닌, 카로틴 및 헤모글로빈 양과 같은 여러 가지 요인에 의해 결정되지만 피부의 과색소 침착과 관련된 주요한 원인은 표피 내 멜라닌색소의 이상적 증가에 기인한다. 과도한 melanin 합성은 인체에 기미, 주근깨, 피부반점을 형성하고 피부노화를 촉진하며 피부암 유발에 관여하는 것으로 알려져 있다 [1-3]. 멜라닌 색소의 생합성은 tyrosinase 효소를 비롯하여 tyrosinase-related protein 1 (TRP1)과 dopachrome tautomerase (TRP2)에 의하여 조절되고 있으며, 그중 tyrosinase는 tyrosine을

기질로 하여 L-dopaquinone으로 전이되는 초기 생합성과 정이후 dihydroxyindole의 산화에 작용한다 [4-6]. 따라서 tyrosinase 활성 억제제를 찾는 연구가 미백제의 개발에 있어서 중요한 부분을 차지하고 있으며, 현재 계속 알려지고 있는 tyrosinase 저해제로 hydroquinone, 4-hydroxyanisole, ascorbic acid 유도체, kojic acid, azelaic acid, corticosteroid, retinoids, arbutin, catechin, 3,4,5-trimethoxy cinnamate thymol ester 등이 있으나, 이들의 안전성과 경제성 등에 문제가 많아 사용에 있어서 어려움이 있다 [7-11]. 또한 현재 기능성 식품, 기능성 화장품 및 치료제 등 각 분야에서 인공물질이 아닌 천연 물질을 이용한 연구가 활발히 진행되어지고 있다 [12-14].

천연 항산화제로는  $\alpha$ -tocopherol, vitamin C, carotenoids, flavonoids 등이 알려져 있는데, 이러한 항산화 효과가 있는 물질들은 동식물에 널리 분포되어 있으며, 특히 많은 연구가 이루어진 분야는 식물성 물질이다. 식물 유래의 2차 대사산

\*Corresponding author

Tel: +82-64-720-2333, Fax: +82-64-720-2331

e-mail: Kingk350@jejubidi.or.kr

### Appendix 3 (*Lindera erythrocarpa* Makino)

Journal	Oriental Pharmacy and Experimental Medicine (OPEM)	and	Grade	SCIE	Language	English	
Year	2010	Volume	10	Number	4	Page	288



*Oriental Pharmacy and Experimental Medicine* 2010 **10**(4), 288-293  
DOI 10.3742/OPEM.2010.10.4.288

### ***Lindera erythrocarpa* Makino extract reduces obesity induced by high-fat diet in rats**

Meejung Ahn<sup>1</sup>, Wonjun Yang<sup>2</sup>, Sohi Kang<sup>2</sup>, Min-Chul Kang<sup>3</sup>, Ryeo Kyeong Ko<sup>3</sup>, Gi-Ok Kim<sup>3\*</sup> and Taekyun Shin<sup>2,3\*</sup>

<sup>1</sup>Department of Anatomy, College of Medicine, Jeju National University, Jeju 690-756, South Korea; <sup>2</sup>Department of Veterinary Anatomy, College of Veterinary Medicine and Veterinary Medical Research Institute, Jeju National University, Jeju 690-756, South Korea; <sup>3</sup>Bio-industry Development center, Jeju Technopark, Jeju 690-121, South Korea

Received for publication September 15, 2010; accepted December 6, 2010

#### SUMMARY

*Lindera erythrocarpa* Makino (LE) is widely distributed on Jeju Island, where it has been used for various traditional therapies. Effects of a crude extract of LE were examined in rats with obesity induced by a high-fat diet (HFD). Anti-obesity effects were followed in rats receiving orally administered vehicle, 100mg/kg extract, or 250 mg/kg LE extract, for 56 days. LE extract (250 mg/kg) suppressed increases in body weight and epididymal fat, with amelioration of fatty changes in the liver. Additionally, serum levels of alanine aminotransferase, aspartate aminotransferase, and total cholesterol were significantly decreased compared with those of vehicle-treated groups ( $p < 0.05$ ). These results suggest that oral administration of LE extract reduced rat obesity induced by HFD, possibly through the reduction of fat accumulation.

**Key words:** *Lindera erythrocarpa* Makino; Obesity; Rat; Cholesterol

#### INTRODUCTION

Obesity is considered to be a disorder of energy balance, occurring when energy expenditure is no longer in equilibrium with daily energy intake, affecting body-weight homeostasis (Van *et al.*, 2008). Obesity can be induced by the intake of high dietary fat, relative to internal fat metabolism. Obesity also refers to the status of an organism that

has accumulated body fat due to various reasons; the primary cause is a high-fat diet. Obesity is reaching epidemic proportions worldwide, and is correlated with various co-morbidities, among which the most relevant are dyslipidemia (Fried *et al.*, 2007), diabetes mellitus type 2 (Pagotto *et al.*, 2008), fatty liver (Marovic, 2008), and cardiovascular diseases such as heart failure and coronary heart disease (Artham *et al.*, 2008).

There have been many studies exploring the potential of various plant extracts for the development of anti-obesity drugs (Birari and Bhutani, 2007). Simple medicinal preparations, from sources including grape-seed (Terra *et al.*, 2010), *Aesculus hippocastanum* (Avci *et al.*, 2010), *Crocus sativus* (Gout *et al.*, 2010), and *Alpinia officinarum* (Xia *et al.*, 2010), often mediate beneficial responses due to

\*Correspondence: Taekyun Shin, Department of Veterinary Anatomy, College of Veterinary Medicine and Veterinary Medical Research Institute, Jeju National University, Jeju 690-756, South Korea. Tel: +82-64 754 3363; Fax: +82- 64 756-3354; E-mail: shint@jejunu.ac.kr  
#Co-correspondence: Gi-Ok Kim, Bio-industry Development center, Jeju Technopark, Jeju 690-121, South Korea. Tel: +82-64 720 2333; Fax: +82- 64 720 2331; E-mail: kimgk350@jejuhidi.or.kr



Appendix 4 (*Lindera erythrocarpa* Makino)

Domestic Patent

Nation Korea

Language Korean

Application No. 10-2008-0087480

Application Date 04. Sep. 2008

International Patent

Nation China, Japan

Language Chinese, Japanese

Application No. PCT/KR2009/005027

Application Date 04. Sep. 2008

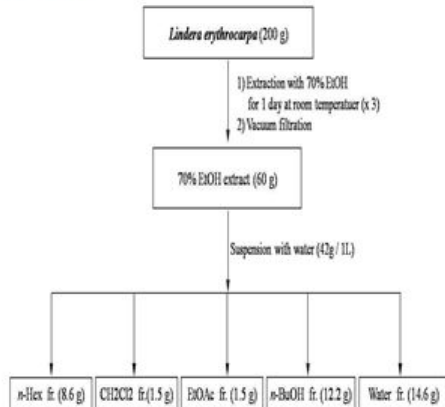
발명의 명칭 비목나무 유래 추출물, 분획물 또는 화합물을 함유하는 피부 미백용 조성물 (A composition for skin whitening comprising extract, fraction or compound from *Lindera erythrocarpa*)

Int. Cl. [A61K 8/97\(2006.01\)](#) [A61Q 19/02\(2006.01\)](#)

대표도면

[크게보기](#)

출원번호(일자)	10-2008-0087480 (20080904)
공개번호(일자)	1020100028440 (20100312)
공고번호(일자)	
등록번호(일자)	
구분/원출원권리	/ 신규
원출원번호(일자)	
Family 출원번호	
최종처분내용	등록결정(일반)
심판사항	
등록상태	공개
국제출원번호(일자)	
국제공개번호(일자)	
심사청구여부(일자)	Y(2008.09.04)
심사청구항수	8



초록  
본 발명은 비목나무 유래 추출물, 분획물 또는 화합물을 함유하는 피부 미백용 조성물에 관한 것으로, 더욱 상세하게는 비목나무를 에탄올로 추출하여 얻은 에탄올 추출물, 이로부터 얻은 용매 분획물 또는 이로부터 분리정제한 화합물을 유효성분으로 하는 피부 미백용 조성물에 관한 것이다. 본 발명 비목나무 유래 추출물, 분획물 또는 화합물을 함유하는 피부 미백용 조성물은 비목나무 추출물, 이의 용매분획물 또는 이로부터 분리정제한 사이클펜타디온 화합물을 유효성분으로서 함유함으로써 기존에 미백제로 알려진 Arbutin보다 더욱 높은 멜라닌 저해 활성을 보이는 매우 뛰어난 효과를 가진다. 비목나무, *Lindera erythrocarpa*, 추출물, 용매분획, 미백, 멜라닌, 사이클펜타디온

Appendix 5 (*Lindera erythrocarpa* Makino)

Domestic Patent

Nation Korea

Language Korean

Application No. 10-2009-0090696

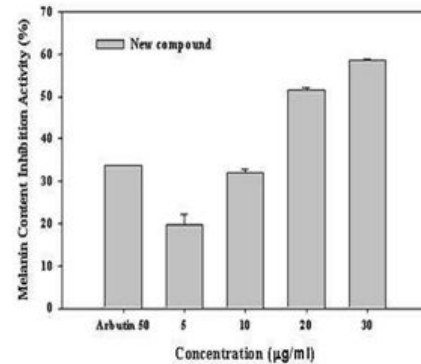
Application Date 24. Sep. 2009

발명의 명칭 비목나무 유래 화합물, 이의 분리 방법 및 이를 함유하는 피부 미백용 조성물 (Compound from *Lindera erythrocarpa*, method for isolating thereof, and composition for skin whitening comprising the same)

Int. Cl	<a href="#">C07C 43/205 (2006.01)</a> <a href="#">A81K 8/33 (2006.01)</a> <a href="#">A81K 8/97 (2006.01)</a> <a href="#">A81Q 19/02 (2006.01)</a>
출원번호(일자)	10-2009-0090696 (20090924)
공개번호(일자)	1020110032931 (20110330)
공고번호(일자)	(20110616)
등록번호(일자)	1010420050000 (20110609)
구분/원출원권리	/ 신규
원출원번호(일자)	
Family 출원번호	
최종처분내용	등록결정(일반)
심판사항	
등록상태	등록
국제출원번호(일자)	
국제공개번호(일자)	
심사청구여부 (일자)	Y(2009.09.24)
심사청구항수	11
초록	본 발명은 비목나무 유래 화합물, 이의 분리 방법 및 이를 함유하는 피부 미백용 조성물에 관한 것으로, 더욱 상세하게는 비목나무( <i>Lindera erythrocarpa</i> ) 추출물의 옹매 분획물로부터 분리한 화합물과 이의 분리 방법 및 상기 화합물을 함유함으로써 멜라닌 생합성을 억제할 수 있는 피부 미백용 조성물에 관한 것이다. 페닐프로판(phenylpropane) 화합물, 비목나무, 추출물, 옹매 분획, 미백, 멜라닌, 티로시나제

대표도면

크게보기



Appendix 6 (*Lindera erythrocarpa* Makino)

**Domestic Patent**  
**Application No.** 10-2010-0110687

**Nation** Korea **Language** Korean  
**Application Date** 08. Nov. 2010

**International Patent**  
**Application No.** PCT/KR2010/007854

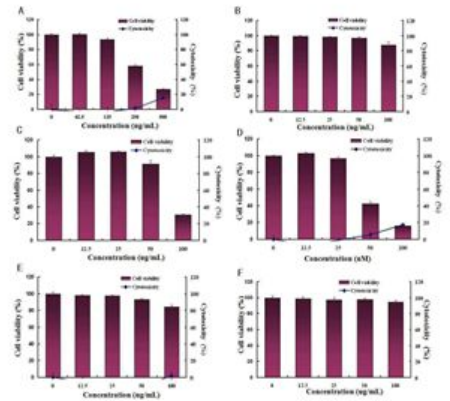
**Nation** China, Japan **Language** Chinese, Japanese  
**Application Date** 08. Nov. 2010

**발명의 명칭** 비목나무 추출물, 이의 분획물, 또는 이로부터 분리한 화합물을 유효성분으로 함유하는 약학적 조성물 (A PHARMACEUTICAL COMPOSITION COMPRISING LINDERA ERYTHROCARPA EXTRACT, FRACTIONS THEREOF, OR COMPOUNDS ISOLATED FROM THEREFORM)

**Int. Cl** [A81K 38/54 \(2006.01\)](#) [A81K 31/21 \(2006.01\)](#) [A81P 35/00 \(2006.01\)](#) [A81P 9/10 \(2006.01\)](#)

**대표도면**  [크게보기](#)

<b>출원번호(일자)</b>	10-2010-0110687 (20101108)
<b>공개번호(일자)</b>	1020110050397 (20110513)
<b>공고번호(일자)</b>	
<b>등록번호(일자)</b>	
<b>구분/원출원권리</b>	/ 신규
<b>원출원번호(일자)</b>	
<b>Family 출원번호</b>	
<b>최종처분내용</b>	공개
<b>심판사항</b>	
<b>등록상태</b>	공개
<b>국제출원번호(일자)</b>	
<b>국제공개번호(일자)</b>	
<b>심사청구여부 (일자)</b>	Y(2010.11.15)
<b>심사청구항수</b>	17



**초록** 본 발명은, 비목나무(*Lindera erythrocarpa*) 추출물, 이의 분획물, 또는 이로부터 분리한 화합물을 유효성분으로 함유하는 약학적 조성물에 관한 것으로, 본 발명의 조성물은 PPAR- $\gamma$  길항제로서 암, 동맥경화, 류마티스 관절염, 다발성경화증, 알츠하이머 또는 비만의 예방 또는 치료에 유용하게 사용될 수 있다.

Appendix 7 (*Lindera erythrocarpa* Makino)

Conference The Korean Society for Biotechnology and Bioengineering  
 Date 06 - 07 Oct 2008 Place JEJU ICC Section Poster

초록 정보

제출번호	0322
발표방법	포스터발표
발표분야	화장품
Title	<b>Identification of Whitening Components from the Leaves of <i>Lindera erythrocarpa</i> in Jeju Island</b>
Author(s)	Ryeo Kyeoung KO, Min-Chul KANG, Ju-Yeop LEE, Jong-Heon HAN, Bong-Seok KIM, Haeng-Bum KIM, Seong-Hyun AN, Gi-Ok KIM and Nam Ho LEE <sup>1</sup> <i>Jeju Bio-Industry Development Center, Jeju Hi-Tech Industry Development Institute, Jeju 690-121, Korea. <sup>1</sup>Department of Chemistry, Cheju National University, Ara-1, Jeju, 690-756, Korea.</i>
Abstract	<i>Lindera erythrocarpa</i> is distributed widely throughout Hanla mountain of Jeju and East Asia. In order to evaluate the utilizing possibility as antioxidant activity and melanin synthesis inhibite effect were investigated using ethanol extract and its fractions from <i>L. erythrocarpa</i> leaf. The EtOAc fractions showed the strongest antioxidant activites: DPPH IC <sub>50</sub> 7.43 ug/ml, Uric acid generation activity IC <sub>50</sub> 5.56 ug/ml, Superoxide generation activity IC <sub>50</sub> 16.86ug/ml, respectively. Phytochemical investigations led to the isolation of nine compound : quercetin(1), quercitrin(2), caffeic acid ethyl ester(3), cinamic acid methyl ester(4), methyl linderone(5), kanakugiol(6), kaempferol-3-O-rhamnopyranoside(7), quercetin-3-O-arabinofuranoside(8) and lucidone(9), as characterized by spectroscopic techniques including 1D, 2D NMR and HR-MS. Lucidone in nine compound was acting as a potent tyrosinase inhibitor(IC <sub>50</sub> 10ug/ml) and melanin content inhibite (IC <sub>50</sub> 8ug/ml) compared to controls (arbutin). We suggesting that the leaf extract of this plant could be used as a source of natural antioxidants useful as potential cosmetic ingredient additives.
Keyword(s)	<i>Lindera erythrocarpa</i> ; Jeju Island; anti-melanin; cosmeceutical cosmetic; NMR;

Appendix 8 (*Lindera erythrocarpa* Makino)

Conference 2011 KSBB Fall Meeting & International Symposim  
Date 05 - 08 Oct 2011 Place Songdo Convensia Incheon Section Poster

**Effects of anti-obesity in separated cyclopentadione from the Leaves of *Lindera erythrocarpa* in Jeju Island**

Yeong-Jun Jin<sup>1</sup>, Ryeo Kyeoung Ko<sup>1</sup>, Su-gyeong Kim<sup>1</sup>, Hoo-Dhon Byun<sup>1</sup>, Cheol-Su Kim<sup>2</sup>, Se-Jae Kim<sup>3</sup>,  
Nam Ho Lee<sup>4</sup> and Gi-Ok Kim<sup>1</sup>

<sup>1</sup>Bio-convergence Center, JEJU TECHNOPARK, Jeju 690-121, Korea

<sup>2</sup>Halla Arboretum, Jeju, 690-816, Korea

<sup>3</sup>Department of Biology, Cheju National University, Jeju, 690-756, Korea

<sup>4</sup>Department of Chemistry Cheju National University, Jeju, 690-756, Korea

TEL: +82-64-720-2372, FAX: +82-64-720-2331

Abstract

*Lindera erythrocarpa* is distributed widely throughout Halla mountain of Jeju and East Asia. In order to evaluate the utilizing possibility as anti-obesity effect, we were investigated using ethanol extract and its sub-fractions from *L. erythrocarpa* bark. We were separated the six compounds (lucidone, methylucidone, linderone, methylinderone, kanakugiol and Jeju-erythrane) of cyclopentadione in methylene chloride solvent sub-fraction and analyzed by spectroscopic techniques including 1D, 2D NMR and LC-MS/MS. Adipocyte differentiation and lipid synthesis were significantly inhibited by EtOH extract and methylene chloride fraction. When six compounds were added during induction of differentiation, lucidone and methylucidone inhibited cell differentiation in dose-dependent manner and methylinderone was revealed cytotoxicity effects. Methylucidone was decreased Peroxisome proliferation activated receptor (PPAR)- $\alpha$  and CCAAT/enhancer binding protein (C/EBP)- $\alpha$  expression at concentrations greater than 25  $\mu$ M, and inhibited time-dependent manner during adipogenesis. Also, the methylucidone was specifically inhibited adipocyte differentiation and lipid synthesis during induced adipocyte but not inhibited other compounds. This result indicated that methylucidone was indirectly regulated the PPAR- $\alpha$  pathway in early stage adipocyte differentiation. This result suggests that methylucidone from *Lindera erythrocarpa* may be possibility of anti-obesity properties as inhibition effect of differentiation.

References

1. Aoyama Y, Konoike T, Kanda A, Naya N, Nakajima M, Total synthesis of human chymase inhibitor methylinderone and structure—activity relationships of its derivatives (2001), Bioorganic & medicinal chemistry letters 11(13), 1695-1697.
2. Leong YW, Hamison LJ, Bennett GJ, Kadir AA, Connolly JD, A dihydrochalcone from *Lindera lucida* (1998), phytochem., 47(5), 891-894.

Appendix 9 (*Aster subulatus* Michx)

Journal	Bulletin (BKCS)	Korean	Chemistry	Society	Grade	SCI	Language	English
Year	2009		Volume	30	Number	5	Page	1167

Notes

Bull. Korean Chem. Soc. 2009, Vol. 30, No. 5 1167

## Notes

### A New Phloroglucinol Glycoside from *Aster subulatus* Michx

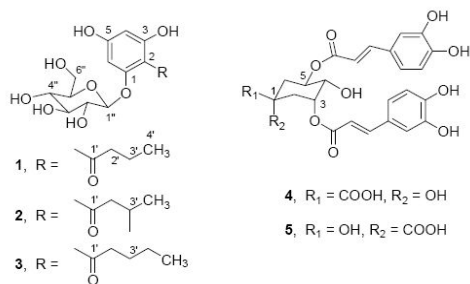
Ryeo Kyeong Ko, Min-Chul Kang, Bong-Seok Kim, Jong-Heon Han, Gi-Ok Kim, and Nam Ho Lee<sup>\*,†</sup>

*Jeju Bio-Industry Development Center, Hi-Tech Industry Development Institute, Jeju 690-121, Korea*  
<sup>†</sup>Department of Chemistry, Cheju National University, Jeju 690-756, Korea. \*E-mail: namho@cheju.ac.kr  
 Received February 11, 2009, Accepted March 18, 2009

**Key Words:** *Aster subulatus*, Compositae, Phloroglucinol glycoside, Dicafeoylquinic acid, DPPH activity

*Aster subulatus* Michx. (Compositae) is an annual grass native to America. In Korea, this species is widely distributed and now been accepted as a naturalized plant.<sup>1</sup> Previous phytochemical study on this plant has resulted in the isolation of flavonoids and their glycosides as well as chlorogenic acid.<sup>2</sup> As a part of our continuing efforts in search of biologically active compounds from plants in Jeju Island,<sup>3</sup> we have found DPPH radical scavenging activities for the ethanol extract of *A. subulatus*. This prompted us to undertake a phytochemical investigation of this plant for its active constituents. Herein, we report the isolation and characterization of a new compound, 1-[(butanoyl)phloroglucinyl]- $\beta$ -D-glucopyranoside (**1**) together with two known compounds, 3,5-dicafeoylquinic acid (**4**) and its epimer, 3,5-dicafeoyl-*epi*-quinic acid (**5**).

The ethanol extract was prepared from the whole plant of *A. subulatus*. The ethyl acetate soluble fraction of the extract was chromatographed over silica gel and reversed-phase silica gel to yield a new phloroglucinol glycoside (**1**) besides two known quinic acid derivatives (**4**, **5**).



Compound **1**, obtained as an amorphous powder, showed a  $[M+Na]^+$  peak at  $m/z$  381.1160 (calcd  $m/z$  381.1162) in the HR-FAB-MS, consistent with the molecular formula  $C_{16}H_{22}O_9$  (six unsaturations). This was supported by  $^{13}C$  and DEPT NMR spectra, which showed signals for all the 16 carbons, including six aromatic, one carbonyl, and nine

aliphatic carbons (Table 1). The UV absorption maxima of **1** in MeOH at 228 and 286 nm suggested the presence of an aromatic ring. The aromatic ring is inferred to be phloroglucinol (1,3,5-trihydroxybenzene) moiety based on the observation of highly downfield shifts of three  $^{13}C$  signals ( $\delta$  162.4, 165.9, 167.8) and upfield shifts of other three  $^{13}C$  signals ( $\delta$  95.5, 98.4, 106.9), typical  $\delta_c$  pattern appeared in phloroglucinol analogue. The aromatic protons at  $\delta$  6.17 (d,  $J=2.0$  Hz) and 5.94 (d,  $J=2.0$  Hz) were placed at H-6 and H-4 based on their HMQC correlation with carbons at  $\delta$  95.5 (C-6) and 98.4 (C-4), respectively. The upfield shift and smaller coupling constant of these protons showed that these *meta* coupled protons are between oxygenated quaternary carbons. Since only two aromatic protons were observed, there should be one substituent connected to aromatic carbon in this 1,3,5-trioxybenzene unit.

The  $^1H$  NMR spectrum showed signals at  $\delta$  0.97 (3H, t,  $J=7.5$  Hz), 3.16 (1H, ddd,  $J=16.5, 7.5, 6.5$  Hz) and 3.09 (1H, ddd,  $J=16.5, 9.0, 7.0$  Hz), and 1.69 (2H, m). These signals were respectively assignable to one methyl and two methylene groups, revealing a propyl side chain in **1**, which was further confirmed by COSY experiment. The propyl group is connected to carbonyl to construct a butanoyl unit, which was verified by HMBC data (Table 1). The carbonyl carbon (C-1') is attached to the aromatic carbon (C-2) of 1,3,5-trioxybenzene nucleus, based on long range ( $^4J$ ) HMBC correlation of H-6 with C-1', probably due to the conjugated  $\pi$ -system of the benzene ring. The presence of a sugar was suggested by the appearance of six oxygen-bearing  $sp^3$  carbons at  $\delta$  101-62 in combination with proton signals at  $\delta$  5.03 and 3.4-3.9. The large coupling constant ( $J=7.5$  Hz) for the anomeric proton at  $\delta$  5.03 (H-1'') having HMQC cross peak with  $\delta$  101.9 indicated the sugar was in  $\beta$ -configuration. The sugar protons at  $\delta$  3.53 (dd,  $J=9.0, 7.5$  Hz, H-2'') and  $\delta$  3.41 (dd,  $J=9.0, 9.0$  Hz, H-4'') all showed axial-axial coupling constants, which suggested that all substituents in this hexose are in equatorial positions. Therefore, the sugar was identified as glucose. In butanoyl substituted phloroglucinols, the glucose unit can be attached to either 1-OH (3-OH) or 5-OH positions. If the substitution is made at 5-OH, it leads to a symmetric benzene nucleus, which show only four aromatic  $^{13}C$  NMR signals. Since it is not observed in **1**, the glucose moiety should be

Appendix 10 (*Aster subulatus* Michx)

Domestic Patent

Nation Korea

Language Korean

Application No. 10-2008-0065646

Application Date 07. July. 2008

발명의 명칭 비자루국화 추출물을 함유하는 피부 상태개선용 조성물 (A composition for improving skin conditions comprising extract of *Aster subulatus* Michx.)

Int. Cl. [A81K 8/97 \(2006.01\)](#) [A81Q 19/00 \(2006.01\)](#) [A81Q 19/02 \(2006.01\)](#)

대표도면

[크게보기](#)

출원번호(일자) 10-2008-0065646 (20080707)

공개번호(일자) 1020100005557 (20100115)

공고번호(일자)

등록번호(일자)

구분/원출원권리 / 신규

원출원번호(일자)

Family 출원번호

최종처분내용 공개

심판사항

등록상태 공개

국제출원번호(일자)

국제공개번호(일자)

심사청구여부 (일자) Y(2008.07.07)

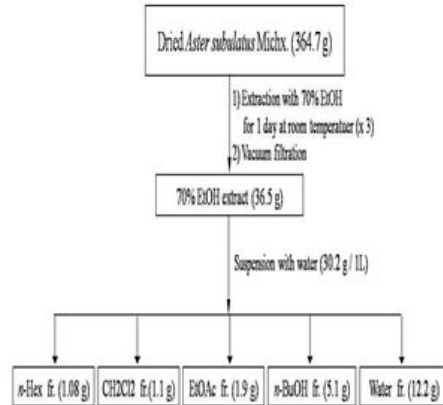
심사청구항수 3

초록

본 발명은 비자루국화 추출물을 함유하는 피부 상태개선용 조성물에 관한 것으로, 더욱 상세하게는 비자루국화를 에탄올로 추출하여 얻은 에탄올 추출물 또는 이로부터 얻은 용매 분획물을 유효성분으로 하는 피부 미백 또는 항염증 활성이 있는 피부 상태개선용 조성물에 관한 것이다.

본 발명의 비자루국화 추출물 또는 이로부터 얻은 용매 분획물은 뛰어난 항산화 활성을 나타내며, 기존에 미백제로 알려진 melasolv보다 더욱 높은 멜라닌 저해 활성을 보이고, NO 생성을 억제하여 항염증 효과를 가지는 것으로 확인되었다.

비자루국화, *Aster subulatus* Michx., 추출물, 용매분획, 항산화, 미백, 멜라닌, 항염증, 산화질소



Appendix 11 (*Aster subulatus* Michx)

Domestic Patent

Nation Korea

Language Korean

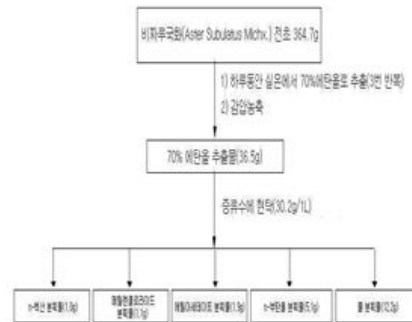
Application No. 10-2009-0034835

Application Date 21. April. 2009

발명의 명칭

비짜루국화 추출물, 분획물 또는 화합물을 포함하는 세포 산화에 의해 야기되는 질환의 예방 및 치료용 조성물 (COMPOSITION FOR PREVENTING AND TREATING DISEASES INDUCED BY CELLULAR OXIDATION COMPRISING EXTRACT, FRACTION OR COMPOUND FROM ASTER SUBULATUS MICHX.)

Int. Cl	<a href="#">C07H 7/04 (2006.01)</a> <a href="#">A61K 38/28 (2006.01)</a> <a href="#">A61P 35/00 (2006.01)</a> <a href="#">C07H 13/02 (2006.01)</a>	대표도면	<a href="#">크게보기</a>
출원번호(일자)	10-2009-0034835 (20090421)		
공개번호(일자)	1020100116090 (20101029)		
공고번호(일자)			
등록번호(일자)			
구분/원출원권리	/ 신규		
원출원번호(일자)			
Family 출원번호			
최종처분내용	공개		
심판사항			
등록상태	공개		
국제출원번호(일자)			
국제공개번호(일자)			
심사청구여부 (일자)	Y(2009.04.21)		
심사청구항수	9		



초록  
본 발명은 비짜루국화 (*Aster Subulatus Michx.*) 추출물, 분획물 또는 화합물을 포함하는 세포 산화에 의해 야기되는 질환을 예방 및 치료하는 용도에 관한 것으로, 본 발명에 따른 비짜루국화 추출물, 분획물 또는 화합물은 지질의 산화, 활성산소의 소거 및 산화적 스트레스를 방지함으로써 노화, 암, 심장질환, 당뇨, 동맥경화 및 고지혈증으로 이루어진 군으로부터 선택되는 세포 산화에 의하여 야기되는 질환의 예방 및 치료용 조성물, 상기 질환들의 예방 및 개선용 건강식품, 또는 피부노화방지용 화장품 조성물에 유용하게 사용될 수 있다.

비짜루국화, 추출물, 산화, 당뇨



Appendix 12 (*Aster subulatus* Michx)

Conference BIO-ISLAND JEJU FORUM

Date 30 Oct 2009

Place JEJU GRAND HOTEL

Section Poster

**Anti-diabetic Activity Effects of A New Phloroglucinol Glycoside Isolated from *Aster subulatus* Michx.**

Ryeo Kyeong Ko,<sup>†</sup> Min-Chul Kang,<sup>†</sup> Yeong-Jun Jin,<sup>†</sup> Ho-Min Choi,<sup>†</sup> Bong-Seok Kim,<sup>†</sup> Jong-Heon Han,<sup>†</sup> Nam Ho Lee<sup>††</sup> and Gi-Ok Kim<sup>†</sup>

<sup>†</sup>Jeju Bio-Industry Development Center, Hi-Tech Industry Development Institute, Jeju 690-121, Korea

<sup>††</sup>Department of Chemistry, Cheju National University, Ara-1, Jeju 690-756, Korea.

In order to develop functional food supplement from plants in Jeju island, we have studied a whole of *Aster subulatus* Michx. *A. subulatus* is an annual grass native to America. In Korea, this species is widely distributed and now been accepted as a naturalized plant. Phytochemical study of the 70 % ethanol extract of *A. subulatus* afforded a new compound along with six known compounds [caffeic acid, caffeic acid ethyl ester, astragaln, 3,5-dicaffeoyl quinic acid, 3,5-dicaffeoyl *epi*-quinic acid,  $\beta$ -stigmasterol]. The identification of the isolated compounds were made from extensive analysis of 1D, 2D NMR spectra and HR-FAB MS experiments. The isolated compounds was inhibited  $\alpha$ -glucosidase activity. We suggesting that *A. subulatus* extract of this plant could be used as a source of natural Anti-diabetic useful as potential food ingredient additives.

**Keywords:** *Aster subulatus* Michx, Anti-diabetic, New Phloroglucinol Glycoside, Food Additives.

Appendix 13 (*Ishige sinicola* (Setchell et Gardner))

Journal	Food and Chemical Toxicology	Grade	SCI	Language	English
Year	2011	Volume	49	Number	4
				Page	864 - 870

Food and Chemical Toxicology 49 (2011) 864–870



Contents lists available at ScienceDirect

Food and Chemical Toxicology

journal homepage: [www.elsevier.com/locate/foodchemtox](http://www.elsevier.com/locate/foodchemtox)



## Diphlorethohydroxycarmalol, isolated from the brown algae *Ishige okamurae*, protects against radiation-induced cell damage in mice

Meejung Ahn<sup>a,b,1</sup>, Changjong Moon<sup>c,1</sup>, Wonjun Yang<sup>b,d</sup>, Eun-Ju Ko<sup>b,d</sup>, Jin Won Hyun<sup>b,e</sup>, Hong Gu Joo<sup>b,d</sup>, Youngheun Jee<sup>b,d</sup>, Nam Ho Lee<sup>b,f</sup>, Jae Woo Park<sup>b,g</sup>, Ryeo Kyeong Ko<sup>h</sup>, Gi Ok Kim<sup>h</sup>, Taekyun Shin<sup>b,d,\*</sup>

<sup>a</sup> Department of Anatomy, College of Medicine, Jeju National University, Jeju 690-756, South Korea

<sup>b</sup> Applied Radiological Science Research Institute, Jeju National University, Jeju 690-756, South Korea

<sup>c</sup> Department of Veterinary Anatomy, College of Veterinary Medicine, Chonnam National University, Gwangju 500-757, South Korea

<sup>d</sup> Laboratory of Veterinary Anatomy, College of Veterinary Medicine and Veterinary Medical Research Institute, Jeju National University, Jeju 690-756, South Korea

<sup>e</sup> Department of Biochemistry, College of Medicine, Jeju National University, Jeju 690-756, South Korea

<sup>f</sup> Department of Chemistry, College of Natural Sciences, College of Medicine, Jeju National University, Jeju 690-756, South Korea

<sup>g</sup> Department of Nuclear and Energy Engineering, College of Engineering, Jeju National University, Jeju 690-756, South Korea

<sup>h</sup> Jeju Technopark, Jeju 690-121, South Korea

### ARTICLE INFO

#### Article history:

Received 14 October 2010

Accepted 8 December 2010

Available online 14 December 2010

#### Keywords:

*Ishige okamurae*  
Diphlorethohydroxycarmalol  
Intestinal crypt assay  
Apoptosis  
Radiation  
Oxidative stress

### ABSTRACT

The aim of this study was to evaluate the radioprotective effects of diphlorethohydroxycarmalol (DPHC), isolated from the brown algae *Ishige okamurae*, in mice subjected to gamma irradiation.

DPHC significantly decreased the level of radiation-induced intracellular reactive oxygen species in cultured Chinese hamster lung fibroblast (V79-4) cells ( $p < 0.05$ ), enhanced cell viability that decreased after exposure to  $\gamma$ -rays, and reduced radiation-induced apoptosis in the V79-4 cells.

Pretreatment with DPHC (100 mg/kg) in mice prior to irradiation significantly protected the intestinal crypt cells in the jejunum ( $p < 0.01$ ) and maintained villi height ( $p < 0.01$ ), compared with those of the vehicle-treated irradiated group. Mice pretreated with DPHC also exhibited dose-dependent increases in the bone marrow cell viability. The dose-reduction factor for gamma irradiation in the DPHC-pretreated mice was 2.05 at 3.5 days after irradiation.

These results suggest that DPHC plays a role in protecting cells from irradiation-induced apoptosis, through the scavenging of reactive oxygen species *in vitro*, and that DPHC significantly protected intestinal progenitor cells and bone marrows cells that were decreased by gamma irradiation *in vivo*.

© 2010 Elsevier Ltd. All rights reserved.

### 1. Introduction

*Ishige okamurae* (Phylum Phaeophyta, Class Phaeophyceae, Order Chordariales, Family Ishigeaceae), an edible brown algae, has been collected from the coast of Jeju island, Korea (Lee and Kang, 1986). Recently, an ethanolic extract of *I. okamurae* was shown to have anti-inflammatory effects via the inhibition of nuclear factor kappa B (NF- $\kappa$ B) (Kim et al., 2009). Diphlorethohydroxycarmalol (DPHC), a phlorotannin isolated from *I. okamurae*, has been shown to have a variety of biological effects, including antioxidant effects (Heo et al., 2008; Zou et al., 2008), anti-viral effects (Ahn et al., 2006), and hypoglycemic effects (Heo et al., 2009). The biological activities of DPHC, described above, prompted us to

examine its use in various types of inflammatory conditions, including radiation injury.

Irradiation has been widely used for the treatment of cancers, but the side effects reduce the patients' quality of life, due to hematopoietic or gastrointestinal injury, apoptosis, and mutagenesis (Rzeszowska-Wolny et al., 2009). In the presence of H<sub>2</sub>O in organism, ionizing radiation including gamma ray leads to formation of reactive oxygen species such as superoxide anion, hydrogen peroxide, hydroxyl radical, and singlet oxygen (Hall et al., 1988). Because reactive oxygen species generated by ionizing radiation damages radiosensitive cells, leading to apoptosis (Moon et al., 2008; Potten and Grant, 1998; Weil et al., 1996), protection of tissues and cells, including intestinal progenitor cells, is an important issue in radiotherapy (Conklin and Walker, 1987; Hall et al., 1988; Weiss and Landauer, 2003).

The search for synthetic or natural compounds that can protect cells against ionizing irradiation is an important topic in radioprotection studies; radiation-induced cellular injury is linked to apoptosis, via oxidative injury, particularly in the proliferating

\* Corresponding author at: Laboratory of Veterinary Anatomy, College of Veterinary Medicine, Jeju National University, Jeju 690-756, South Korea. Tel.: +82 64 754 3363; fax: +82 64 756 3354.

E-mail address: [shint@jeju.ac.kr](mailto:shint@jeju.ac.kr) (T. Shin).

<sup>1</sup> These authors contributed equally to this work.

Appendix 14 (*Ishige sinicola* (Setchell et Gardner))

Domestic Patent

Nation Korea

Language Korean

Application No.

10-2011-49717

Application Date

25. May. 2011

관인생략  
출원번호통지서

출원일자 2011.05.25  
 특기사항 심사청구(유) 공개신청(무)  
 출원번호 10-2011-0049717 (접수번호 1-1-2011-0392623-34)  
 출원인명칭 제주대학교 산학협력단(2-2004-016727-0) 외 1명  
 대리인성명 위병갑(9-2004-000155-3)  
 발명자성명 신태균 현진원 안미정 양원준 감소희 고려경 김기욱  
 발명의명칭 디플로르에도하이드록시카르마를 화합물을 유효성분으로 함유하는 간 손상 예방 또는 치료용 조성물

특 허 청 장

<< 안내 >>

1. 귀하의 출원은 위와 같이 정상적으로 접수되었으며, 이후의 심사 진행상황은 출원번호를 통해 확인하실 수 있습니다.
2. 출원에 따른 수수료는 접수일로부터 다음날까지 동봉된 납입영수증에 성명, 납부자번호 등을 기재하여 가까운 우체국 또는 은행에 납부하여야 합니다.  
\* 납부번호 : 0131(기관코드) + 접수번호
3. 귀하의 주소, 연락처 등의 변경사항이 있을 경우, 즉시 [출원인코드 정보 변경(경정), 정정신고서]를 제출하여야 출원 이후의 각종 통지서를 정상적으로 받을 수 있습니다.  
\* 특허로(patent.go.kr) 접속 > 민원서비스다운로드 > 특허법 시행규칙 별지 제5호 서식
4. 특허(실용신안등록)출원은 명세서 또는 도면의 보정이 필요한 경우, 등록결정 이전 또는 의견서 제출기간 이내에 출원서에 최초로 첨부된 명세서 또는 도면에 기재된 사항의 범위 안에서 보정할 수 있습니다.
5. 국내출원건을 외국에도 출원하고자 하는 경우에는 국내출원일로부터 일정한 기간 내에 외국에 출원하여야 우선권을 인정 받을 수 있습니다.  
\* 우선권 인정기간 : 특허·실용신안은 12월, 상표·디자인은 6월 이내  
\* 미국특허상표청의 선출원을 기초로 우리나라에 우선권주장출원 시, 선출원이 미공개상태이면, 우선일로부터 16개월 이내에 미국특허상표청에 [전자적교환허가서(PTO/SB/39)]를 제출하거나 우리나라에 우선권 증명서류를 제출하여야 합니다.
6. 본 출원사실을 외부에 표시하고자 하는 경우에는 아래와 같이 하여야 하며, 이를 위반할 경우 관련법령에 따라 처벌을 받을 수 있습니다.  
\* 특허출원 10-2010-0000000, 상표등록출원 40-2010-0000000
7. 기타 심사 절차에 관한 사항은 동봉된 안내서를 참조하시기 바랍니다.

Appendix 15 (*Dictyota coriacea* (Holmes) Hwang, Kim, et Lee)

Journal	KSBB Journal	Grade	SCIE	Language	Korean
Year	2008	Volume	23	Number	4
				Page	311 - 316

한국생물공학회지 제23권 제4호  
 Korean J. Biotechnol. Bioeng.  
 Vol. 23, No. 4, 311-316(2008)

제주도 근해에 자생하는 참가죽그물바탕말 (*Dictyota coriacea*)  
 추출물의 멜라닌 억제 효과 및 항염증 효과

강민철 · 이주엽 · 고려경 · 김행범 · 홍승호 · 김기옥  
 (재)제주하이테크산업진흥원 생물자원산업화지원센터<sup>1</sup> 제주대학교 교육대학 과학교육과  
 (접수 : 2008. 4. 27., 게재승인 : 2008. 8. 5.)

Melanin Inhibitory Effect and Anti-inflammatory Effects of *Dictyota coriacea* Extracts Derived from Adjacent Sea of the Jeju Island

Min-Chul Kang, Ju-Yeop Lee, Ryeo Kyeoung Ko, Haeng-Bum Kim, Seung-Ho Hong<sup>1</sup>, and Gi-Ok Kim<sup>†</sup>  
 Jeju Bio-Industry Development Center, Jeju Hi-Tech Industry Development Institute, Jeju 690-121, Korea  
<sup>1</sup>Department of Science Education, Teachers College, Cheju National University, Jeju 690-781, Korea  
 (Received : 2008. 4. 27., Accepted : 2008. 8. 5.)

We investigated several biological activities using the ethanol extract and its fractions from *Dictyota coriacea* to evaluate the usefulness of its extract as a functional biomaterial. The ethanol extract and n-hexane and ethylacetate fractions showed dependently inhibitory effect on tyrosinase activity and melanin content in B16F10 cells. The ethanol extract and its fractions showed inhibitory effect on Tyrosinase and TRP-1 gene transcription but didn't showed inhibitory effect on TRP-2 gene transcription. Also, the n-hexane and ethylacetate fractions dose-dependently inhibited the NO production in a RAW 264.7 cells. These results suggest that extract of *Dictyota coriacea* could be used as functional biomaterial in developing a skin whitening agent having the anti-inflammatory activity.

**Key Words** : *Dictyota coriacea*, tyrosinase activity, melanin content, anti-inflammatory activity

서 론

동양인들은 최고 고운 피부에 대한 열망이 과거에서부터 미의 상징으로 여겨져 동양권에서는 미백화장품에 대한 관심과 함께 그에 대한 연구가 집중되어 왔다. 인간의 피부색깔은 환경, 인종, 성별 등의 요인과 멜라닌, 카로틴 및 헤모글로빈 양과 같은 여러 가지 요인에 의해 결정되지만 피부의 과색소 침착과 관련된 주요한 원인은 표피 내 멜라닌색소의 이상적 증가에 기인한다. 과도한 melanin 합성은 인체에 기미, 주근깨, 피부반점을 형성하고 피부노화를 촉진하며 피부암 유발에 관여하는 것으로 알려져 있다(1-2). 멜라닌 색소의 생합성은 tyrosinase 효소를 비롯하여 tyrosinase-related protein 1 (TRP1)과 dopachrome tautomerase (TRP2)에 의하여 조절되고 있으며, 그중 tyrosinase는 tyrosine을 기질로 하여 L-dopaquinone으로 전이되는 초기

생합성과정 이후 dihydroxyindole의 산화에 작용한다(3-5). 따라서 tyrosinase 활성 억제제를 찾는 연구가 미백제의 개발에 있어서 중요한 부분을 차지하고 있으며, 현재 계속 알려지고 있는 tyrosinase 저해제로 hydroquinone, 4-hydroxyanisole, ascorbic acid 유도체, kojic acid, azelaic acid, corticosteroid, retinoids, arbutin, catechin, 3,4,5-trimethoxy cinnamate thymol ester 등이 있으나, 이들의 안전성과 경제성 등에 문제가 많아 사용에 있어서 어려움이 있다(6-9). 한편 자외선에 의해 그 생성이 촉진되며 멜라닌합성을 활성화시키고 염증과 피부노화를 유도하는 물질 중에 하나인 nitric oxide (NO)는 작고 비교적 불안정하며 독성이 있는 무기 저분자 라디칼이다. NO를 생성하는 효소(NOS: nitric oxide synthase)에는 constitutive NOS (c-NOS)와 inducible NOS (iNOS)가 보고되어 있다. cNOS에 의한 NO생성은 생체 내 항상성 조절에 중요한 역할을 하지만(10), iNOS는 cNOS와는 달리 lipopolysaccharide (LPS), interferon- $\gamma$  (IFN- $\gamma$ ), interleukin-1 $\beta$  (IL-1 $\beta$ ) 및 tumor necrosis factor- $\alpha$  (TNF- $\alpha$ ) 등의 자극에 의해 대식세포, 혈관평활근세포, 내피세포, 간세포와 심근세포 등에서 발현된다(11). 이들 조직에서 발현되는 iNOS는 장시간 동안 많은 양의 NO를 생성하게 되어 염증과 종양을

<sup>†</sup> Corresponding Author : Jeju Bio-Industry Development Center, Hi-Tech Industry Development Institute, Jeju 690-121, Korea  
 Tel : +82-64-720-2333, Fax : +82-64-720-2331  
 E-mail : Kimgk350@jejubidi.or.kr

Appendix 16 (*Styrax obassia* Siebold & Zucc)

Domestic Patent

Nation Korea

Language Korean

Application No. 10-2011-0076709

Application Date 01. Aug. 2011

【서지사항】

【서류명】 특허출원서

【출원구분】 특허출원

【출원인】

【명칭】 재단법인 제주테크노파크

【출원인코드】 2-2005-039314-6

【대리인】

【명칭】 특허법인 유아이피

【대리인코드】 9-2008-100141-2

【지정된변리사】 전상우, 김동진

【포괄위임등록번호】 2009-041221-1

【발명의 국문명칭】 쪽동백나무 조추출물, 이의 분획물 또는 그 분획물에서 분리된 생리활성물질을 유효성분으로 함유하는 식품조성물 또는 약학 조성물

【발명의 영문명칭】 A food composition or pharmaceutical composition comprising *Styrax obassia* Siebold & Zucc extract, fraction thereof, or bioactive substances isolated from the fraction

【발명자】

【성명】 김기옥

【성명의 영문표기】 KIM, Gi Ok

【주민등록번호】 \*\*\*\*\*-\*\*\*\*\*

【우편번호】 690-121

Appendix 17 (*Styrax obassia* Siebold & Zucc)

Conference 2011 KSBB Fall Meeting & International Symposim  
Date 05-08 Oct 2011 Place Songdo Convensia Incheon Section Poster

**Chemical Constituents and anti-obesity effects from the leaves of *Styrax obassia* Siebold & Zucc in Jeju Island**

Ryeo Kyeoung Ko<sup>1</sup>, Yeong-Jun Jin<sup>1</sup>, Su-gyeong Kim<sup>1</sup>, Hoo-Dhon Byun<sup>1</sup>, Min-Cheol Kang<sup>1</sup>, Cheol-Su Kim<sup>2</sup>, Se-Jae Kim<sup>3</sup>, Nam Ho Lee<sup>4</sup> and Gi-Ok Kim<sup>1</sup>

<sup>1</sup>Bio-convergence Center, JEJU TECHNOPARK, Jeju 690-121, Korea

<sup>2</sup>Halla Arboretum, Jeju, 690-816, Korea

<sup>3</sup>Department of Biology, Cheju National University, Jeju, 690-756, Korea

<sup>4</sup>Department of Chemistry Cheju National University, Jeju, 690-756, Korea

TEL: +82-64-720-2372, FAX: +82-64-720-2331

Abstract

*Styrax obassia* Siebold & Zucc is belong to the Styracaceae family and is distributed widely throughout Korea, Japan and China. In order to evaluate the utilizing possibility as anti-obesity effect, we were investigated using ethanol extract and its sub-fractions from *S. obassia* leaves. *S. obassia* BuOH fraction was more decreased the Peroxisome proliferation activated receptor (PPAR)- $\alpha$ , CCAAT/enhancer binding protein (C/EBP)- $\alpha$  and p2 than *S. obassia* extract. In other words,  $\beta$ -catenin and cyclin D1 protein were reduced during a dipocyte differentiation and then increased PPAR- $\alpha$  expression. When treated with *S. obassia* extracts were inhibited the both of  $\beta$ -catenin, cyclin D1. The n-Butanol solvent sub-fraction was completely inhibited the a dipocyte differentiation than the other sub-fractions. Therefore, we were isolated two compounds type of saponin from n-BuOH solvent sub-fraction of *S. obassia*. Jegosaponin A and B was analyzed by spectroscopic techniques including 1D, 2D NMR and LC-MS/MS. Jegosaponin B was more effect of inhibition the differentiation than jegosaponin A in dose-dependent manner. This result suggests that jegosaponin A and B from *S. obassia* may be possibility of anti-obesity properties as inhibition effect of differentiation.

Reference

1. Yoshikawa K, Hirai H, Tanaka M, Arihara S, Antisweet natural products. SV. Structures of jegosaponins A-D from *Styrax japonica* sieb. et zucc(2000), Chem. Pharm. Bull. 28(7), 1093-1096.
2. Yoon WJ, Lee NH, Hyun CG, Limonene suppresses lipopolysaccharide-induced production of nitric oxide, prostaglandin E2, and pro-inflammatory cytokines in RAW 264.7 macrophages (2010), J. of Oleo Science, 59(8), 415-421.
3. Gregoire FM, Smas CM, Sul HS, Understanding a dipocyte differentiation (1998), physiol Rev. 78(3),

## Acknowledgments (감사의 글)

일 년에 걸친 학위논문 작성이 끝나는 이 시점.

한 장 반 남짓 되는 마지막 글에 무엇을 써야할지 선뜻 떠오르질 않습니다. 논문 작성에서 가장 어려운 부분이 감사의 글이 아닌가 싶습니다. 직장업무와 병행하며 보냈던 3년간의 박사과정은 석사과정 때와는 다른 경험을 선사하였습니다. 그 간의 감정 상태를 그래프로 도식해보는다면 인간이 느낄 수 있는 모든 감정선들이 뒤죽박죽 섞여진 형태를 보이겠지만, 오늘이 있기까지 최고의 방해꾼이자 격려자는 어떤 누구도 아닌 바로 저 자신이라는 것을 깨닫게 해준 소중한 시간 이었습니다. 또한 이 자리를 빌어 목표를 향해 한발 한발 내딛는 제게 따뜻한 등불이 되어주신 소중한 이들에게 감사의 마음을 전하고자 합니다.

언제나 성령이 되어 어두운길 보지 않고 밝은 길로 인도해 주신 주님께 감사드립니다.

**지도교수님께** : 지금까지 부족한 저를 잘 보듬어주시고 뒤에서 묵묵히 지켜봐주신 이남호 교수님. 학교 울타리를 벗어나 사회에서 보여주신 교수님 모습은 참으로 멋지셨습니다. 그 모습 기억하고 본받아 저 또한 멋진 사람이 되도록 노력하고자 합니다. 지도교수님으로써, 화학자로서 그리고 선배님으로써 존경하고, 사랑합니다.

**화학과 교수님께** : 늘 따뜻한 관심과 조언으로 학문의 길을 보여주신 정덕상 교수님, 김덕수 교수님, 변종철 교수님, 강창희 교수님, 이선주 교수님, 김원형 교수님. 매 학기마다 많은 것을 가르쳐 주시며, 학생들이 발전 할 수 있게 토대가 되어주신 노력들에 대한 고마움은 제가 앞으로도 계속 잊지 못할 것 같습니다. 감사합니다.

**유기화학실험실 식구들과 화학과 선후배님께** : 실험실로 입실하던 그 날부터 든든한 버팀목이 되어주셨던 백종석 박사님, 윤진석 선생님, 오태현 박사님, 김정

미 박사님과 김상숙 박사님. 값진 조언과 힘을 불어넣어주신 한충훈 박사님, 고희철 박사님, 이정아 박사님. 함께 입학하여 박사수로 하기까지 서로 의지하며 힘이 되어준 이동은 선생님, 최지영 선생님, 송정민 선생님 그리고 화학과 선배님들과 유기화학실험실 후배님들에게도 고맙다는 말씀을 전하며, 앞으로 하고자 하는 분야에서 최고가 될 수 있도록 기원 드립니다.

**강삼식 교수님께 :** 교수님께서 제게 천연물화학 공부를 다시 시작할 수 있다는 용기를 주셨고, 천연물 화학자로서 자부심을 안겨 주셨습니다. 우연치 않은 기회에 교수님께 첫 인사 올린 그 날 이후부터 줄곧 저의 롤 모델 이셨습니다. 교수님 앞에서 논문심사를 받게 되어 제겐 더 없는 큰 영광 이였고, 지켜봐주시겠다는 말씀에 힘입어 더욱 정진하겠습니다. 늘 행복하시고 건강하세요.

**(재)제주테크노파크 연구원님께 :** 박사과정을 무사히 끝낼 수 있게 모든 면에서 지원해주신 김성규 센터장님과 김기옥 단장님. 생리활성연구를 해주신 진영준 연구원님, 강민철 연구원님과 이주엽 연구원님. 늘 따뜻한 격려와 응원의 메시지를 보내준 바이오융합센터의 현창구 박사님, 박지권 박사님, 김봉석 전임연구원님, 한중현 전임연구원님, 이경후 연구원님, 현지영 연구원님, 김수경 연구원님, 김민진 연구원과 정책기획단의 진관훈 박사님, 강신해 박사님, 임소진 박사님께 자리를 빌어 감사 인사드립니다.

**가족들에게 :** 존경하는 외할머니, 영원한 나의 영웅이신 아버지와 어머니, 역할 모델이 되어준 큰오빠, 큰언니, 작은오빠, 작은언니, 삼촌, 숙모, 이모, 이모부. 제 곁에서 가장 소중한 당신들의 기도와 무한한 신뢰가 있었기에 가능할 수 있었다는 것 잘 알고 있습니다. 앞으로 제게 주신 사랑 갚아 가면서 살겠습니다. 감사합니다.

**앙상블 단원들에게. :** 무미건조하게 바쁘기만 하던 제게 하나의 휴식처가 되주었고, 항상 행복한 미소를 짓게 해주신 유상근 단장님, 김경택 지휘자님, 황경수 교수님, 혜경언니, 미정언니, 형관 선생님, 수연이, 미선과 제주플루트카론앙상블 단원들 모두에게 감사의 인사드립니다.



친구들에게. : 바쁘다는 핑계로 연락 한번 먼저 건내본 적 없는 무관심한 친구에게 언제나 곁에 머물러 주며 때때마다 응원을 보내 준 나의 친구들. 수경, 은영 언니, 유미, 지연, 수빈언니, liang, 진식, ali. 고맙습니다.

제겐 더없이 소중한 분들께 인사를 드리고 나니 두 장이 훌쩍 넘어갑니다. 석사학위 논문 내 감사의 글은 한 장 반도 채 되지 않았는데, 그 새 인사를 드릴 수 있는 분들이 이만큼 많아졌습니다. 이 모든 것, 당신들의 도움이 있었기에 가능했다는 것 잘 알고 깊이 간직하겠습니다.

세계 있어 박사 학위는 깊고 넓은 학문바다를 향해 하는 여객선의 승선표가 되어줄 것이라 생각합니다. 힘찬 뱃고동 소리와 함께 앞으로 나아가기 위해서는 지금과는 비교할 수 없는 더 많은 노력을 계속 기울여야 가능하겠지요. 각오를 다지며 떨리던 손을 움켜쥐고 실험방 문을 처음 두드리던 7년 전 그 날의 마음처럼 조금씩 계속 정진하며 나아가겠습니다.

고맙습니다.

사랑합니다.

2012년 1월  
고려경 올림